REC-ERC-82-9

HYDRAULIC MODEL STUDIES OF LANDSLIDE-GENERATED WATER WAVES— MORROW POINT RESERVOIR

April 1982

Engineering and Research Center

U.S. Department of the Interior

Bureau of Reclamation

7-2090 (4-81)
Bureau of Reclamation

TECHNICAL REPORT STANDARD TITLE PAGE

1. REPORT NO. REC-ERC-82-9	3. RECIPIENT'S CATALOG NO.
4. TITLE AND SUBTITLE Hydraulic Model Studies of Landslide-Generated Water Waves—Morrow Point Reservoir	5. REPORT DATE April 1982
	6. PERFORMING ORGANIZATION CODE
7. AUTHOR(S) C. A. Pugh	8. PERFORMING ORGANIZATION REPORT NO. REC-ERC-82-9
9. PERFORMING ORGANIZATION NAME AND ADDRESS Bureau of Reclamation Engineering and Research Center Denver, Colorado 80225	10. WORK UNIT NO.
	11. CONTRACT OR GRANT NO.
12. SPONSORING AGENCY NAME AND ADDRESS Same	13. TYPE OF REPORT AND PERIOD COVERED
	14. SPONSORING AGENCY CODE DIBR

15. SUPPLEMENTARY NOTES
Microfiche and/or hard copy available at the Engineering and Research Center, Denver, Colo. Both color hard copies and slides of appendix B (microfiche) available at a cost of $ 31.00 and $ 72.00, respectively per set. (Prices subject to change.) To order, see appendix B.
Editor-JMT

16. ABSTRACT
A physical model study of landslide-generated water waves was conducted to determine the potential for waves overtopping Morrow Point Dam in the event of a rapid landslide into the reservoir located near Cimarron, Colo. The model landslides were designed to simulate the potential prototype landslide dynamics. This report describes the model design, construction, and testing. Dimensionless graphs and equations were developed from the model data which may be used for general cases in the prediction of wave heights for design and operational purposes. This is the first study relating slide volume and direction as well as velocity to wave height. The test results were also used to calibrate a general numerical model developed by a consulting firm for the Bureau of Reclamation.

17. KEY WORDS AND DOCUMENT ANALYSIS
a. *DESCRIPTORS*--Landslide/ slip surface/ waves/ hydraulic model/ bores/ dam overtopping/ safety of dams/ reservoir slopes/ instrumentation/ celerity/ wave heights/ translatory waves/ solitary waves/ oscillatory waves/ gravity waves/ freeboard

b. *IDENTIFIERS*-- Colorado River Storage Project/ Upper Colorado Region/ Gunnison River

c. *COSATI Field/Group* 13C, 13M *COWRR:* 1402, 1313.1 *SRIM:* 50B, 50D

18. DISTRIBUTION STATEMENT *Available from the National Technical Information Service, Operations Division, 5285 Port Royal Road, Springfield, Virginia 22161.* (Microfiche and/or hard copy available from NTIS)	19. SECURITY CLASS (THIS REPORT) UNCLASSIFIED	21. NO. OF PAGES 53
	20. SECURITY CLASS (THIS PAGE) UNCLASSIFIED	22. PRICE

REC-ERC-82-9

HYDRAULIC MODEL STUDIES OF LANDSLIDE-GENERATED WATER WAVES—MORROW POINT RESERVOIR

by

Clifford A. Pugh

April 1982

Hydraulics Branch
Division of Research
Engineering and Research Center
Denver, Colorado

SI METRIC

UNITED STATES DEPARTMENT OF THE INTERIOR ☆ BUREAU OF RECLAMATION

ACKNOWLEDGMENTS

This hydraulic model study was conducted by the author under the supervision of T. J. Rhone, Head of the Hydraulic Structures Section, and the general supervision of D. L. King, Chief, Hydraulics Branch. The studies were accomplished through the cooperation of the Hydraulics Branch, Division of Research; the Embankment Dams Section, Dams Branch; and the Office of Dam and Structural Safety.

The contributions of D. W. Harris to the direction of the study; of Dr. Hr. T. Falvey and T. J. Rhone for their valuable technical review and direction; of J. A. Kinkaid and L. E. Elgin for their contributions to model layout and instrumentation; of the laboratory shops for expert model construction; and W. Lambert for excellent photography are very much appreciated.

As the Nation's principal conservation agency, the Department of the Interior has responsibility for most of our nationally owned public lands and natural resources. This includes fostering the wisest use of our land and water resources, protecting our fish and wildlife, preserving the environmental and cultural values of our national parks and historical places, and providing for the enjoyment of life through outdoor recreation. The Department assesses our energy and mineral resources and works to assure that their development is in the best interests of all our people. The Department also has a major responsibility for American Indian reservation communities and for people who live in Island Territories under U.S. administration.

The information contained in this bulletin regarding commercial products or firms may not be used for advertising or promotional purposes and is not to be construed as an endorsement by the Bureau of Reclamation of any product or firm.

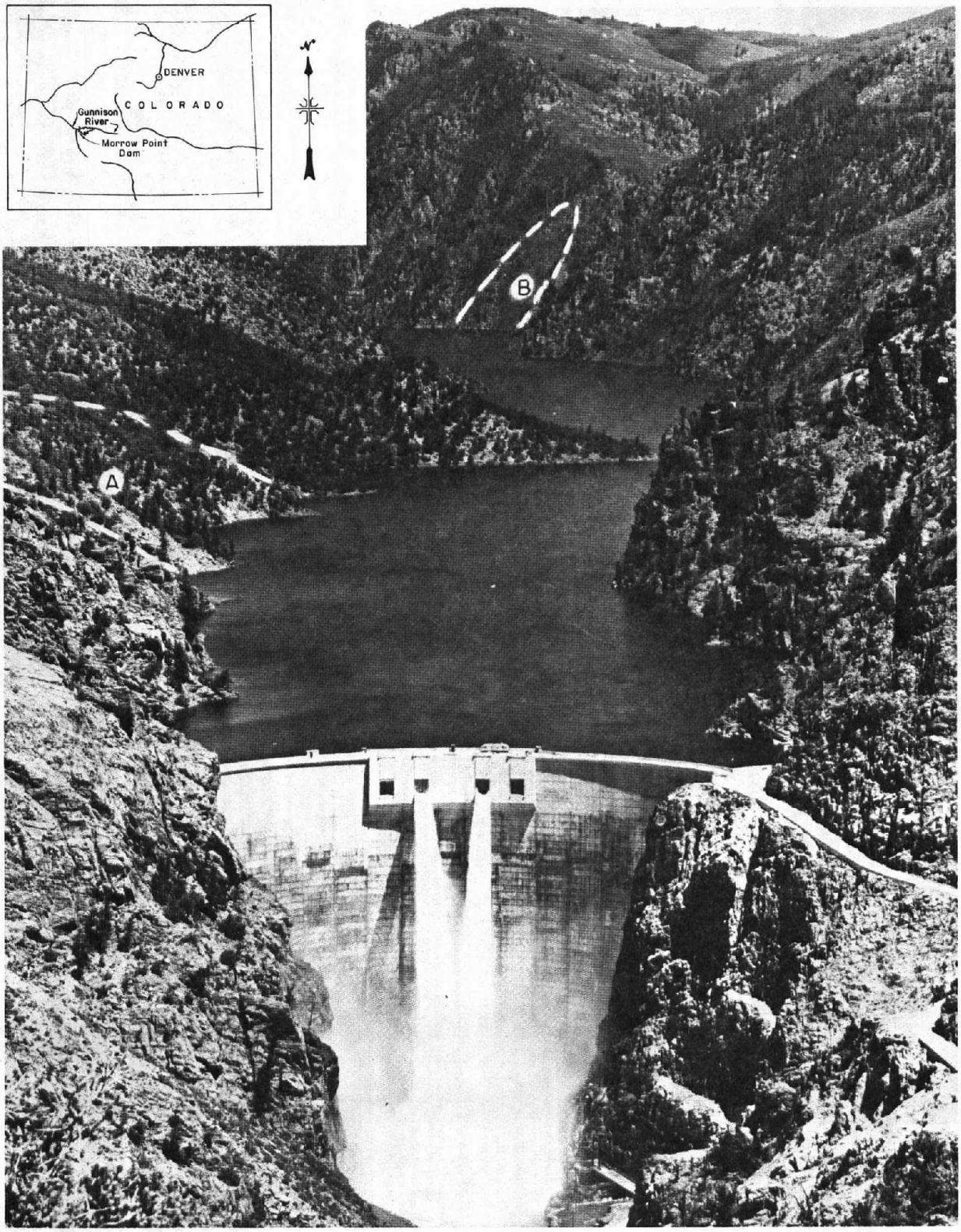

Frontispiece—Photograph of Morrow Point Dam with location map in upper left corner. P801-D-79707

CONTENTS

	Page
Acknowledgments	ii
Glossary	vii
Purpose	1
Introduction	1
Conclusions	1
The model	3
Description	3
Landslide simulation	3
Estimate of potential prototype landslide momentum	5
Designing the model landslide	5
Dimensional analysis	6
Scale relations	7
Data collection	9
Test results	11
Wave forms	11
Wave celerities (*c*)	15
Water overtopping the dam	15
Dimensionless plots	16
Bibliography	20
Appendix A	21
Appendix B	39

TABLES

Table		
1	Reservoir cross sectional data	15
2	Landslide data — dimensionless parameters	16

FIGURES

Figure		
1	Plan of reservoir area showing location of landslides and wave probes	2
2	Morrow Point landslide model photographs	4
3	Schematic diagram of the model landslide	5
4	Schematic diagram of forces used to represent the model landslide	5
5	Cross section through prototype landslide "A"	7
6	Computed model momentum versus prototype momentum (slide "A")	8
7	Capacitance probes during a test at landslide "A"	10
8	Position-velocity transducer (PVT)	11
9	Sequence photographs — landslide "A"	12
10	Types of gravity waves	14
11	Wave height in front of slides (*x*-direction) versus slide Froude number	17
12	Maximum wave height in front of slides versus volume parameter	18
13	Maximum wave height beside slides (*y*-direction) versus slide Froude number	18
14	Maximum wave height beside slides versus volume parameter	19
15	Wave height at dam versus slide Froude number	20
16	Maximum wave heights at dam for various distances and slide volumes	20

GLOSSARY

a	Acceleration of slide
A	End area of displaced water or submerged end area of slide
c	Wave celerity
d	Average depth of water
dx	Incremental distance in x-direction
dy	Incremental distance in y-direction
F_s	Spring force
F_b	Buoyant force along slope
F_w	Slide gravity force along slope
F_x	Friction force in x-direction
F_y	Friction force in y-direction
$\mathcal{F}$	Slide Froude number
g	Acceleration of gravity
i	Slide angle
k	Spring constant
ℓ	Distance from a slide in the y-direction
L	Landslide length
M	Momentum
m	Mass
Q	Discharge
s	Travel distance of slide
t	Time
u	Depth averaged velocity in direction of slide (x-direction)
v	Depth averaged velocity perpendicular to slide (y-direction)
v_s	Slide velocity
v_o	Initial slide velocity
V	Volume of water displaced
W_s	Gravity force of the slide
W	Top width of reservoir
x'	Spring stretch
x	Horizontal axis (in direction of slide)
y	Horizontal axis (perpendicular to slide direction)
η	Wave height above the undisturbed water surface
ρ	Density of water
γ_w	Specific force of water
ξ	Depth of water at slide
$\tan \phi_s$	Coefficient of dynamic sliding friction

PURPOSE

The purpose of this model study was to accurately determine the characteristics of waves generated by landslides into Morrow Point Reservoir, a feature of the Colorado River Storage Project. The data will also be used to calibrate a general numerical model being developed under contract to simulate landslides and the resulting waves for a variety of situations.

INTRODUCTION

Many serious problems are associated with rockfalls or landslides into reservoirs or other bodies of water. Areas of concern include: (1) loss of life; (2) failure of dams; (3) overtopping of dams by waves which could result in damage to the dam, intake structures, spillways, powerhouses, and downstream flooding; (4) upstream flooding due to river blockages; (5) damage to shoreline structures and boats; and (6) loss of reservoir capacity due to the final position of slide material [1][1].

A number of major landslide areas are located upstream from Morrow Point Dam. These landslides have moved very slowly and are not presently considered a hazard. However, under certain conditions (such as earthquake or heavy rainfall when pressures along the slip surface are increased), it is possible that a slide could break free and plunge into the reservoir at velocities greater than 30 m/s (100 ft/s). It is not the intention of the author to imply that high speed landslides will occur at Morrow Point. The study was conducted to determine the magnitude of waves in the event such a landslide occurs.

A literature review was conducted by the Bureau of Reclamation to determine the extent of the landslide hazard at Morrow Point Dam [2]. This study used several empirical methods to evaluate the potential for landslide-generated waves at Morrow Point Dam [2]. The different methods gave an order of magnitude difference in predicted wave heights. A 6- to 15-m (20- to 50-ft) high wave was predicted for slide "A", located 760 m (2500 ft) upstream from the dam (fig. 1). It was concluded that a well documented, easy to use method to perform landslide-generated wave calculations was needed, especially where the slide is located some distance from the dam or around bends in the reservoir.

Because of the literature review, this particular model study was conducted. The USBR (Bureau of Reclamation) has also entered into a contract with a consulting firm to develop a computer code (numerical model) to predict the generation of waves due to landslides and the propagation of the waves through a reservoir and over the top of a dam. The numerical model includes landslide simulation, refraction, and shoaling. Therefore, it should be applicable to a variety of possible landslides at different reservoirs and other bodies of water. The results obtained from this model study are also being used for calibration and partial verification of the numerical model.

Morrow Point Dam is a double-curvature, thin-arch concrete dam constructed by the USBR and located on the Gunnison River 40 km (25 mi) east of Montrose, Colorado, and is part of the Colorado River Storage Project. It is 143 m (468 ft) high and 4 m (12 ft) thick at the crest. Blue Mesa Dam is located upstream and Crystal Dam downstream from Morrow Point Dam. The frontispiece depicts Morrow Point Dam and Reservoir with the spillways operating.

CONCLUSIONS

The physical model study of landslide-generated water waves in Morrow Point Reservoir resulted in the following conclusions:

- The direction of the landslide as well as the volume of water displaced and slide velocity are important to the wave height in the vicinity of the landslide. Waves directly in line with the slide direction were two to three times higher than waves not in line with the slide.

- Waves distant from the slide were solitary waves. Waves in the river downstream from the dam were bore waves. The maximum wave height at the dam due to slide "A" was 20 m (65 ft). The maximum wave height in the river downstream was 7 m (23 ft). Landslides at locations "B" and "C" could result in waves at the dam as high as 8.5 m (28 ft) and 6.9 m (22.5 ft), respectively.

[1]Numbers in brackets refer to entries in the Bibliography.

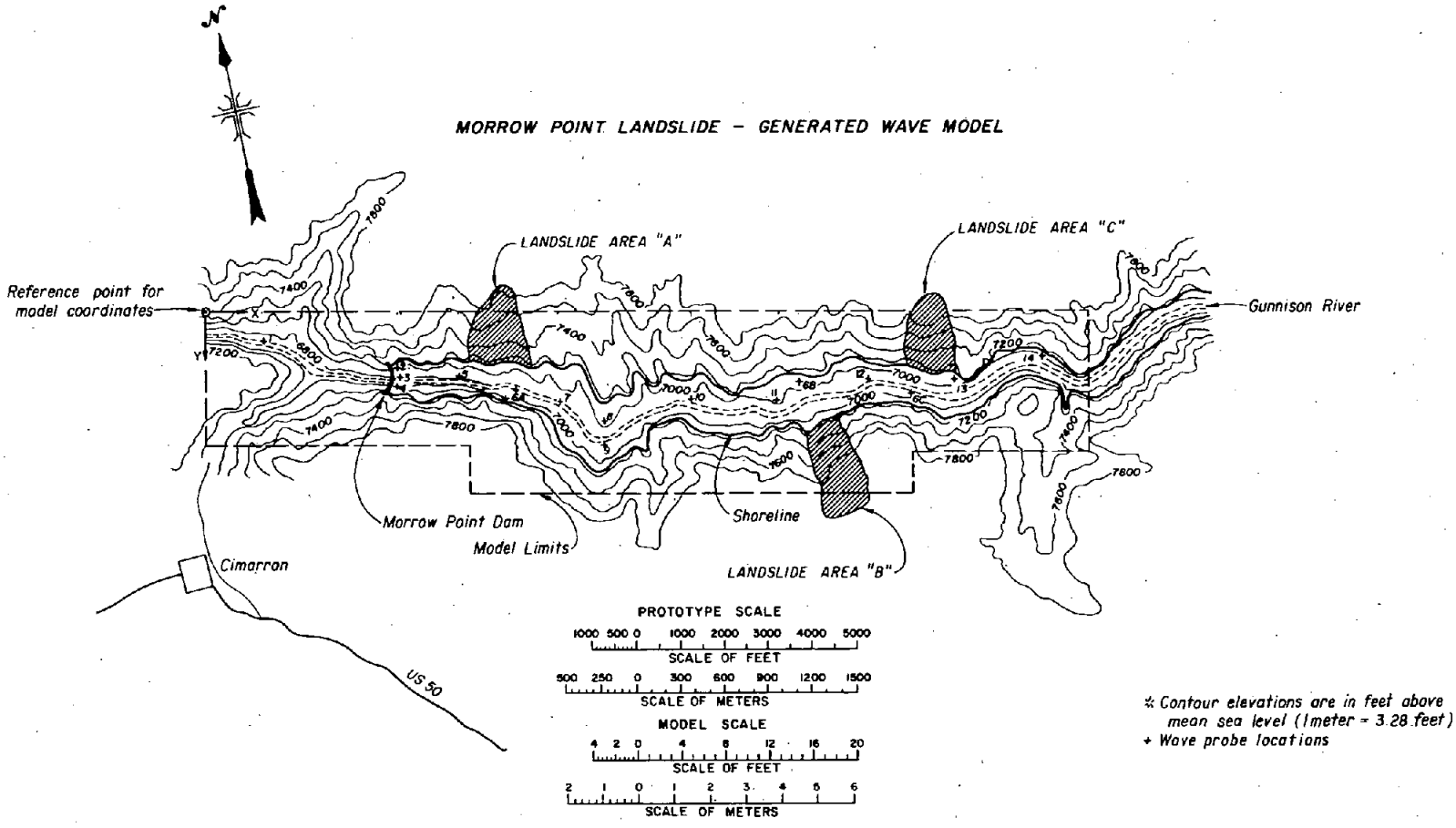

Figure 1.—Plan of reservoir area showing location of landslides and wave probes.

- Nondimensional relationships were developed to predict wave heights for Morrow Point Reservoir and other cases as a function of slide velocity, water depth at the slide, volume of water displaced, and distance from the slide.

- The celerity (c) of solitary waves is accurately predicted by the following equation [3]:

$$c = \sqrt{g(d+\eta)}$$

- Wave recording for various slide volumes and velocities at landslides "A," "B," and "C" are presented in appendix B.

THE MODEL

Description

The model included 4.8 km (3 mi) of reservoir and 1.3 km (0.8 mi) of the canyon downstream from the dam. Three landslide areas designated "A," "B," and "C" were studied. Figure 1 is a plan of the reservoir area showing the location of the landslides and the model limits.

The model was constructed to an undistorted scale of 1:250. The model topography was formed by projecting contour maps onto plywood with a vertical reflecting projector. The contours were then traced onto the plywood. Cuts were made along the contour lines and the pieces were placed in the model in "steps" according to the contour elevations. The location of the topography was controlled by using a grid system. The topography was finished by stretching expanded metal lath over the contours and applying a 19-mm (¾-in) layer of concrete to the lath. The final contours were accurate to within ± 1.5 m (± 5 ft) of the prototype scale (assuming the reference maps were accurate). The elevation of the dam was accurate to within ± 0.3 m (± 1 ft). The contours generally extended to elevation 2256 m (7400 ft),[2] however, in the areas directly across from the landslides, contours extended to elevation 2377 m (7800 ft). Figures 2a and b show photographs of the model during construction and after completion.

[2]Elevations are referenced to mean sea level.

Landslide Simulation

As a landslide enters the water, a wave is generated by a combination of factors which include: (1) displacement of the water and (2) pressure and viscous drag forces between the slide and the water. If the landslide velocity is greater than the wave celerity (wave velocity) of the displaced water, the motion of the slide and the shape must be correctly simulated. However, if the slide velocity is less than the wave celerity, the primary wave motion will be created by the displacement of water with pressure and viscous drag forces having little effect on wave generation. That is, the relative velocity of the slide with respect to the wave celerity will be negative. The wave being generated by the displacement of water will move away from the slide faster than the slide enters the water; therefore, the viscous and pressure drag forces will be negligible.

In previous physical models of landslides, bags of rocks or sand were pushed, dropped, or slid into the water. In most cases, the precise dynamics of the slide material entering the water were questionable. In addition, the geometry, slide friction, and mode of the prototype landslide were only approximated in those models. Therefore, considerable doubt can be cast on the validity of the landslide simulations.

Since the wave celerity is important to landslide simulation, an estimate for wave celerity is needed. An approximation for wave celerity (c) is given by Chow [3]:

$$c = \sqrt{g(d+\eta)} \qquad (1)$$

where: g = acceleration of gravity
η = wave height above the undisturbed water surface
d = average depth of water

Using empirical methods [2], a wave of height of 15 m (50 ft) was calculated at slide "A" for a slide velocity of approximatly 30 m/s (100 ft/s) in a water depth of 110 m (360 ft). From equation (1), a celerity of 35 m/s (115 ft/s) is computed. Since the slide velocity is less than the wave celerity, the major factor creating the wave is the displacement of water. The viscous

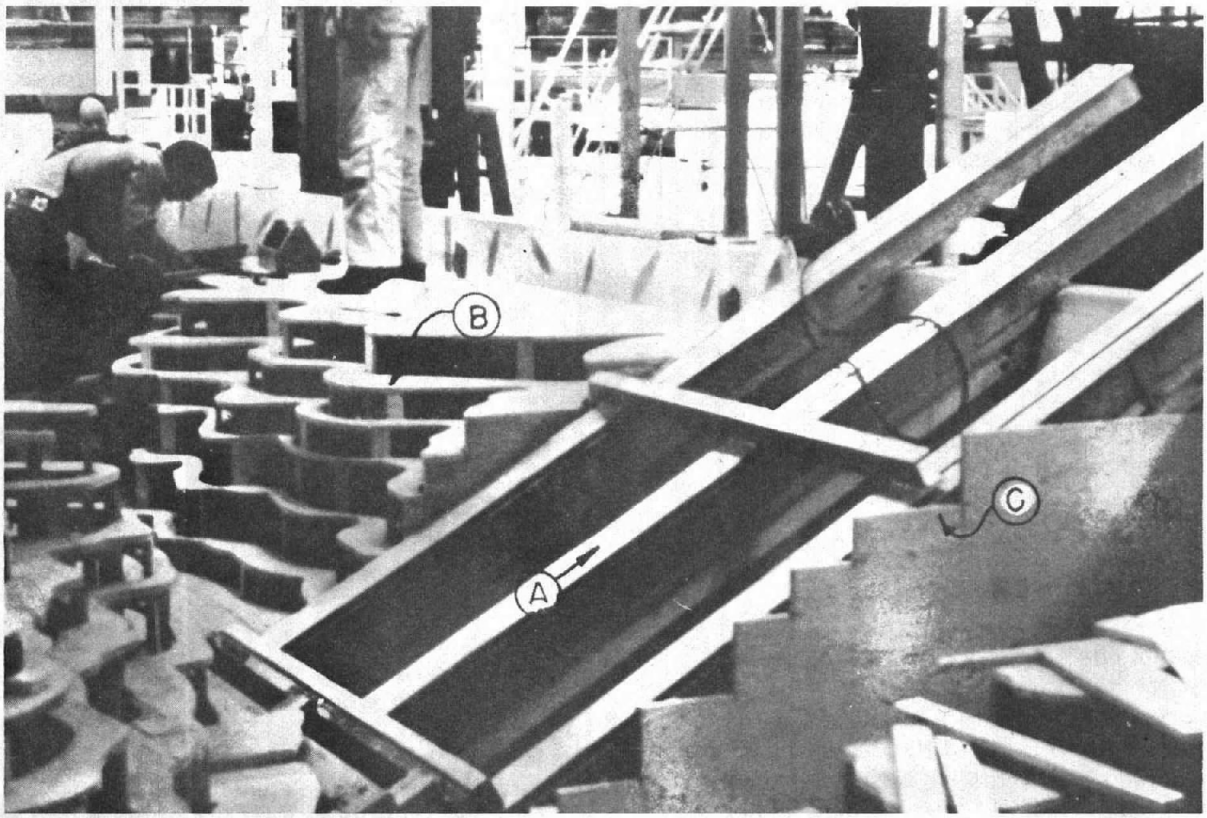

Figure 2a.—Model under construction - Ⓐ landslide sled and framework, Ⓑ contour steps, Ⓒ contour support framework. P801-D-79708

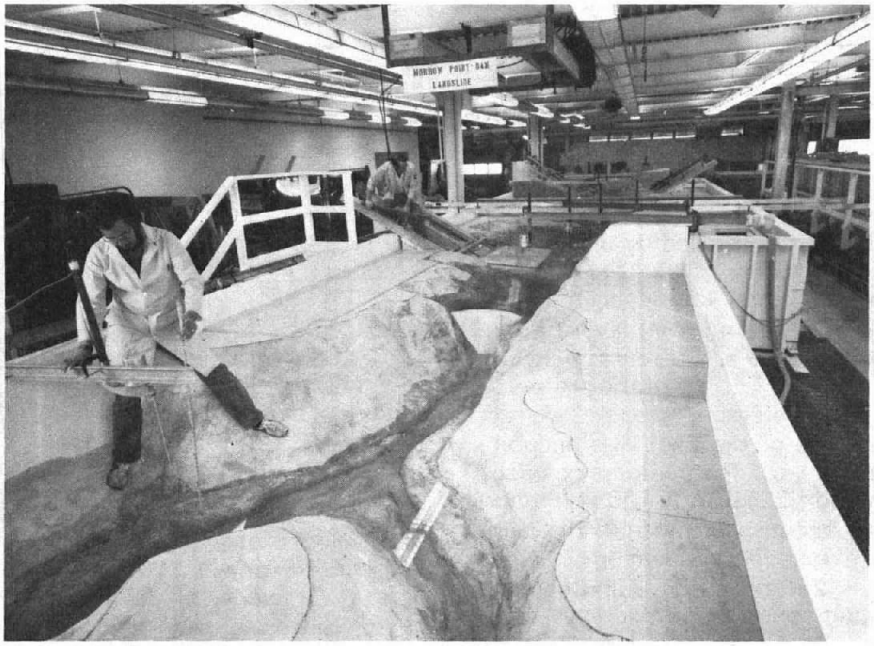

Figure 2b.—Completed model. P801-D-79709

and pressure drag forces are minor; which means that simulation of underwater slide dynamics should not be necessary and a rather simple model of the slide can be used to produce the waves.

The approach taken in this study was to use a wedge-shaped slide and measure the position, velocity, and time accurately during the slide. Since the geometry of the slide is known, the rate of change of displaced water and its velocity can be calculated for any position as the slide progresses. Their product multiplied by the water density gives the momentum flux of the water at each instant of time. The force of the water which produces the landslide-generated waves is a function of the rate of change of momentum. Therefore, the momentum versus time relationship was used as a basis for comparison between the model and potential prototype landslides. Figure 3 is a schematic diagram of the model landslide. The momentum calculation was made according to the following equation:

$$M(t) = A(t)L\rho v_s(t) \qquad (2)$$

where: M = momentum of displaced water
A = end area of displaced water
L = landslide length
ρ = density of water
v_s = slide velocity
(t) = a function of time

The model landslide was scaled to match the length of the prototype landslide and enters the water at the same angle. The volume of the model landslide was designed to match the prototype volume when it reaches the bottom of the valley. The angle of the front face of the model landslide determines the volume.

Estimate of potential prototype landslide momentum.—In addition to the rate of displacement of water by the slide and total volume of displacement by the slide, the momentum versus time relationship for the prototype slides and model slides was matched. To compute a velocity for the prototype slides, equation (3) (according to Slingerland and Voight [4]) was used incrementally for the total displaced position. Once the toe of the slide had reached the bottom of the reservoir, an overrun of material from the uphill portion of the slide was estimated. This produced a momentum versus time graph which was S-shaped.

$$v_s = v_o + \sqrt{2\,gs\,[\sin(i) - \tan\phi_s \cos(i)]} \qquad (3)$$

where: v_s = slide velocity
v_o = initial slide velocity
g = acceleration of gravity
s = travel distance of slide
i = slide angle
$\tan\phi_s$ = coefficient of dynamic sliding friction including pore pressure and roughness effects. (May be taken as 0.25 ± 0.12.)

Designing the model landslide.—A computer program was written to determine whether potential (computed) prototype slide dynamics could be matched in the model. Figure 4 is a schematic diagram of the forces used in the computer program to represent the model landslide.

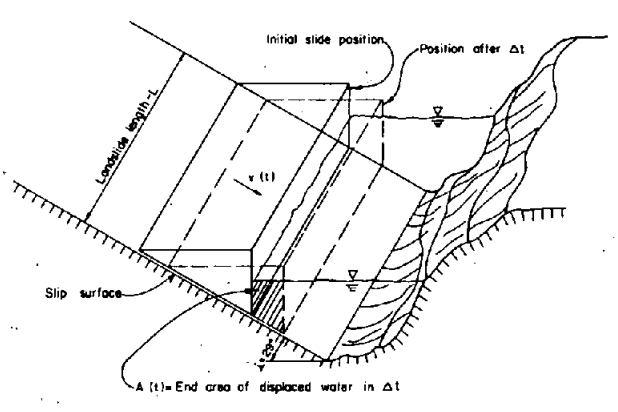

Figure 3.—Schematic diagram of model landslide.

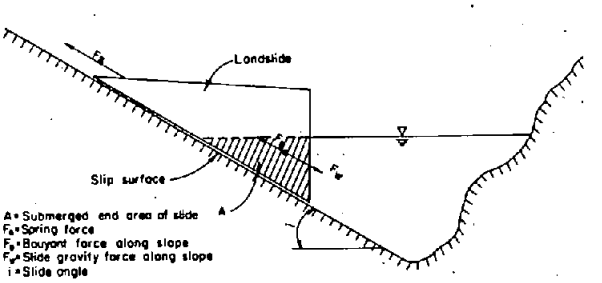

Figure 4.—Schematic diagram of forces used to represent the model landslide.

$$F_s = kx' \quad (4)$$

$$F_b = \gamma_w A L \sin i \quad (5)$$

$$F_w = W_s \sin i \quad (6)$$

where: k = spring constant
x' = spring stretch
γ_w = specific force of water
A = submerged end area of slide
L = landslide length
i = slide angle
W_s = gravity force of the slide
F_s = spring force
F_b = buoyant force along slope
F_w = slide gravity force along slope

Newton's second law of motion (eq 7) and the equations of motion (8, 9) were used to compute the location and velocity of the model landslide for each time step. The momentum of displaced water for each time step was then computed using equation (2).

$$F = ma \text{ or } a = \frac{F}{m} \quad (7)$$

$$v_s = v_o + at \quad (8)$$

$$s = v_o t + \tfrac{1}{2} at^2 \quad (9)$$

where: F = force
m = mass of slide
(The remaining variables were previously defined.)

The friction drag force between the model landslide and the water was minor because the wave celerity and the slide velocity were approximately equal. Therefore, the dynamic pressure forces on the face of the slide and friction drag were not considered in the analysis. The slide friction was also minor in the model landslide because it was mounted on rollers.

When the computer program was run without a spring force, it was apparent that the time the slide took to reach the bottom of the reservoir was too short and the momentum was too high. Therefore, an extension spring was added to slow the slide. This simulates the dynamics of the thinner and longer prototype slide (fig. 5) striking the bottom of the reservoir, breaking up, overriding, and slowing the rate of increase in the momentum, resulting in an S-shaped momentum versus time curve.

The initial position, slide gravity force, spring constant, and position where the spring engages were varied for the model slide in the computer program until the momentum versus time relationship matched the computed prototype landslide dynamics. In addition to momentum and time, the volume also matched in the model and prototype. Figure 6 compares results obtained from the computer program for different conditions with the computed prototype momentum for slide "A".

When the model landslide was constructed, the computed dynamics were very close to the measured dynamics requiring only slight adjustments to match the computed prototype momentum curve.

Dimensional Analysis

The differential equations describing shallow-water, long-wave motion can be derived from continuity and the Navier-Stokes equations [4].

$$\frac{\partial \eta}{\partial t} + \frac{\partial}{\partial x} u(\eta + d) + \frac{\partial}{\partial y} v(\eta + d) = \frac{\partial \xi}{\partial t} \quad (10)$$

$$\frac{\partial u}{\partial t} + u\frac{\partial u}{\partial x} + v\frac{\partial u}{\partial y} + g\frac{\partial \eta}{\partial x} + F_x = 0 \quad (11)$$

$$\frac{\partial v}{\partial t} + u\frac{\partial v}{\partial x} + v\frac{\partial v}{\partial y} + g\frac{\partial \eta}{\partial y} + F_y = 0 \quad (12)$$

where: t = time
x = horizontal axis (in the direction of the slide)
y = horizontal axis (perpendicular to slide direction)
u, v = depth-averaged velocities in the x and y directions, respectively
F_x, F_y = components of bottom friction force
ξ = depth of water at slide

These depth-averaged equations describe the mean velocities in a prism whose height equals water depth and whose width and depth are equal to the incremental distances dx and dy, respectively.

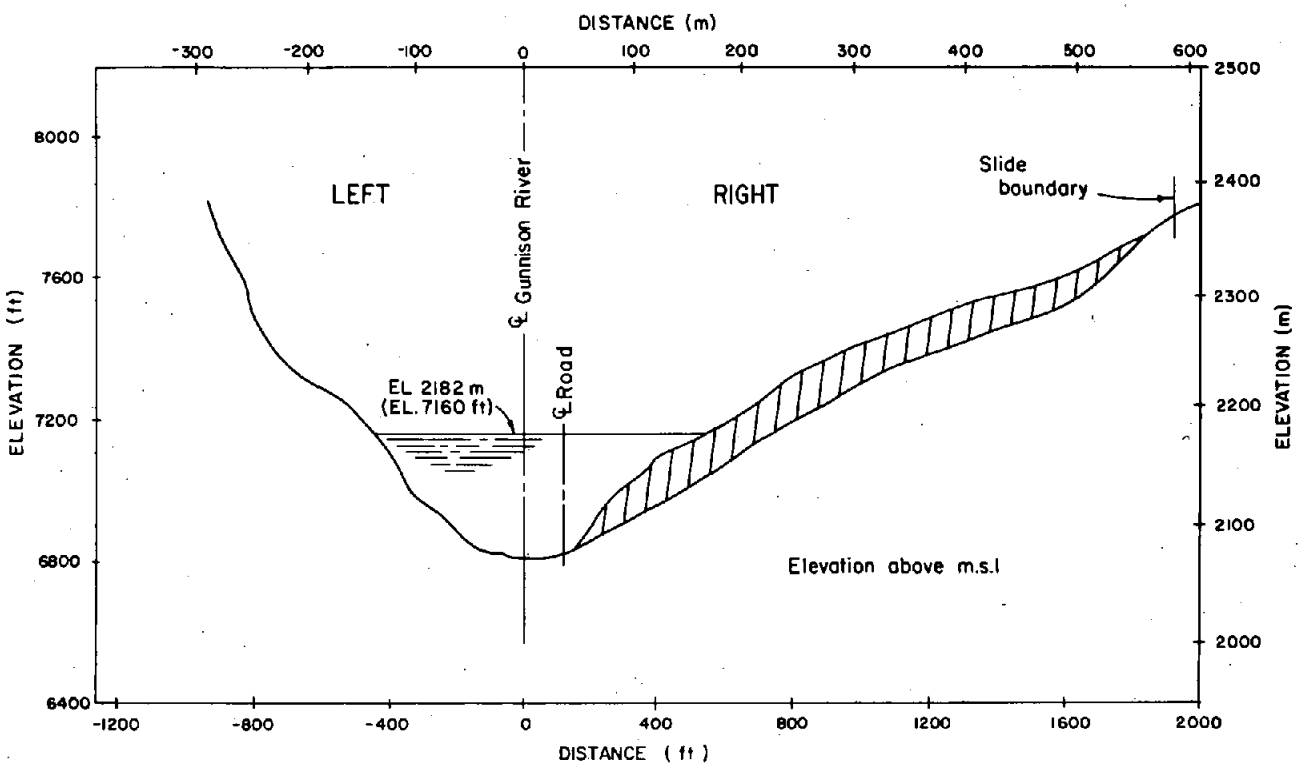

Figure 5.—Cross section through prototype landslide "A" looking downstream.

The following boundary conditions were used to make the differential equations dimensionless, according to a procedure described in "Hydraulic Laboratory Techniques" [5]:

$$t = \frac{\bar{t}\ell}{\sqrt{gd}};\ u = \bar{u}v_s;\ v = \bar{v}\sqrt{gd}$$

$$\eta = \bar{\eta}d;\ \xi = \bar{\xi}d;\ x = \bar{x}d;\ y = \bar{y}\ell$$

where: $(\bar{t}, \bar{u}, \bar{v}, \bar{\eta}, \bar{\xi}, \bar{x}, \bar{y})$ are dimensionless ratios

ℓ = distance from the slide in the y-direction

v_s = velocity of the slide

After substituting the boundary conditions in equations (10, 11, and 12) and normalizing, the dimensionless differential equations (neglecting friction) are:

$$\frac{\partial\bar{\eta}}{\partial\bar{t}} + \left(\frac{\ell}{d}\right)\left(\frac{v_s}{\sqrt{gd}}\right)(\bar{\eta}+1)\frac{\partial\bar{u}}{\partial\bar{x}} + (\bar{\eta}+1)\frac{\partial\bar{v}}{\partial\bar{y}} = \frac{\partial\bar{\xi}}{\partial\bar{t}} \quad (13)$$

$$\frac{\partial\bar{u}}{\partial\bar{t}} + \left(\frac{\ell}{d}\right)\left(\frac{v_s}{\sqrt{gd}}\right)\bar{u}\frac{\partial\bar{u}}{\partial\bar{x}} + \bar{v}\frac{\partial\bar{u}}{\partial\bar{y}} + \left(\frac{\ell}{d}\right)\left(\frac{\sqrt{gd}}{v_s}\right)\frac{\partial\bar{\eta}}{\partial\bar{x}} = 0 \quad (14)$$

$$\frac{\partial\bar{v}}{\partial\bar{t}} + \left(\frac{v_s}{\sqrt{gd}}\right)\left(\frac{\ell}{d}\right)\bar{u}\frac{\partial\bar{v}}{\partial\bar{x}} + \bar{v}\frac{\partial\bar{v}}{\partial\bar{y}} + \frac{\partial\bar{\eta}}{\partial\bar{y}} = 0 \quad (15)$$

From these equations, the main parameters affecting the wave height and wave propagation are a velocity parameter, $v_s/\sqrt{gd}$, a distance parameter, ℓ/d, and the time rate of change of displacement, $\partial\bar{\xi}/\partial\bar{t}$.

Scale Relations

As shown in the preceding section, inertia and gravity are the predominant forces; therefore,

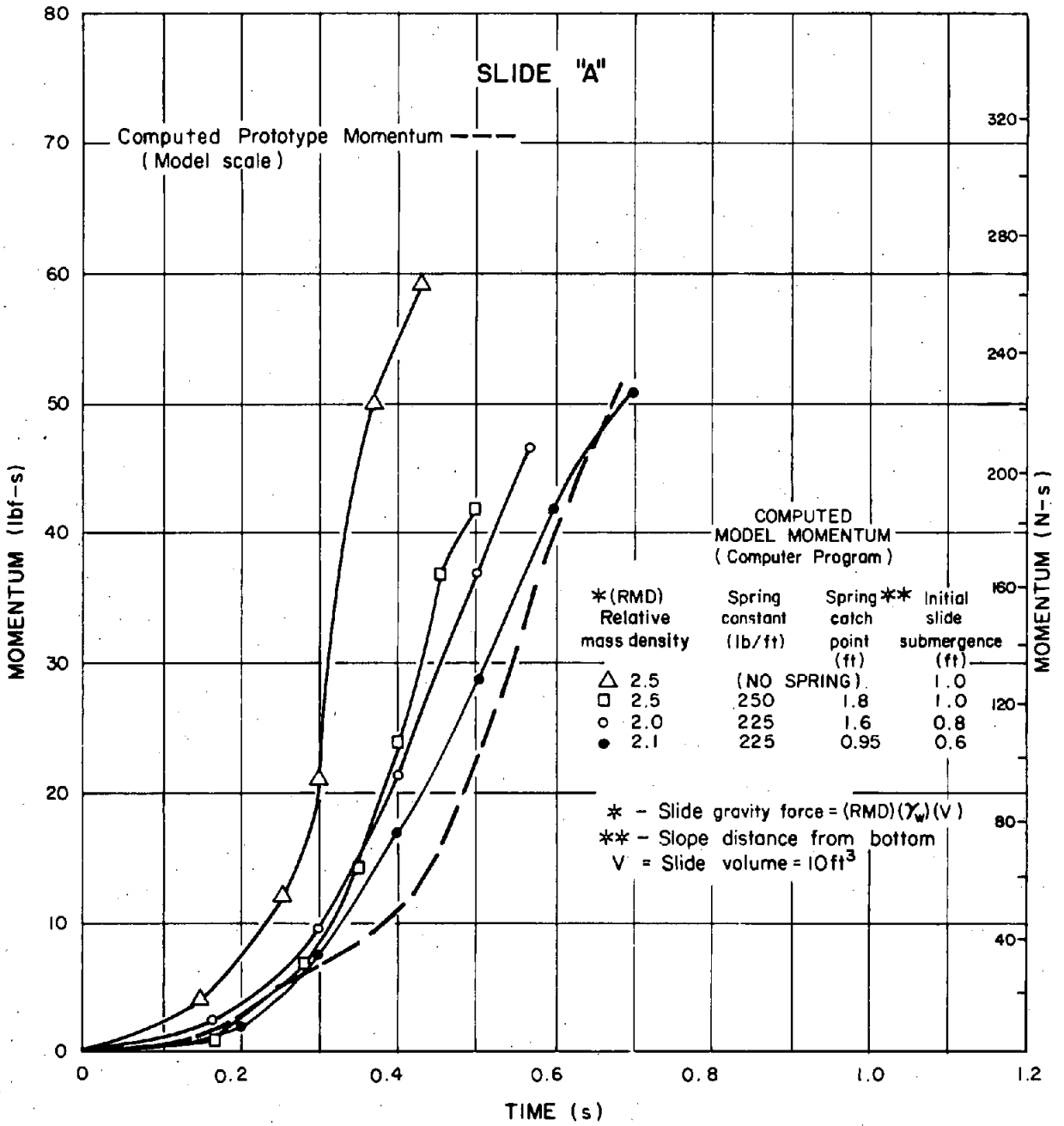

Figure 6.—Computed model momentum versus prototype momentum.

the Froude number ($v/\sqrt{gd}$) was used to scale from model to prototype. The scale relations for this study (based on the Froude law) are listed below:

Quantity ratio	Model:Prototype
Length*	$L_r = 1:250$
Area	$A_r = L_r^2 = 1:6.25 \times 10^4$
Volume	$V_r = L_r^3 = 1:1.56 \times 10^7$
Time	$t_r = L_r^{1/2} = 1:15.81$
Velocity	$v_r = L_r/t_r = 1:15.81$
Force	$F_r = L_r^3 = 1:1.56 \times 10^7$
Momentum	$M_r = F_r t_r = L_r^{7/2} = 1:2.47 \times 10^8$
Discharge	$Q_r = L_r^{5/2} = 1:9.88 \times 10^5$

*(geometric scale)

Data Collection

Waterlevel measurements were taken at 14 locations throughout the reservoir and in the river downstream from the dam (see figs. 1 and A-1* for measurement locations). Position and velocity of the model landslide were also measured.

The water surface measurements were made using commercially available capacitance probes. The capacitance probes were 3-mm (⅛-in) diameter stainless steel rods with a Teflon sheath. The rods cause very little disturbance or wake, yet were stiff enough to maintain their positions. Depending on their location, the probes were either 250 or 450 mm (10 or 18 in) in length. Figure 7 shows capacitance probes during a test at landslide "A." Each capacitance probe was self contained (i.e., the electronics and power supply were contained in the enclosure attached to the top of the probe). The power input required is 120 V a.c. Both a 4- to 20-mA current output and a 0- to 10-V d-c output are available. The maximum response time between readings is 50 milliseconds, and the probes are accurate to ±1 mm.

The position and velocity of the slide were measured with a PVT (position-velocity transducer), (fig. 8). This device has a cable with constant retracting tension. The cable is attached to the landslide and extends and retracts as the landslide moves. The PVT is excited by a 15-V d-c power supply. The output is 0 to 10 volts. The velocity measurements were made using a self-excited tachometer in the transducer. Positions can be determined within ±1 mm and velocities to ±6 mm/s.

All electronic measurements were taken and recorded with the aid of a microprocessor and data acquisition system. The system has an internal clock capable of reading elapsed time in milliseconds. Using all 16 channels and the clock, the system was capable of taking about 12 readings per second. Voltage readings were made with an internal voltmeter in the data acquisition system. The microprocessor scanned the velocity channel at a high rate to initiate tests. When the slide was released, a changed reading on the velocity channel signaled the start of the test, tripped the clock, and readings were begun on all 16 channels. The calculator memory was capable of storing data for about 20 seconds; the data were then stored on magnetic disk and this cycle of data recording and storage continued until the test was terminated. A 4-second gap in the data occurred while the data were being stored on disk; however, the data of primary interest and importance were obtained in the first 20 seconds.

The PVT and water level transducers were calibrated before testing. All the instruments demonstrated excellent linearity between output voltage and reading. The calibrations were checked throughout the testing program to ensure that the calibration coefficients did not drift. It was found that a salt buildup on the Teflon sheath caused the calibration coefficients to drift if the probes were left in the water. The probes were therefore cleaned every day prior to testing which stabilized the calibration. Checks of the calibration coefficients indicated very little change when the probes were cleaned.

*Figure A-1 is located in appendix A.

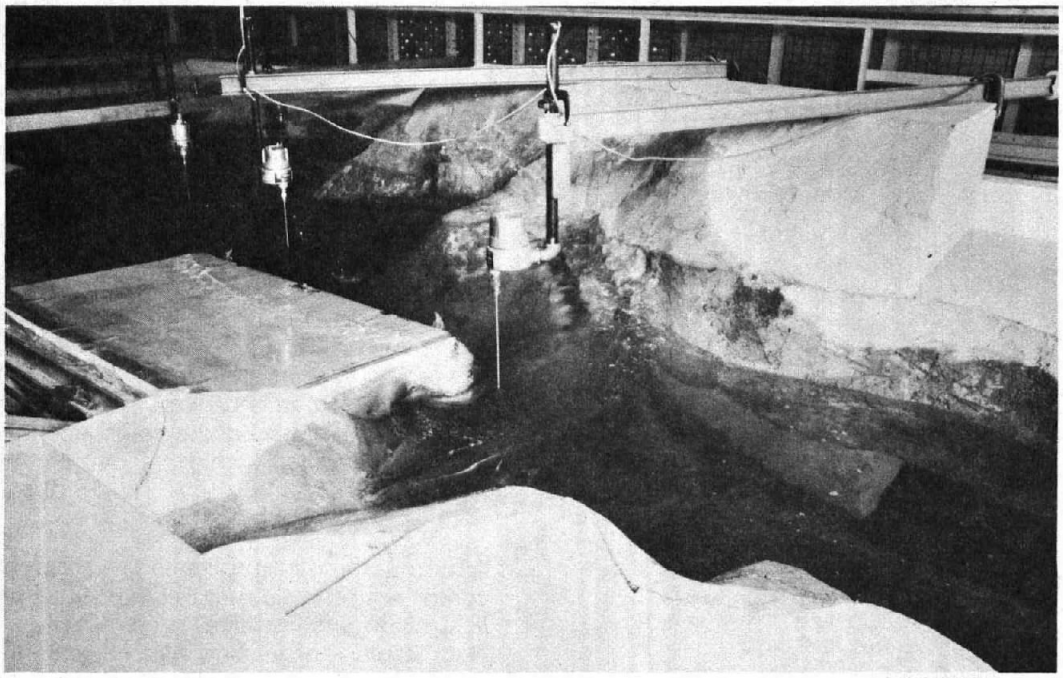

a. View across reservoir (landslide "A" fully submerged). P801-D-79710

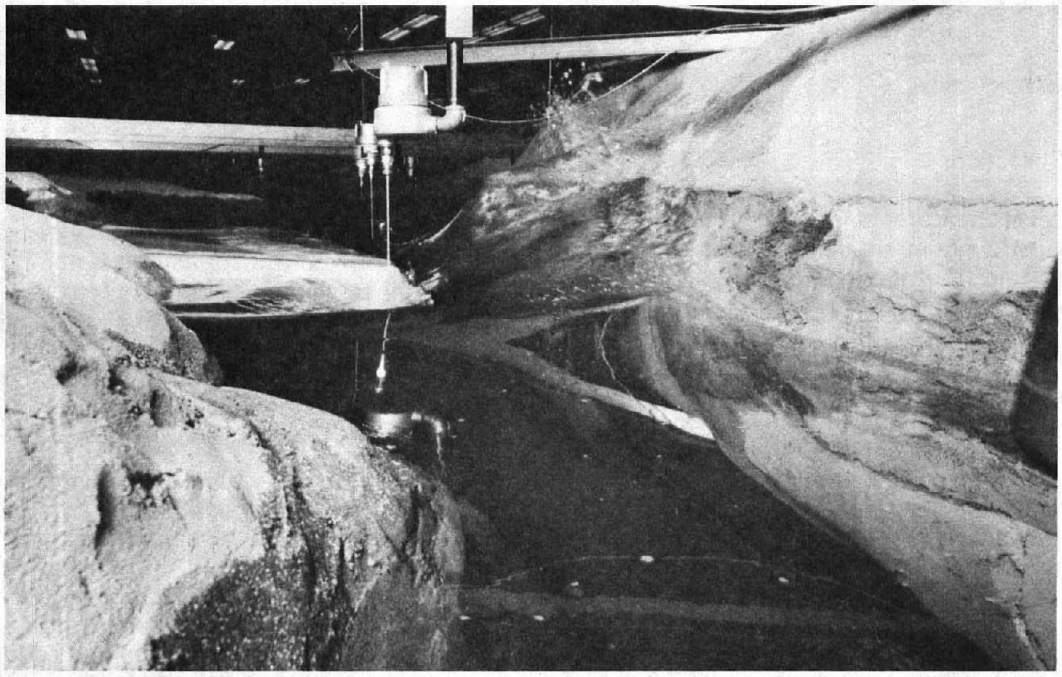

b. View of wave approaching dam. P801-D-79711

Figure 7.—Capacitance probes during test at landslide "A." Note wave crest climbing topography and approaching dam (to the right).

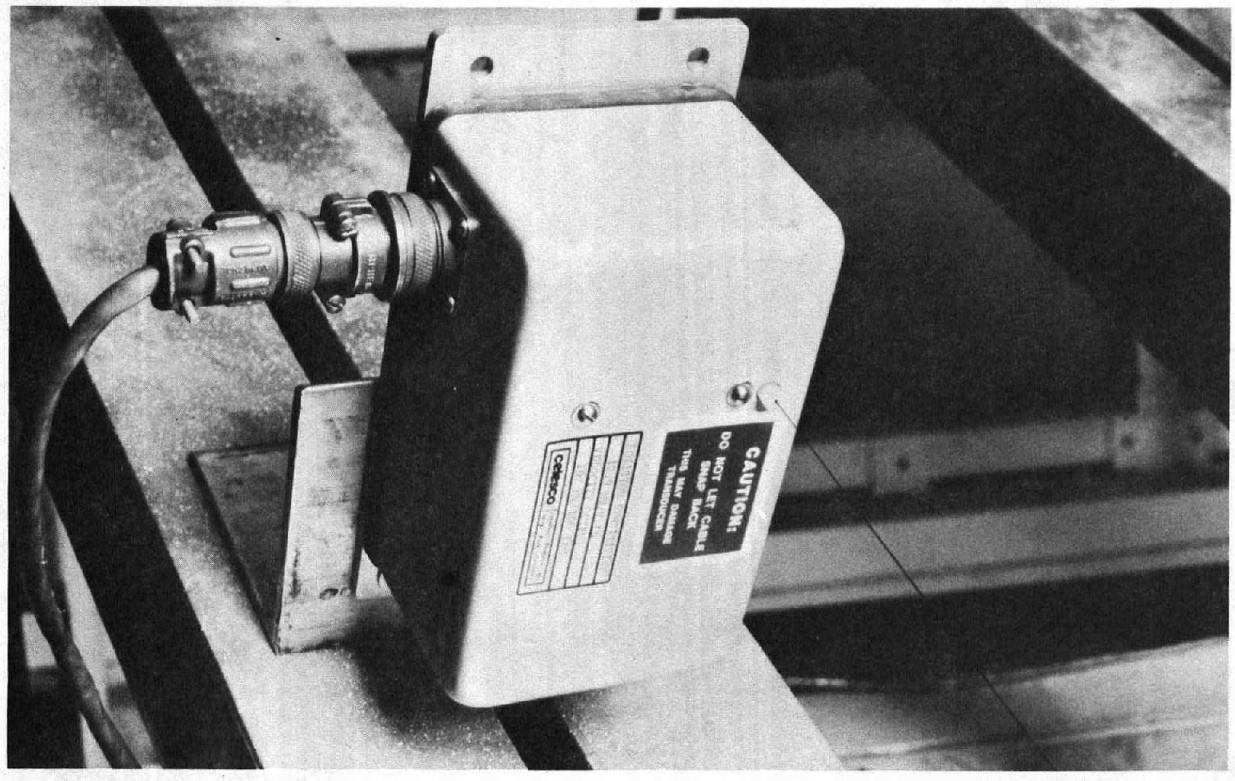

Figure 8.—Position-velocity transducer (PVT). P801-D-79712

Test Results

The primary data consisted of waterlevel recordings, and position, and velocity measurements of the landslides. The position and velocity readings were converted to slide momentum by considering the slide geometry (as discussed previously). A range of tests was run at each landslide location. Figure 9 shows a test at landslide "A." The full-scale wave overtopping the dam would be about 20 m (66 ft) high.

Appendix A and B contain the results of the tests. Tests with "A" in the name indicate a landslide at location "A," similarly with "B" and "C." The locations of the probes are given on Figure A-1* for reference. Probe No. 6 was located in front of the slide being tested and was designated 6A, 6B, or 6C, depending on the slide location.

The momentum versus time graph for each test is plotted in addition to a projection of potential prototype momentum for slides "A," "B," or "C." These momentum plots are given on figures A-2 through A-32. The momentum plots are given in model scale for simplicity. A range of momentums and volumes was covered by the tests; each test was not intended to match the potential prototype momentum.

Figures B-1** through B-32 show the wave traces at each probe for the tests. From these plots, maximum wave heights can be determined and the form of the wave and the propagation through the reservoir and over the dam can be observed. The wave plots are all referenced to the reservoir level before the test. Freeboard at the dam was generally about 2 m (7 ft) during the model tests.

Wave Forms

Gravity waves are created as a result of any momentary change in the local depth of the water [3]. The wave is then propagated by a

*Indicates figures located in appendix A.

**Indicates figures located in appendix B.

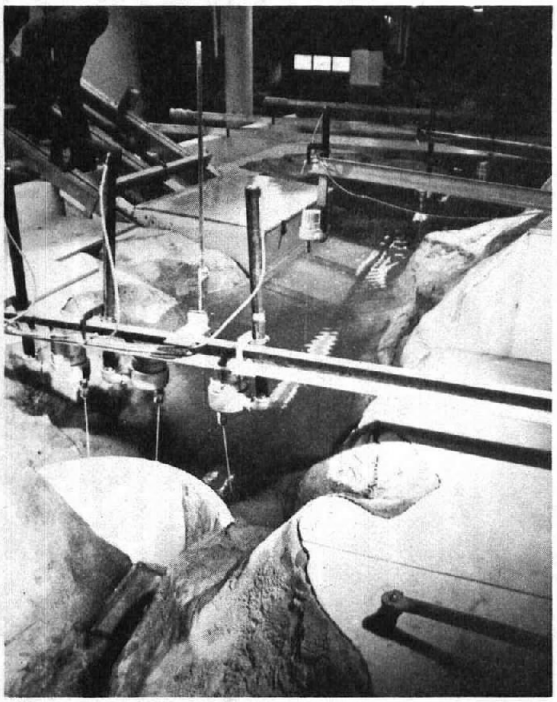

a. Immediately after slide was released (time ≅ 0.1 s). P801-D-79713

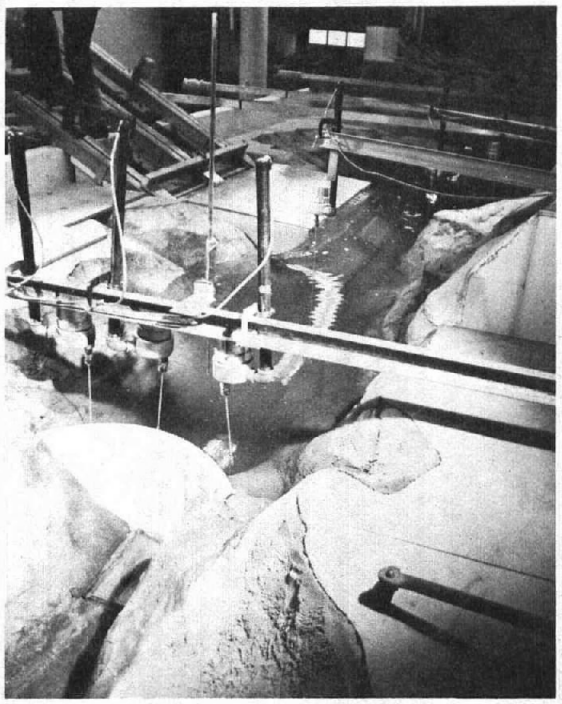

b. Slide partially into water (time ≅ 0.4 s). P801-D-79714

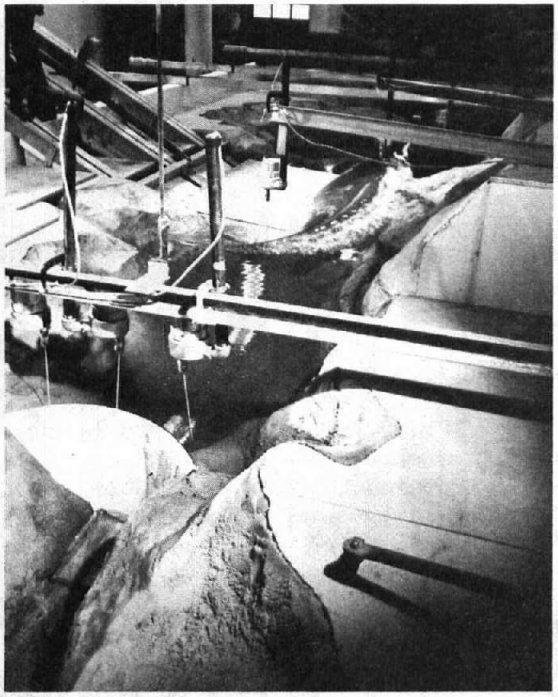

c. Slide completely into water (time ≅ 0.7 s). P801-D-79715

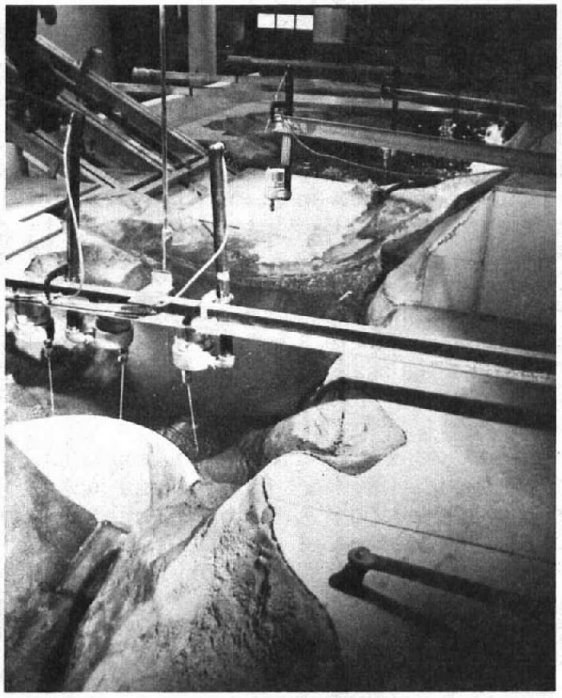

d. Water across from slide at maximum height uphill (time ≅1.0 s). P801-D-79716

Figure 9.—Sequence photographs - landslide "A" (model times shown).

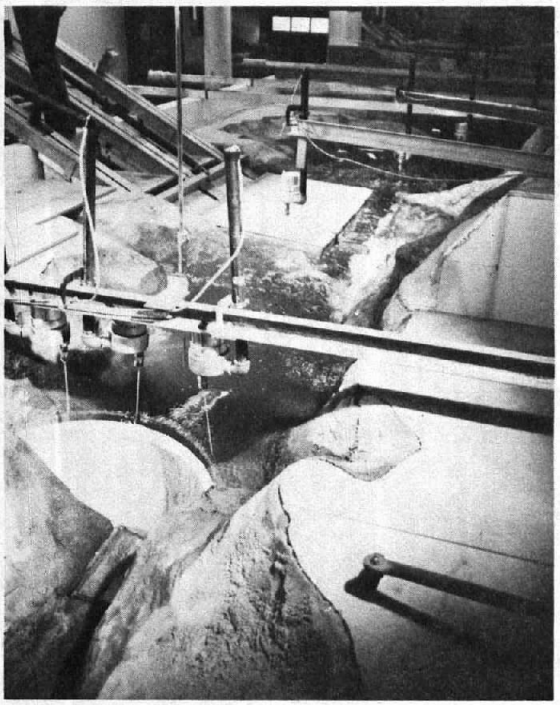

e. Wave starting to overtop dam (time ≅ 1.3 s). P801-D-79717

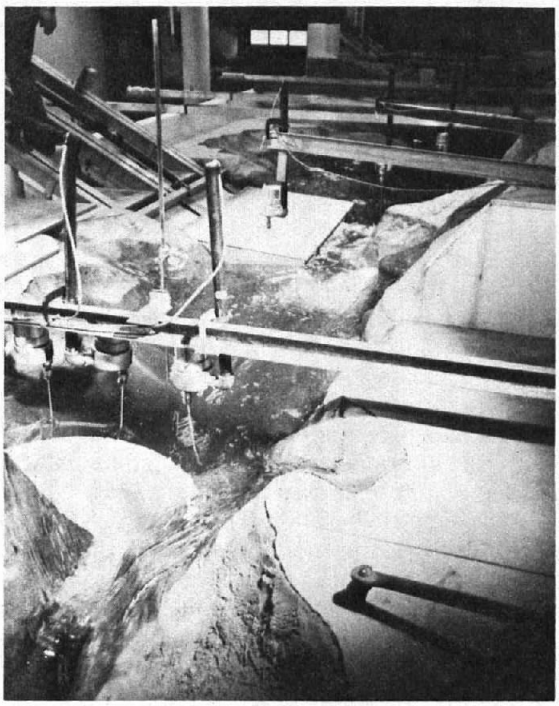

f. Dam overtopping wave at peak (time ≅ 1.9 s). P801-D-79718

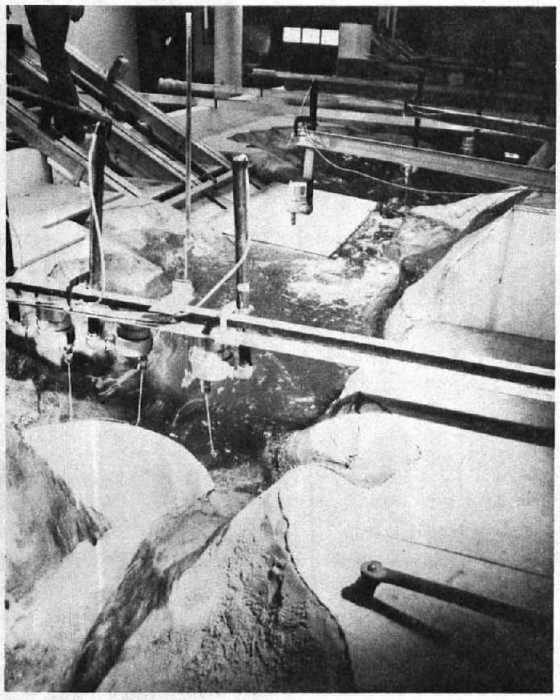

g. Dam overtopping wave receding (time ≅ 2.5 s). P801-D-79719

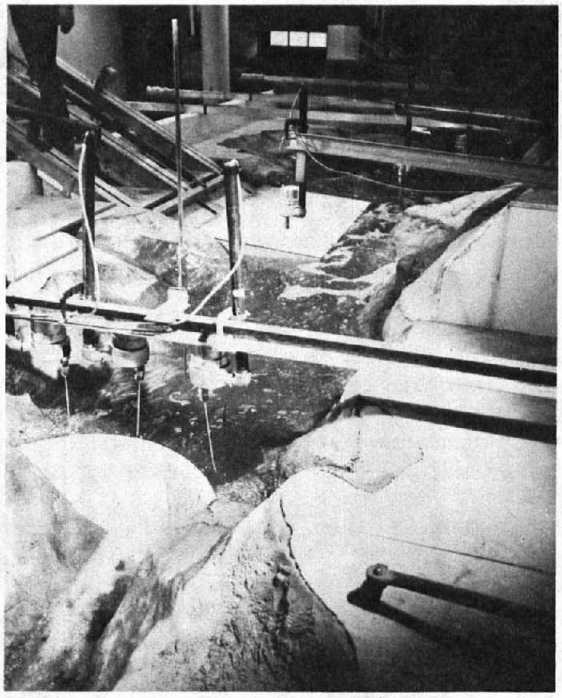

h. Secondary waves at dam (time ≅ 3.4 s). P801-D-79720

Figure 9.—Sequence photographs - landslide "A" (model times shown)—Continued.

gravity force. There are several types of gravity waves; however, the primary ones of interest in this study can be classified as oscillatory or translatory. In oscillatory waves, the particles of water do not actually travel with the wave but tend to oscillate about a mean position in an orbital path as the wave passes (fig. 10a).

In translatory waves, the wave particles associated with the wave are transported with the wave at essentially the wave velocity. Three types of translatory waves of interest to this study are: solitary waves, hydraulic bore waves (surges), and seiches. A solitary wave is a single disturbance, propagated essentially unaltered in form over long distances at a constant velocity [6]. Figure 10b shows a solitary wave with water particle trajectories. The solitary wave lies entirely above the normal water surface and moves smoothly and quietly without surface turbulance. Hydraulic bore waves have a sharp and steep advancing front with the appearance of a moving hydraulic jump [3]. A bore wave indicates a change in stage from subcritical to supercritical. Figure 10c shows a bore wave.

Seiches are changes in surface elevation over a long period in enclosed basins. Seiches are usually not even noticeable to an observer. The water surface rises and falls gradually as the water flows from one end of the basin to the other until surface elevation equalizes. Seiches resulting from landslides in the Morrow Point model were not studied because the entire reservoir was not modeled and a wave absorber at the upstream end of the model damped reflected waves.

Solitary waves are nondispersive so their amplitudes do not decrease rapidly as they travel away from the source. For these, bends should have little effect on the amplitude. On the other hand, oscillatory waves are dispersive and bends would influence their amplitudes.

The model data indicate that waves in the vicinity of the landslide were oscillatory. The peaks were sharp and high and they dissipated quickly. As the wave traveled away from the slide around bends in the reservoir, a solitary wave developed. The amplitude of the solitary wave was lower than the waves at the slide; however, the period was longer and the wave traveled long distances through the reservoir. The form of the waves can be observed on the wave plots provided in appendix B. Note that, in the vicinity

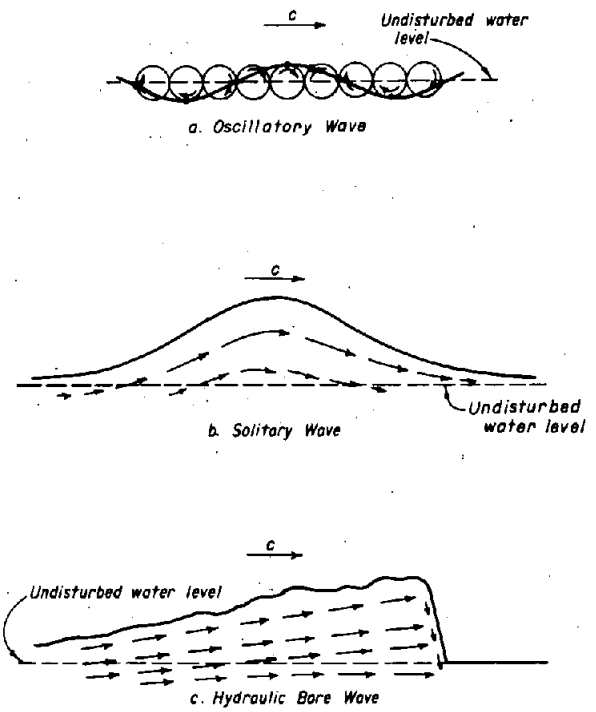

Figure 10.—Types of gravity waves.

of the slide, the wave peaks are very high and sharp with many small oscillations. As the wave travels away from the source, it smooths out as the amplitude decreases and the period increases.

The distant waves were also entirely above the initial water surface, indicating solitary waves. The amplitudes of the solitary waves increased as the reservoir narrowed and decreased as the reservoir widened. When the wave reached the dam, the amplitude increased due to the wave being partially reflected by the dam.

Waves in the river downstream from the dam were bore waves. The wave overtopping the dam in test SLA91 resulted in a 7-m (23-ft) high wave in the river with a very steep front, indicating a bore wave (see fig. B-4).

The wave in the river caused by test SLB51 was about 4 m (13 ft) high (fig. B-15). The second peak (about 55 seconds after the first wave) at probe location 1 was caused by the initial wave reflecting off the downstream end of the model; therefore, the second wave at probe location 1 should be disregarded.

Waves in the reservoir a distance away from the slide were solitary waves in all cases except one. For test B4511, (fig. B-17) the wave near the dam was a bore wave. The front of the wave rose steeply and abruptly and did not have the characteristic S-shape of the solitary waves in the other tests. Compare the shape of the waves at probe location 5 in tests B4511 and B4521 (fig. B-17 with fig. B-18) for an example of a bore wave versus a solitary wave. It is interesting to note that test B4511 was also the only test in which the maximum slide velocity (v_s) exceeded the approximate wave celerity at the slide ($\sqrt{gd}$.), i.e., the slide Froude number was supercritical.

Two slides were run within the same test at locations A and B. In test SBA11 slide "B" was released first. Slide "A" was released as the solitary wave from slide "B" was passing location A. The maximum wave at the dam was 22.9 m (75 ft), see figure B-9. The maximum wave height in the river was 15.8 m (52 ft), more than twice the height of the wave caused by slide "A" only. However, the probability of the slides releasing in this sequence is very low. In test SAB11, slides "A" and "B" were released simultaneously. The maximum waves during this test were not much different than in tests with the slides released individually. Therefore, tests with the landslides released individually should be adequate to assess wave potential.

Wave Celerities

The wave celerities for solitary waves (a distance from the slide) matched celerities calculated from equation (1) closely when the average water depth was used. A solitary wave occupies the entire cross section of the reservoir; the entire water surface moves up and down as the wave passes. Therefore, the average water depth which includes the effect of side slopes, affects the wave celerity.

The average water depth was computed by dividing the cross sectional area (A) of the reservoir by the surface width (W). For example, between probe locations 12 and 14 (see fig. 1), the average depth was 52 m (171 ft) and the maximum depth was 85 m (279 ft). The computed wave celerity for a wave height of 9 m (30 ft) (using the average depth) was 24 m/s (79 ft/s.) The wave celerity determined from the wave plots in this area was also 24 m/s (79 ft/s). If the maximum depth is used, the computed wave celerity is 33 m/s (108 ft/s) or about 38 percent higher. Table 1 gives cross sectional data for Morrow Point Reservoir. Using the cross sectional data and equation (1), celerities can be computed throughout the reservoir for solitary waves.

Table 1.—*Reservoir cross sectional data*

*Location (probe nos.)	Max d m	(ft)	Average d** m	(ft)
3–5	114	(374)	69	(227)
5–6A	110	(360)	67	(221)
6A–7	105	(345)	62	(204)
7–8, 9	104	(340)	57	(188)
8, 9–10	104	(340)	59	(194)
10–11	101	(330)	57	(186)
11–12	98	(320)	54	(176)
12–13	85	(280)	49	(161)
13–14	84	(274)	56	(184)

*Location - between probes
**Average $d = A/W$

The wave celerities for oscillatory waves (close to the slide) more closely matched celerities from equation (1) when the maximum water depth was used. The wave data indicate that the celerity in the vicinity of slide "A" was about 39 m/s (128 ft/s). Using the maximum water depth of 114 m (374 ft) and a 20-m (66-ft) wave height, equation (1) predicts a wave celerity of 36 m/s (118 ft/s). This indicates that oscillatory waves, in the vicinity of the slide, are more of a local phenomenon affected by local water depth.

Water Overtopping the Dam

Discharge over the dam is a function of the depth of water overtopping the dam since the dam acts as a weir. The weir equation, $Q = CLH^{3/2}$ [7], was used to compute incremental discharge for each time step during test SLA91. Their weir coefficient (C) was estimated to be 4.0 from "Design of Small Dams" [7]. The maximum computed discharge was 41 910 m³/s (1 480 000 ft³/s) at the wave peak. The volume of water overtopping was computed by multiplying the computed discharge by the differential time, and adding the incremental volumes to obtain the total overtopping volume.

The total computed overtopping volume was 6.12×10^5 m³ (2.16×10^7 ft³).

The water overtopping the dam was also captured in the downstream channel and the volume measured. The volume overtopping for slide SLA91 was 6.19×10^5 m³ (2.19×10^7 ft³). Therefore, the computed volume using the weir equation was within 2 percent of the measured volume.

The volume overtopping the dam was about 14 percent of the slide volume. The average discharge for the main overtopping wave was approximately 14 200 m³/s (500 000 ft³/s) over a 40-second period.

The volume of water overtopping the dam during test SLB51 was about 2.43×10^5 m³ (8.58×10^6 ft³) resulting in an average of 2800 m³/s (100 000 ft³/s) during an estimatd 80-second dam overtopping period. The estimated peak discharge is 10 000 m³/s (350 000 ft³/s); the overtopping volume was about 7 percent of the total slide volume.

Dimensionless Plots

Some empirical relationships were developed using data from the Morrow Point model tests in terms of dimensionless parameters. The most important parameters affecting wave heights and propagation were identified in a previous section on Dimensional Analysis.

The relationships presented in this section should be useful for general cases in predicting wave heights for design and operational purposes. The graphs are presented in terms of slide velocity, volume of water displaced, distance from the slide to the point of interest, and water depth at the slide.

Using the dimensionless parameters, plots were made from the data collected on the Morrow Point model. Table 2 lists the landslide data used in the graphs. Figure 11 is a dimensionless plot of η/d in the x-direction versus the slide Froude number, $\mathbb{F} = v_s/\sqrt{gd}$. The numbers adjacent to the data points represent a dimensionless displacement parameter (V/d^3), where V is the volume of water displaced by the slide.

For a given displacement the wave height increases with velocity up to a point and then levels off. Added velocity does not increase the wave height for slide Froude numbers ($\mathbb{F}$) greater than 0.6. Note that the Froude number in the x-direction ($\mathbb{F}_x$) would be cos i ($\mathbb{F}$), or $\mathbb{F}_x$ = 0.87 $\mathbb{F}$ for the Morrow Point tests. $\mathbb{F}_x$ can be used to relate the graphs in this report to other cases with different reservoir side slopes.

Curves were interpolated between the data points on figure 11 for constant volumes. The maximum wave heights on these curves were then plotted on a semilogrithmic graph of

Table 2.—*Landslide data — dimensionless parameters*

Test	$\mathbb{F}$	V/d^3
SA611	0.44	2.51
SLA71	.57	2.98
SLA81	.58	3.10
SLA91	.58	3.07
SA101	.39	2.58
SA111	.57	2.71
SA121	.38	2.29
SA131	.32	2.43
SAB11	.65	2.89
B4511	1.03	2.34
B4521	.77	2.14
B4531	.53	2.35
B4541	.70	2.34
SLB11	.67	3.02
SLB21	.67	3.25
SLB31	.68	3.39
SLB41	.83	3.36
SLB51	.84	3.34
SLB71	.94	3.52
C4521	.78	2.79
C4531	.78	2.78
C4551	.76	2.83
C4561	.60	2.53
C4571	.35	1.84
SLC21	.42	2.99
SLC41	.71	4.30
SLC51	.75	4.29
SLC61	.91	4.24
SLC71	.89	4.31
SLC81	.92	4.14

v_s = slide velocity (maximum)
d = water depth at slide (maximum)
g = gravitational force
V = volume of water displaced
$\mathbb{F}$ = slide Froude number ($v_s/\sqrt{gd}$)
V/d^3 = displacement parameter

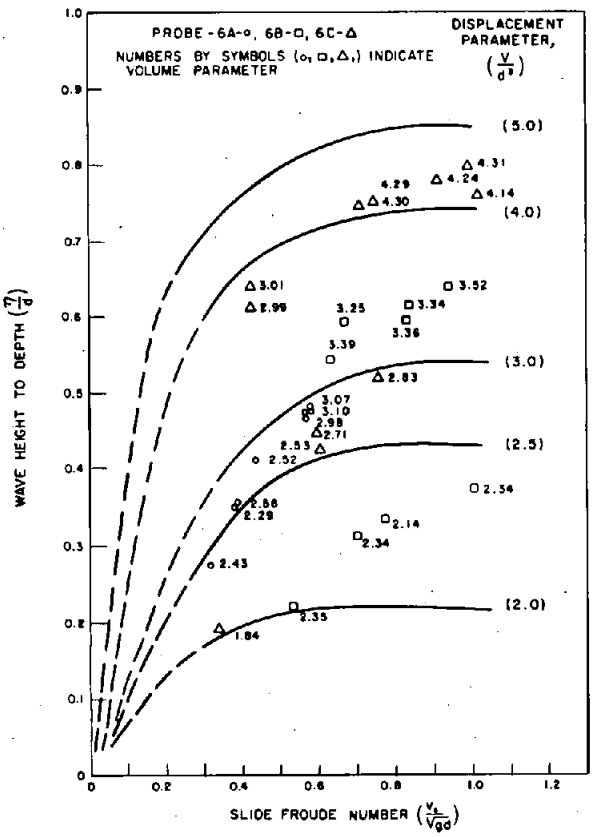

Figure 11.—Wave height in front of slides (x-direction) versus slide Froude number

volume versus wave height in the x-direction (fig. 12). The data plots as a straight line described by the following equation:

$$\eta/d = 1.458 \log (V/d^3) - 0.169 \qquad (16)$$

This equation can be used to determine the maximum wave height directly in front of a slide. The same procedure was used to determine maximum wave height in the y-direction (beside the slide). Figure 13 shows the relationship between slide velocity, slide volume, and wave height. The maximum wave heights from figure 13 were plotted on figure 14 versus slide volume. The following equation defines maximum wave height in the y-direction:

$$\eta/d = 0.351 \log (V/d^3) + 0.06 \qquad (17)$$

The effect of distance from the slide (ℓ/d) on wave height was then evaluated. Figure 15 is a plot of wave height at the dam (probe location 3) versus the slide Froude number ($\mathbb{F}$). The wave heights peak at $\mathbb{F}$ = 0.5 to 0.6 then decrease with increased slide velocity. Curves of constant volume (V/d^3) = 3 were interpolated for each slide at various distances from the dam. The maximum wave heights versus distance from the slide (ℓ/d) were then plotted on a semilogarithmic graph on figure 16. The following equation was determined for maximum wave height at the dam versus distance and volume of water displaced:

$$(\eta/d) = \frac{0.351 \log (V/d^3) + 0.08}{10^{\left(\frac{\ell}{d}/56\right)}} \qquad (18)$$

A family of curves (for different volumes) was also plotted on figure 16 using equation (18). The numerator of equation (18) represents the intercept or the maximum wave height at the slide in the y-direction. The denominator represents the rate of decay of the wave with distance. The wave height caused by the Vaiont slide was plotted to illustrate that the relationship is valid for other cases. The rate of wave decay may vary slightly for other bodies of water because of differences in topography. At greater distances from the slide the decay rate may change. The greatest distance tested in this study was (ℓ/d) = 35.

Slingerland and Voight [2,4] developed an empirical equation for first wave height which is very similar in form to equations (16, 17, and 18). The Slingerland and Voight equation uses a dimensionless kinetic energy term rather than the dimensionless displacement parameter suggested in this study. Also, equations (16, 17, and 18) account for the wave height as related to the direction of the slide and distance from the slide. The direction of the slide and distance are not accounted for in the Slingerland and Voight equation.

The Slingerland and Voight equation [2] predicts a 15.25-m (50-ft) wave height due to slide "A," compared to a 20.7-m (68-ft) prediction using equation (18).

The data presented on figure 15 indicate that a slide Froude number of about 0.5 produces the highest waves at points distant from the slide. This phenomenon may be explained by examining the hydrodynamics in the slide area. As the slide velocity increases, the wave height and velocity in the x-direction (across the reservoir) increase.

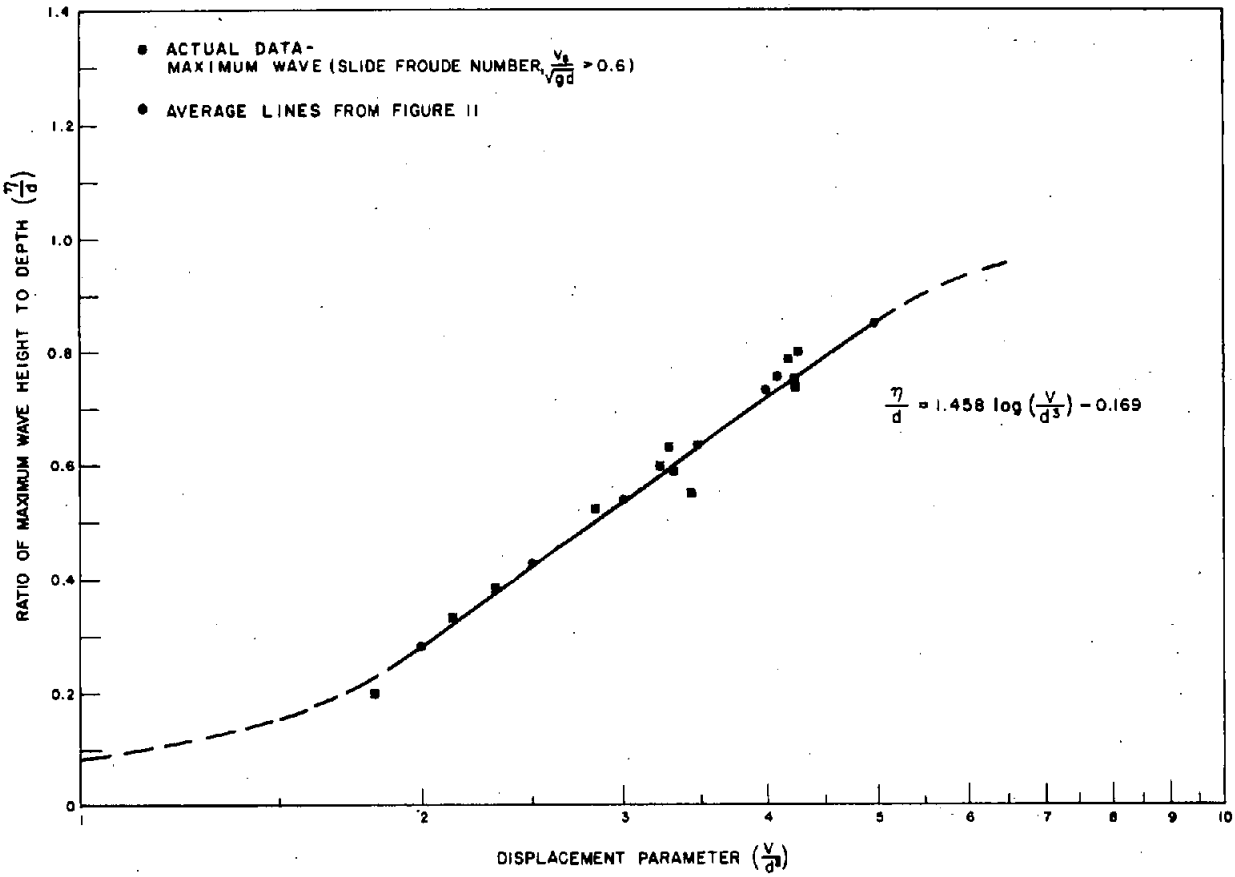

Figure 12.—Maximum wave height in front of slide versus volume parameter.

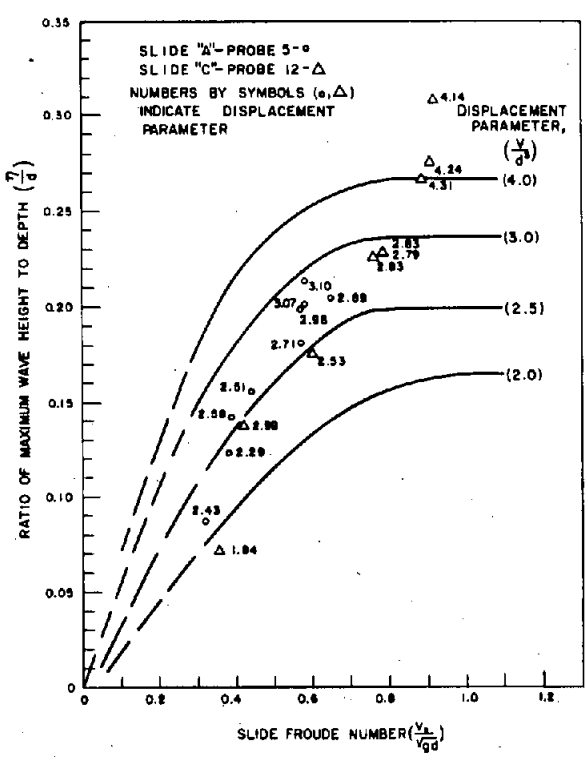

Figure 13.—Maximum wave height beside slides (y-direction) versus slide Froude number.

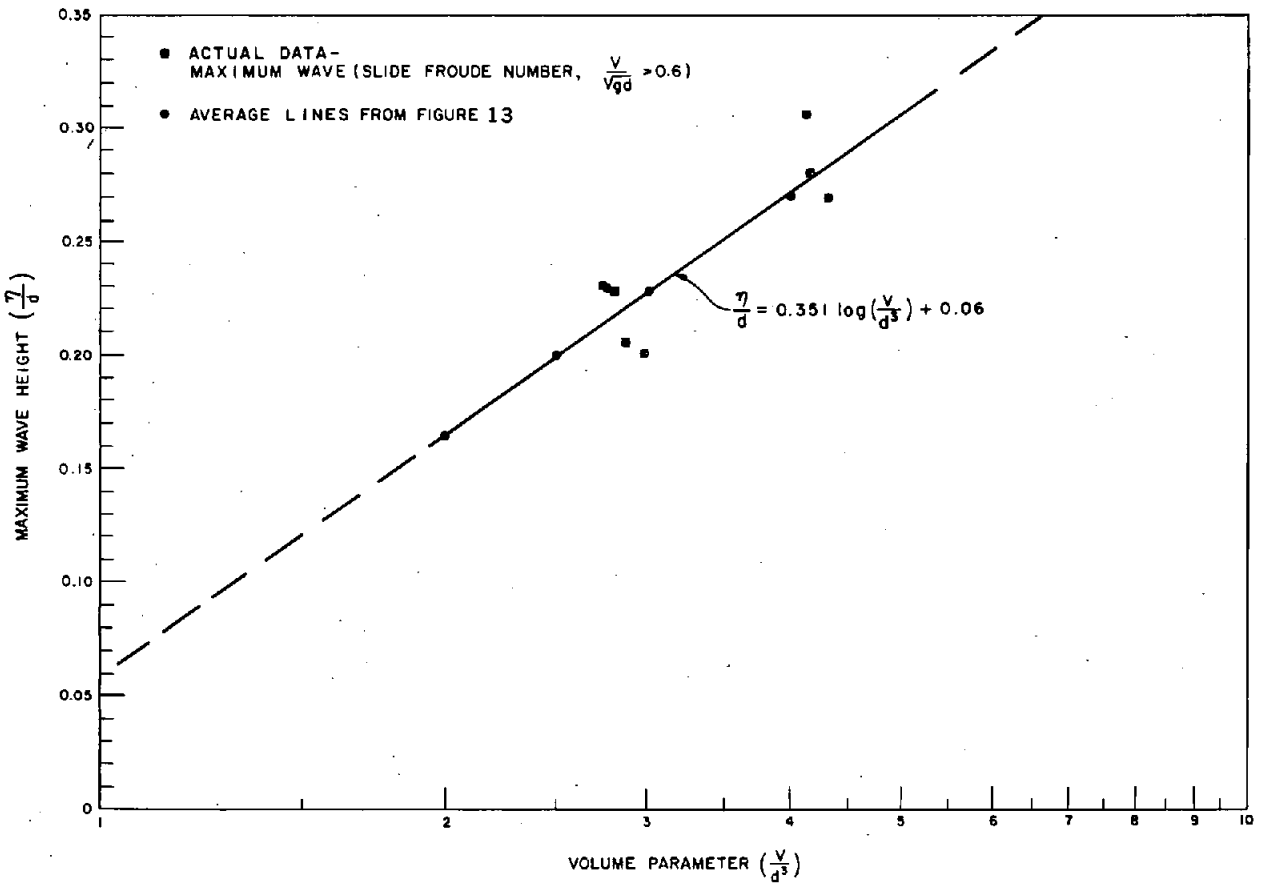

Figure 14.—Maximum wave height beside slide versus volume parameter.

When the slide Froude number exceeds 0.5, the wave in the x-direction is traveling fast enough to pass across the lake and climb the opposite shore before the wave in the y-direction is fully formed. At lower slide velocities, the wave in the x-direction contributes more to the formation of the wave in the y-direction.

To determine the maximum wave height close to a slide for slower slides (slide Froude numbers, $\mathbb{F} < 0.6$), use figures 11 or 13, depending on the point where the wave height is desired. Wave attenuation with distance can then be determined by assuming the same decay rate shown on figure 16. Thus, the following equation can be used to determine wave height for various distances from the dam to the slide:

$$(\eta/d) \text{ at dam} = \frac{(\eta/d) \text{ at slide}}{10^{\left(\frac{\ell}{d}/56\right)}} \qquad (19)$$

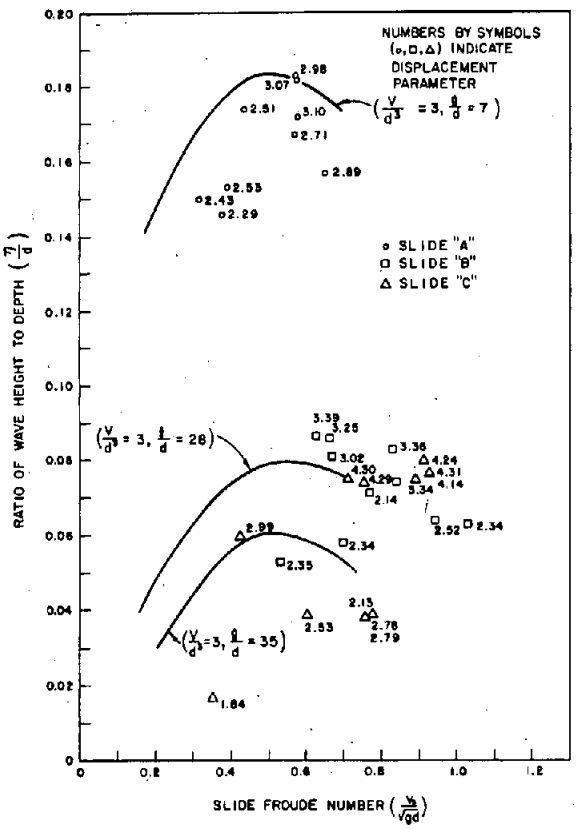

Figure 15.—Wave height at dam versus slide Froude number.

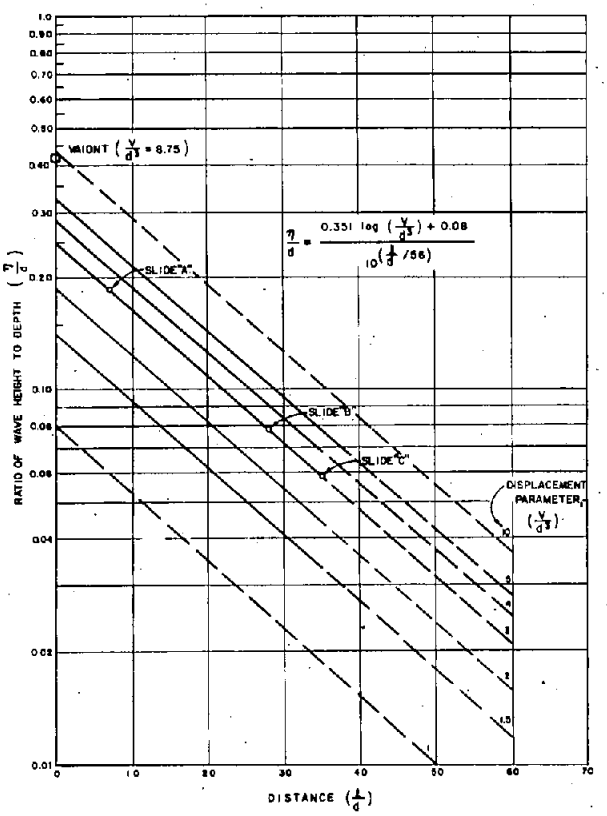

Figure 16.—Maximum wave heights at dam for various distances and slide volumes.

BIBLIOGRAPHY

[1] Raney, D. C., and H. L. Butler, "Landslide Generated Wave Model," J. Hyd. Div., Proc., Am. Soc. Civ. Eng., Paper 12425, vol. 102, pp. 1269–1282, September 1976.

[2] Pugh, C. A., and D. W. Harris, "Prediction of Landslide-Generated Water Waves," Paper, Int. Comm. on Large Dams, 14th Congress, Q54, R20, Rio de Janeiro, Brazil, May 1982.

[3] Chow, V. T., *Open Channel Hydraulics,* McGraw-Hill Inc., N.Y. pp. 537–540, 1959.

[4] Slingerland, R. L., and B. Voight, "Occurrences, Properties, and Predictive Models of Landslide Generated Water Waves," Rockslides and Avalanches, vol. 2, Elsevier Science Publishing, N.Y., 1979.

[5] "Hydraulic Laboratory Techniques," Water and Power Resources Service (Bureau of Reclamation), 1980.

[6] Morris, H. M., *Applied Hydraulics in Engineering,* The Ronald Press Company, N.Y., 1963.

[7] "Design of Small Dams," Bureau of Reclamation, 2d ed. (rev.), pp. 373–378, 1977.

APPENDIX A

Appendix A presents model landslide data and wave data for 31 tests on the Morrow Point model.

Figure A-1 gives locations of the wave measurement probes and landslides during the tests.

Tests with "A" in the name indicate a landslide at location "A," similarly with "B" and "C." Table A-1 lists landslide data for the tests.

Figures A-2 through A-32 are momentum versus time plots for the tests. Projections of potential prototype momentum are shown on each graph for comparison. These figures are given in model scale for simplicity (scale relations are listed in the main report).

TABLE

Table		Page
A-1	Model landslide data	22

FIGURES

Figure		Page
A-1	Morrow Point wave probe locations	29
A-2	Momentum versus time — test SA611	30
A-3	Momentum versus time — test SLA71	30
A-4	Momentum versus time — test SLA81	30
A-5	Momentum versus time — test SLA91	30
A-6	Momentum versus time — test SA101	31
A-7	Momentum versus time — test SA111	31
A-8	Momentum versus time — test SA121	31
A-9	Momentum versus time — test SA131	31
A-10	Momentum versus time — test SBA11	32
A-11	Momentum versus time — test SAB11	32
A-12	Momentum versus time — test SLB11	32
A-13	Momentum versus time — test SLB21	32
A-14	Momentum versus time — test SLB31	33
A-15	Momentum versus time — test SLB41	33
A-16	Momentum versus time — test SLB51	33
A-17	Momentum versus time — test SLB71	33
A-18	Momentum versus time — test B4511	34
A-19	Momentum versus time — test B4521	34
A-20	Momentum versus time — test B4531	34
A-21	Momentum versus time — test B4541	34
A-22	Momentum versus time — test SLC21	35
A-23	Momentum versus time — test SLC41	35
A-24	Momentum versus time — test SLC51	35
A-25	Momentum versus time — test SLC61	35
A-26	Momentum versus time — test SLC71	36
A-27	Momentum versus time — test SLC81	36
A-28	Momentum versus time — test C4521	36
A-29	Momentum versus time — test C4531	36
A-30	Momentum versus time — test C4551	37
A-31	Momentum versus time — test C4561	37
A-32	Momentum versus time — test C4571	37

Table A-1.—*Model landslide data*

Test	Time (s)	Momentum* (lb-s)	Volume*,** (ft^3)	Velocity* (ft/s)
SA611	0.016	0.0	2.14	0.11
	.103	.3	2.28	1.07
	.189	2.0	2.70	1.83
	.276	5.6	3.33	2.39
	.362	11.9	4.29	2.85
	.449	19.2	5.45	2.99
	.536	27.4	6.81	3.02
	.623	32.3	8.24	2.73
	.710	32.9	9.64	2.26
SLA71	0.016	0.0	1.30	0.15
	.101	.5	1.47	1.44
	.186	2.9	1.91	2.44
	.271	8.3	2.63	3.20
	.356	17.0	3.69	3.65
	.440	28.5	5.08	3.88
	.525	39.7	6.73	3.77
	.610	47.4	8.45	3.42
	.694	48.7	10.20	2.82
SLA81	0.016	0.0	1.14	0.51
	.102	.7	1.34	1.76
	.188	3.6	1.82	2.74
	.273	9.8	2.63	3.39
	.358	19.9	3.76	3.93
	.443	31.5	5.26	3.94
	.528	42.7	6.98	3.78
	.614	51.0	8.85	3.42
	.699	1.8	10.40	.10
SLA91	0.016	0.0	1.16	0.24
	.103	.5	1.32	1.54
	.190	2.8	1.74	2.48
	.277	8.8	2.51	3.37
	.364	18.0	3.62	3.79
	.451	30.0	5.08	3.95
	.538	40.0	6.79	3.66
	.625	48.2	8.60	3.34
	.712	48.3	10.33	2.72

*SI METRIC CONVERSIONS

To Convert	From	To	Multiply by
Length	Feet (ft)	Meters (m)	0.3048
Momentum	Pound-seconds (lb-s)	Newton-seconds (N-s)	4.448
Volume	Cubic feet (ft^3)	Cubic meters (m^3)	0.02832
Velocity	Feet per second (ft/s)	Meters per second (m/s)	0.3048

**Initial volume of water displaced by slide was taken as volume at t = 0.016 seconds. Volume displaced = volume − volume (initial).

Table A-1.—*Model landslide data*—Continued

Test	Time (s)	Momentum* (lb-s)	Volume*,** (ft^3)	Velocity* (ft/s)
SA101	0.016	0.0	2.73	0.17
	.102	.3	2.91	0.92
	.186	1.8	3.31	1.61
	.271	4.8	3.92	2.10
	.356	9.7	4.77	2.46
	.441	16.2	5.85	2.68
	.526	21.2	7.00	2.56
	.611	24.7	8.23	2.32
	.696	25.4	9.38	1.96
	.782	23.2	10.43	1.55
SA111	0.016	0.0	1.45	0.25
	.104	.6	1.66	1.51
	.190	3.6	2.17	2.56
	.277	10.5	3.04	3.38
	.364	20.8	4.27	3.79
	.451	33.4	5.87	3.90
	.537	44.1	7.65	3.66
	.624	52.5	9.55	3.34
SA121	0.015	0.0	3.18	0.21
	.101	.4	3.40	1.01
	.185	2.0	3.82	1.63
	.270	5.4	4.49	2.13
	.355	10.2	5.37	2.38
	.440	16.6	6.48	2.60
	.525	21.9	7.66	2.52
	.610	25.7	8.91	2.32
	.695	25.7	10.02	1.93
SA131	0.016	0.0	3.21	0.26
	.103	.3	3.40	.93
	.190	1.7	3.81	1.48
	.277	4.4	4.45	1.81
	.364	8.4	5.25	2.12
	.451	12.8	6.22	2.19
	.538	16.2	7.19	2.10
	.625	18.2	8.22	1.87
	.712	17.9	9.17	1.55
	.799	14.3	9.91	1.10
	.886	9.6	10.46	0.68
SAB11	0.016	0.0	1.48	0.28
	.103	.5	1.67	1.35
	.189	2.9	2.11	2.37
	.276	9.4	2.92	3.36
	.362	21.6	4.19	4.12
	.449	37.6	5.88	4.41
	.536	52.4	7.92	4.19
	.622	60.5	10.12	3.61

Table A-1.—*Model landslide data*—Continued

Test	Time (s)	Momentum* (lb-s)	Volume*,** (ft^3)	Velocity* (ft/s)
B4511	0.016	0.0	0.00	0.45
	.104	.0	.00	1.83
	.190	.0	.00	2.89
	.277	.7	.08	4.09
	.363	2.6	0.26	5.17
	.450	9.1	0.77	6.08
	.537	22.7	1.76	6.63
	.624	39.6	3.26	6.26
	.711	45.8	4.90	4.83
B4521	0.016	0.0	0.21	0.35
	.103	.2	0.27	1.80
	.190	1.1	0.42	2.57
	.276	3.7	0.73	3.62
	.363	9.2	1.29	4.40
	.450	18.8	2.17	4.93
	.537	28.5	3.30	4.74
	.623	30.0	4.49	3.62
B4531	0.016	0.0	1.11	0.46
	.104	.5	1.27	1.53
	.190	2.4	1.60	2.48
	.277	6.4	2.14	3.20
	.364	11.6	2.88	3.39
	.450	14.8	3.71	2.93
	.537	12.8	4.42	2.00
	.623	7.9	4.93	1.07
B4541	0.016	0.0	0.45	0.37
	.103	.3	.58	1.44
	.190	1.6	.80	2.54
	.276	5.3	1.24	3.60
	.362	11.5	1.92	4.13
	.449	20.8	2.88	4.48
	.536	25.7	3.96	3.82
	.623	20.0	4.90	2.33
SLB11	0.016	0.0	0.24	0.37
	.102	.1	.27	1.68
	.187	.9	.42	2.70
	.272	3.8	.78	3.62
	.357	10.0	1.50	4.09
	.442	19.8	2.63	4.28
	.527	26.3	3.98	3.62
	.612	30.5	5.36	3.07
	.697	26.2	6.58	2.13

Table A-1.—*Model landslide data*— Continued

Test	Time (s)	Momentum* (lb-s)	Volume*,** (ft^3)	Velocity* (ft/s)
SLB21	0.016	0.0	0.24	0.49
	.103	.1	.28	1.74
	.190	1.1	.44	2.80
	.276	4.5	.85	3.84
	.363	11.9	1.67	4.28
	.449	22.1	2.91	4.28
	.536	30.4	4.37	3.79
	.623	30.3	5.83	3.79
	.710	27.6	7.06	2.08
SLB31	0.016	0.0	0.24	0.43
	.102	.1	.27	1.58
	.187	.9	.41	2.73
	.271	3.8	.78	3.59
	.356	9.8	1.48	4.05
	.441	17.3	2.50	3.94
	.526	23.6	3.73	3.49
	.611	26.1	5.00	2.83
	.696	23.6	6.08	2.08
	.781	16.0	6.90	1.24
	.866	6.6	7.35	.48
SLB41	0.016	0.0	0.00	0.36
	.103	.0	.00	1.64
	.189	.0	.00	2.71
	.276	1.7	.23	3.99
	.363	4.4	.46	4.99
	.449	13.0	1.26	5.35
	.535	23.3	2.56	4.69
	.621	33.2	4.13	4.14
	.708	35.3	5.72	3.18
	.794	30.8	7.04	2.26
SLB51	0.015	0.0	0.00	0.61
	.102	.0	.00	1.62
	.189	.0	.00	3.00
	.275	1.8	.23	4.18
	.361	4.8	.49	4.99
	.448	14.0	1.33	5.41
	.534	26.2	2.72	4.96
	.621	35.5	4.40	4.16
	.707	38.4	6.08	3.26

Table A-1.—*Model landslide data*—Continued

Test	Time (s)	Momentum* (lb-s)	Volume*,** (ft^3)	Velocity* (ft/s)
SLB71	0.015	0.0	0.00	0.43
	.103	.0	.00	1.77
	.190	.0	.00	3.01
	.277	.0	.00	4.05
	.364	2.6	.26	5.14
	.451	9.4	.80	6.04
	.538	22.8	2.05	5.73
	.625	36.8	3.80	4.99
	.711	43.8	5.73	3.94
	.798	37.4	7.38	2.61
C4521	0.016	0.0	0.10	0.49
	.102	.1	.13	1.35
	.187	.5	.21	2.47
	.272	1.8	.39	3.16
	.357	4.8	.73	3.93
	.443	10.3	1.30	4.44
	.528	18.3	2.11	4.69
	.613	23.6	3.10	4.06
	.698	13.1	4.02	1.73
C4531	0.016	0.0	0.10	0.36
	.103	.1	.12	1.34
	.190	.4	.19	2.26
	.277	1.6	.35	3.14
	.364	4.4	.69	3.81
	.451	9.8	1.25	4.38
	.538	17.9	2.07	4.68
	.625	22.8	3.07	3.95
	.711	10.6	4.01	1.40
C4551	0.016	0.0	0.12	0.20
	.101	.1	.15	1.72
	.186	.5	.24	2.15
	.271	1.9	.43	3.16
	.356	4.9	.78	3.83
	.441	10.9	1.36	4.53
	.526	18.3	2.20	4.54
	.611	23.1	3.17	3.90
	.696	15.5	4.09	2.01
C4561	0.016	0.0	0.50	0.04
	.102	.1	.53	.81
	.188	.5	.66	1.65
	.275	2.2	.92	2.64
	.361	5.0	1.34	3.07
	.447	10.0	1.93	3.61
	.534	14.1	2.69	3.30
	.621	14.4	3.44	2.53
	.707	8.5	4.06	1.22

Table A-1.—*Model landslide data*—Continued

Test	Time (s)	Momentum* (lb-s)	Volume*,** (ft^3)	Velocity* (ft/s)
C4571	0.016	0.0	1.38	0.27
	.103	.2	1.49	1.08
	.189	1.3	1.73	1.90
	.275	2.9	2.11	2.08
	.362	4.9	2.58	2.13
	.449	6.7	3.06	2.06
	.535	6.9	3.54	1.66
	.622	5.6	3.96	1.12
SLC21	0.016	0.0	1.69	0.28
	.103	.4	1.86	1.30
	.189	2.5	2.32	2.03
	.276	6.5	3.05	2.45
	.362	11.1	3.94	2.54
	.449	14.2	4.92	2.26
	.535	16.3	5.89	2.00
SLC41	0.016	0.0	0.00	0.27
	.103	.6	.22	1.48
	.190	1.3	.27	2.58
	.276	3.6	.51	3.66
	.363	9.1	1.10	4.28
	.449	16.8	2.12	4.10
	.536	25.8	3.40	3.92
	.623	29.7	4.77	3.21
	.709	28.0	6.04	2.39
SLC51	0.016	0.0	0.00	0.37
	.104	.0	.00	1.71
	.190	1.4	.26	2.74
	.277	3.5	.50	3.58
	.364	9.7	1.11	4.51
	.451	16.6	2.12	4.03
	.538	26.0	3.42	3.92
	.625	30.0	4.80	3.22
	.712	1.1	6.03	.09
SLC61	0.016	0.0	0.00	0.41
	.102	.0	.00	1.73
	.187	.0	.00	2.55
	.273	.0	.00	3.52
	.358	2.2	.24	4.59
	.443	6.5	.61	5.44
	.529	16.3	1.57	5.33
	.614	27.4	2.97	4.75
	.699	32.7	4.53	3.72
	.784	5.9	5.96	.51

Table A-1.—*Model landslide data*—Continued

Test	Time (s)	Momentum* (lb-s)	Volume*,** (ft^3)	Velocity* (ft/s)
SLC71	0.016	0.0	0.00	0.57
	.103	.0	.00	1.73
	.190	.0	.00	2.80
	.276	.0	.00	3.72
	.363	2.7	.29	4.77
	.450	7.9	.78	5.23
	.537	19.4	1.88	5.32
	.623	30.8	3.41	4.66
	.710	35.8	5.04	3.66
	.797	6.5	6.06	.55
SLC81	0.016	0.0	0.00	0.50
	.103	.0	.00	1.43
	.190	.0	.00	2.42
	.276	.0	.00	3.37
	.363	.0	.00	4.39
	.449	3.9	.40	5.05
	.536	12.5	1.16	5.55
	.623	24.6	2.51	5.06
	.710	35.8	4.15	4.44
	.796	37.2	5.82	3.29

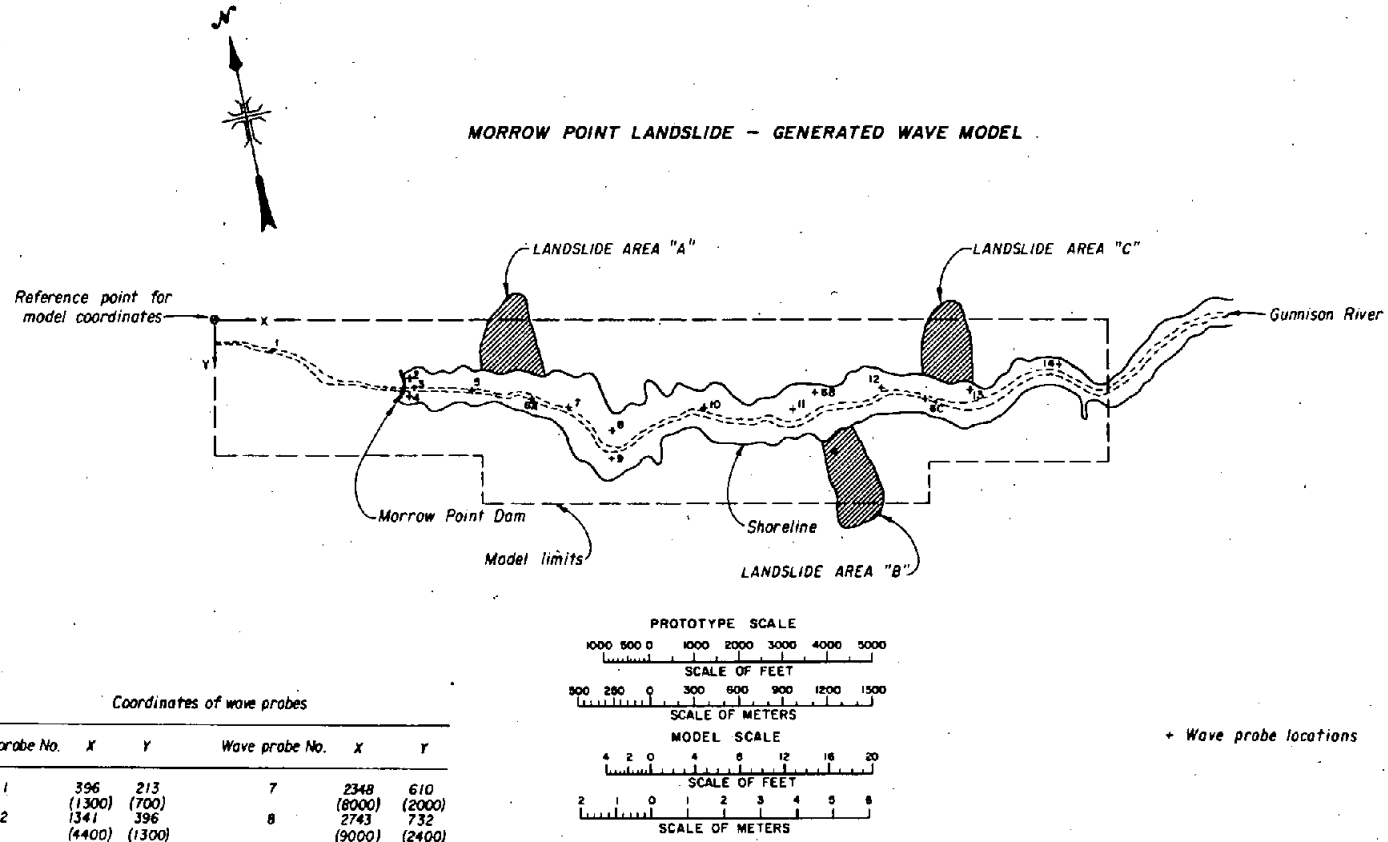

Coordinates of wave probes

Wave probe No.	X	Y	Wave probe No.	X	Y
1	396 (1300)	213 (700)	7	2348 (8000)	610 (2000)
2	1341 (4400)	396 (1300)	8	2743 (9000)	732 (2400)
3	1356 (4450)	457 (1500)	9	2743 (9000)	914 (3000)
4	1341 (4400)	518 (1700)	10	3353 (11000)	610 (2000)
5	1768 (5800)	457 (1500)	11	3962 (13000)	610 (2000)
6A	2134 (7000)	549 (1800)	12	4572 (15000)	457 (1500)
6B	4115 (13500)	488 (1600)	13	5182 (17000)	457 (1500)
6C	4877 (16000)	549 (1800)	14	5791 (19000)	305 (1000)

Coordinates are given as distance from the reference point in m (ft).

The coordinates of a point on the center of the dam crest are: X = 1344 m (4410 ft), Y = 457 m (1500 ft).

Figure A-1.—Morrow Point wave probe locations.

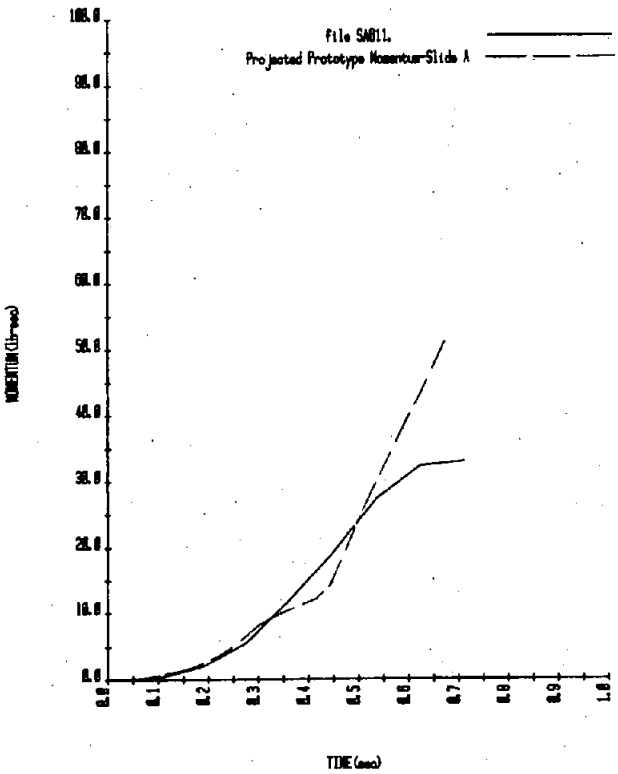

Figure A-2.—Momentum versus time — test SA611.

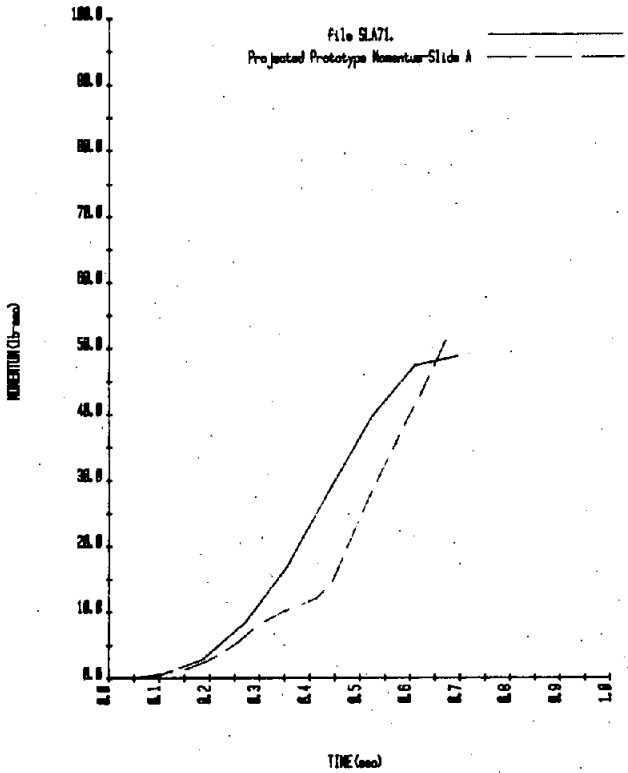

Figure A-3.—Momentum versus time — test SLA71.

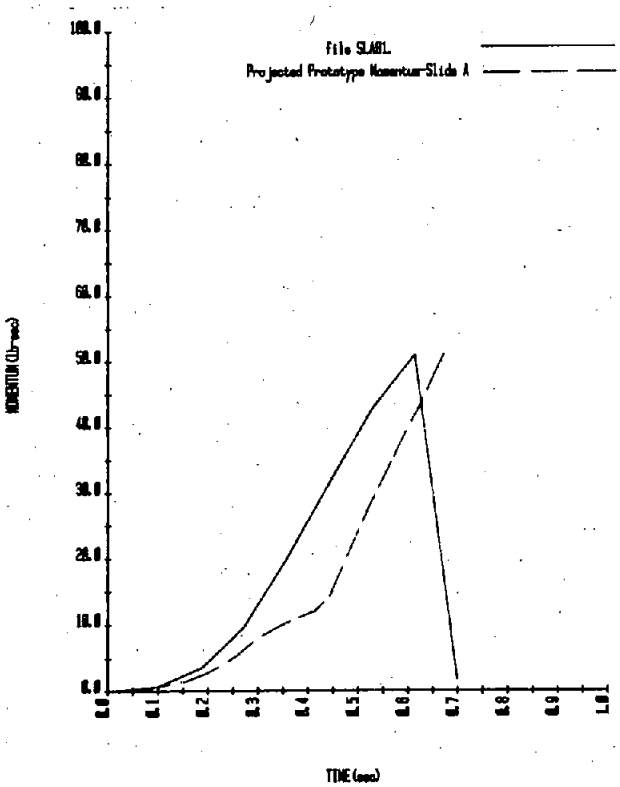

Figure A-4.—Momentum versus time — test SLA81.

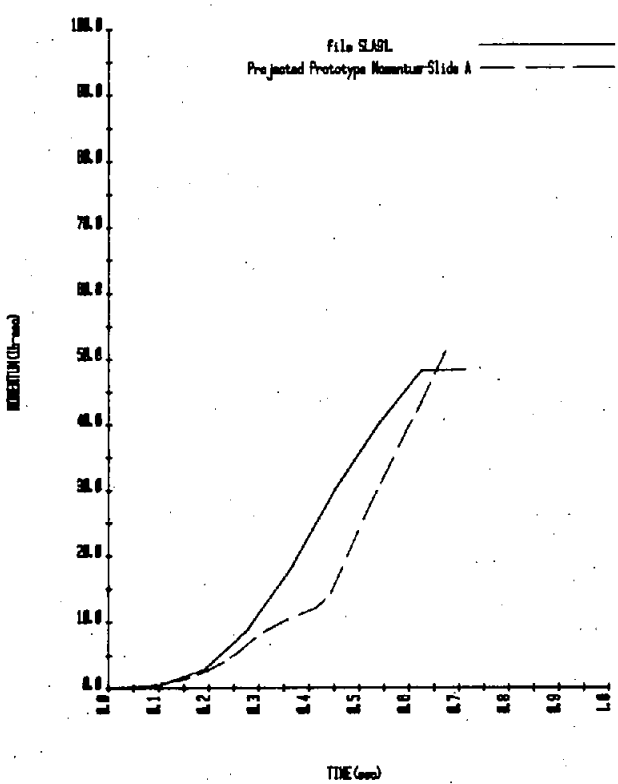

Figure A-5.—Momentum versus time — test SLA91.

To convert lb-sec to Newton-sec multiply by 4.448

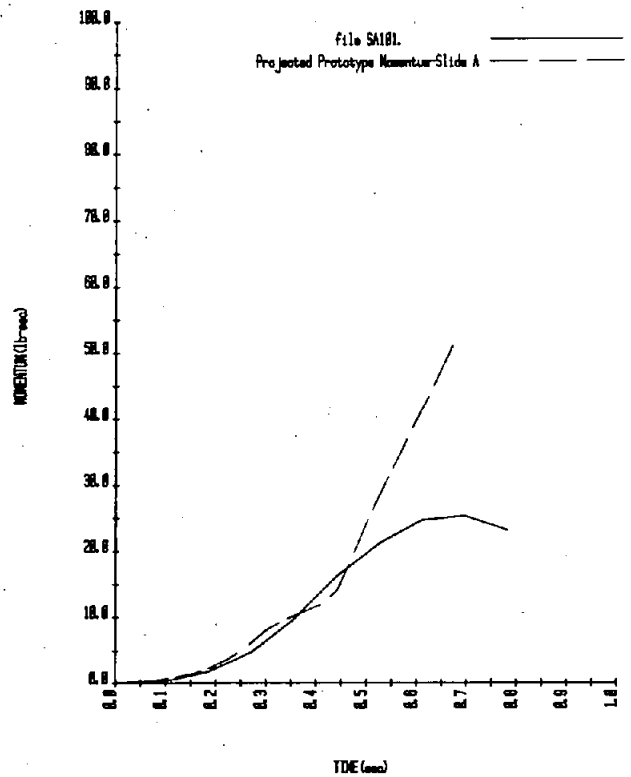

Figure A-6.—Momentum versus time — test SA101.

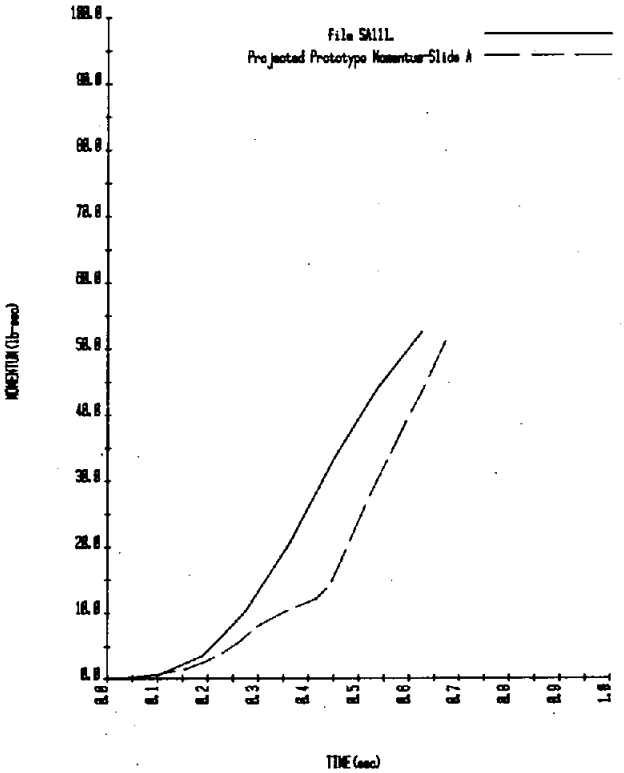

Figure A-7.—Momentum versus time — test SA111.

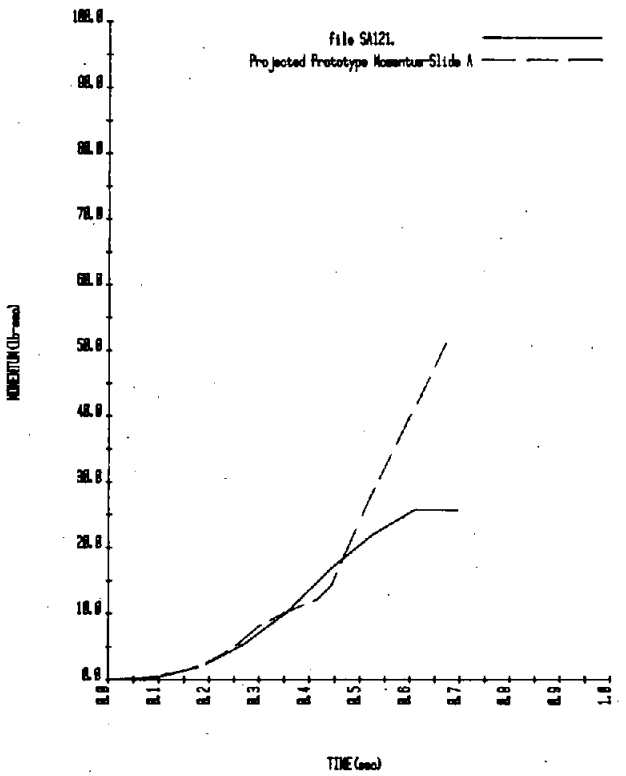

Figure A-8.—Momentum versus time — test SA121.

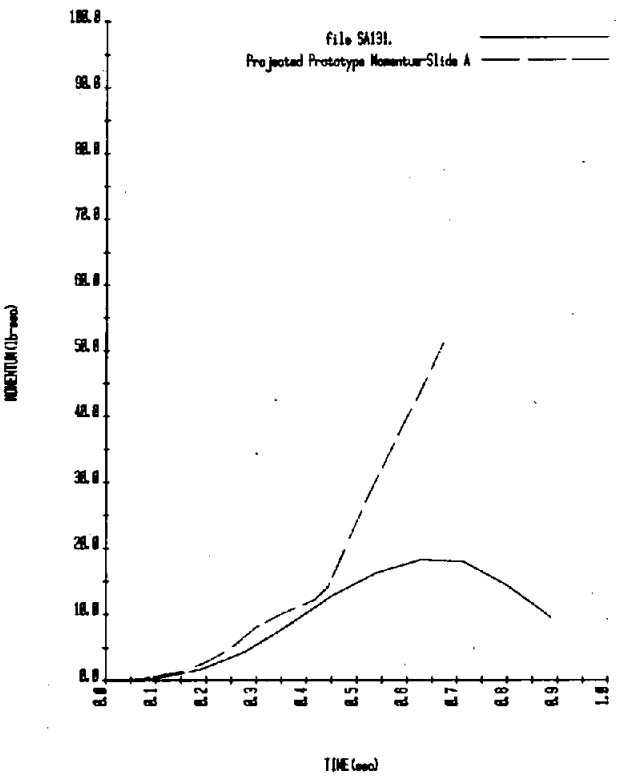

Figure A-9.—Momentum versus time — test SA131.

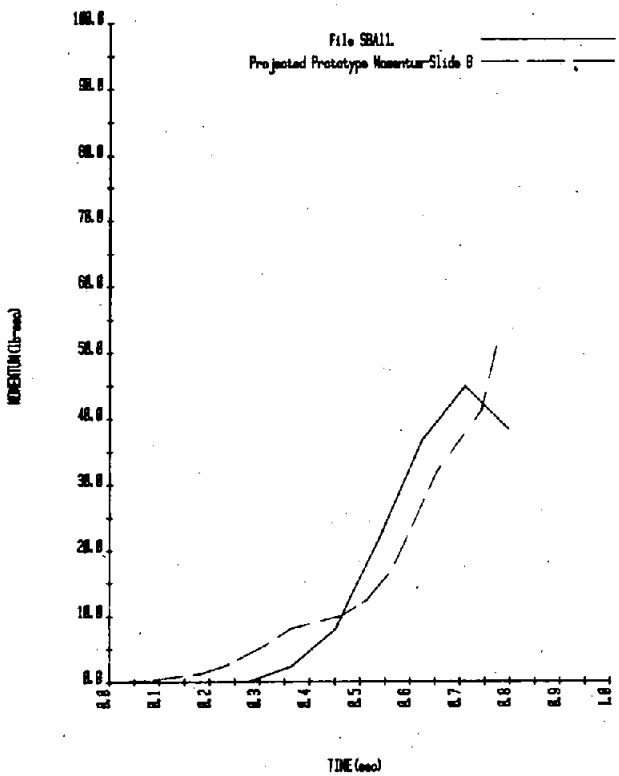

Figure A-10.—Momentum versus time — test SBA11.

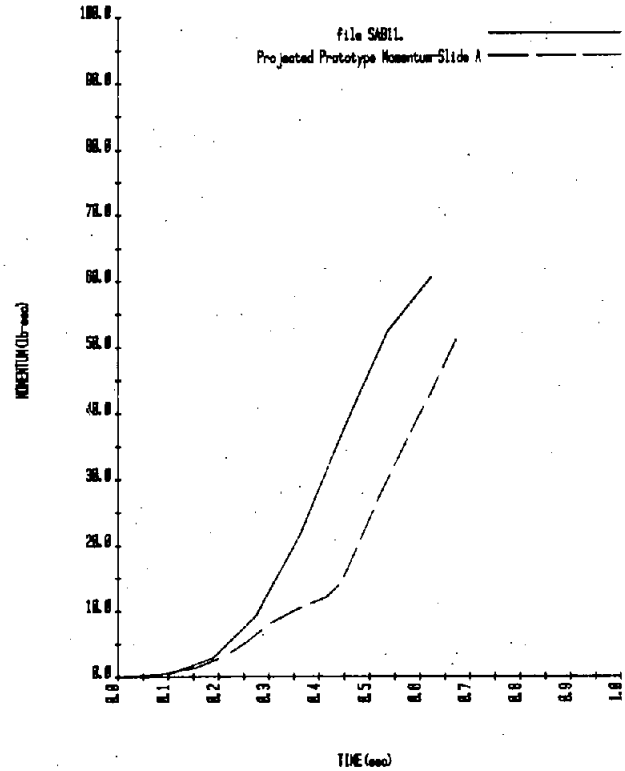

Figure A-11.—Momentum versus time — test SAB11.

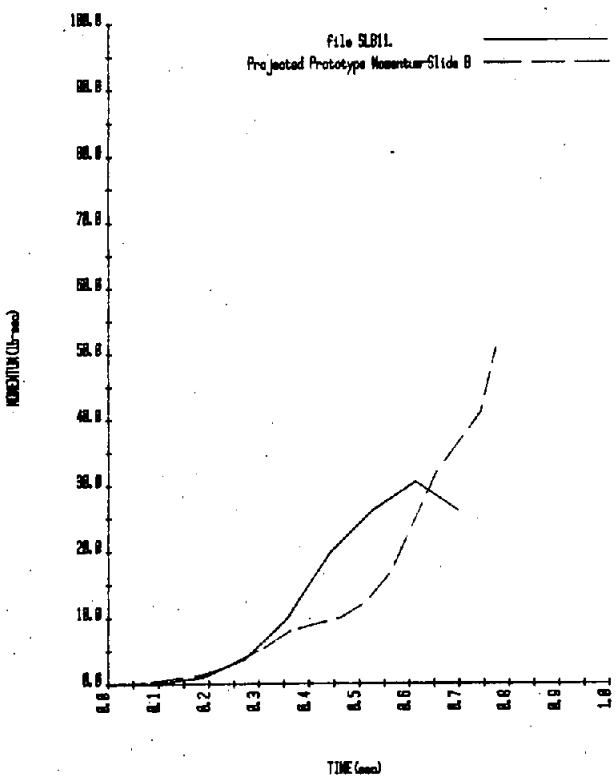

Figure A-12.—Momentum versus time — test SLB11.

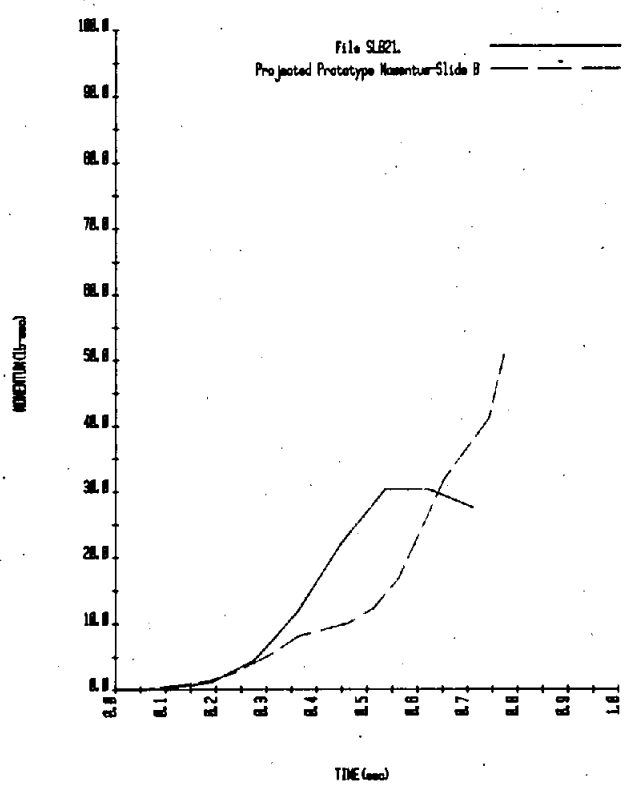

Figure A-13.—Momentum versus time — test SLB21.

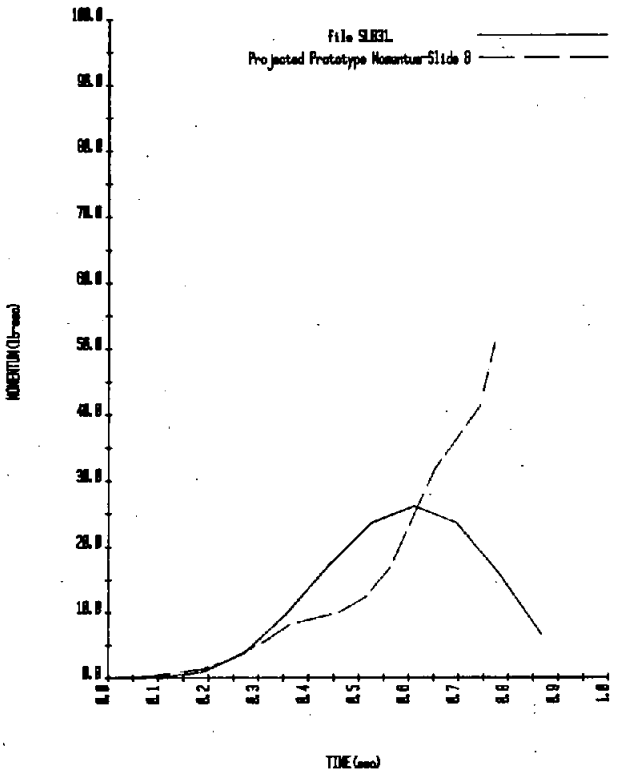

Figure A-14.—Momentum versus time — test SLB31.

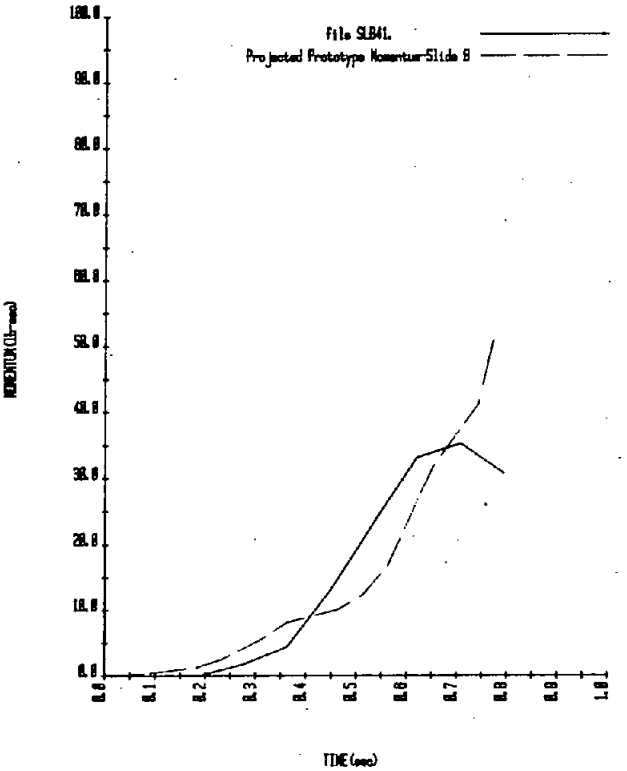

Figure A-15.—Momentum versus time — test SLB41.

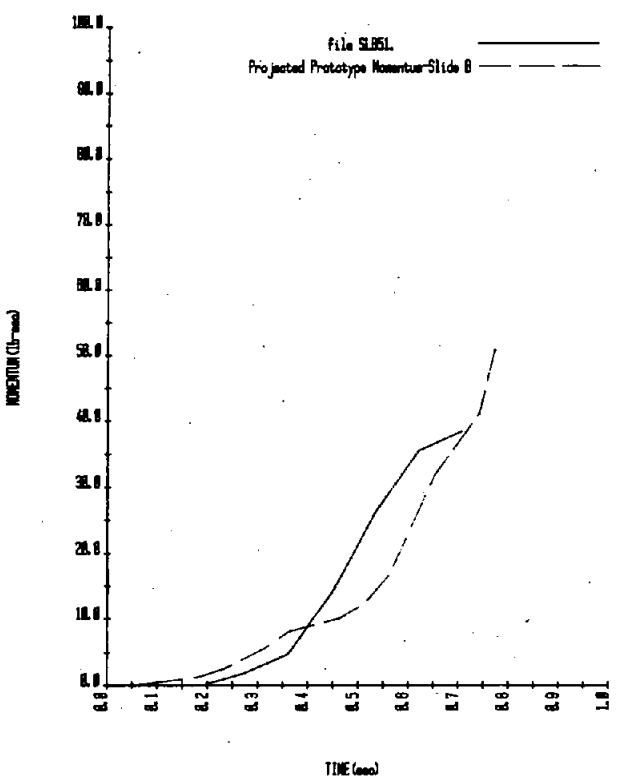

Figure A-16.—Momentum versus time — test SLB51.

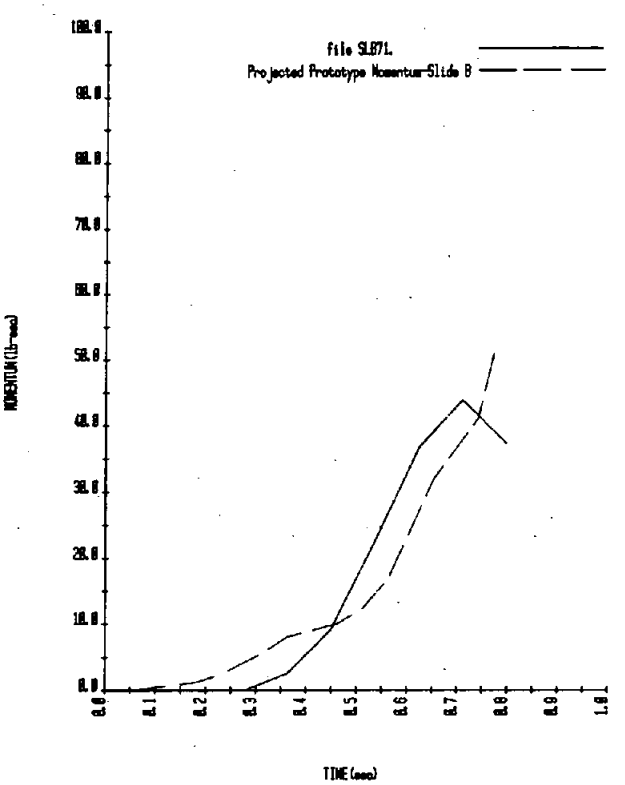

Figure A-17.—Momentum versus time — test SLB71.

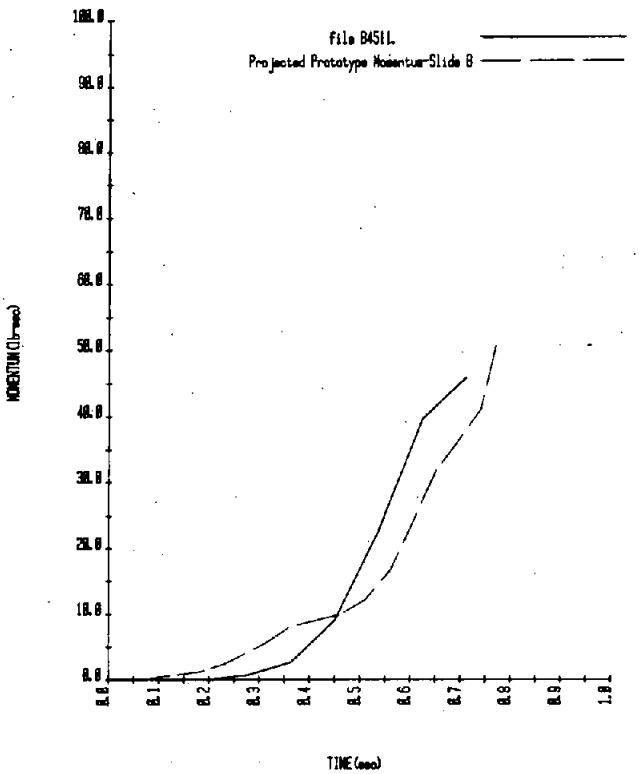

Figure A-18.—Momentum versus time — test B4511.

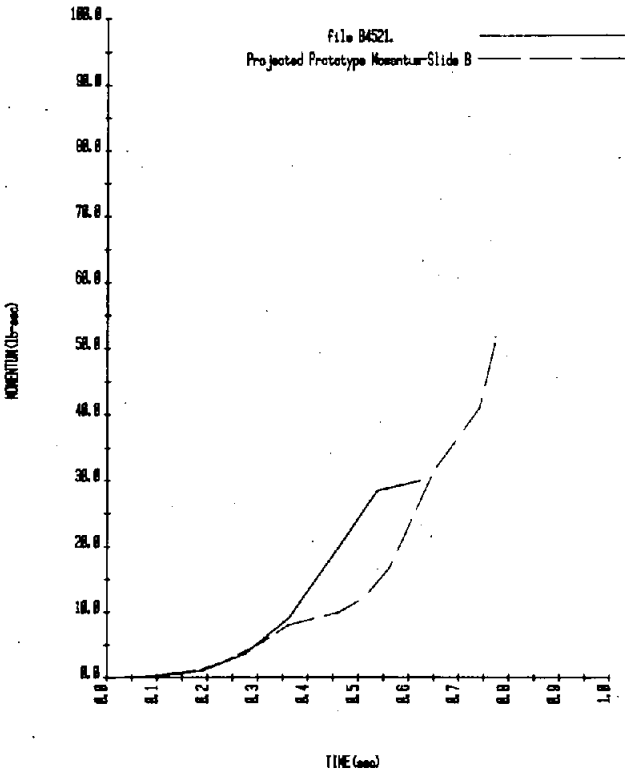

Figure A-19.—Momentum versus time — test B4521.

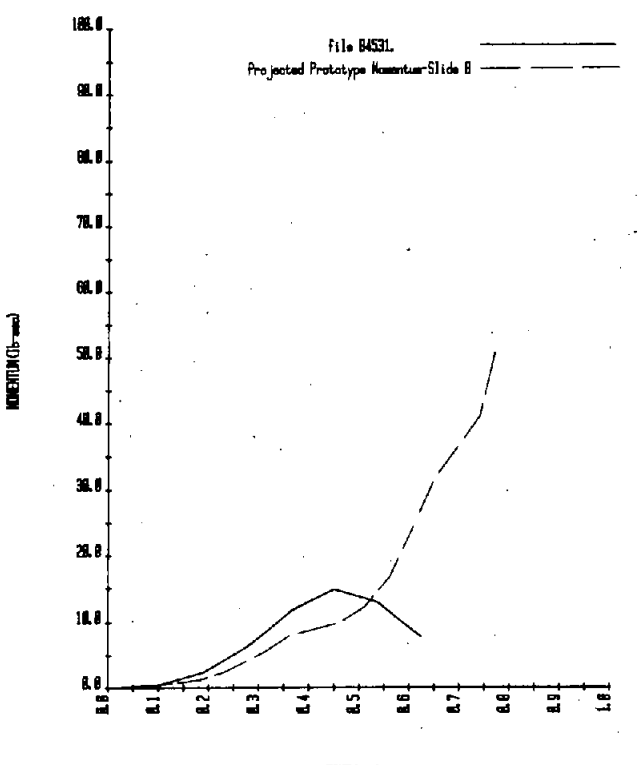

Figure A-20.—Momentum versus time — test B4531.

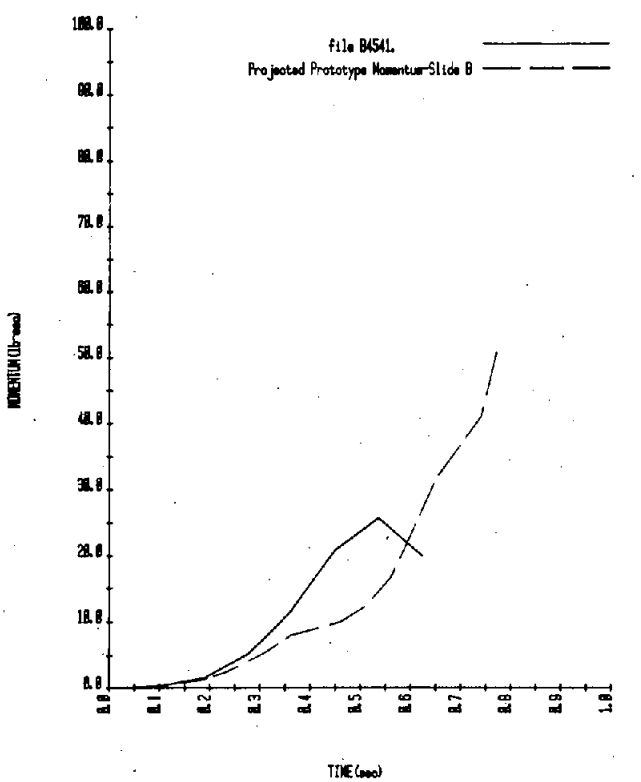

Figure A-21.—Momentum versus time — test B4541.

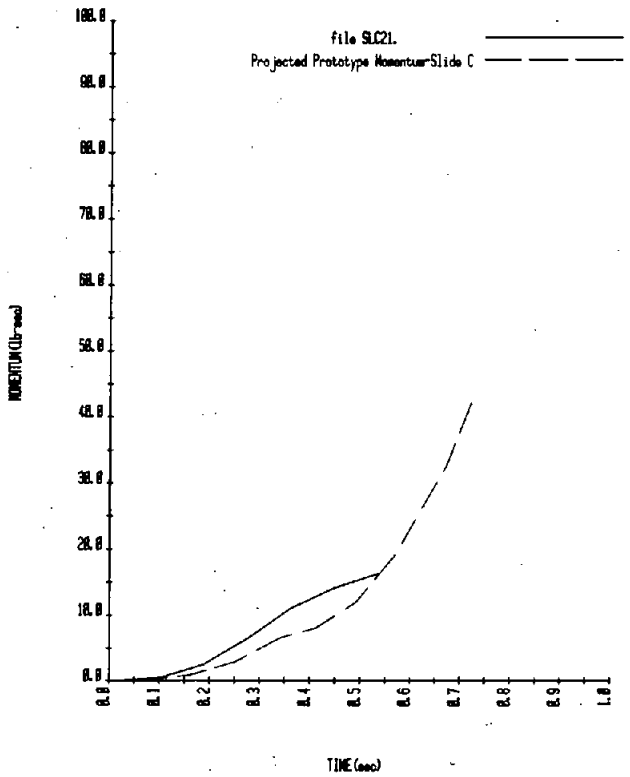

Figure A-22.—Momentum versus time — test SLC21.

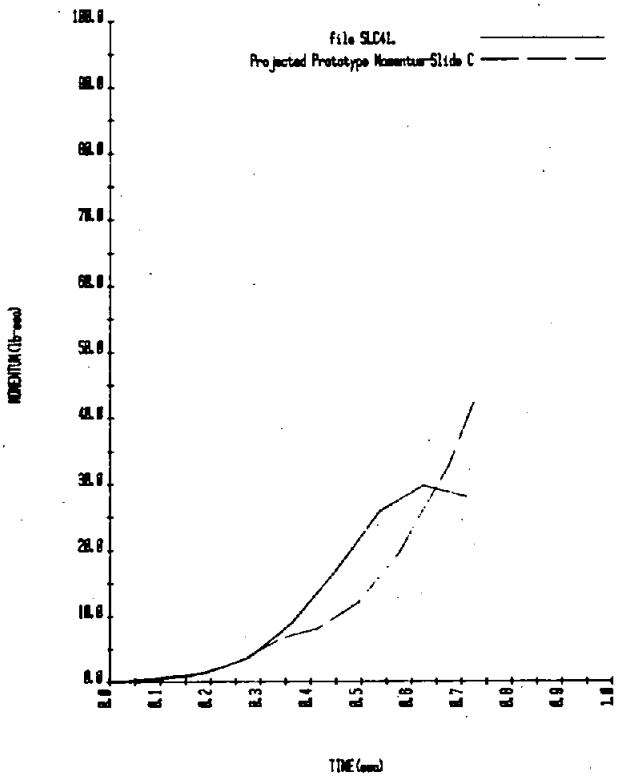

Figure A-23.—Momentum versus time — test SLC41.

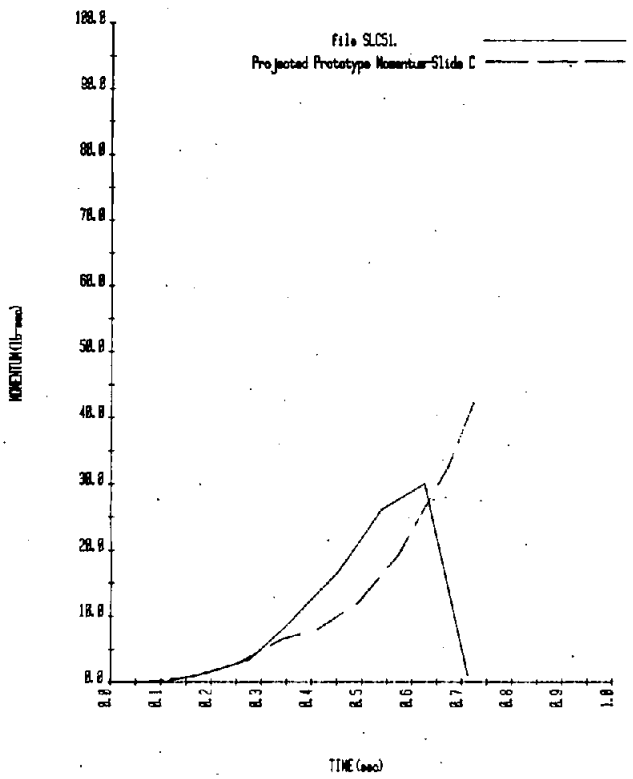

Figure A-24.—Momentum versus time — test SLC51.

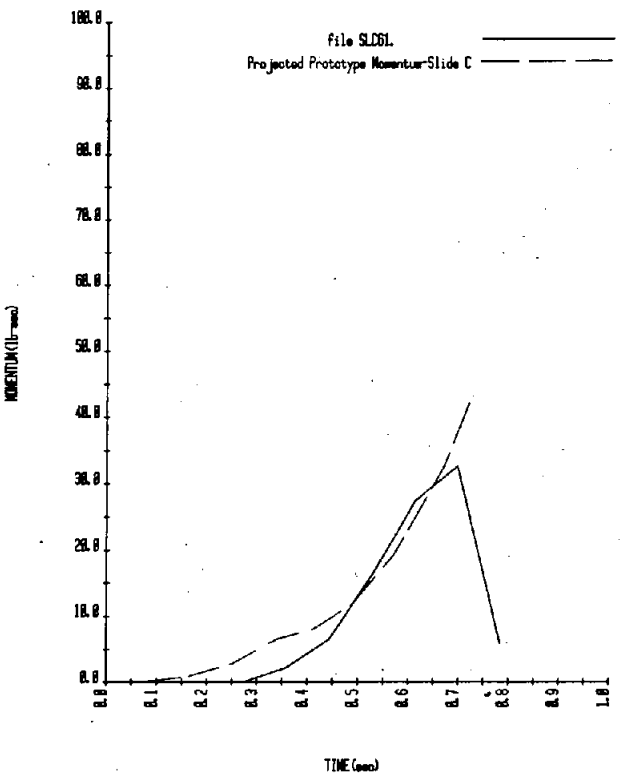

Figure A-25.—Momentum versus time — test SLC61.

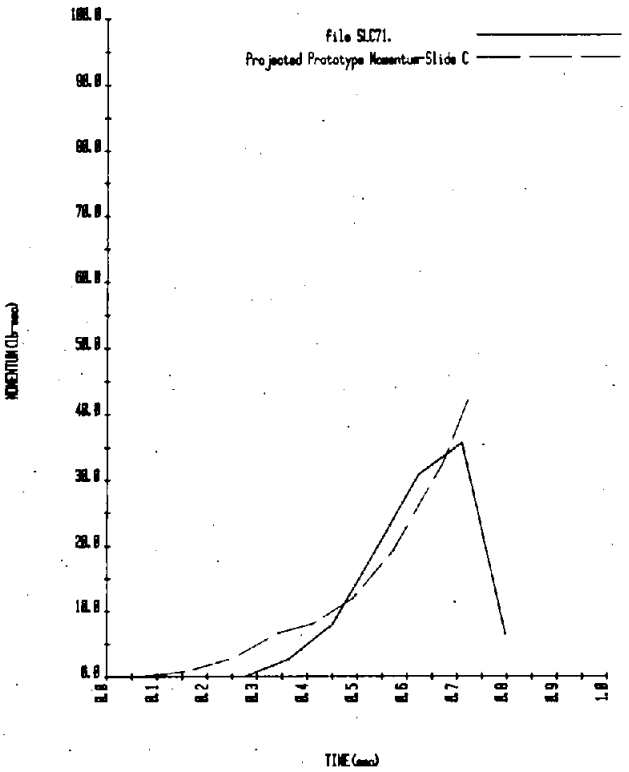

Figure A-26.—Momentum versus time — test SLC71.

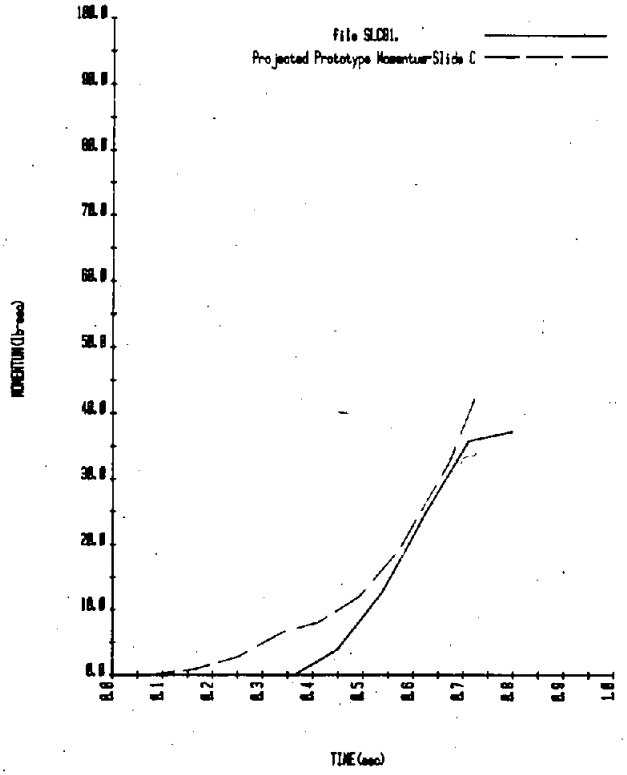

Figure A-27.—Momentum versus time — test SLC81.

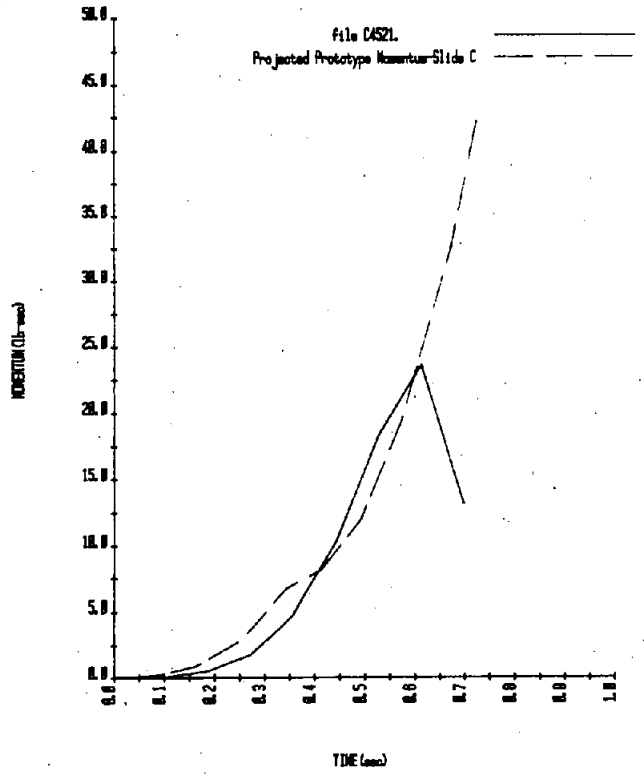

Figure A-28.—Momentum versus time — test C4521.

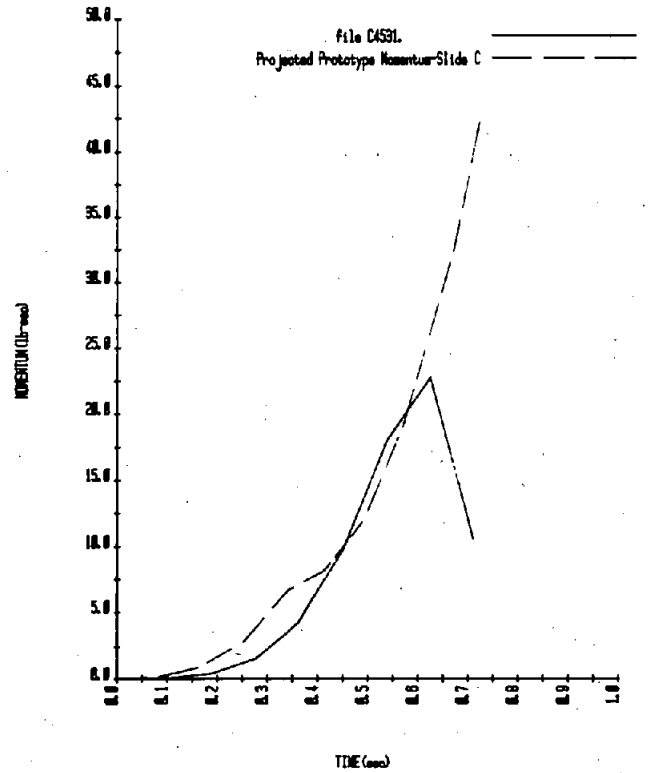

Figure A-29.—Momentum versus time — test C4531.

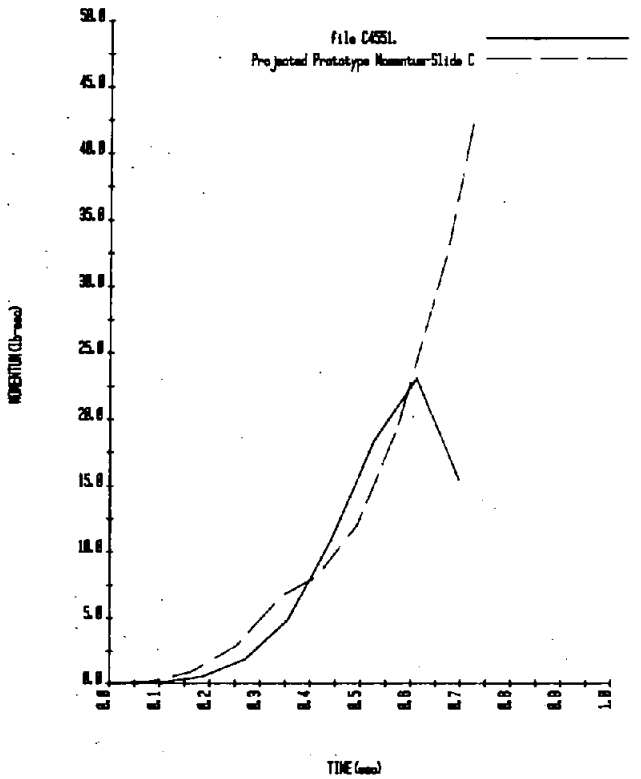

Figure A-30.—Momentum versus time — test C4551.

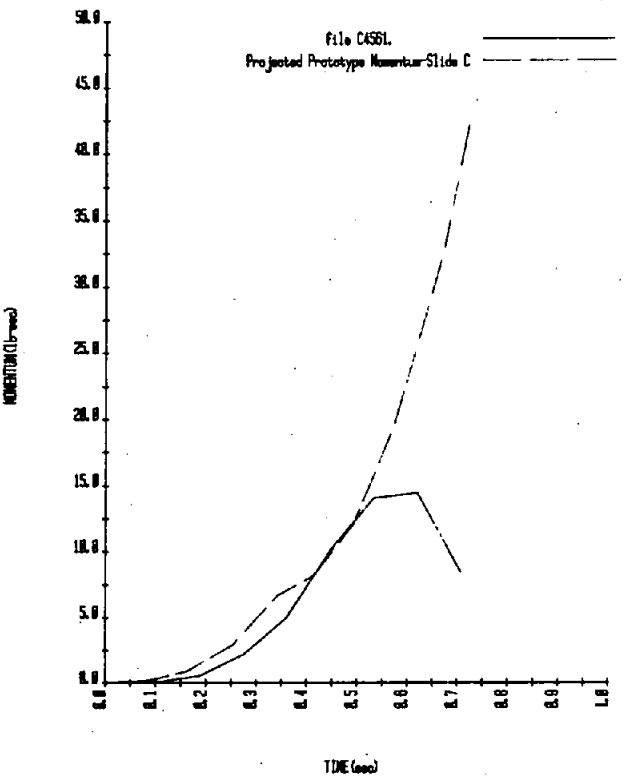

Figure A-31.—Momentum versus time — test C4561.

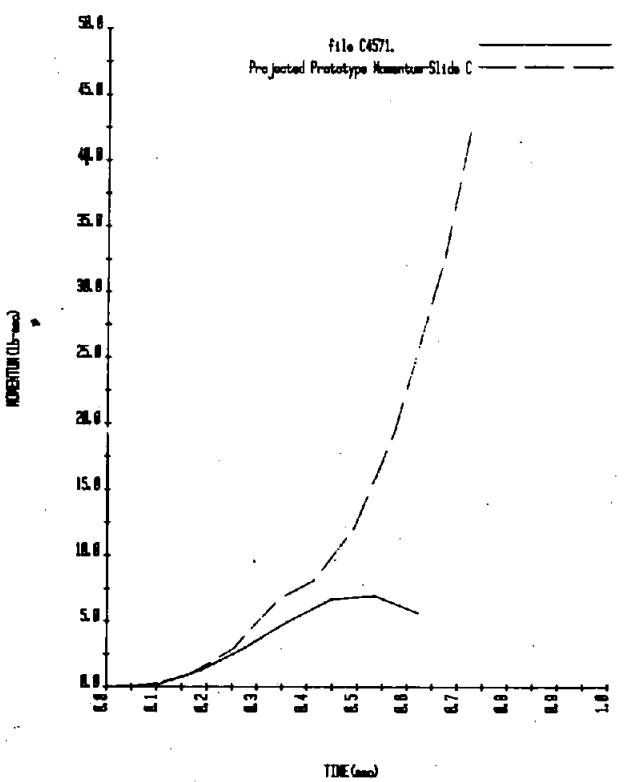

Figure A-32.—Momentum versus time — test C4571.

APPENDIX B

Figures B-1 through B-31 are wave traces for the 14 wave measurement locations. Figure B-32 contains wave traces for one test over a period of four cycles of measurement and illustrates how the water surface levels off a few feet higher than the water surface before the tests. Sample wave traces (B-4, B-9, B-10, B-15, B-17, B-18, and B-24) which are referenced in the main body of the report are included as part of appendix B. The entire test results (fig. B-1 through B-32) are contained on 2 color-microfiche located in a pocket attached inside the back cover.

Both color hard copies and slides of appendix B (microfiche) are available at a cost of $ 31.00 and $ 72.00, respectively per set (Prices are subject to change) from Bureau of Reclamation, Engineering and Research Center, PO Box 25007, Denver Federal Center, Bldg. 67, Denver, CO 80225, Attn: 922,

APPENDIX B FIGURES

Figure		Page
B-4	Wave height versus time — test SLA91	41
B-9	Wave height versus time — test SBA11	43
B-10	Wave height versus time — test SAB11	45
B-15	Wave height versus time — test SLB51	47
B-17	Wave height versus time — test B4511	49
B-18	Wave height versus time — test B4521	51
B-24	Wave height versus time — test SLC61	53

MICROFICHE FIGURES

		MF Numbers*
B-1	Wave height versus time — test SA611	1–5
B-2	Wave height versus time — test SLA71	6–10
B-3	Wave height versus time — test SLA81	11–15
B-4	Wave height versus time — test SLA91	16–20
B-5	Wave height versus time — test SA101	21–25
B-6	Wave height versus time — test SA111	26–30
B-7	Wave height versus time — test SA121	31–35
B-8	Wave height versus time — test SA131	36–40
B-9	Wave height versus time — test SBA11	41–45
B-10	Wave height versus time — test SAB11	46–50
B-11	Wave height versus time — test SLB11	51–54
B-12	Wave height versus time — test SLB21	55–59
B-13	Wave height versus time — test SLB31	60–64
B-14	Wave height versus time — test SLB41	65–69
B-15	Wave height versus time — test SLB51	70–74
B-16	Wave height versus time — test SLB71	75–79
B-17	Wave height versus time — test B4511	80–84
B-18	Wave height versus time — test B4521	85–89
B-19	Wave height versus time — test B4531	90–94
B-20	Wave height versus time — test B4541	95–99
B-21	Wave height versus time — test SLC21	100–104
B-22	Wave height versus time — test SLC41	105–109
B-23	Wave height versus time — test SLC51	110–114
B-24	Wave height versus time — test SLC61	115–119
B-25	Wave height versus time — test SLC71	120–124
B-26	Wave height versus time — test SLC81	125–129
B-27	Wave height versus time — test C4521	130–133

MICROFICHE FIGURES—Continued

		MF Numbers*
B-28	Wave height versus time — test C4531	134–137
B-29	Wave height versus time — test C4551	138–142
B-30	Wave height versus time — test C4561	143–147
B-31	Wave height versus time — test C4571	148–152
B-32	Wave height versus time — test SLA9 (4 Files)	153

*MF Numbers = Microfiche numbers

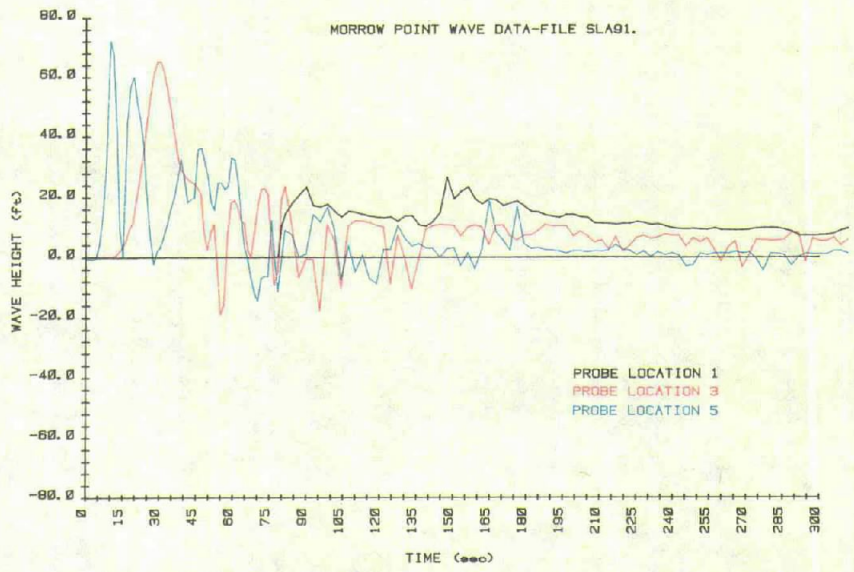

Figure B-4.—Wave height versus time — test SLA91 (1 of 5).

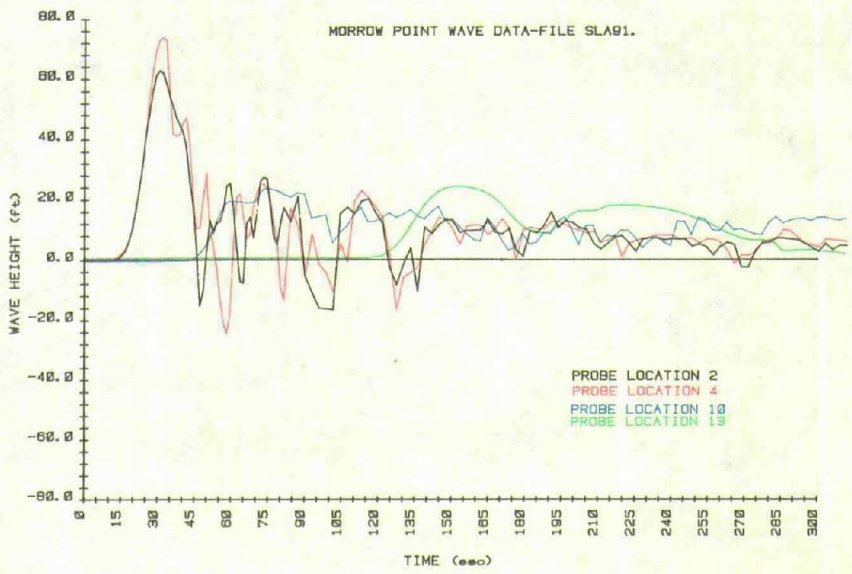

Figure B-4.—Wave height versus time — test SLA91 (2 of 5).

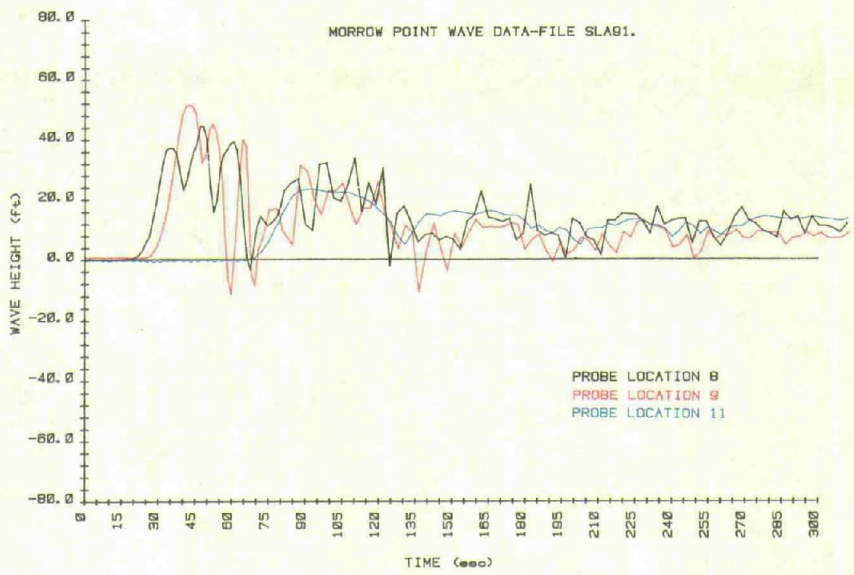

Figure B-4.—Wave height versus time — test SLA91 (3 of 5).

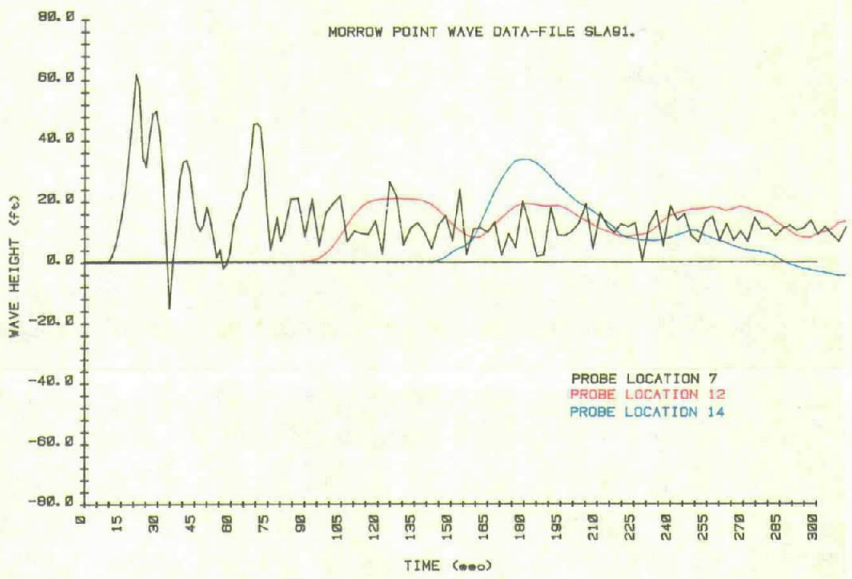

Figure B-4.—Wave height versus time — test SLA91 (4 of 5).

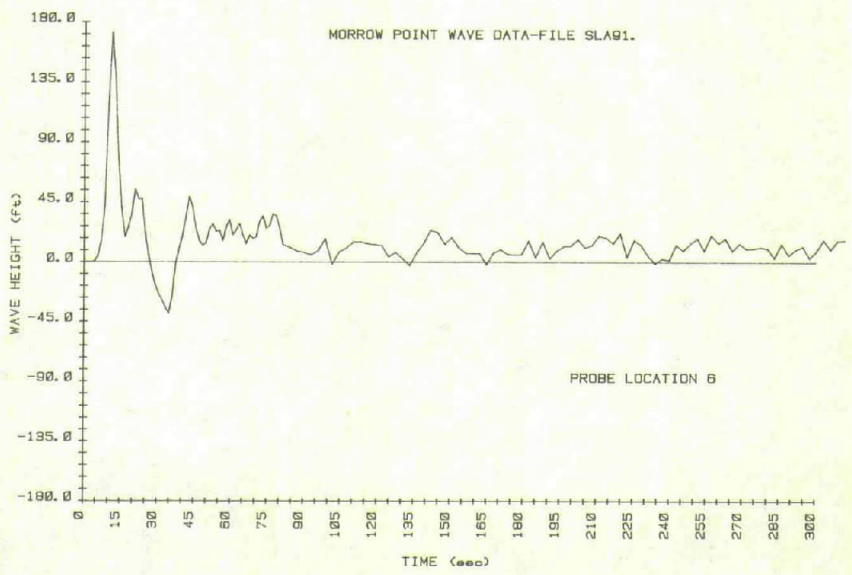

Figure B-4.—Wave height versus time — test SLA91 (5 of 5).

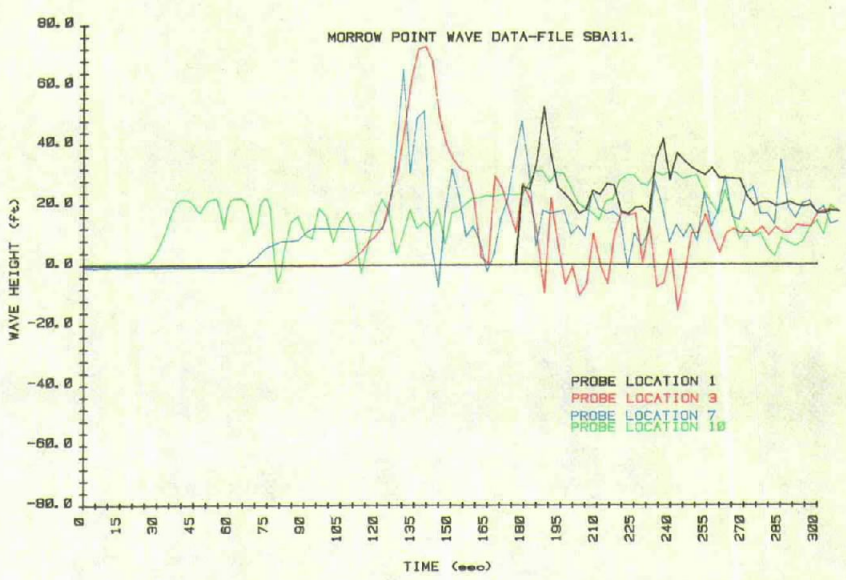

Figure B-9.—Wave height versus time — test SBA11 (1 of 5).

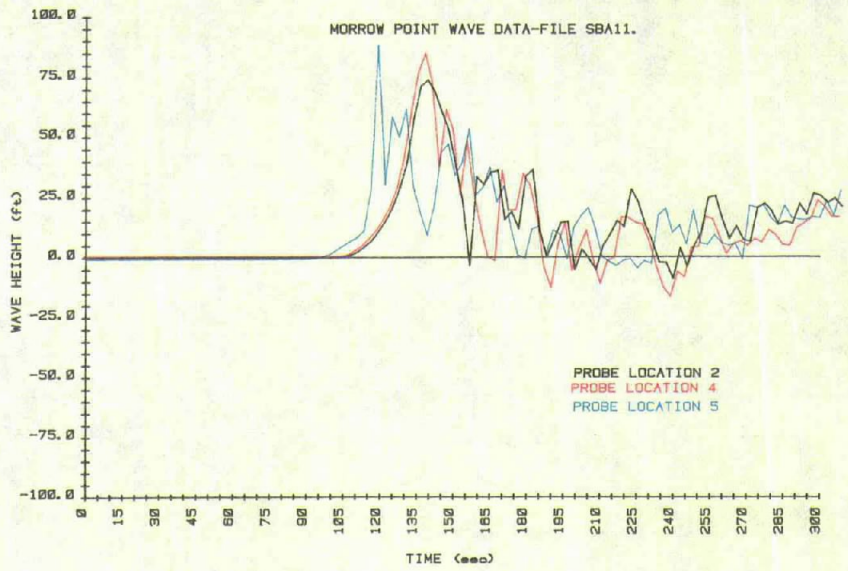

Figure B-9.—Wave height versus time — test SBA11 (2 of 5).

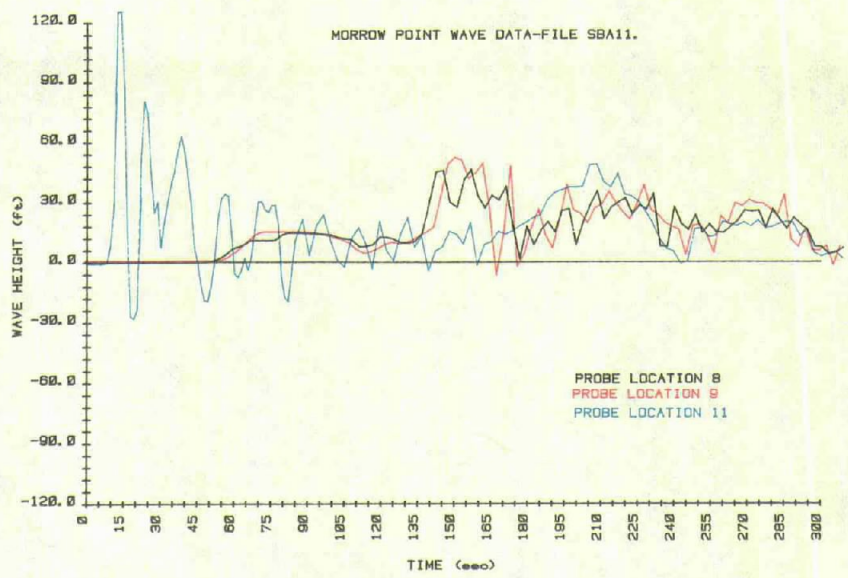

Figure B-9.—Wave height versus time — test SBA11 (3 of 5).

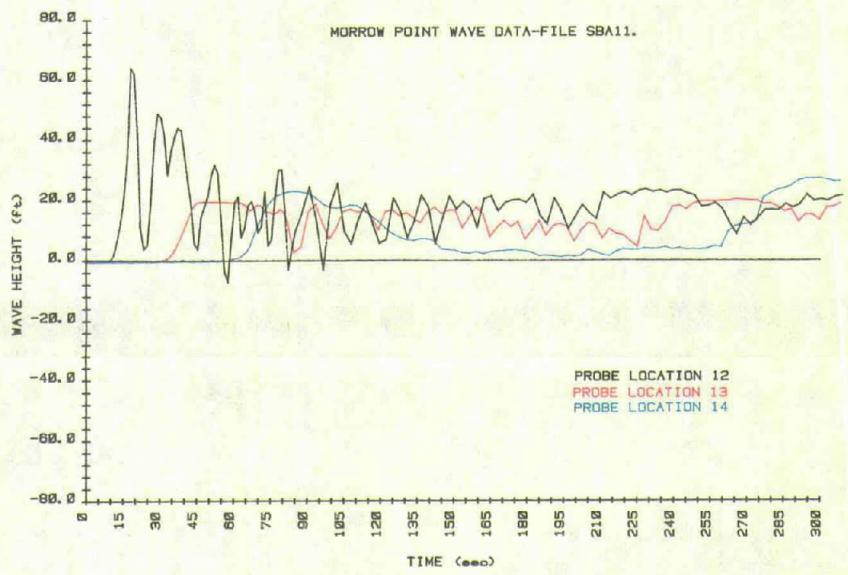

Figure B-9.—Wave height versus time — test SBA11 (4 of 5).

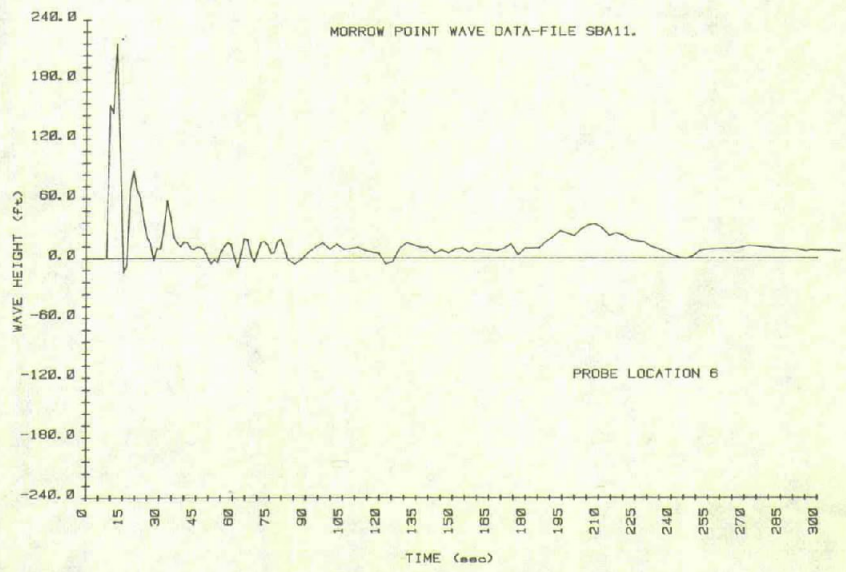

Figure B-9.—Wave height versus time — test SBA11 (5 of 5).

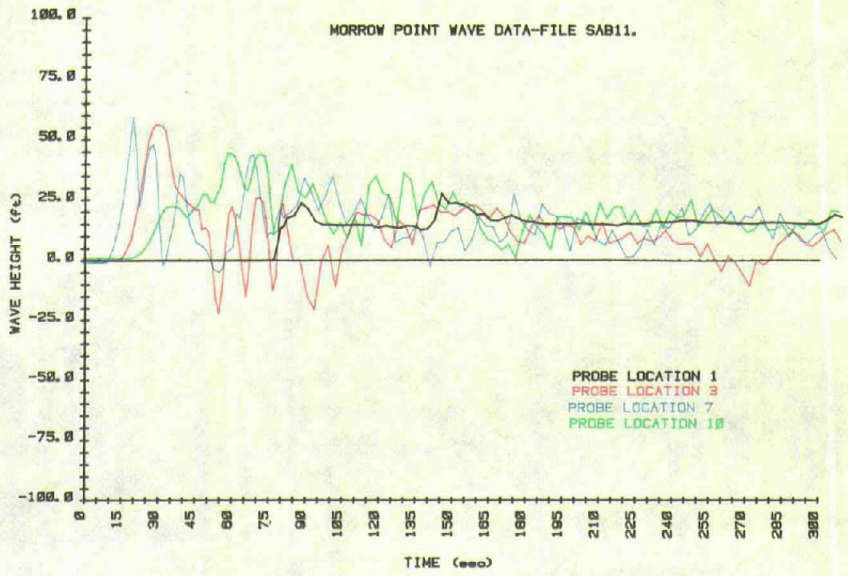

Figure B-10.—Wave height versus time — test SAB11 (1 of 5).

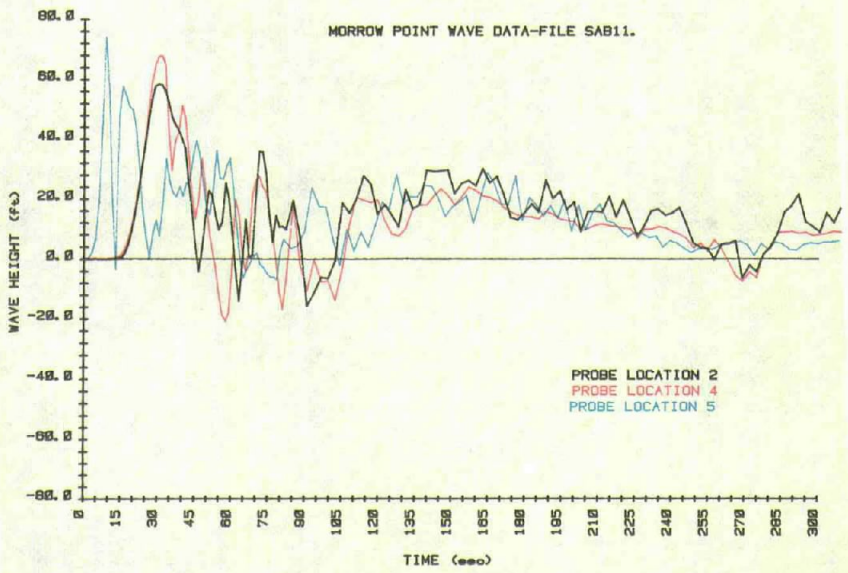

Figure B-10.—Wave height versus time — test SAB11 (2 of 5).

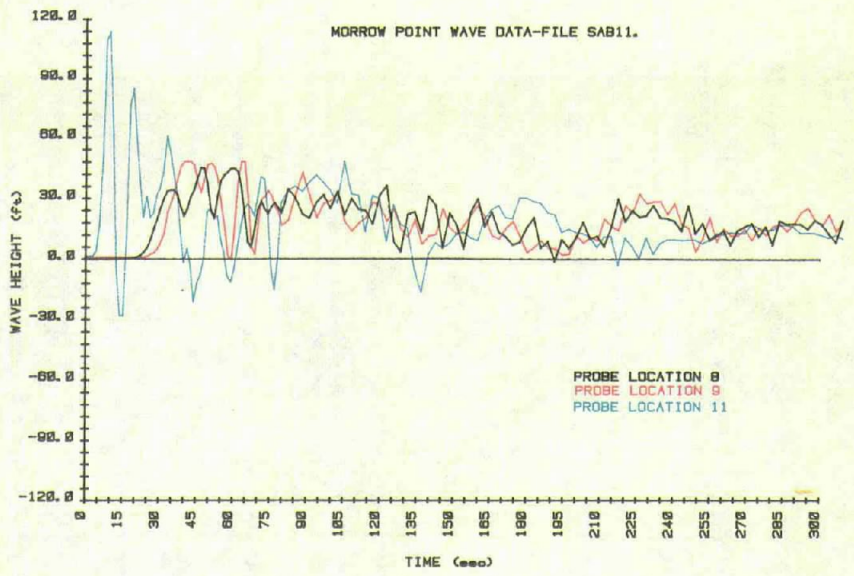

Figure B-10.—Wave height versus time — test SAB11 (3 of 5).

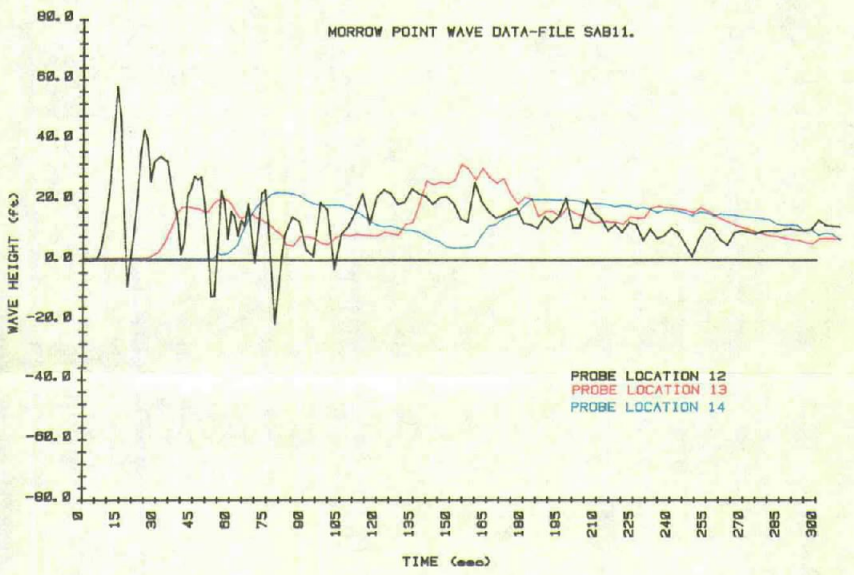

Figure B-10.—Wave height versus time — test SAB11 (4 of 5).

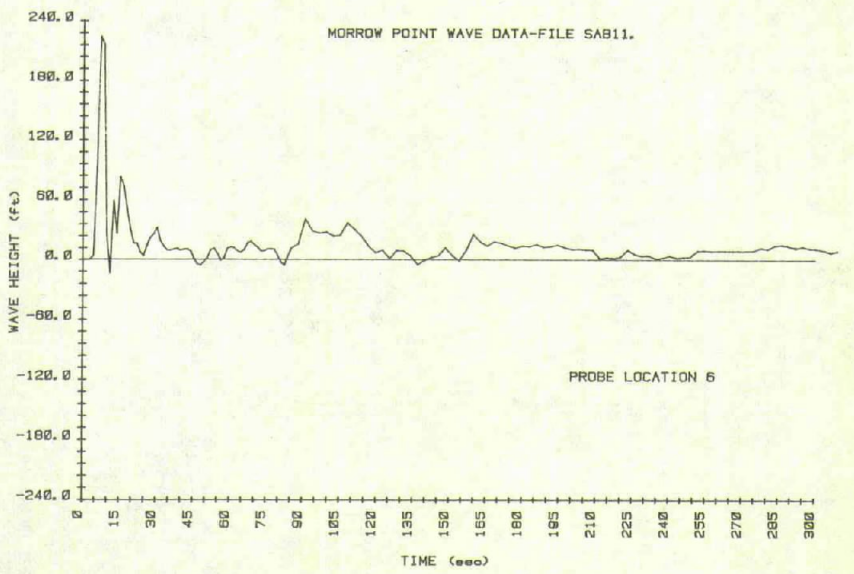

Figure B-10.—Wave height versus time — test SAB11 (5 of 5).

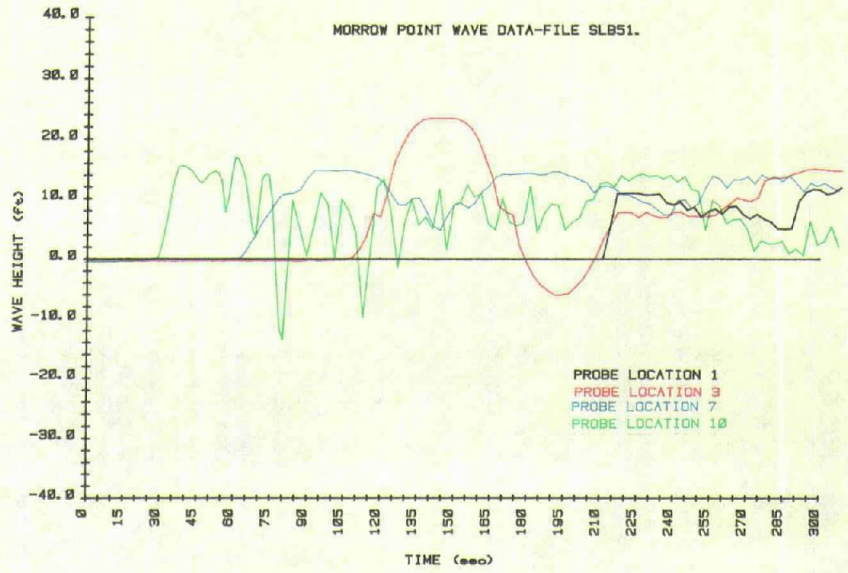

Figure B-15.—Wave height versus time — test SLB51 (1 of 5).

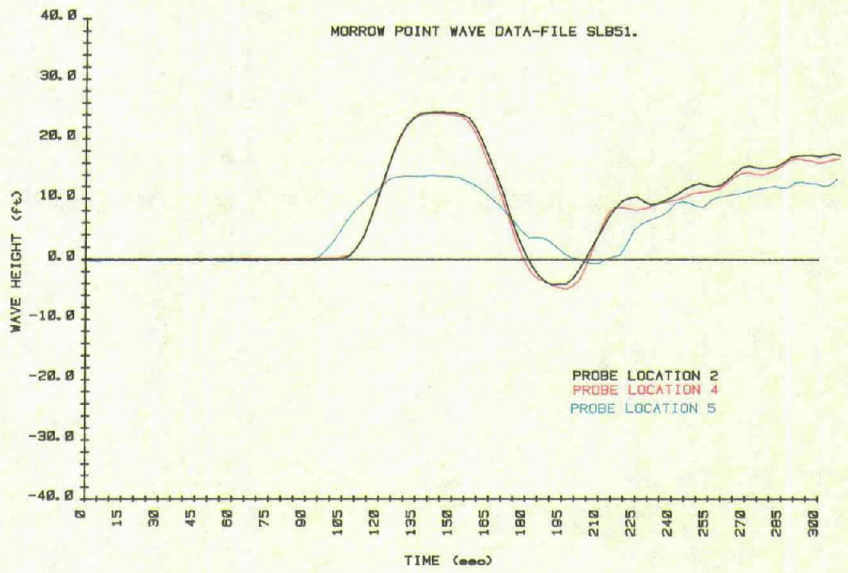

Figure B-15.—Wave height versus time — test SLB51 (2 of 5).

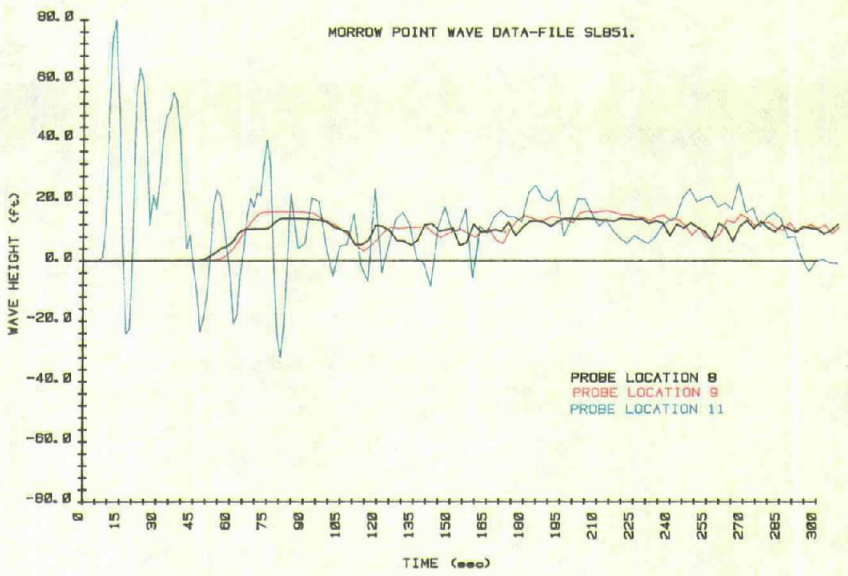

Figure B-15.—Wave height versus time — test SLB51 (3 of 5).

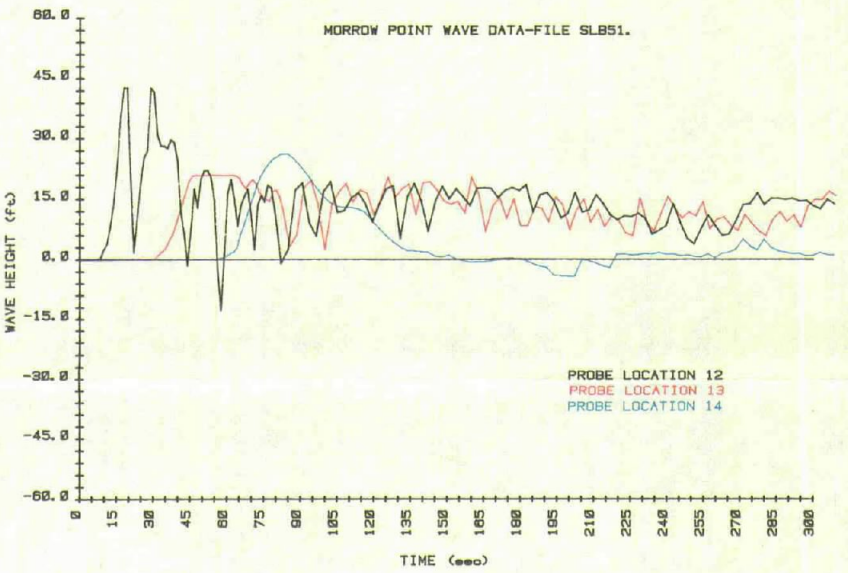

Figure B-15.—Wave height versus time — test SLB51 (4 of 5).

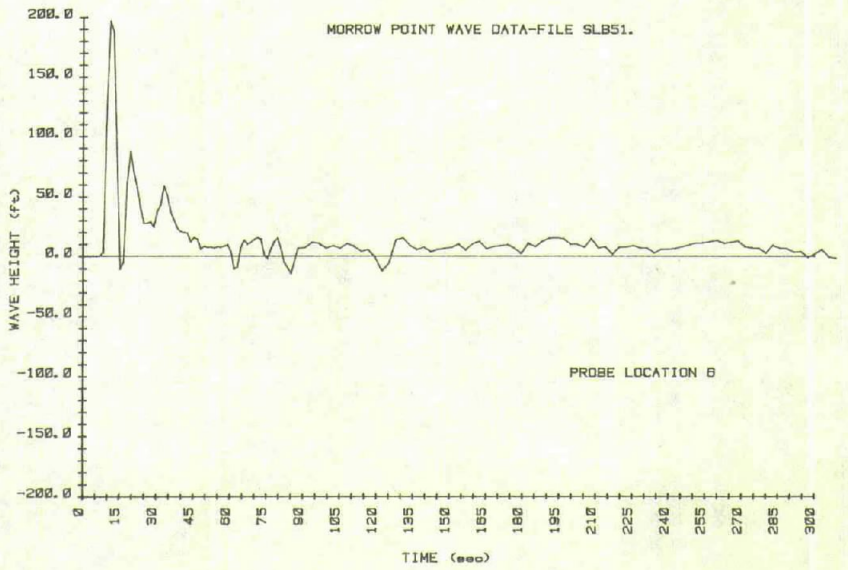

Figure B-15.—Wave height versus time — test SLB51 (5 of 5).

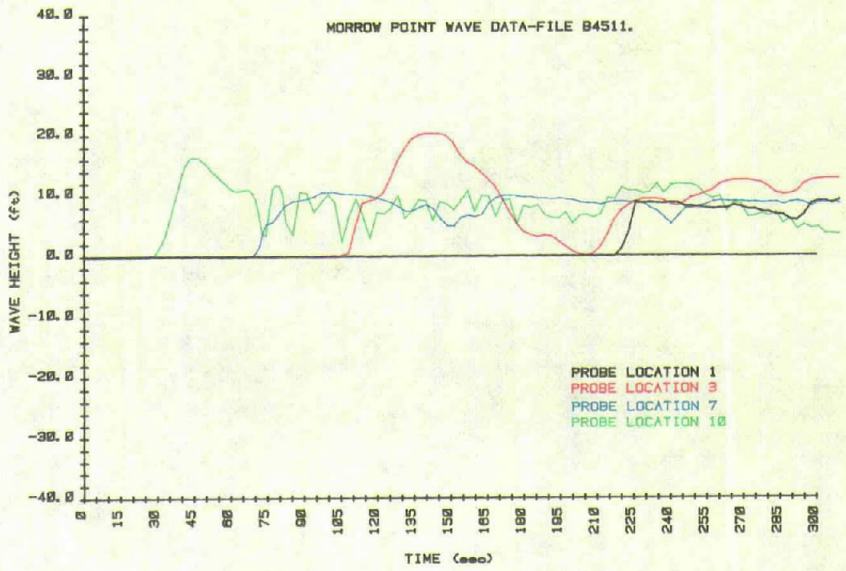

Figure B-17.—Wave height versus time — test B4511 (1 of 5).

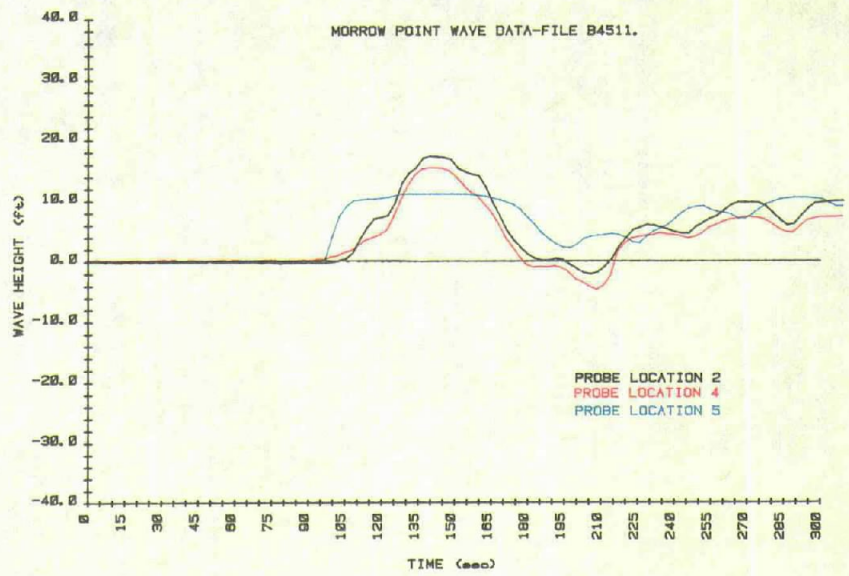

Figure B-17.—Wave height versus time — test B4511 (2 of 5).

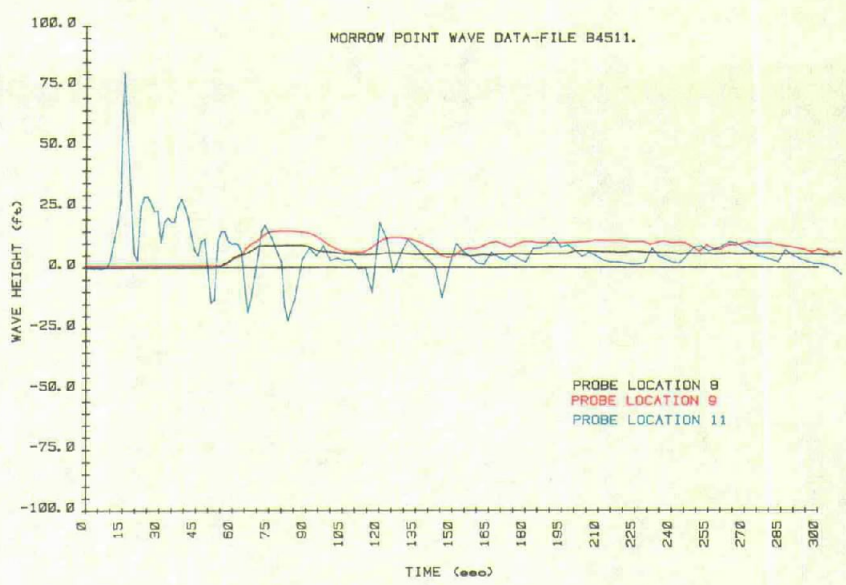

Figure B-17.—Wave height versus time — test B4511 (3 of 5).

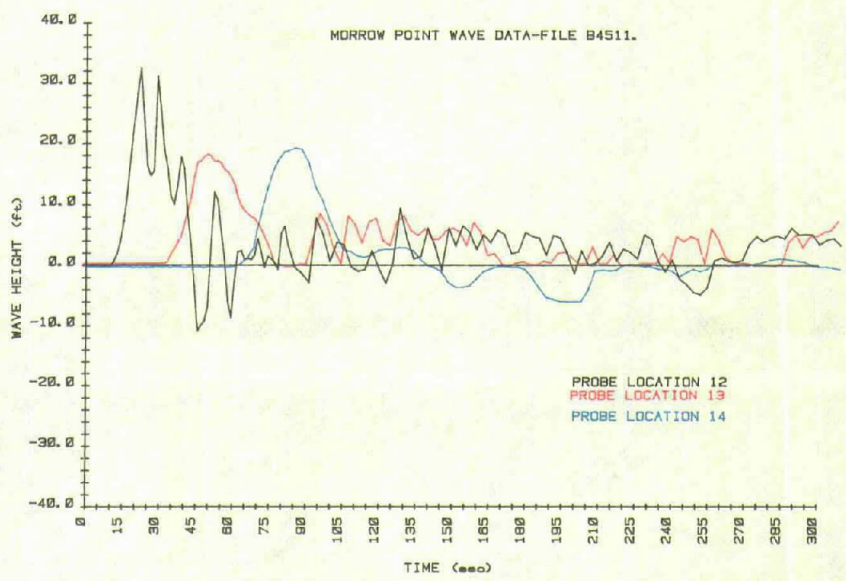

Figure B-17.—Wave height versus time — test B4511 (4 of 5).

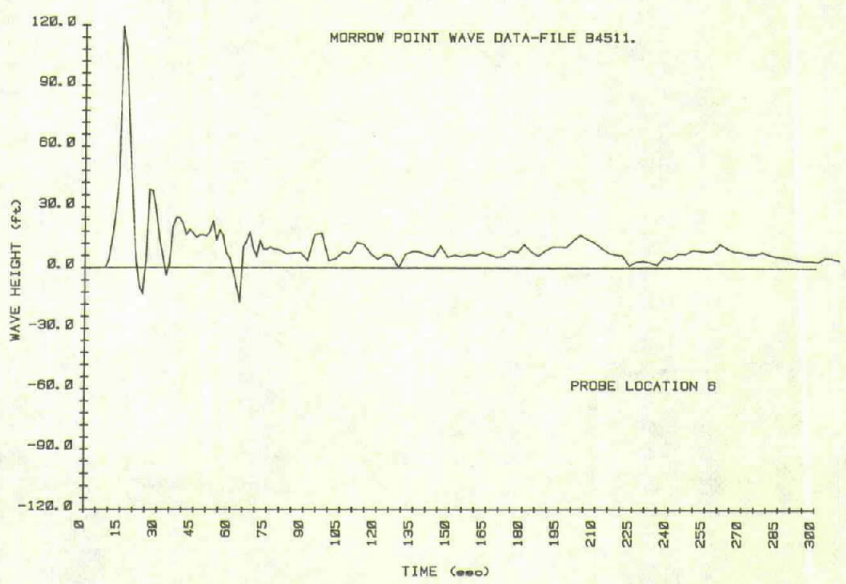

Figure B-17.—Wave height versus time — test B4511 (5 of 5).

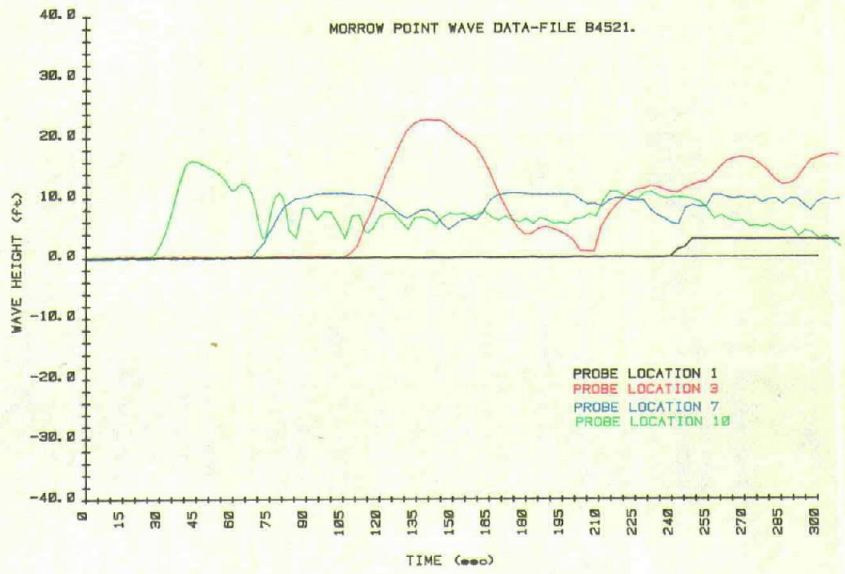

Figure B-18.—Wave height versus time — test B4521 (1 of 5).

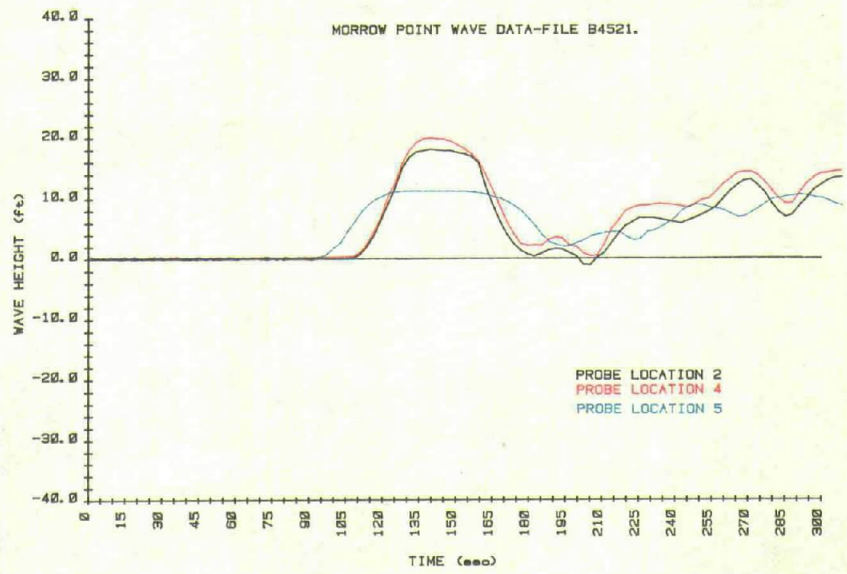

Figure B-18.—Wave height versus time — test B4521 (2 of 5).

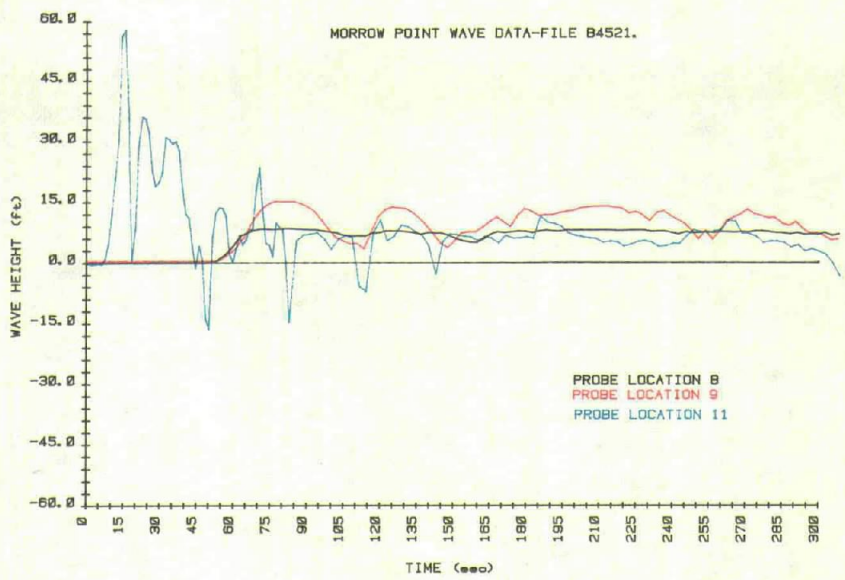

Figure B-18.—Wave height versus time — test B4521 (3 of 5).

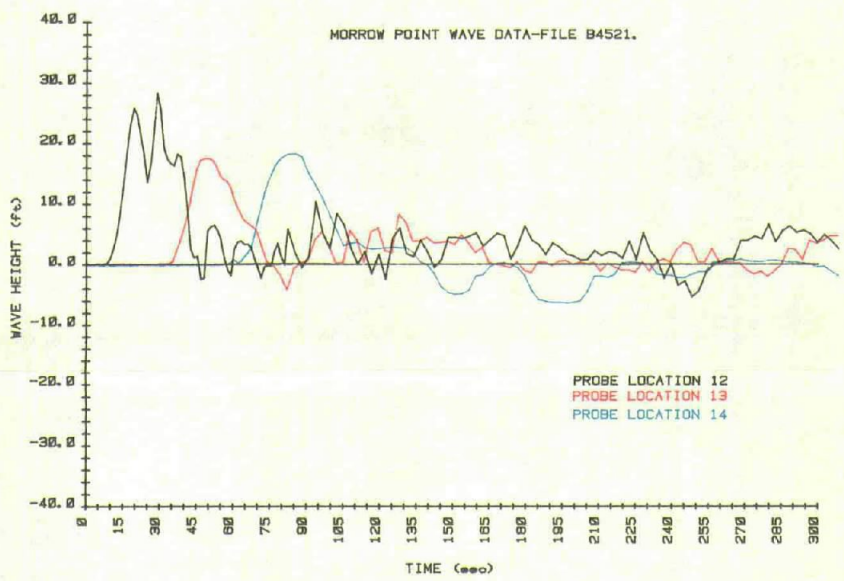

Figure B-18.—Wave height versus time — test B4521 (4 of 5).

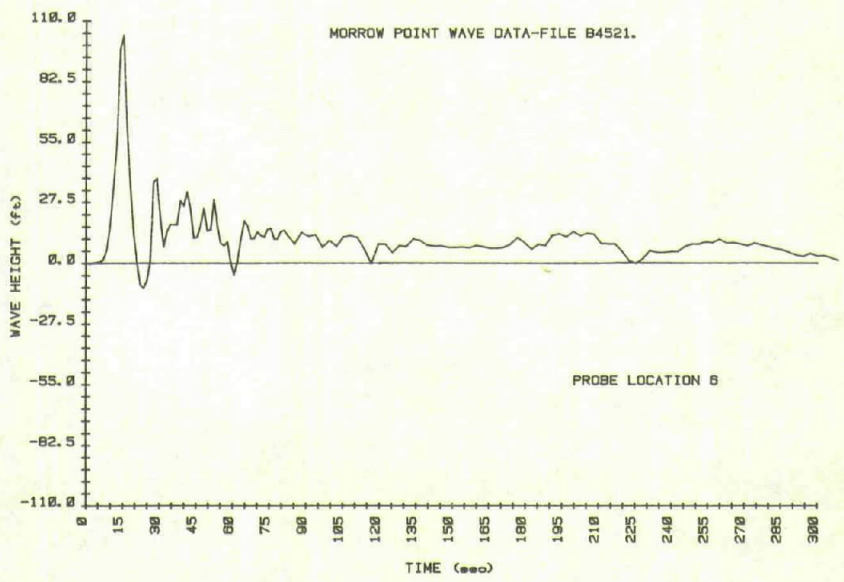

Figure B-18.—Wave height versus time — test B4521 (5 of 5).

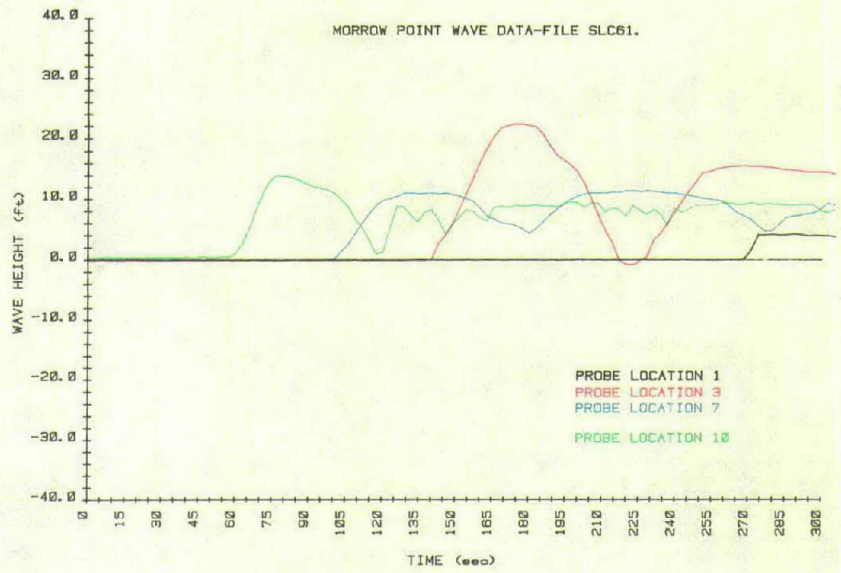

Figure B-24.—Wave height versus time — test SLC61 (1 of 5).

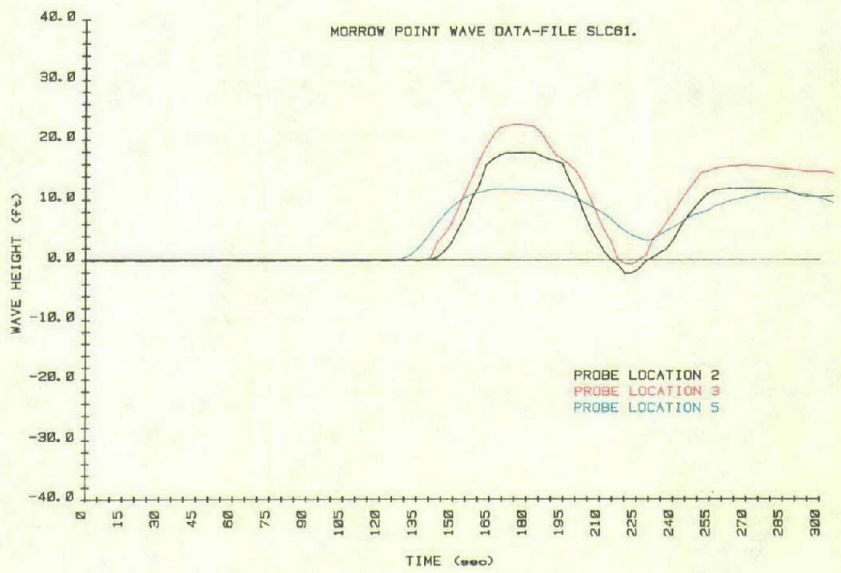

Figure B-24.—Wave height versus time — test SLC61 (2 of 5).

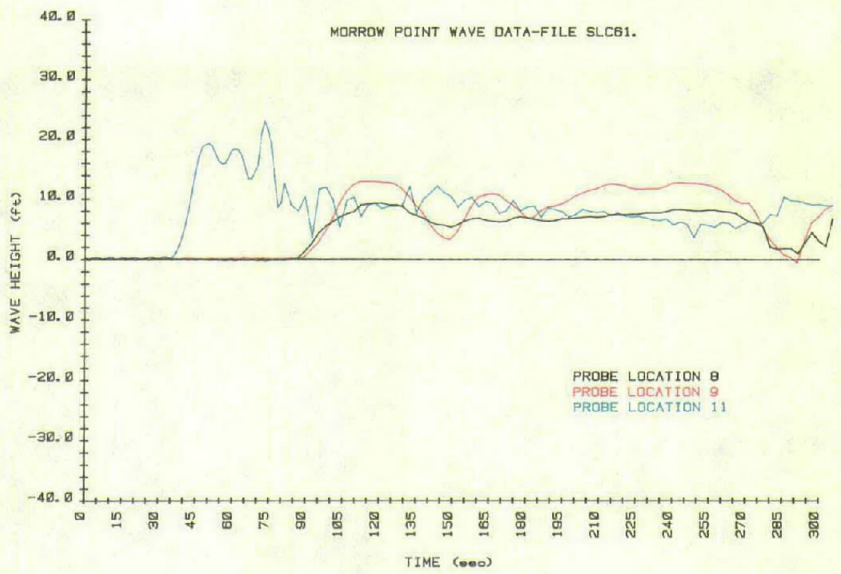

Figure B-24.—Wave height versus time — test SLC61 (3 of 5).

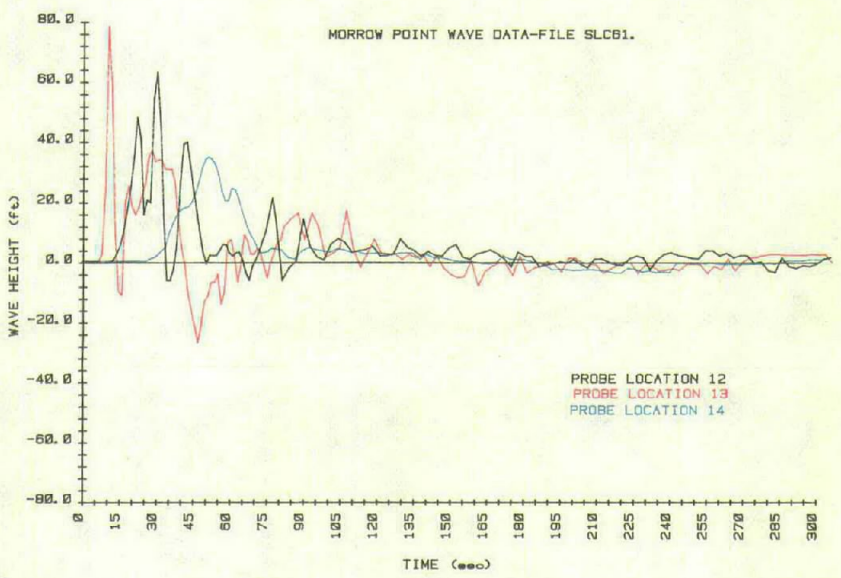

Figure B-24.—Wave height versus time — test SLC61 (4 of 5).

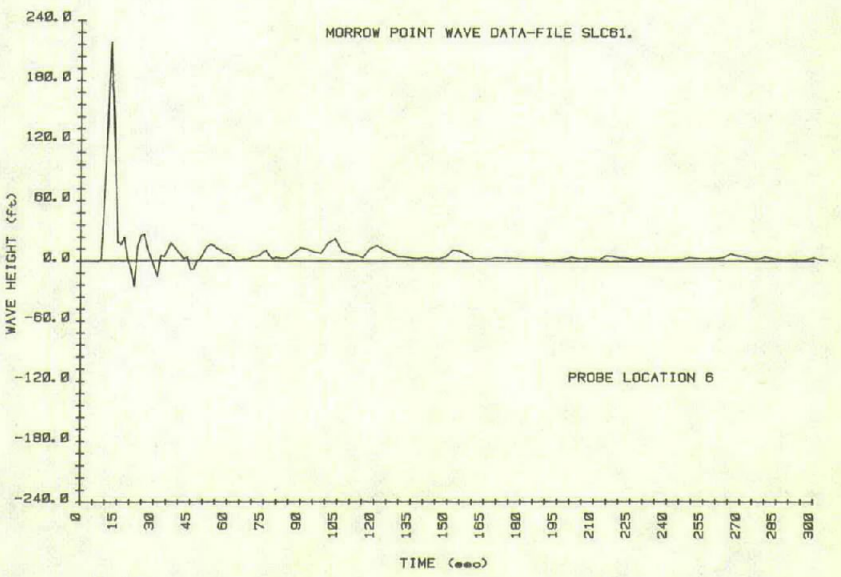

Figure B-24.—Wave height versus time — test SLC61 (5 of 5).

GPO 834-809

A free pamphlet is available from the Bureau of Reclamation entitled, "Publications for Sale". It describes some of the technical publications currently available, their cost, and how to order them. The pamphlet can be obtained upon request to the Bureau of Reclamation, E&R Center, PO Box 25007, Denver Federal Center, Bldg. 67, Denver, CO 80225, Attn: 922.

Burgi
D-1533

DEPARTMENT OF THE INTERIOR
MARCH 3, 1849

U.S. DEPARTMENT OF THE INTERIOR

BUREAU OF RECLAMATION

UNITED STATES DEPARTMENT OF THE INTERIOR
Bureau of Reclamation
Engineering and Research Center
P.O. Box 25007
Building 67, Denver Federal Center
Denver, Colorado 80225

THESE ARE REPRODUCTIONS OF RESEARCH REPORTS ISSUED BY THE BUREAU OF RECLAMATION, ENGINEERING AND RESEARCH CENTER. THEY WERE MICROFILMED BY THE MICROGRAPHICS UNIT OF THE E & R CENTER IN A MANNER AND ON MICROFILM WHICH MEETS THE RECOMMENDED REQUIREMENTS OF THE AMERICAN NATIONAL STANDARD INSTITUTE (ANSI) FOR PERMANENT MICROPHOTOGRAPHIC REPRODUCTIONS.

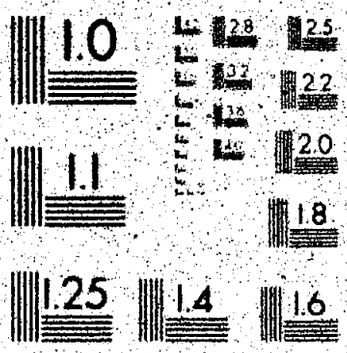

24X

MICROCOPY RESOLUTION TEST CHART
NATIONAL BUREAU OF STANDARDS
STANDARD REFERENCE MATERIAL 1010a
(ANSI and ISO TEST CHART No. 2)

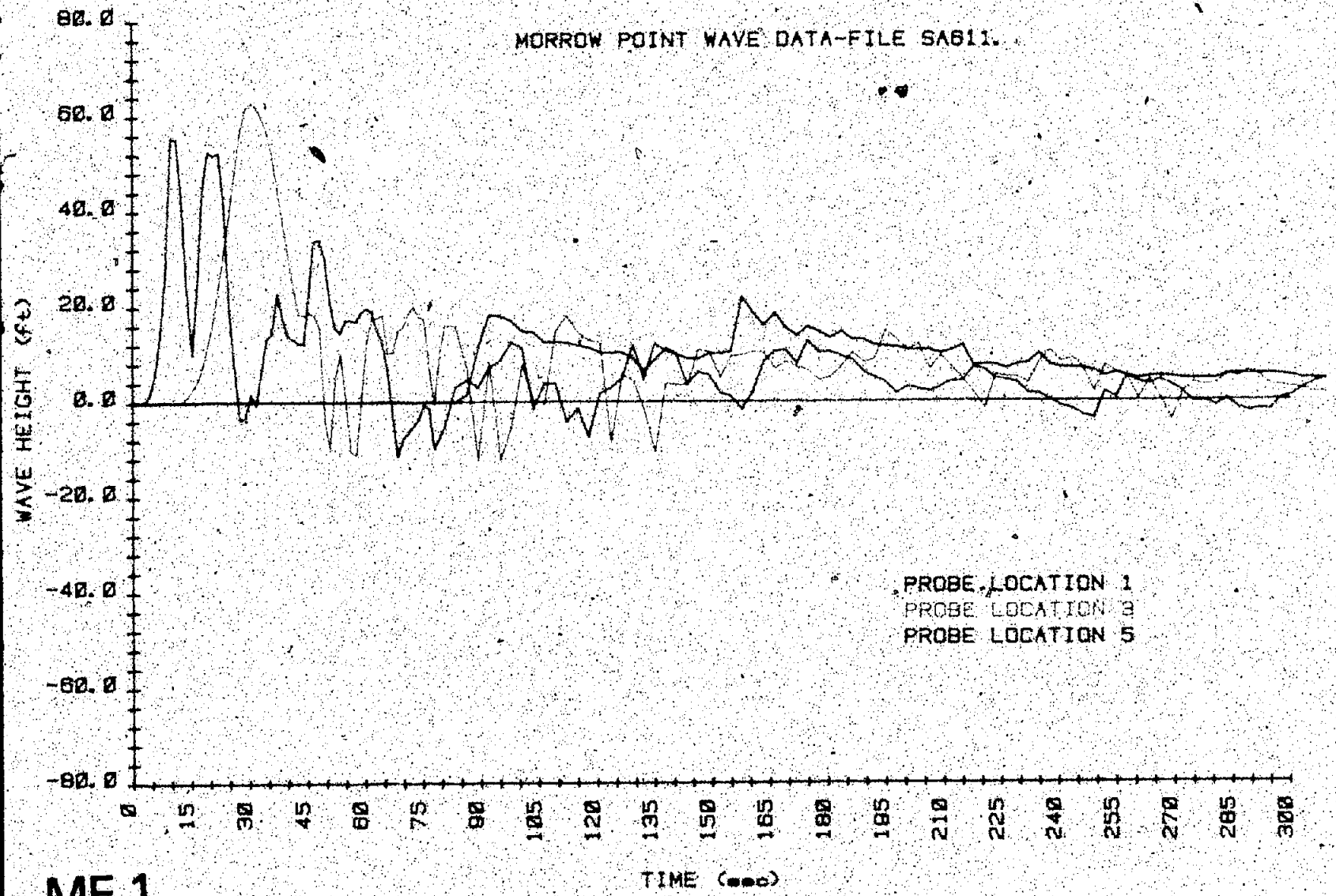

MF 1

Figure B-1.—Wave height versus time — test SA611 (1 of 5).

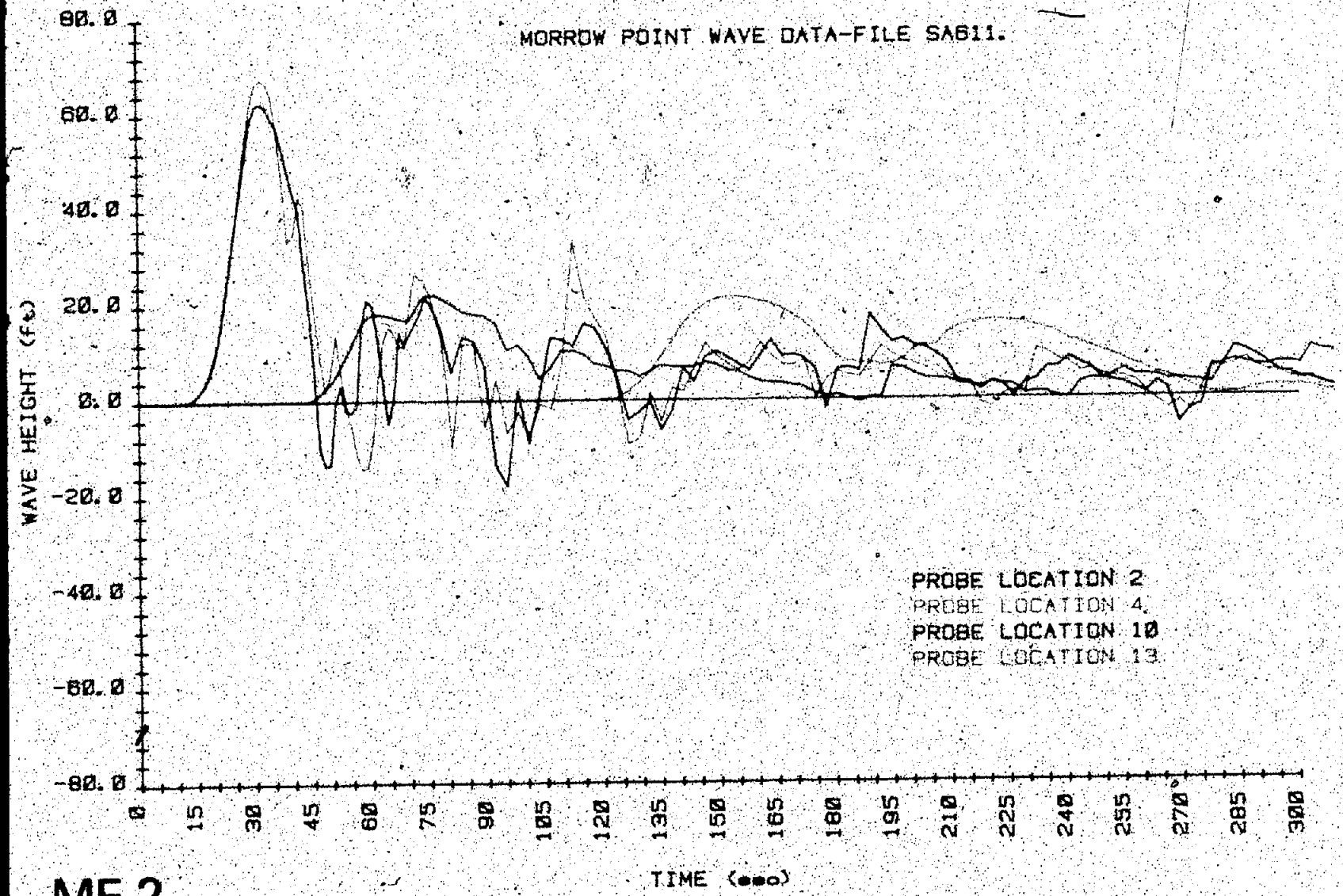

MF 2

Figure B-1. – Wave height versus time – test SA611 (2 of 5).

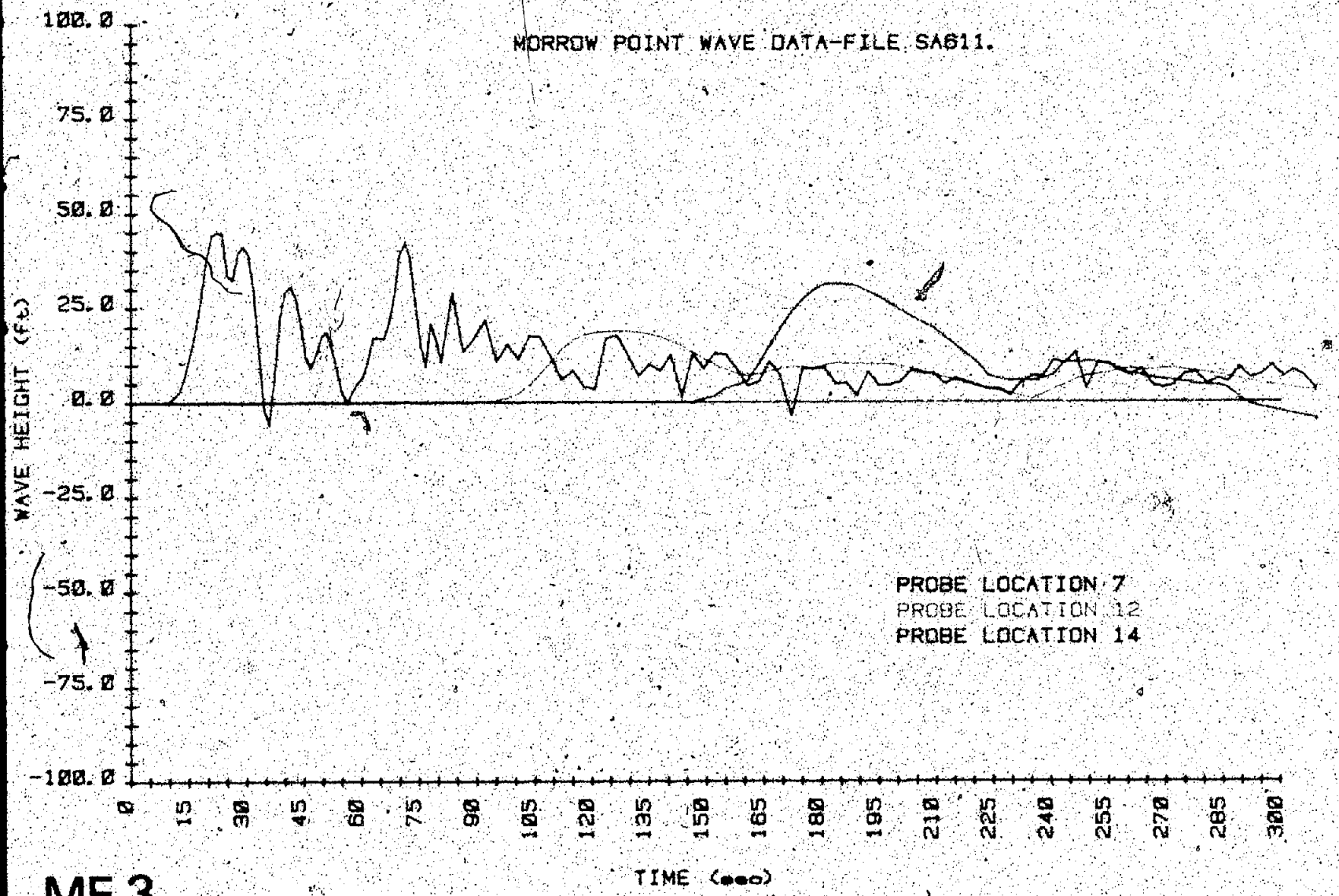

MF 3

Figure B 1. Wave height versus time — test SA611 (3 of 5)

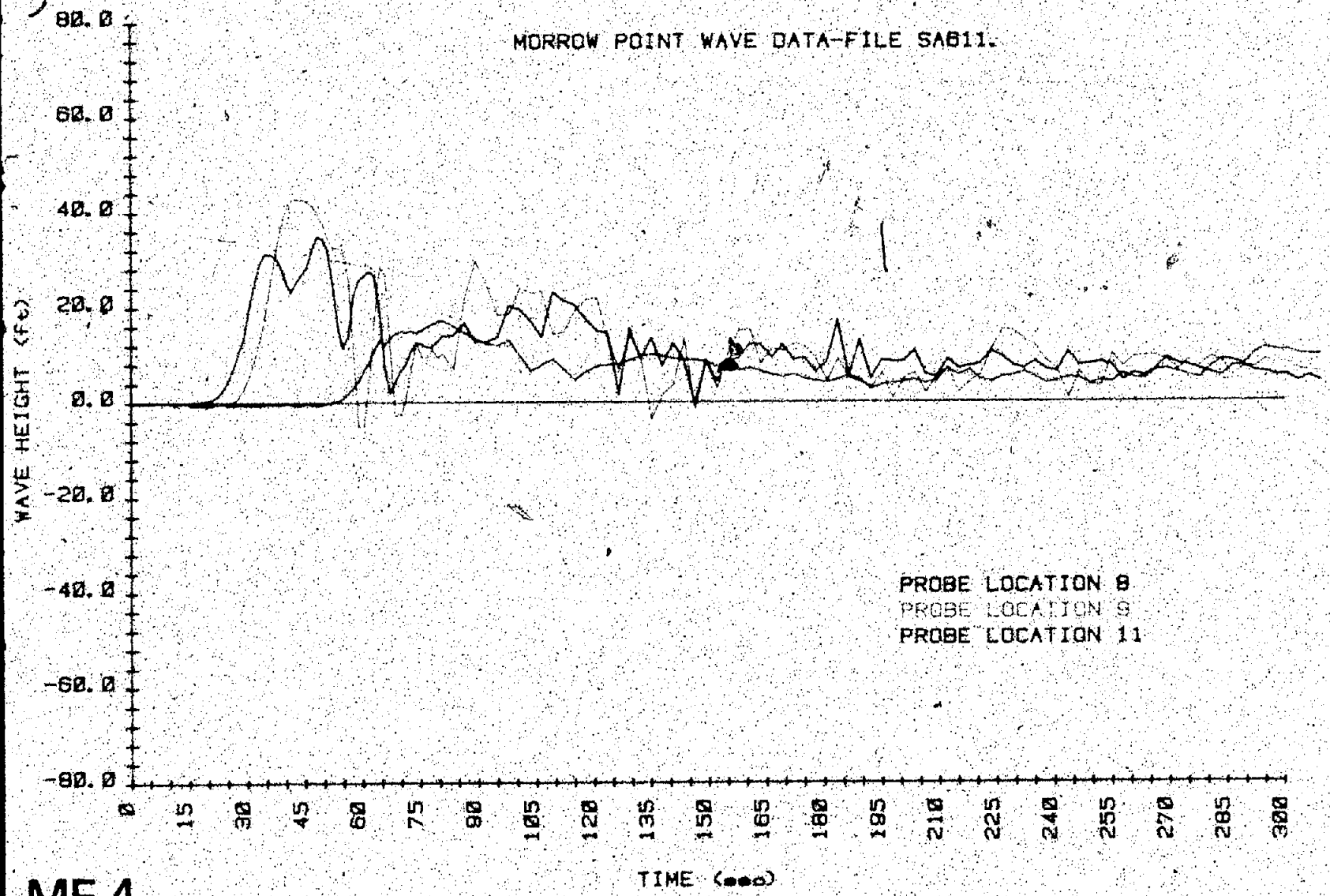

MF 4

Figure B.1 Wave height versus time — test SA611 (4 of 5)

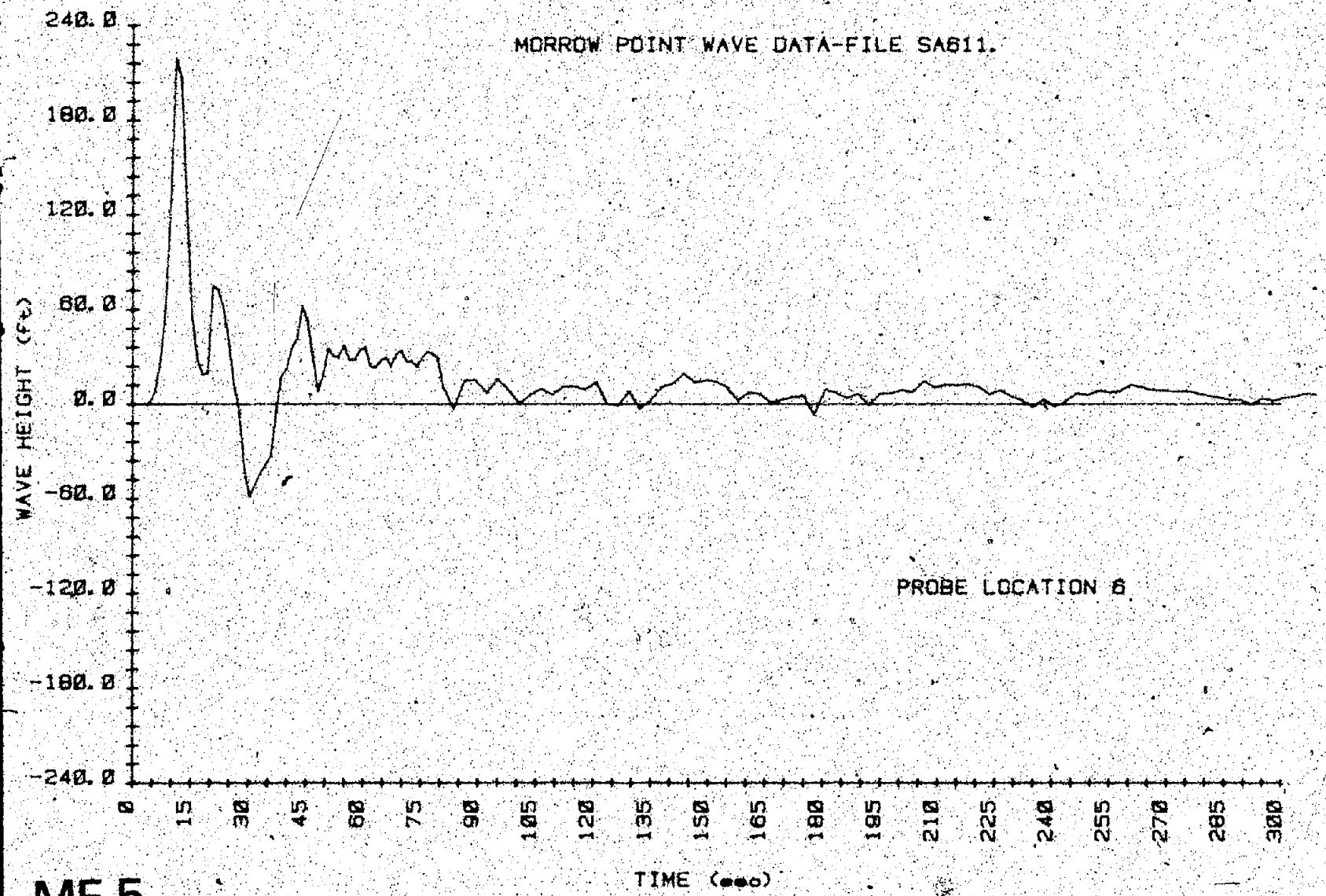

MF 5

Figure B-1. Wave height versus time – test SA611 (5 of 5).

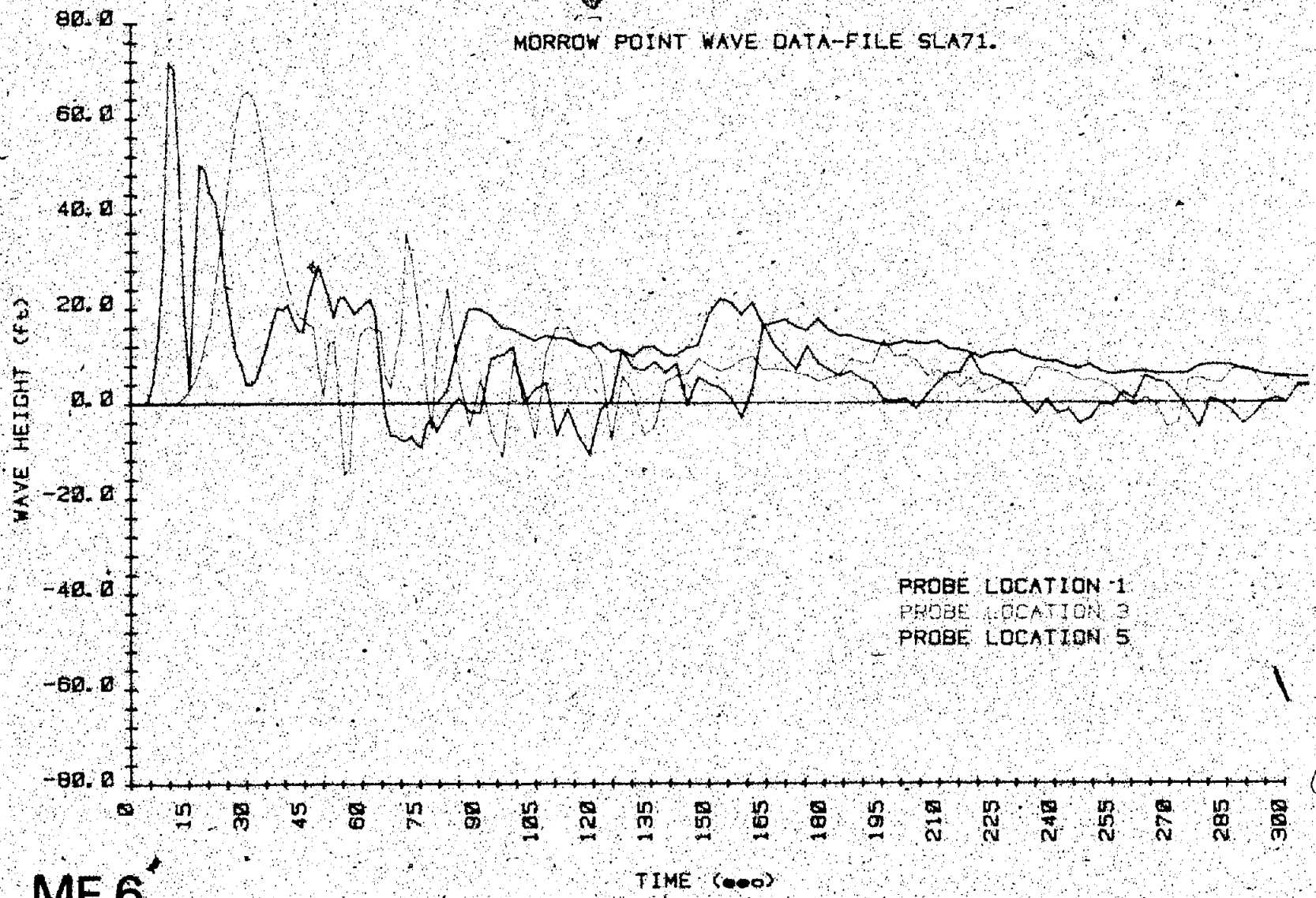

MF 6

Figure B-2. Wave height versus time — test SLA71 (1 of 5).

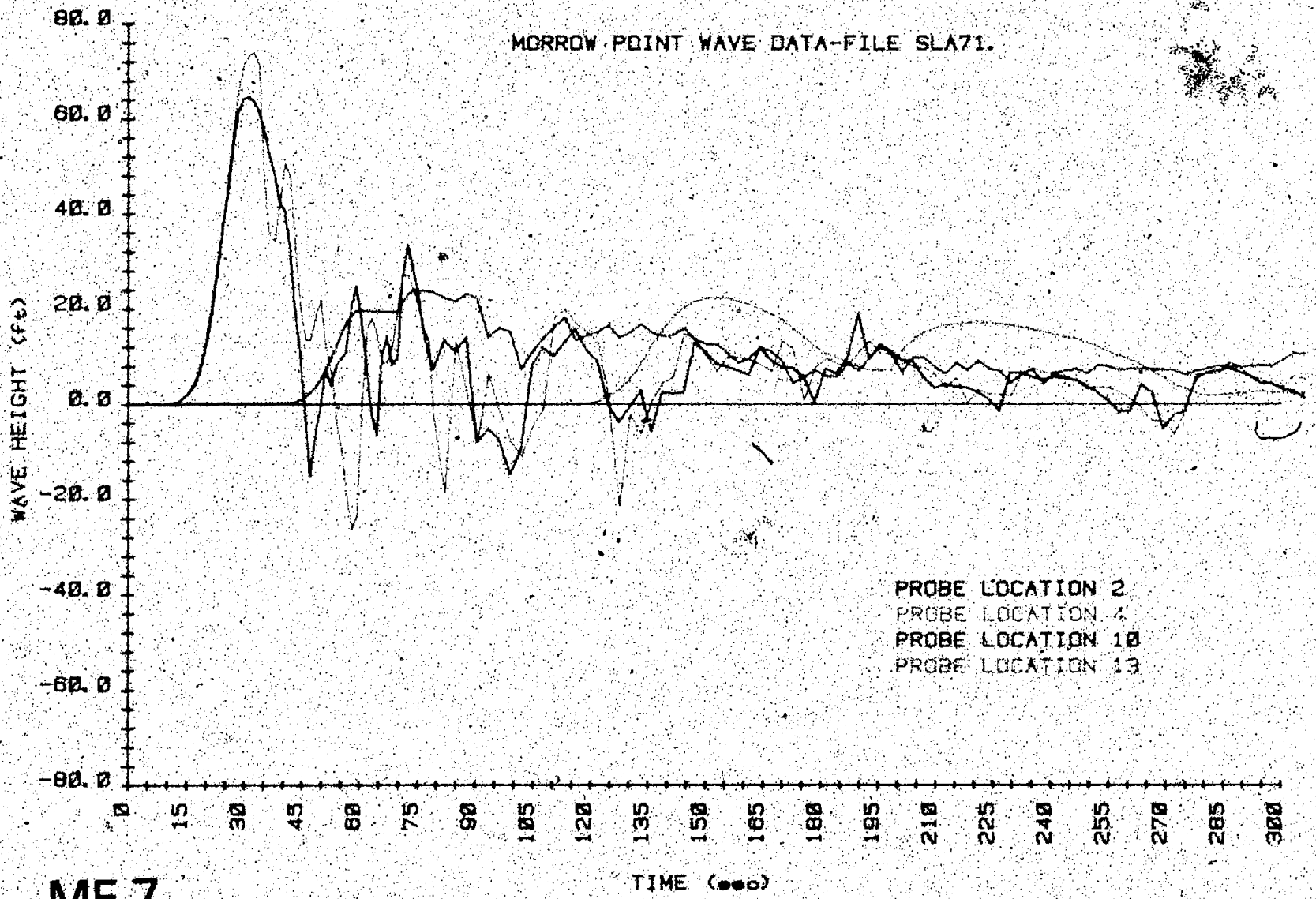

MF 7

Figure B-2.—Wave height versus time — test SLA71 (2 of 5)

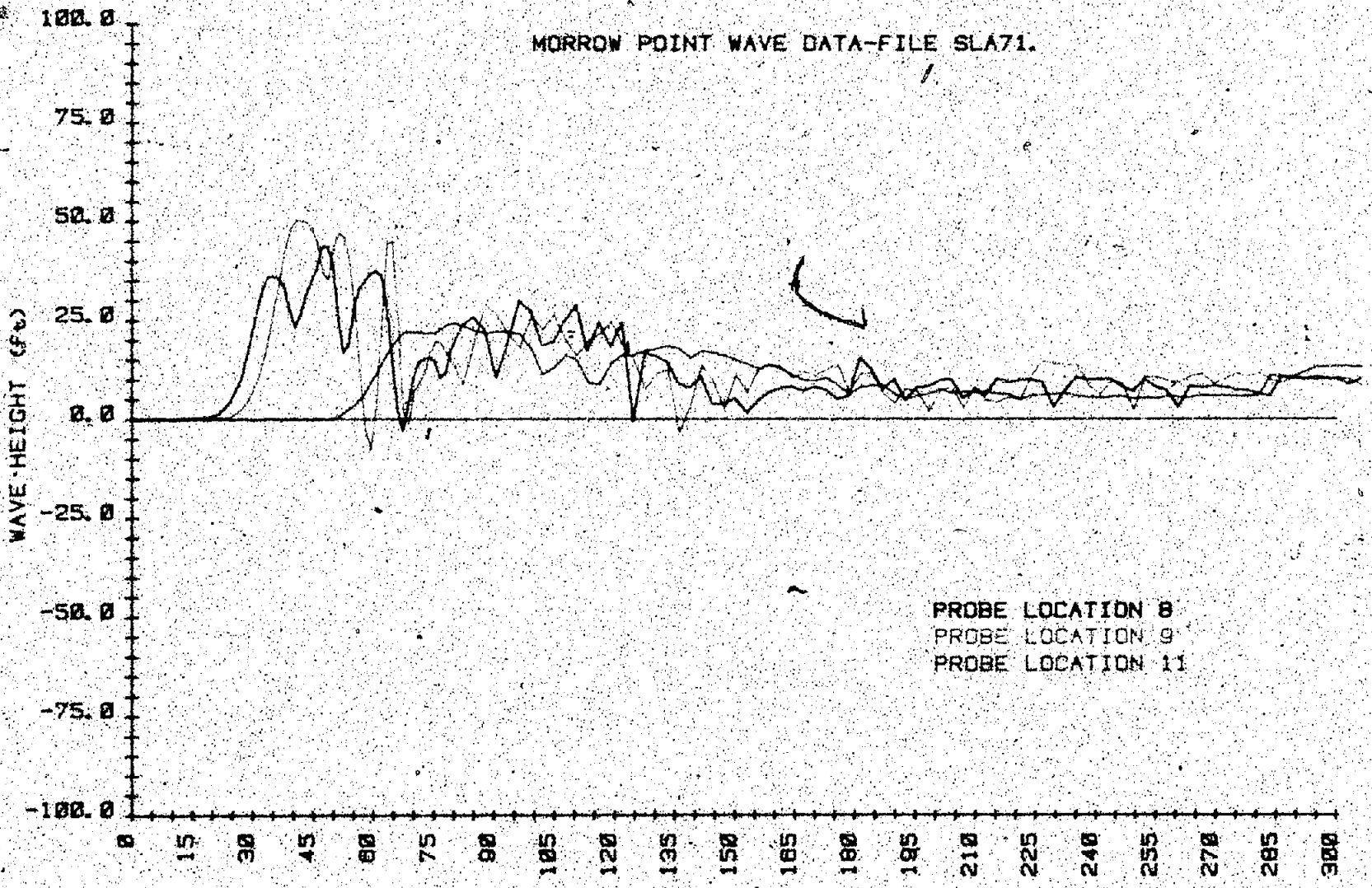

MF 8

Figure B-2 – Wave height versus time – test SLA71 (3 of 5).

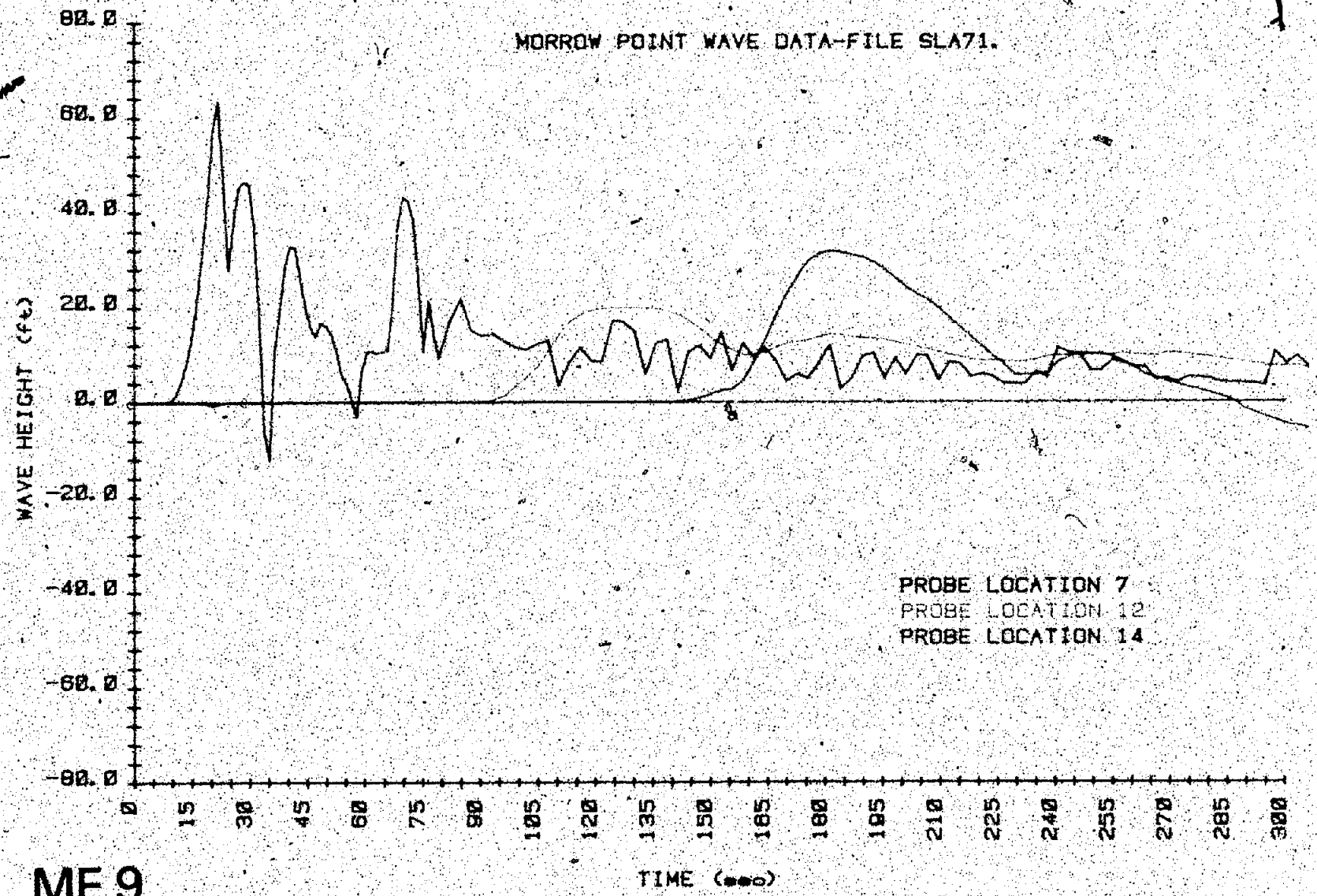

MF 9

Figure B-2.—Wave height versus time — test SLA71 (4 of 5).

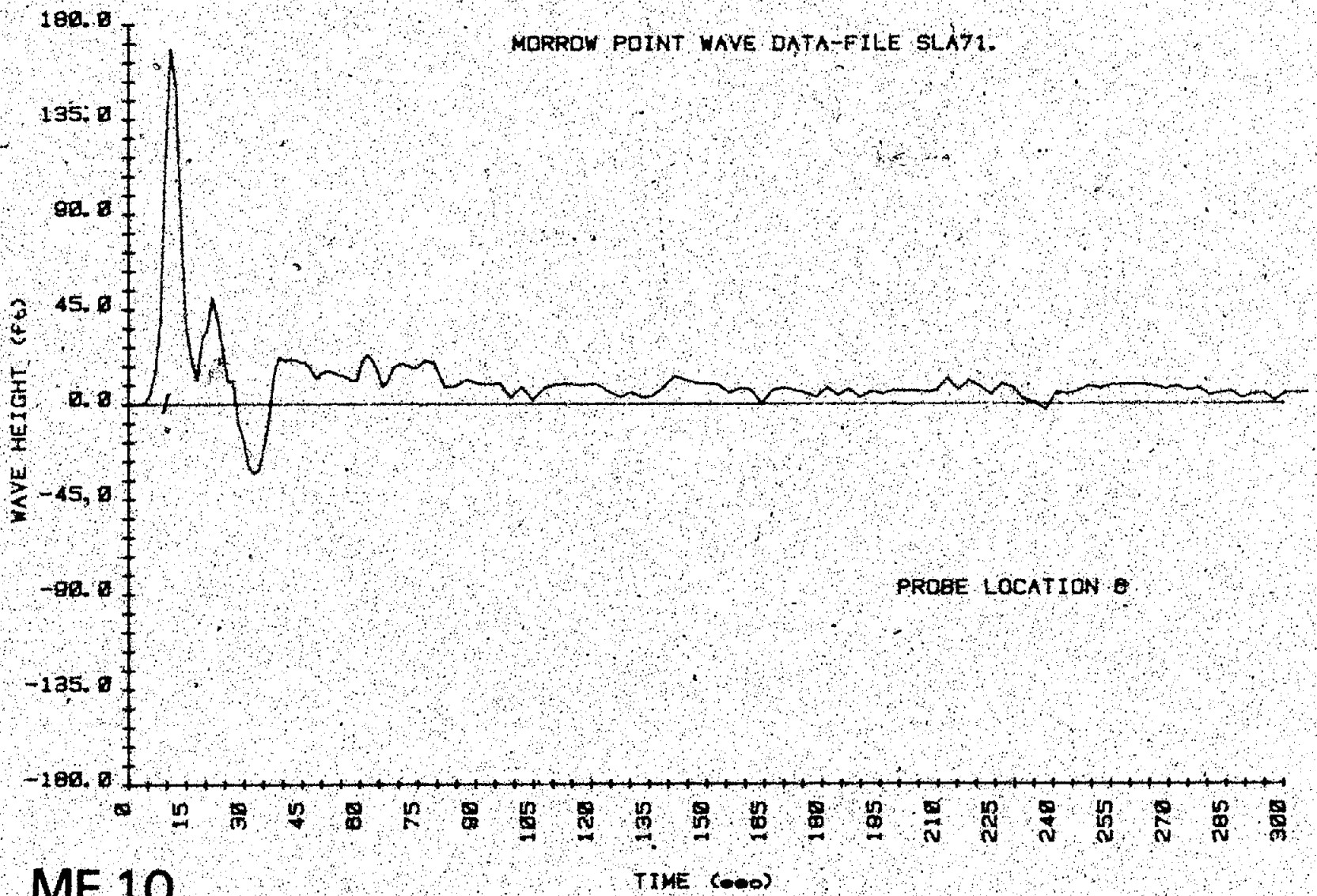

MF 10

Figure B-2 – Wave height versus time — test SLA71 (5 of 5).

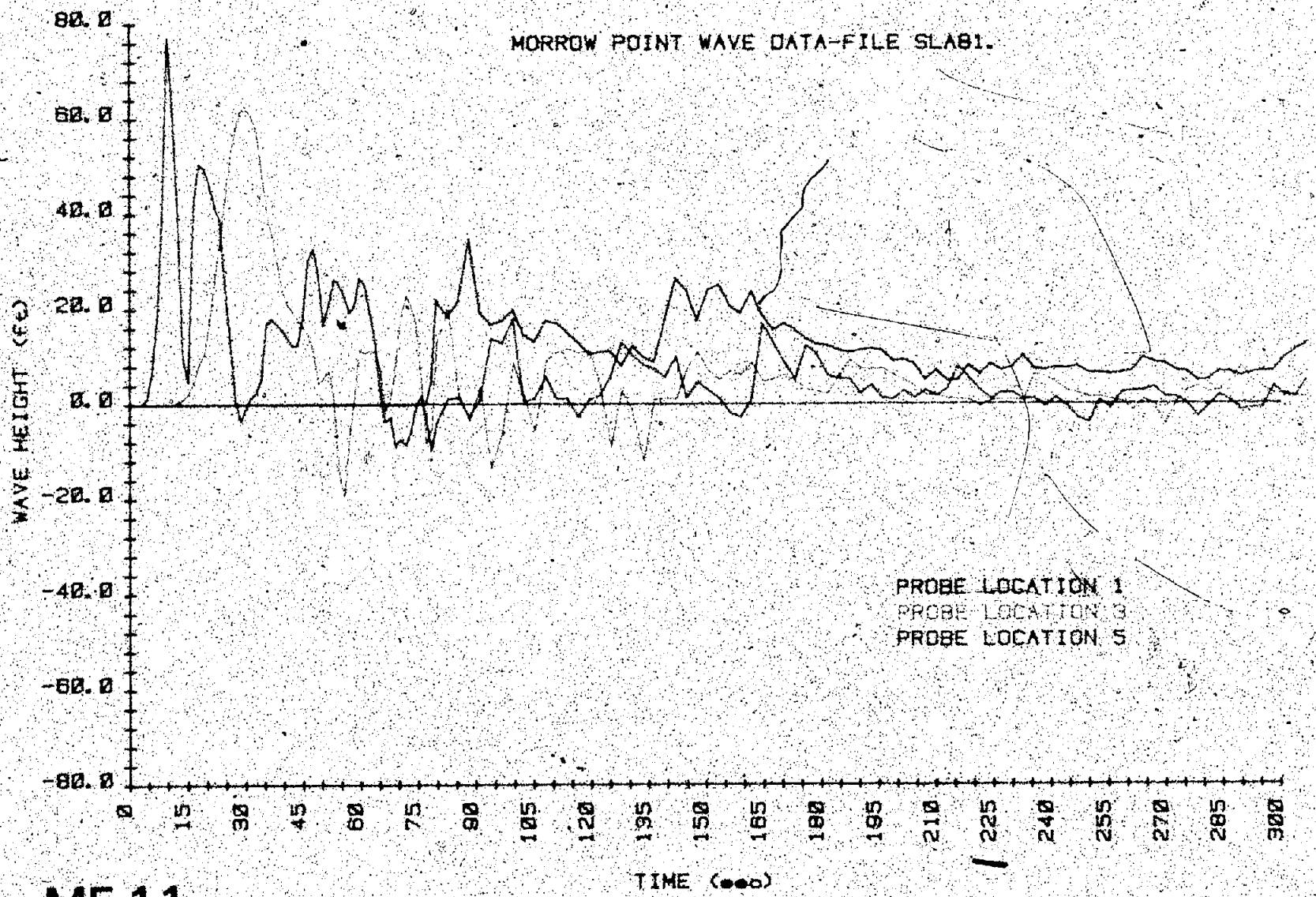

MF 11

Figure B-3. – Wave height versus time – test SLA81 (1 of 5)

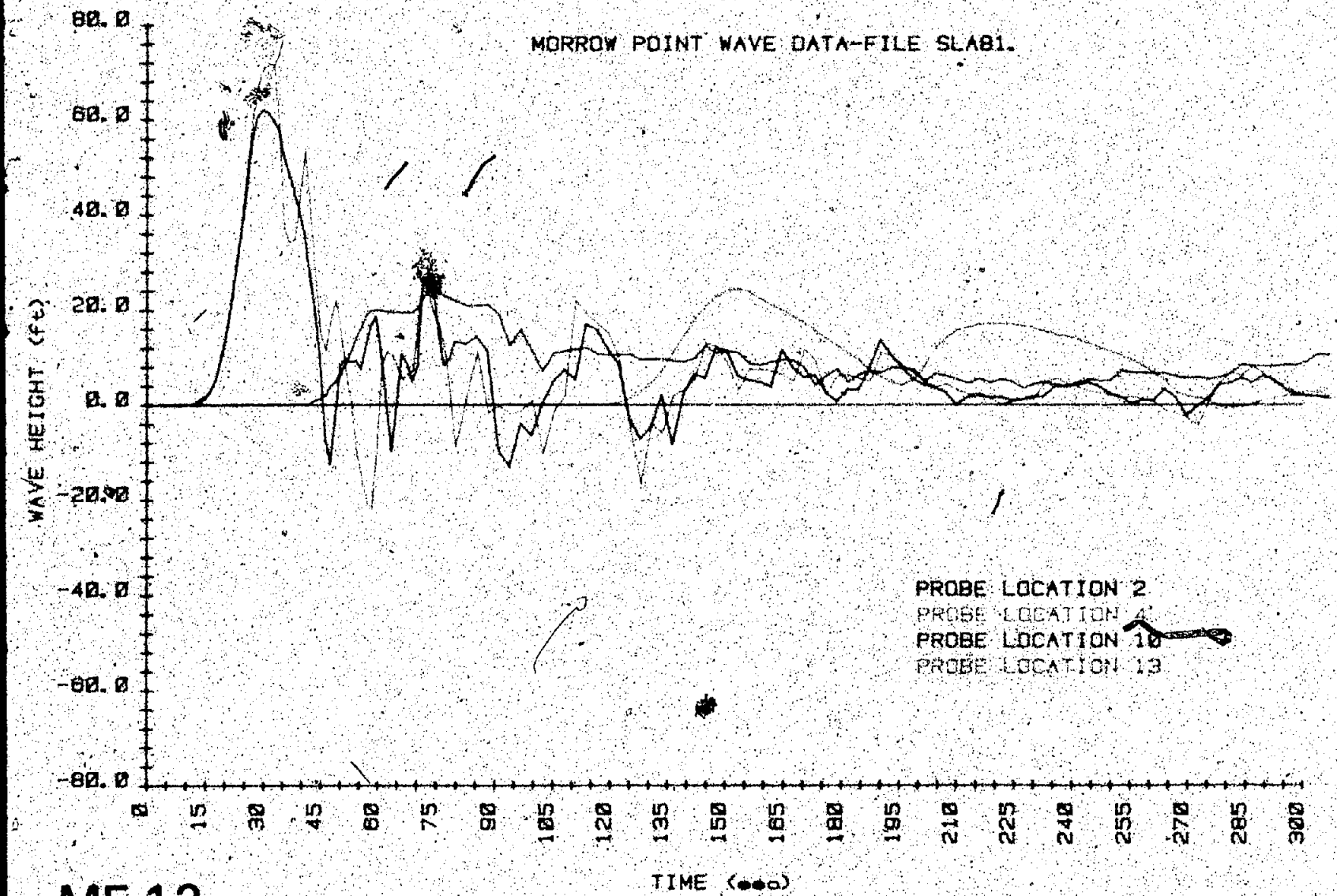

MF 12

Figure B-3. –Wave height versus time – test SLA81 (2 of 5).

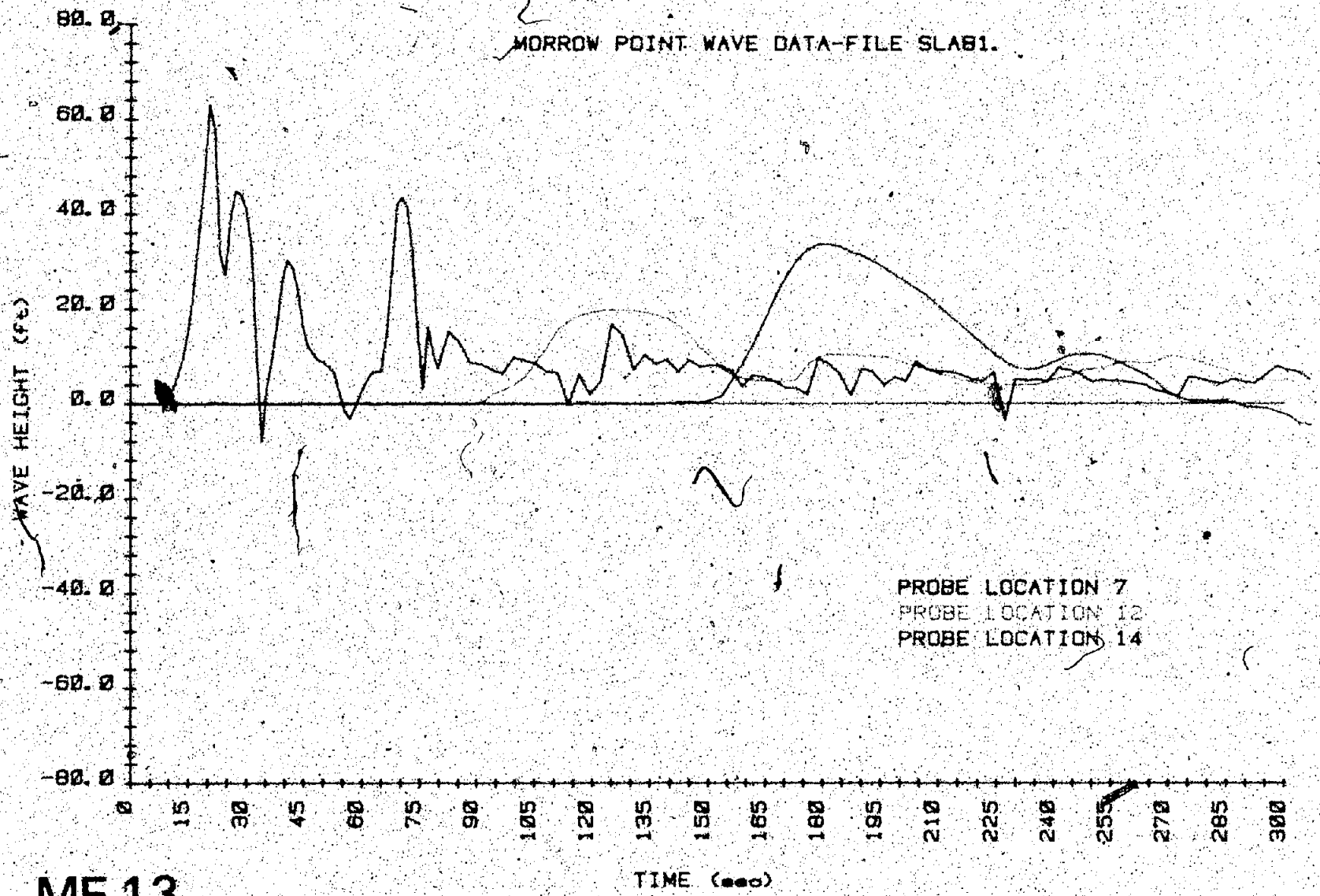

MF 13

Figure 8-3. Wave height versus time — test SLA81 (3 of 5).

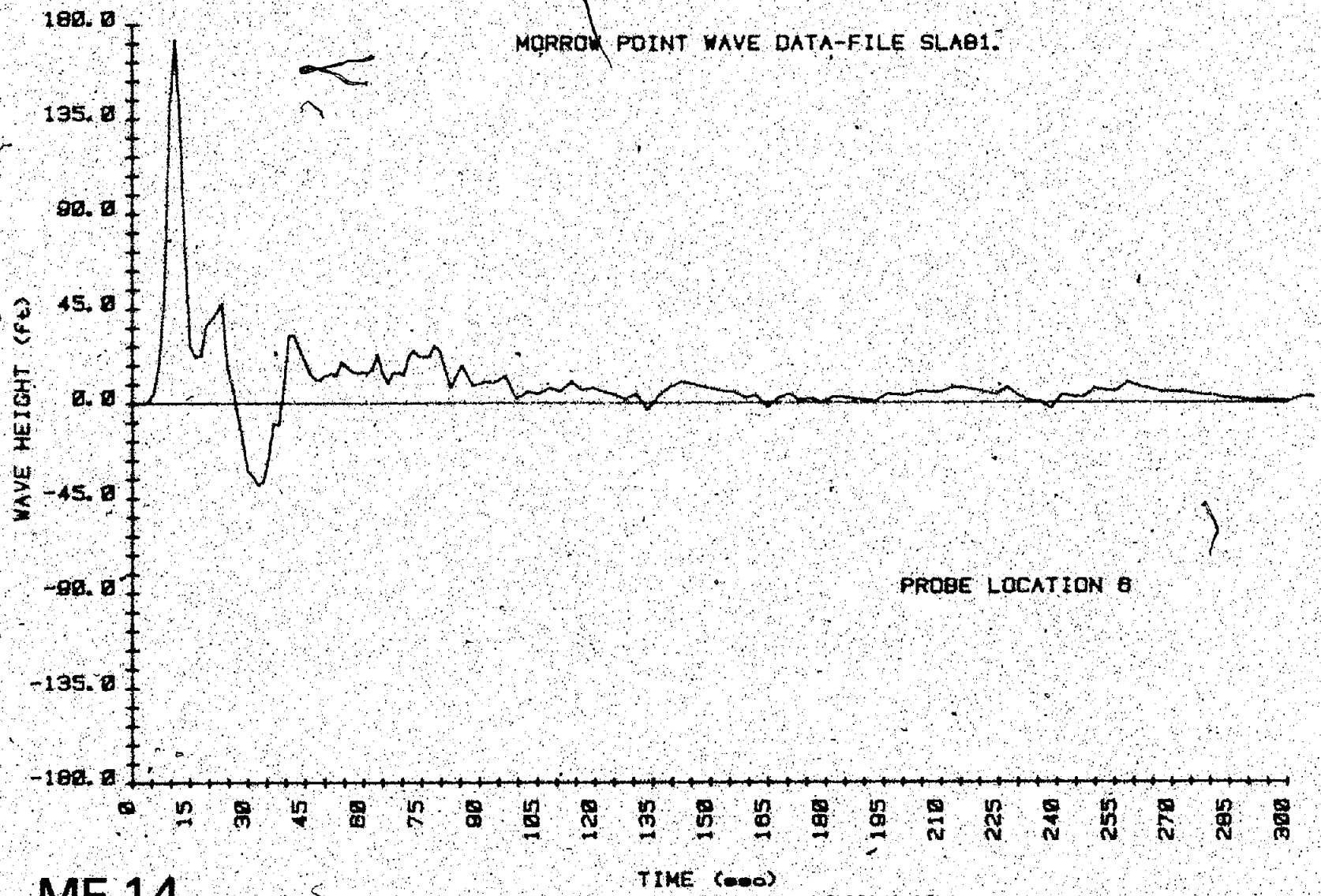

MF 14

Figure B-3. – Wave height versus time – test SLA01 (4 of 5).

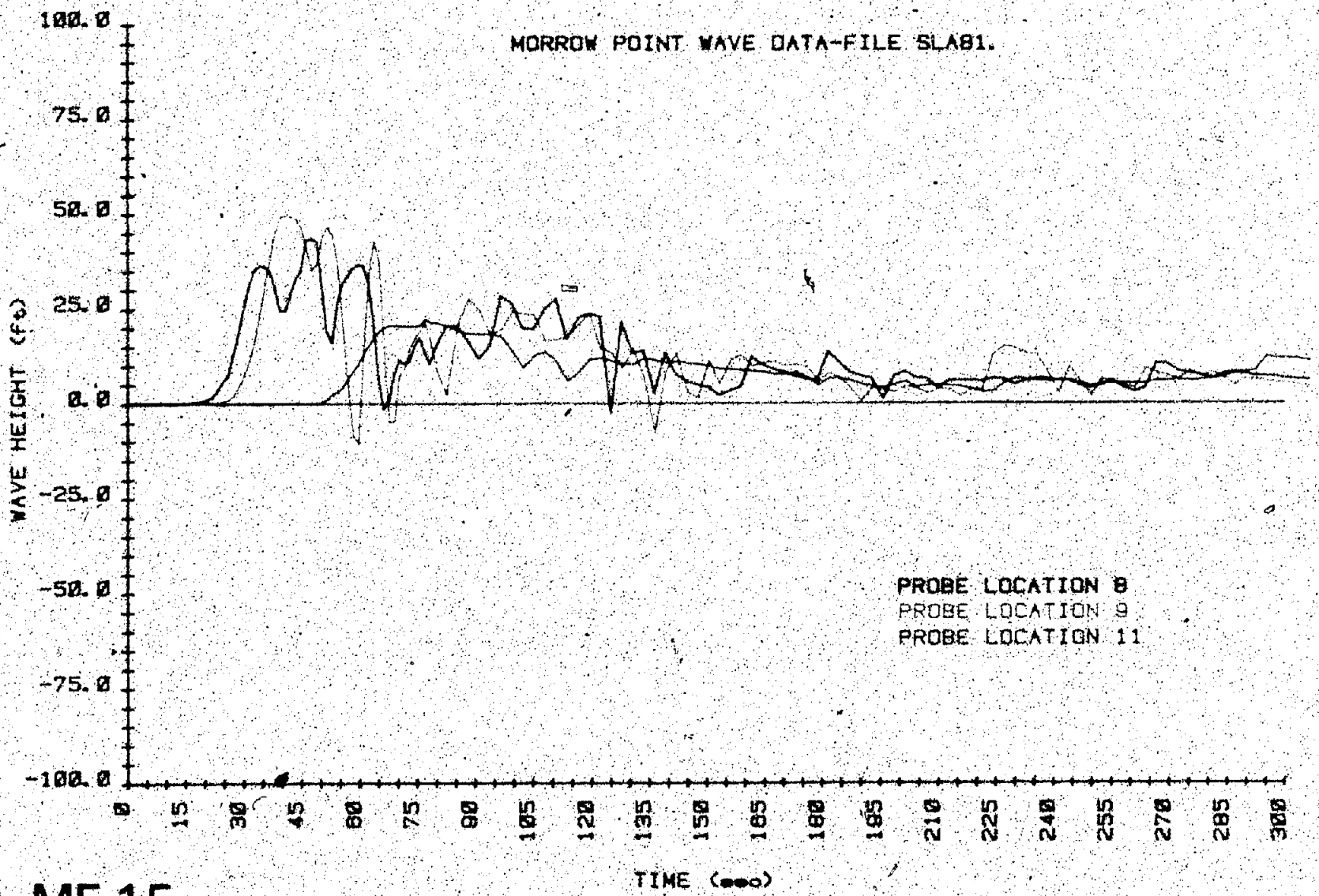

Figure B-3. – Wave height versus time – test SLA81 (5 of 5).

MF 15

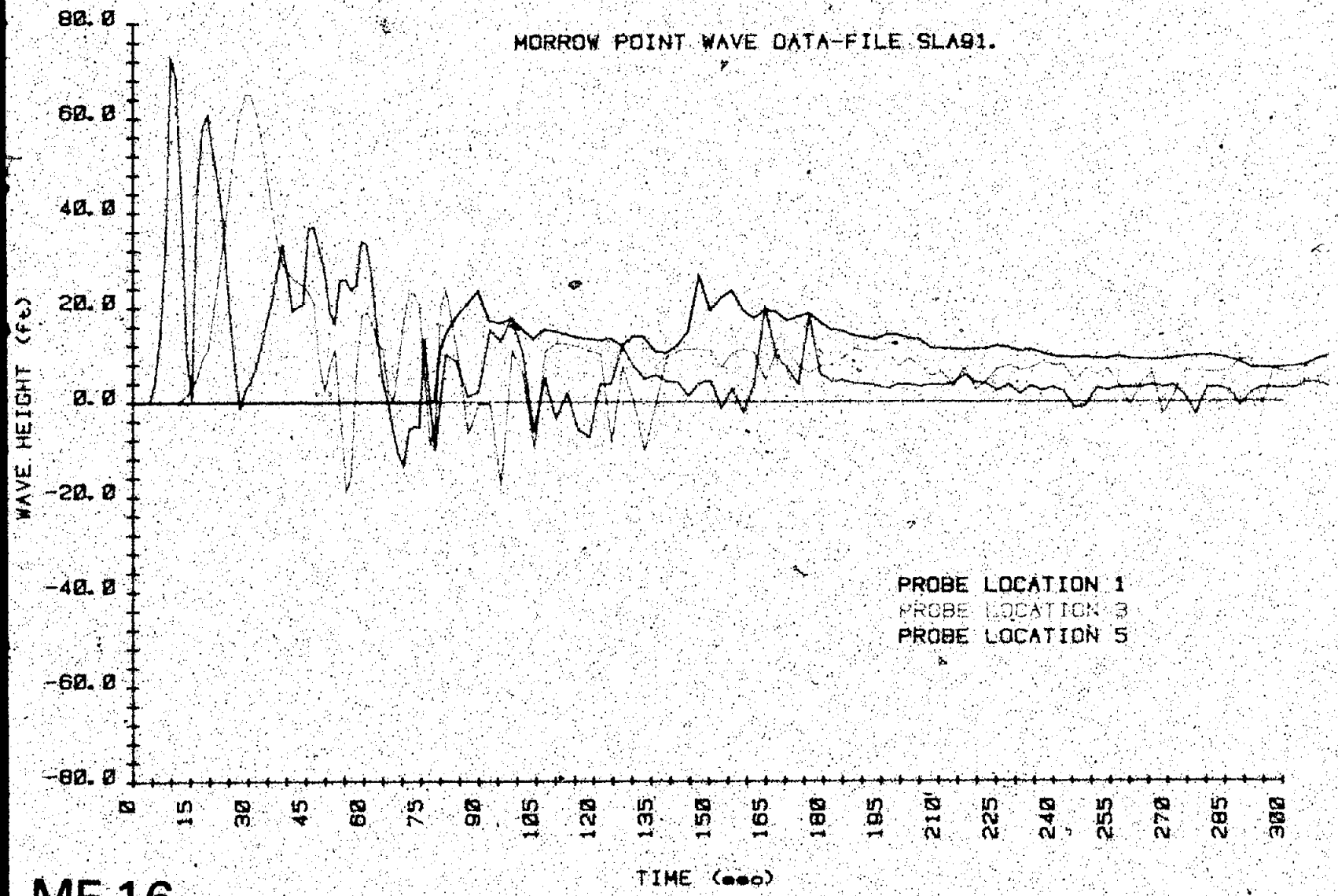

MF 16

Figure B-4. – Wave height versus time – test SLA91 (1 of 5).

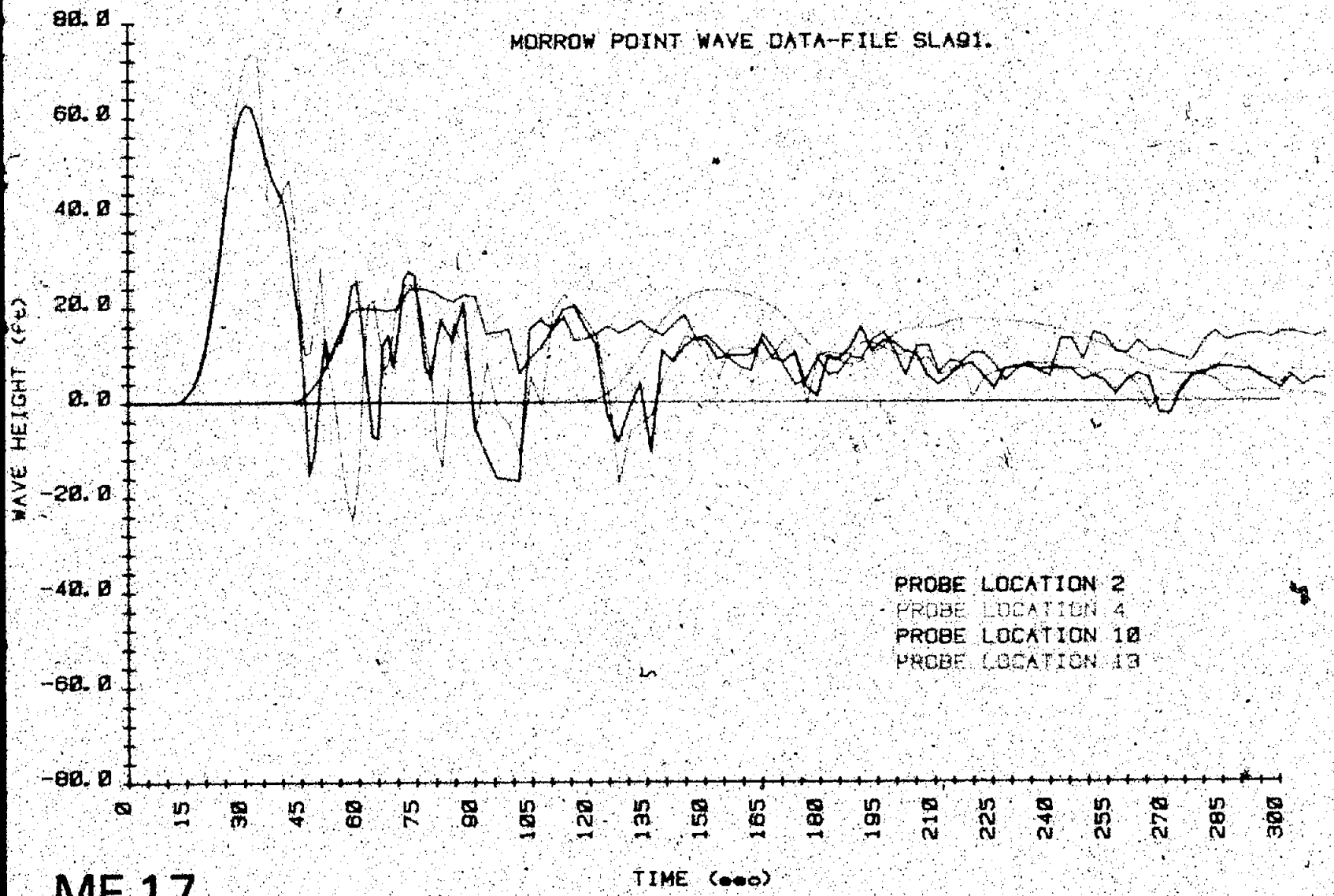

MF 17

Figure 8.4. – Wave height versus time – test SLA91 (2 of 5)

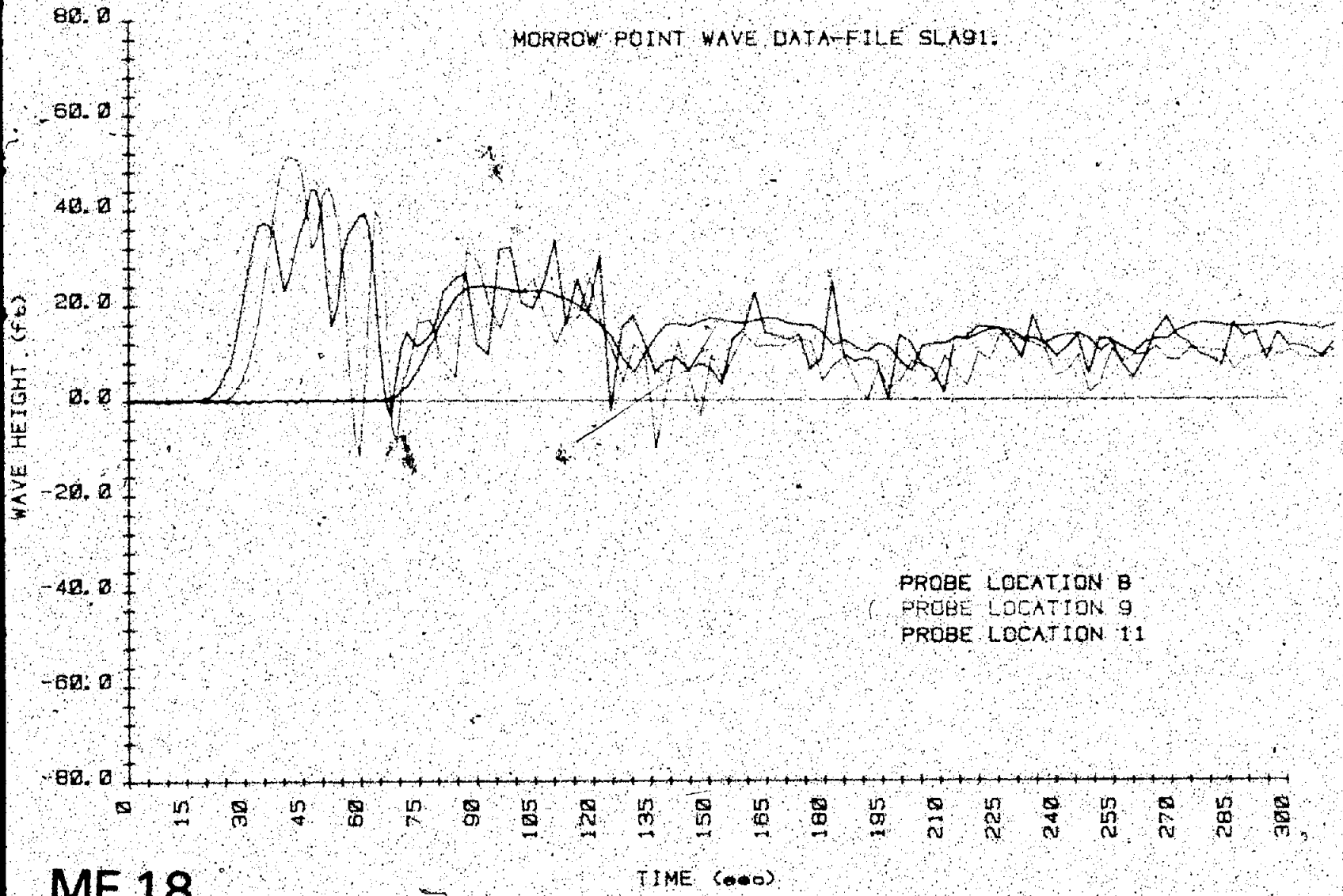

MF 18

Figure B-4. Wave height versus time — test SLA91 (3 of 5)

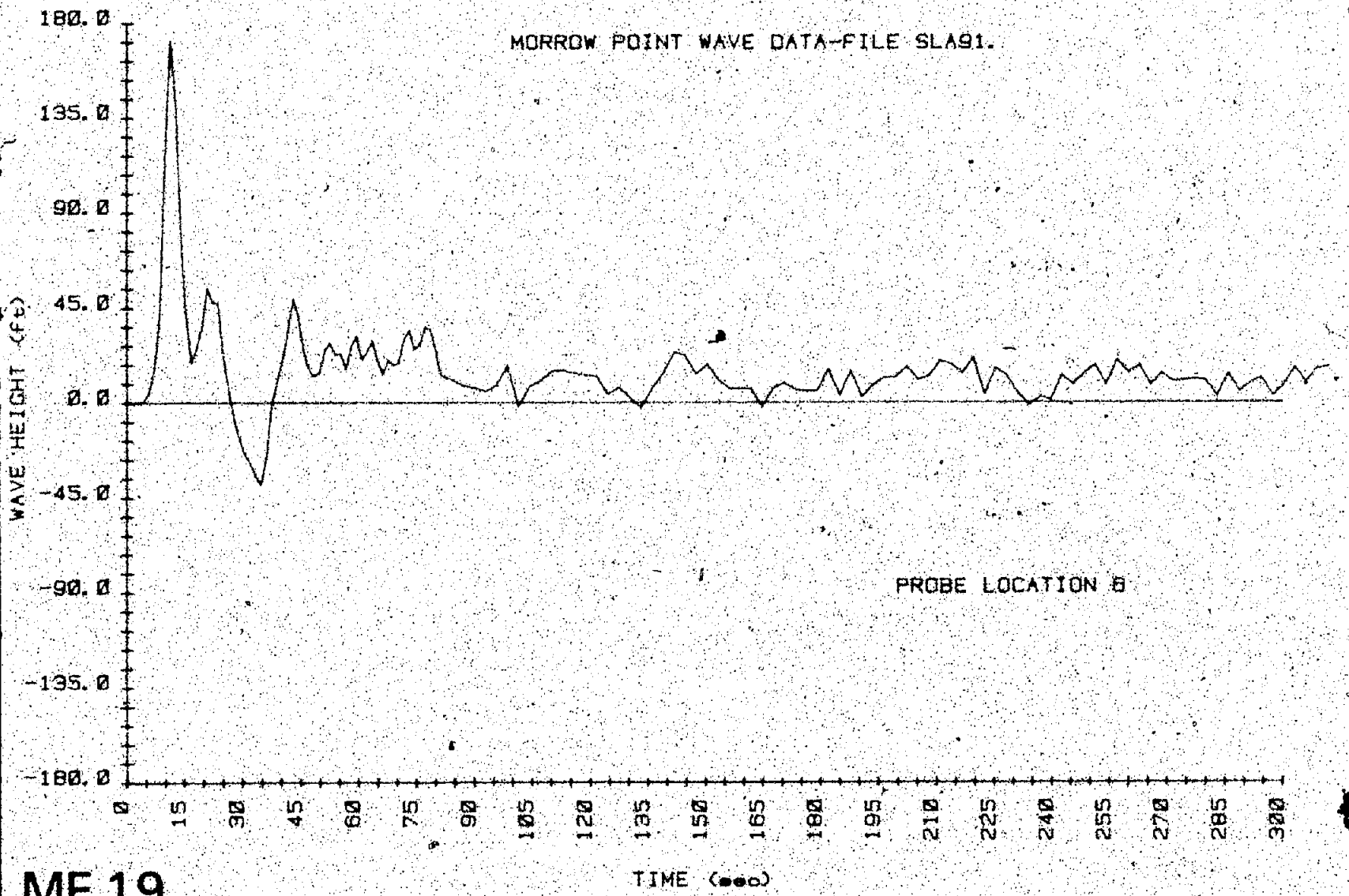

MF 19

Figure B-4. - Wave height versus time. - test SLA91 (4 of 5).

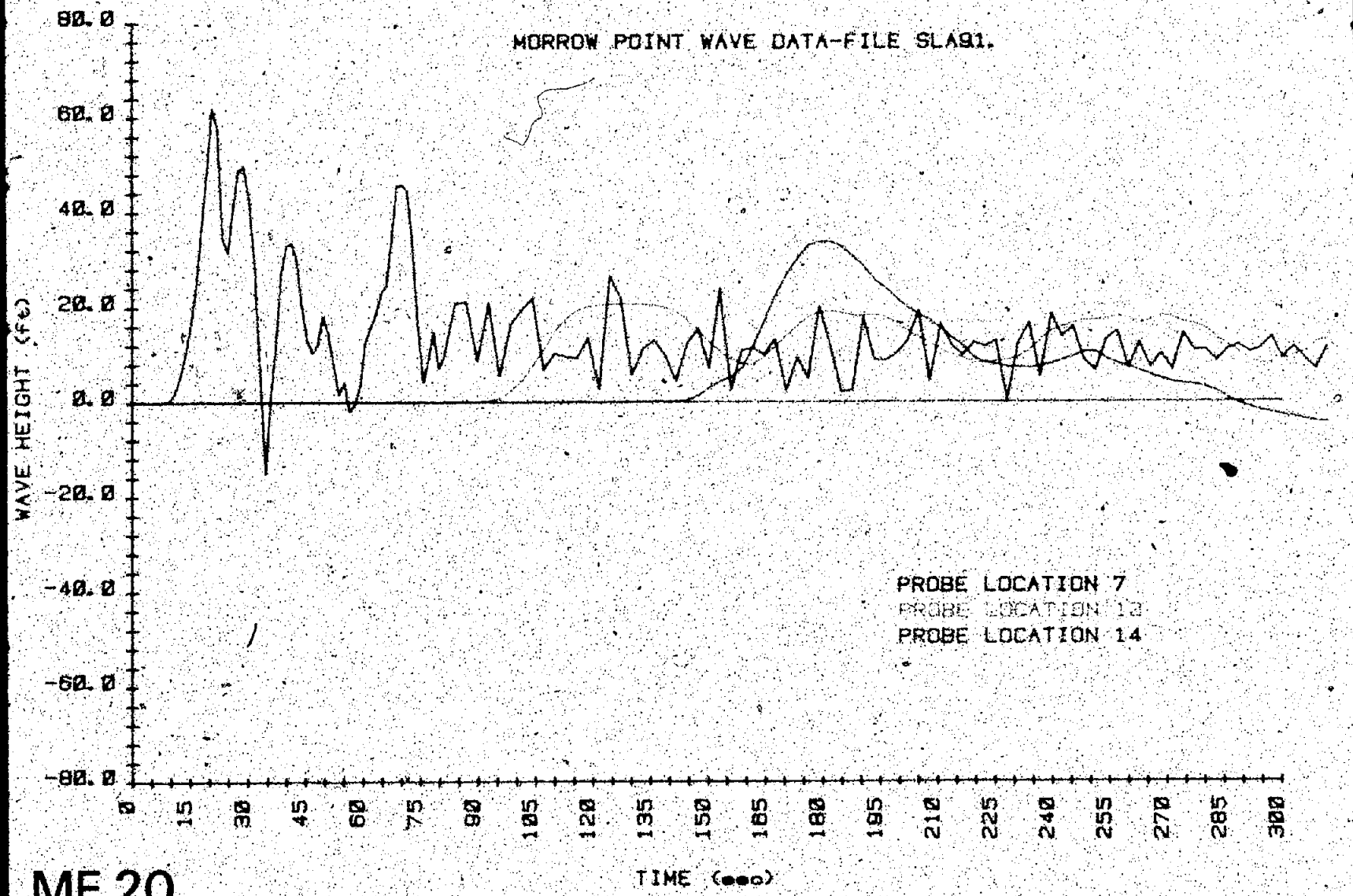

MF 20

Figure B-4. Wave height versus time - test SLA91 (5 of 5).

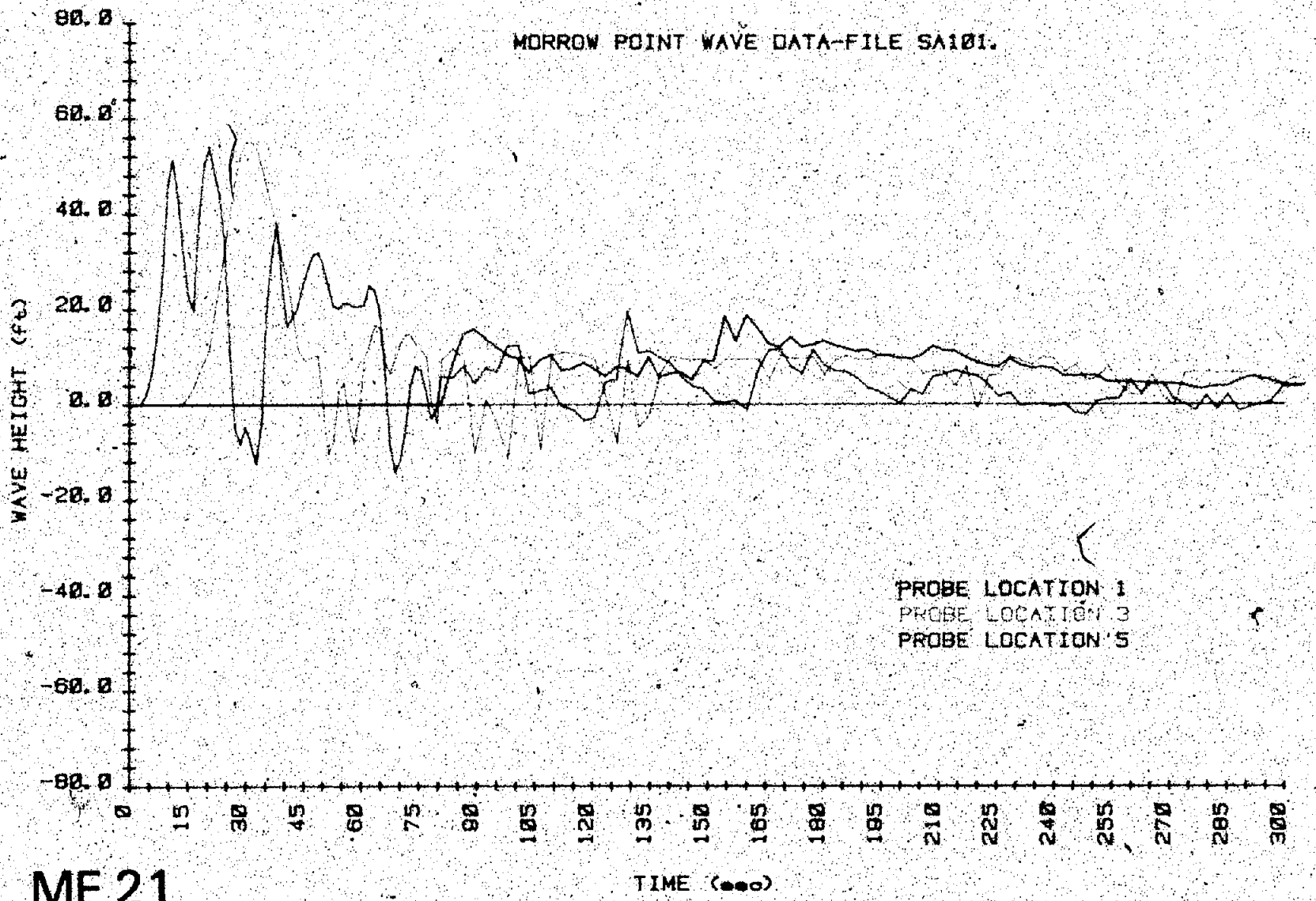

MF 21

Figure B-5. – Wave height versus time – test SA101 (1 of 5)

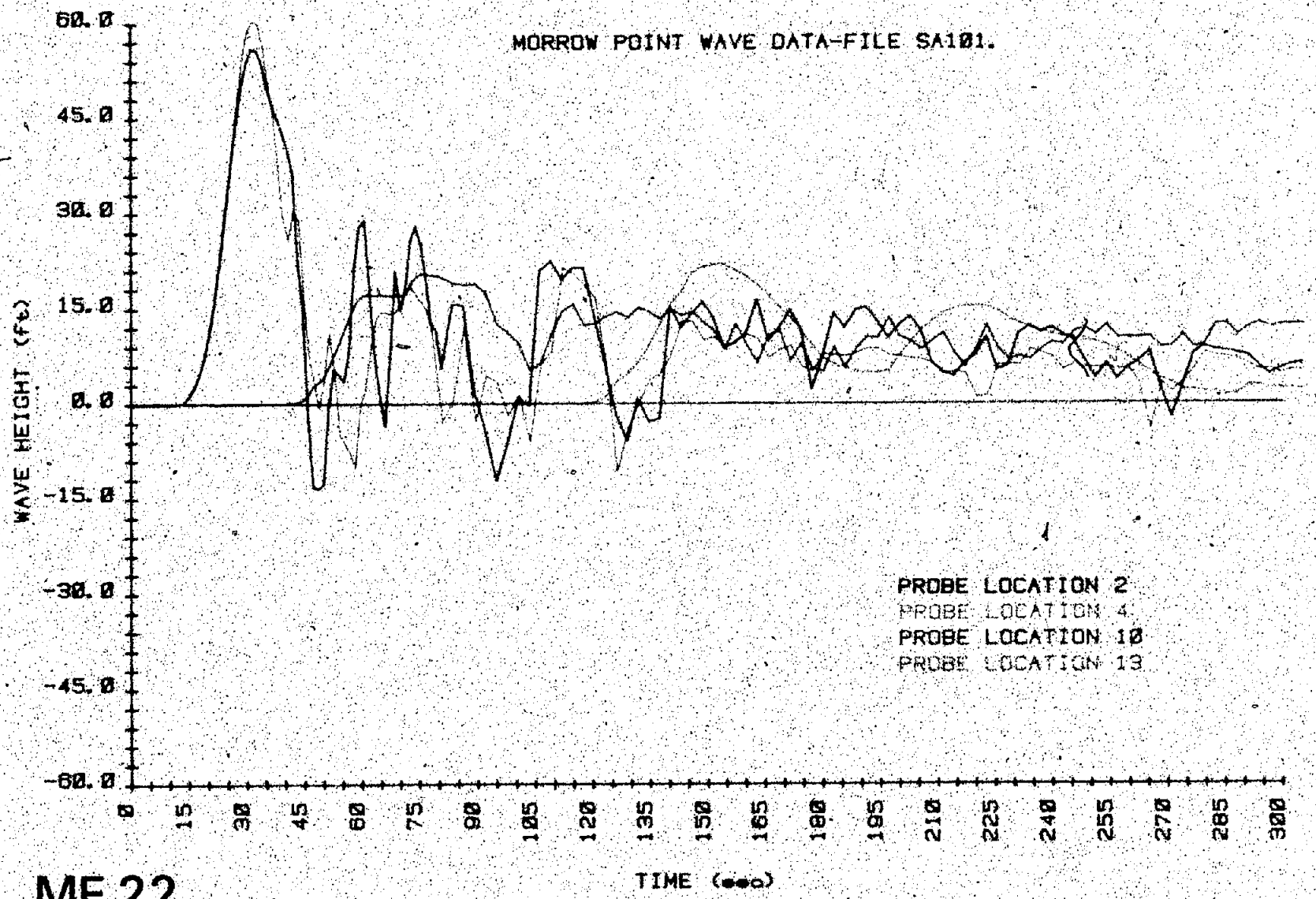

MF 22

Figure B-5.—Wave height versus time — test SA101 (2 of 5)

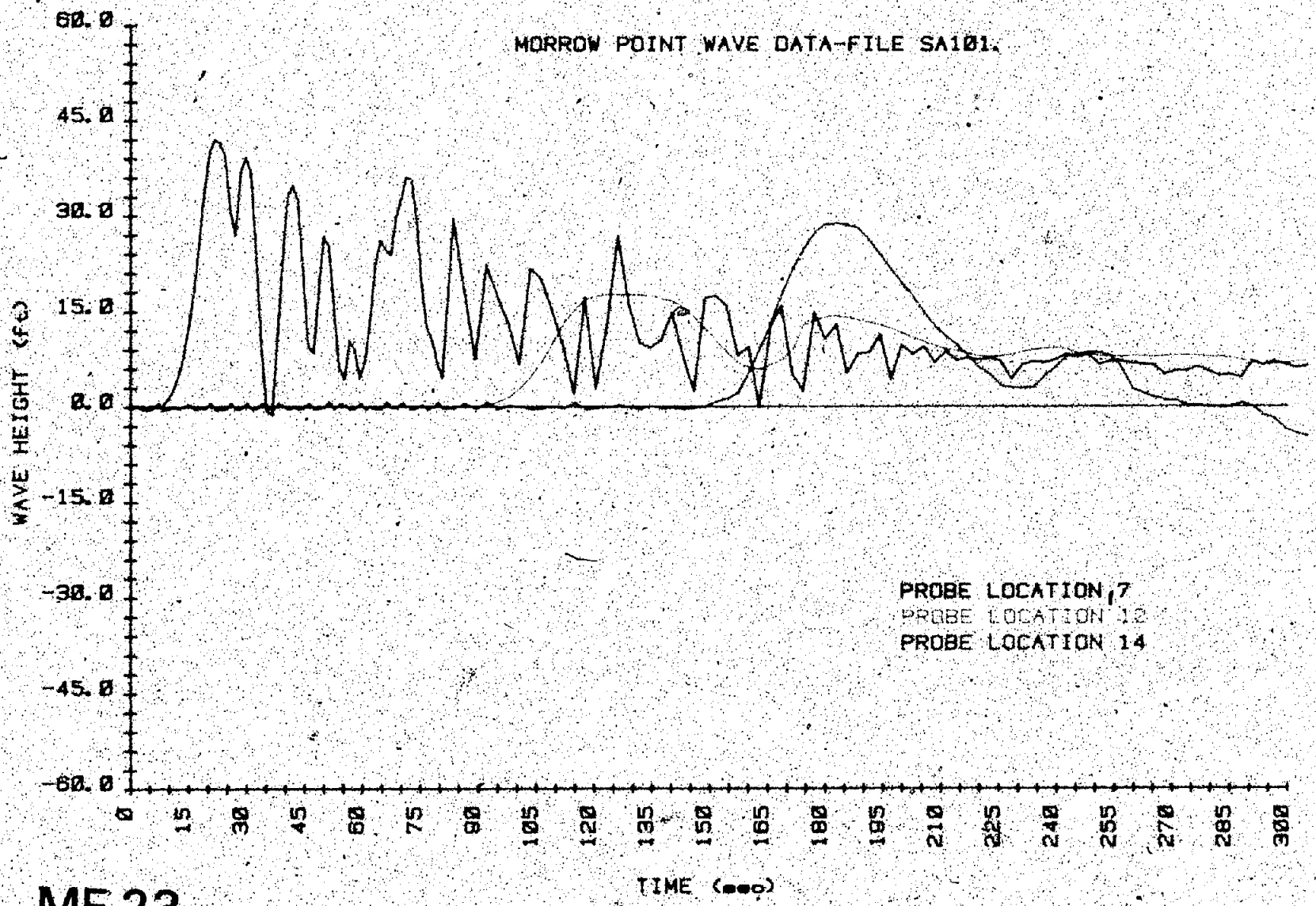

MF 23

Figure B-5. – Wave height versus time – test SA101 (3 of 5)

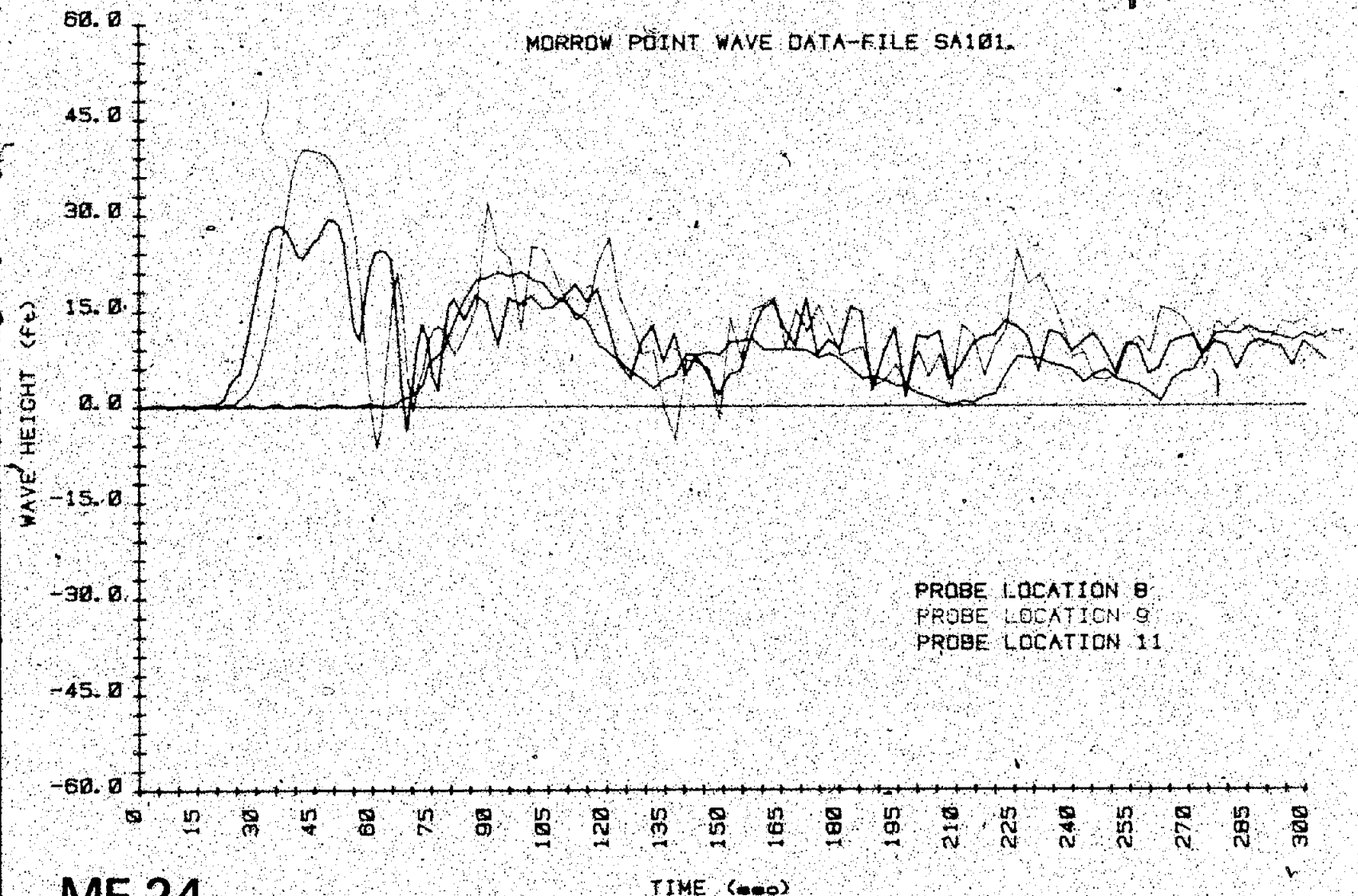

MF 24

Figure B-5. – Wave height versus time – test SA101 (4 of 5).

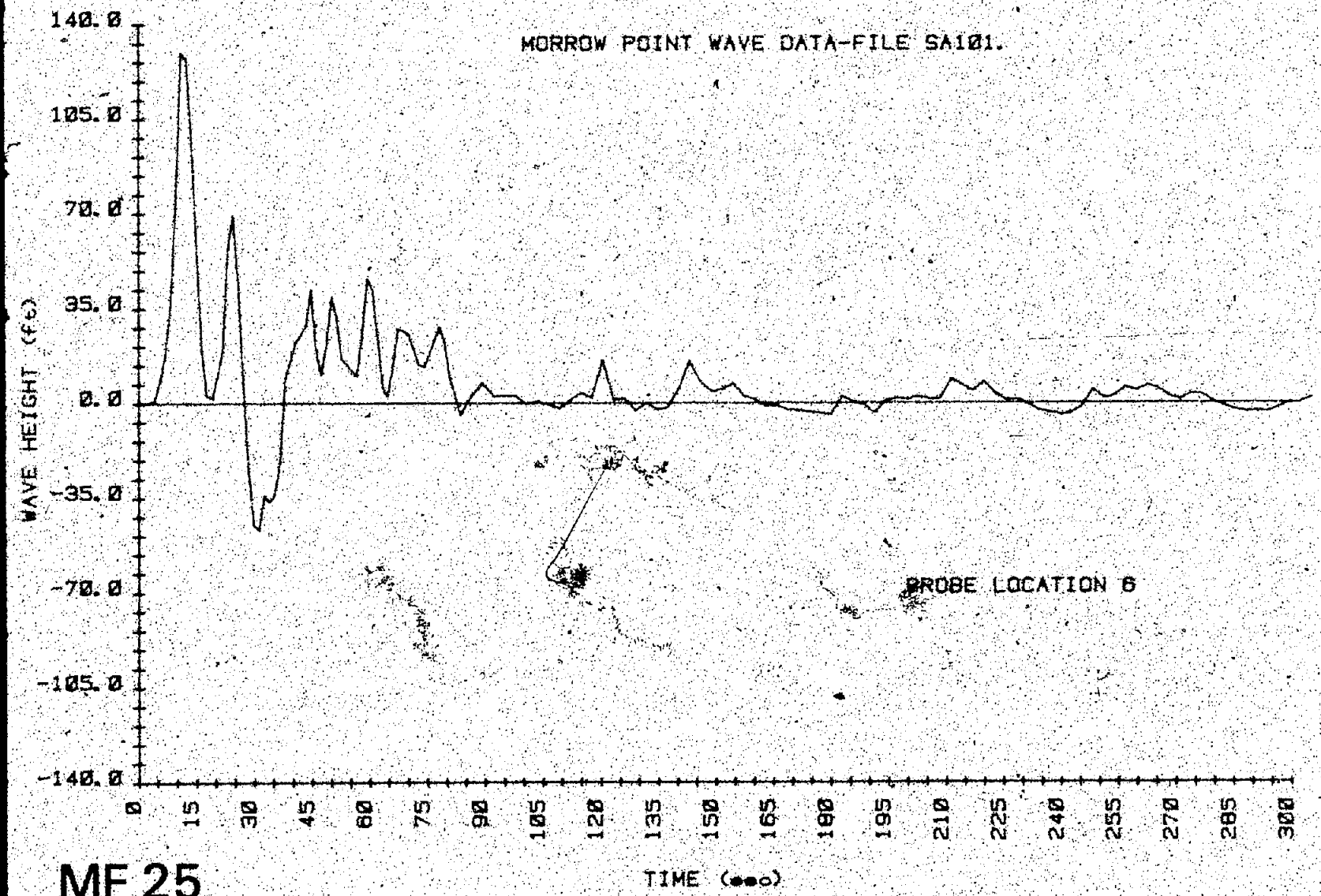

MF 25

Figure B-5. – Wave height versus time – test SA101 (5 of 5)

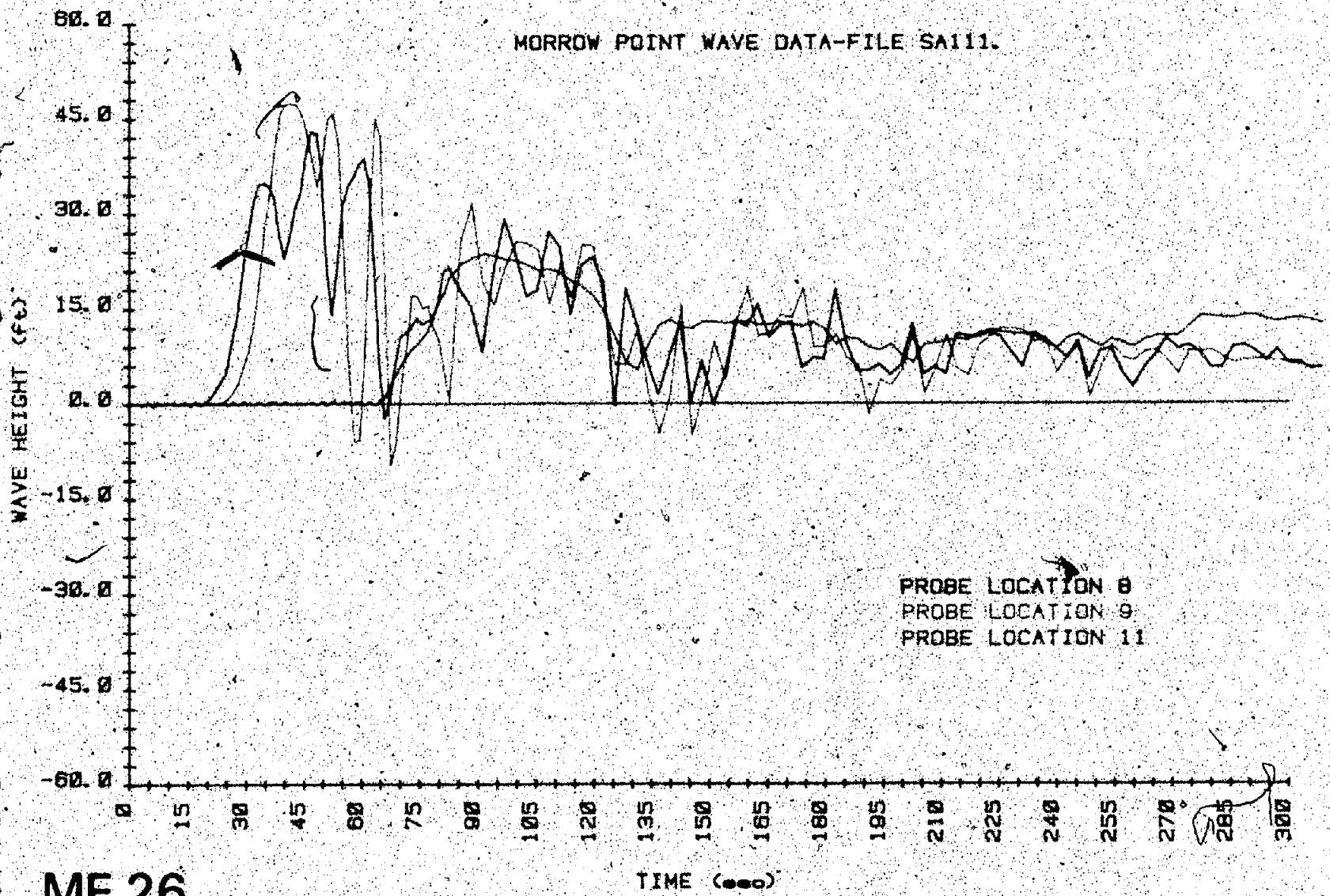

MF 26

Figure 8-8. – Wave height versus time – test SA111 (1 of 5)

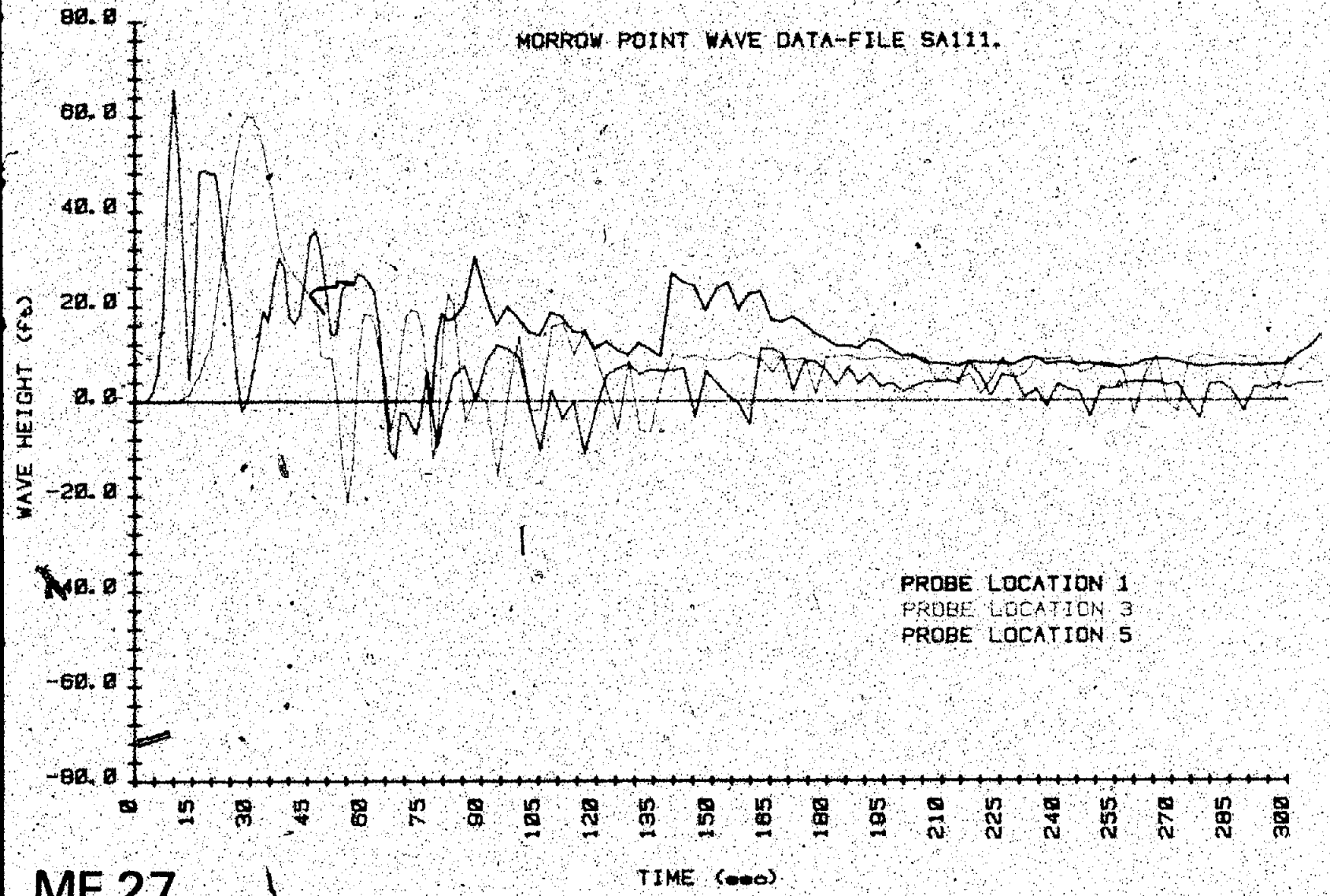

MF 27

Figure B-6. Wave height versus time — test SA111 (2 of 5).

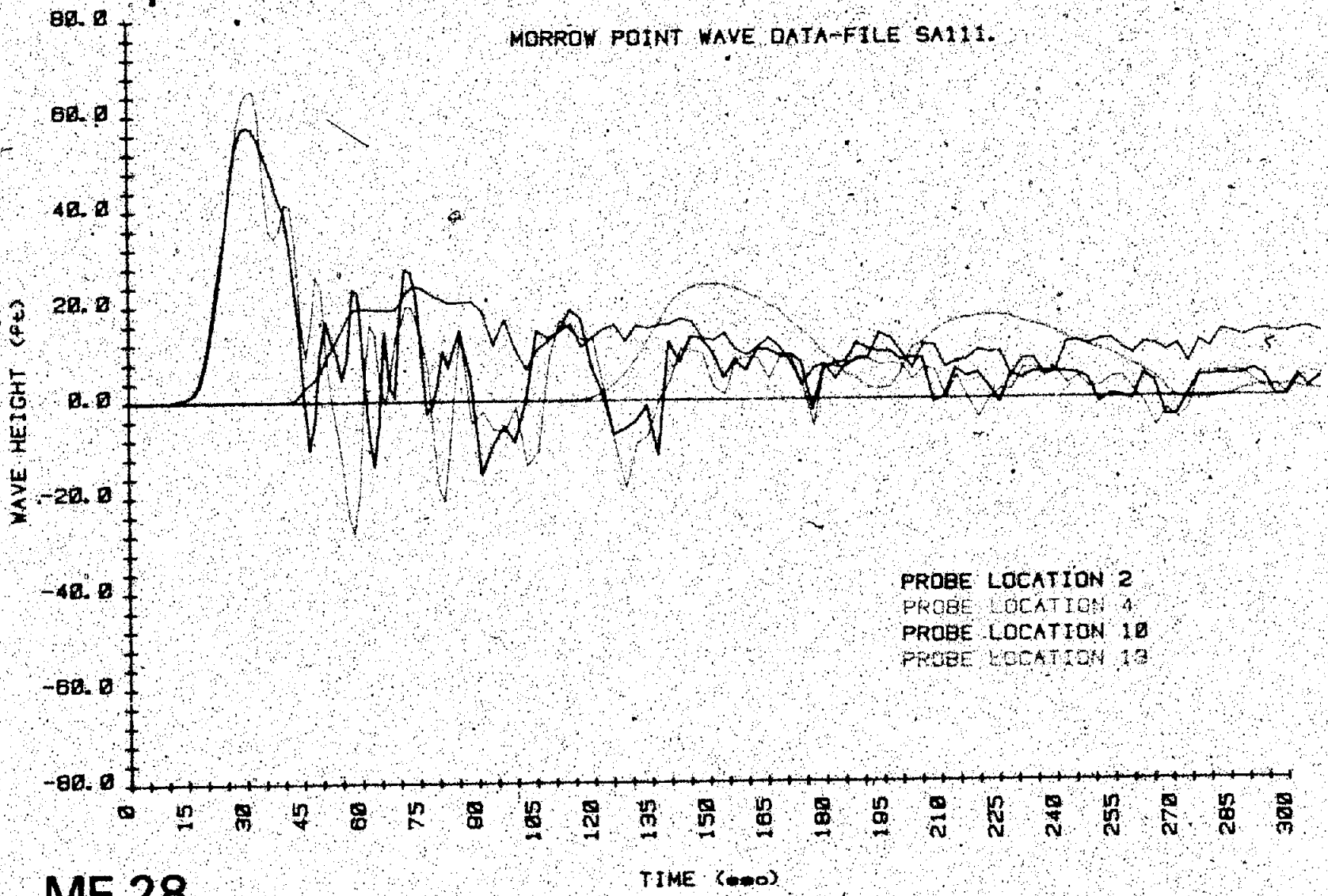

MF 28

Figure B-6. – Wave height versus time — test SA111 (3 of 5).

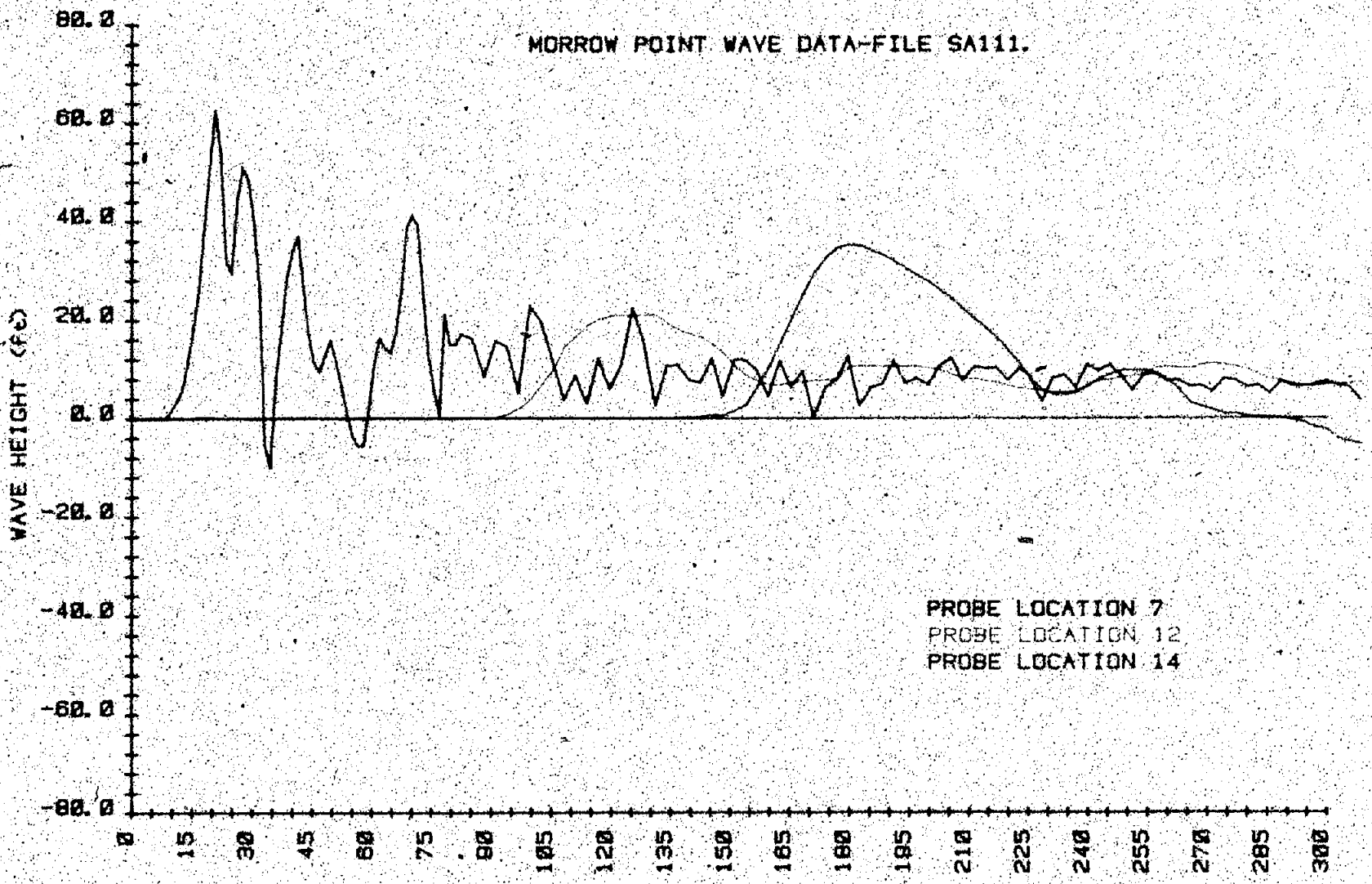

MF 29

Figure B-6.--Wave height versus time -- test SA111 (4 of 5).

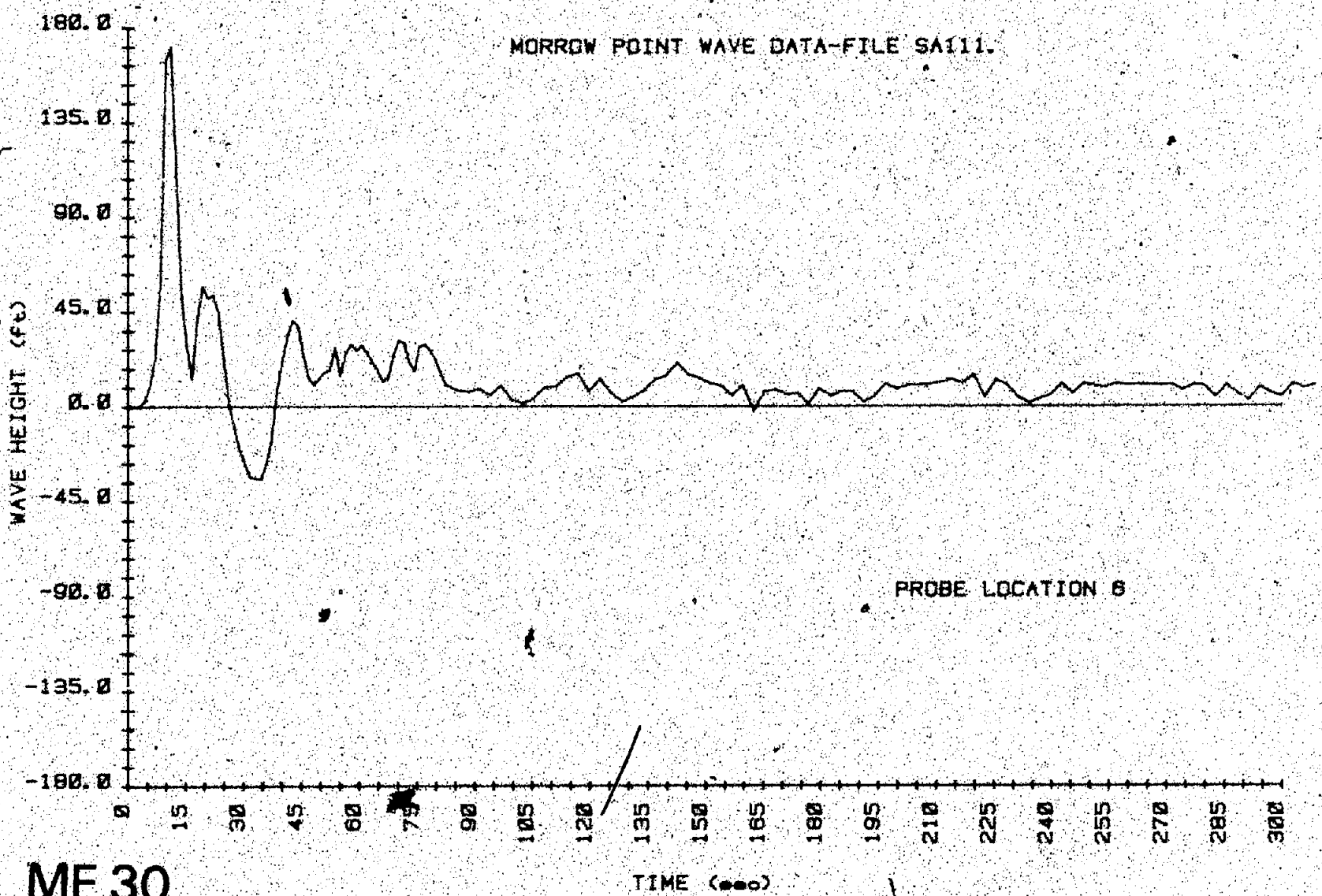

Figure B-6. – Wave height versus time – test SA111 (5 of 5).

MF 30

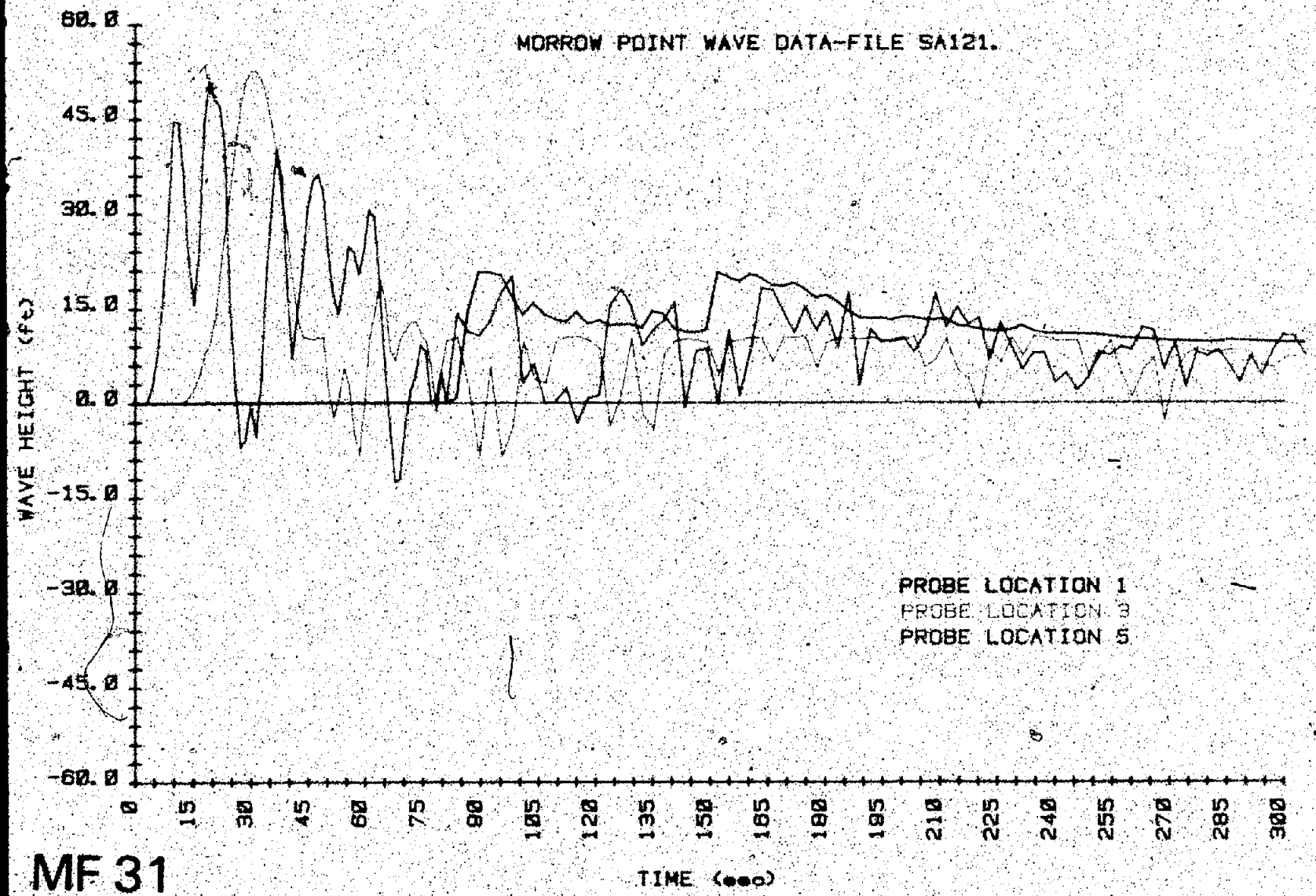

MF 31

Figure B-7. Wave height versus time — test SA121 (1 of 5).

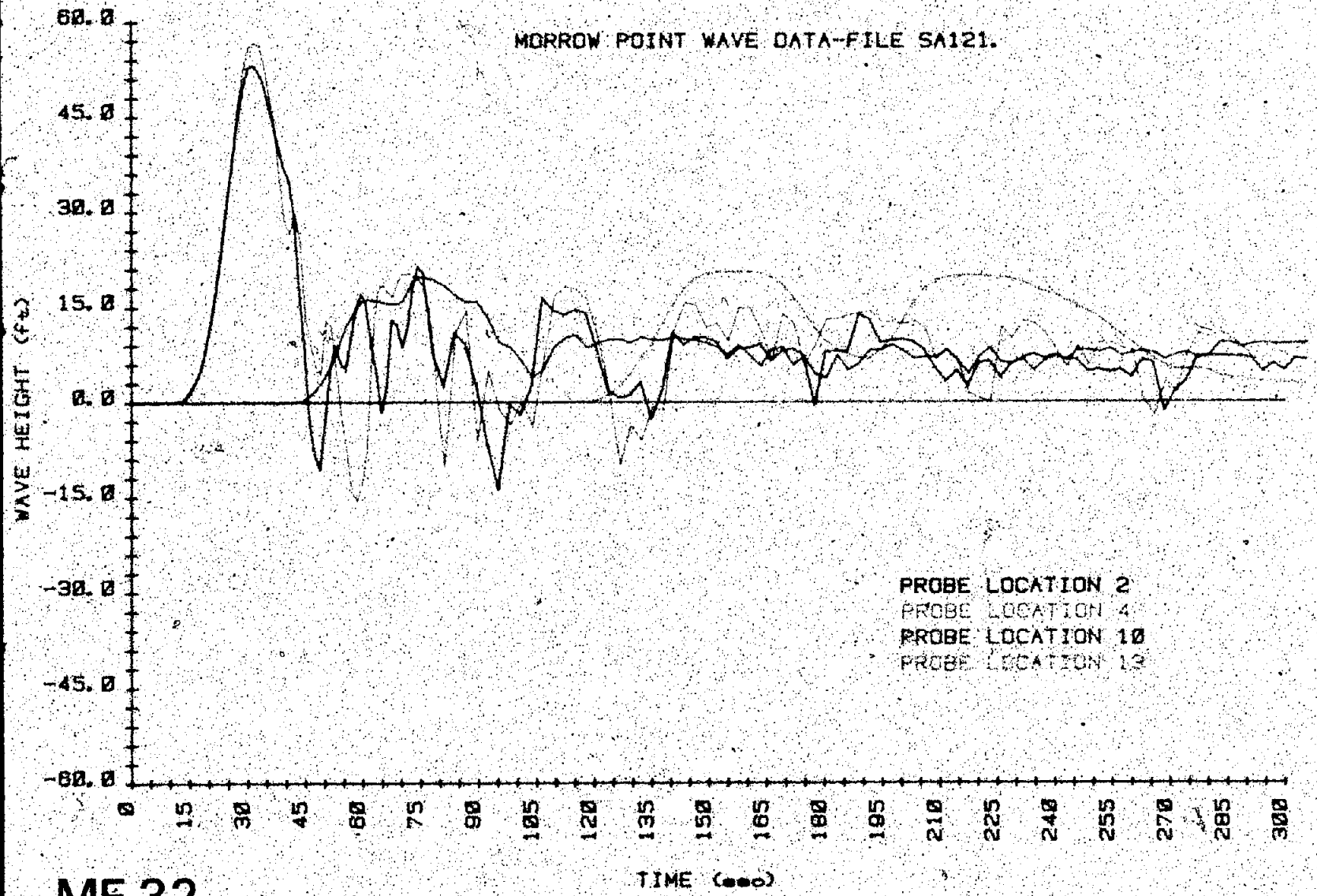

MF 32

Figure B-7.—Wave height versus time — test SA121 (2 of 5)

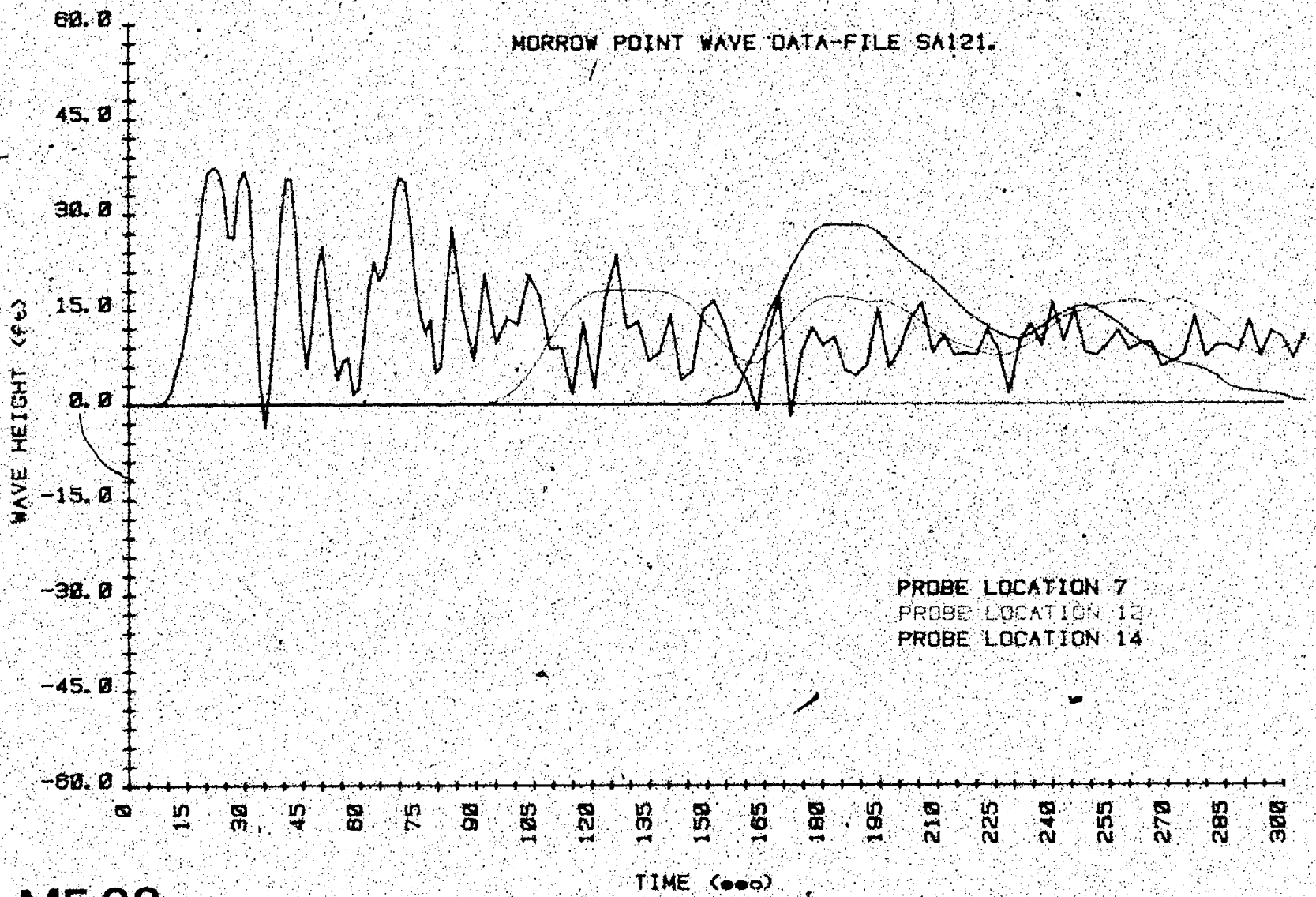

MF 33

Figure B-7. Wave height versus time — test SA121 (3 of 5).

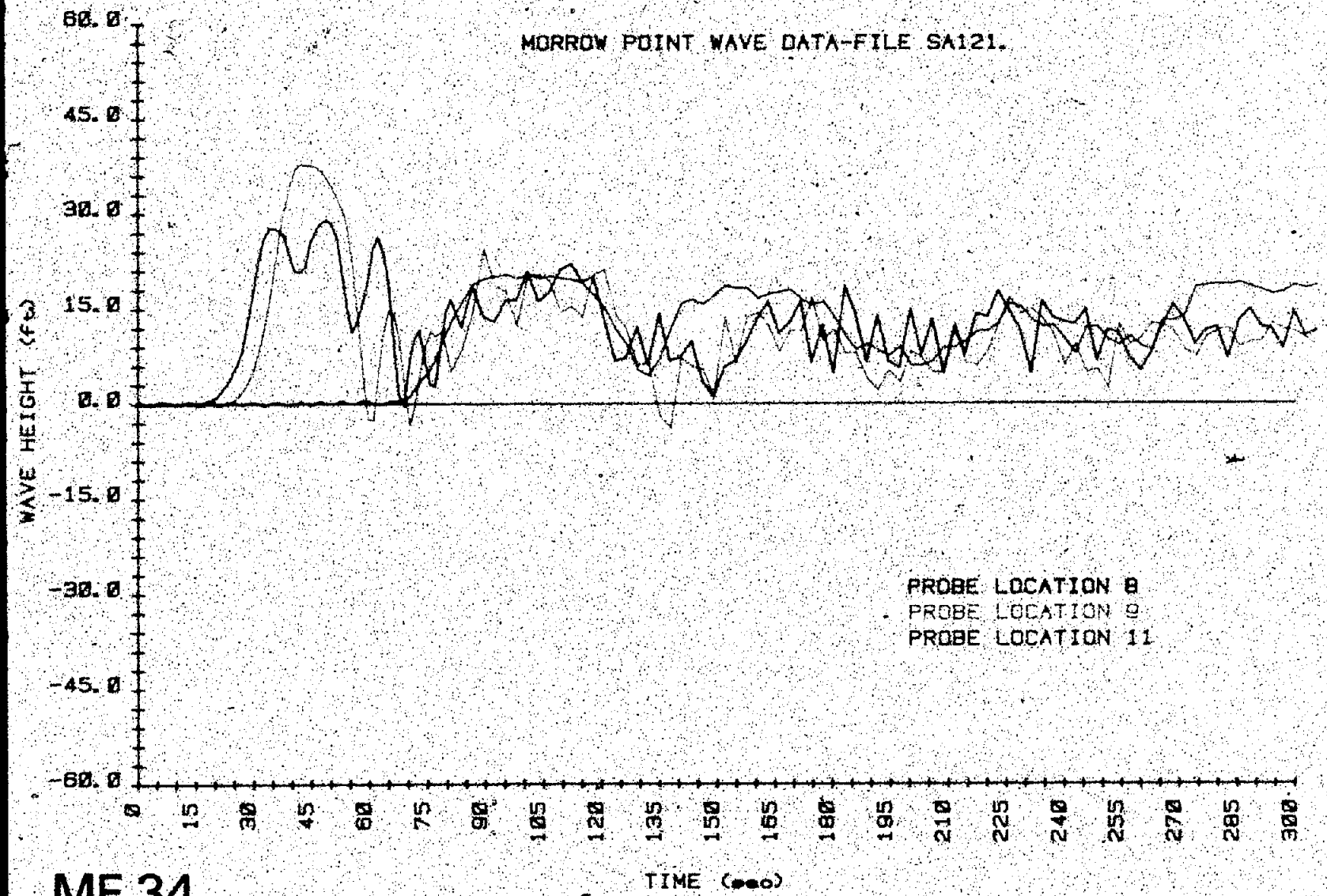

MF 34

Figure B-7. Wave height versus time — test SA121 (4 of 5).

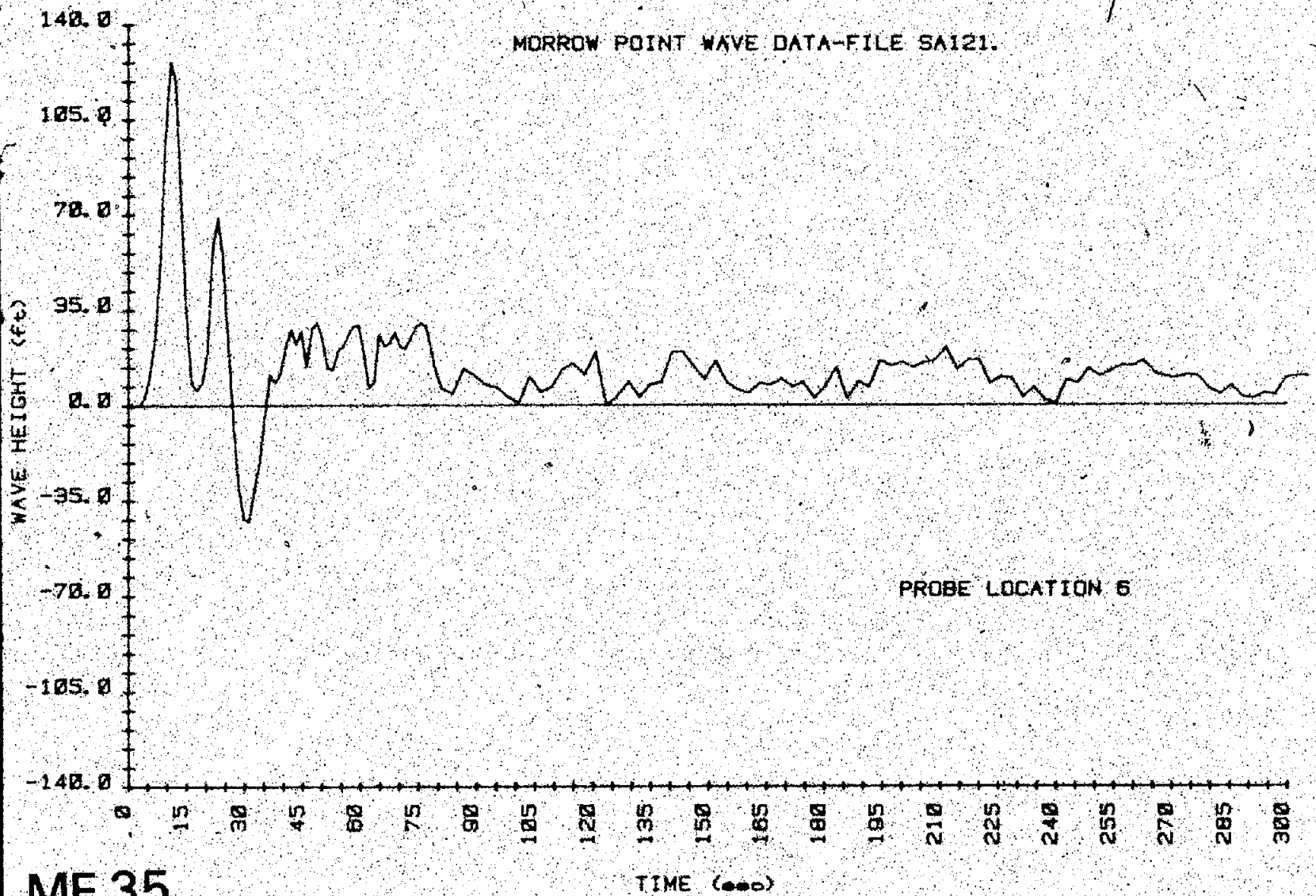

MF 35

Figure B-7. - Wave height versus time -- test SA121 (5 of 5)

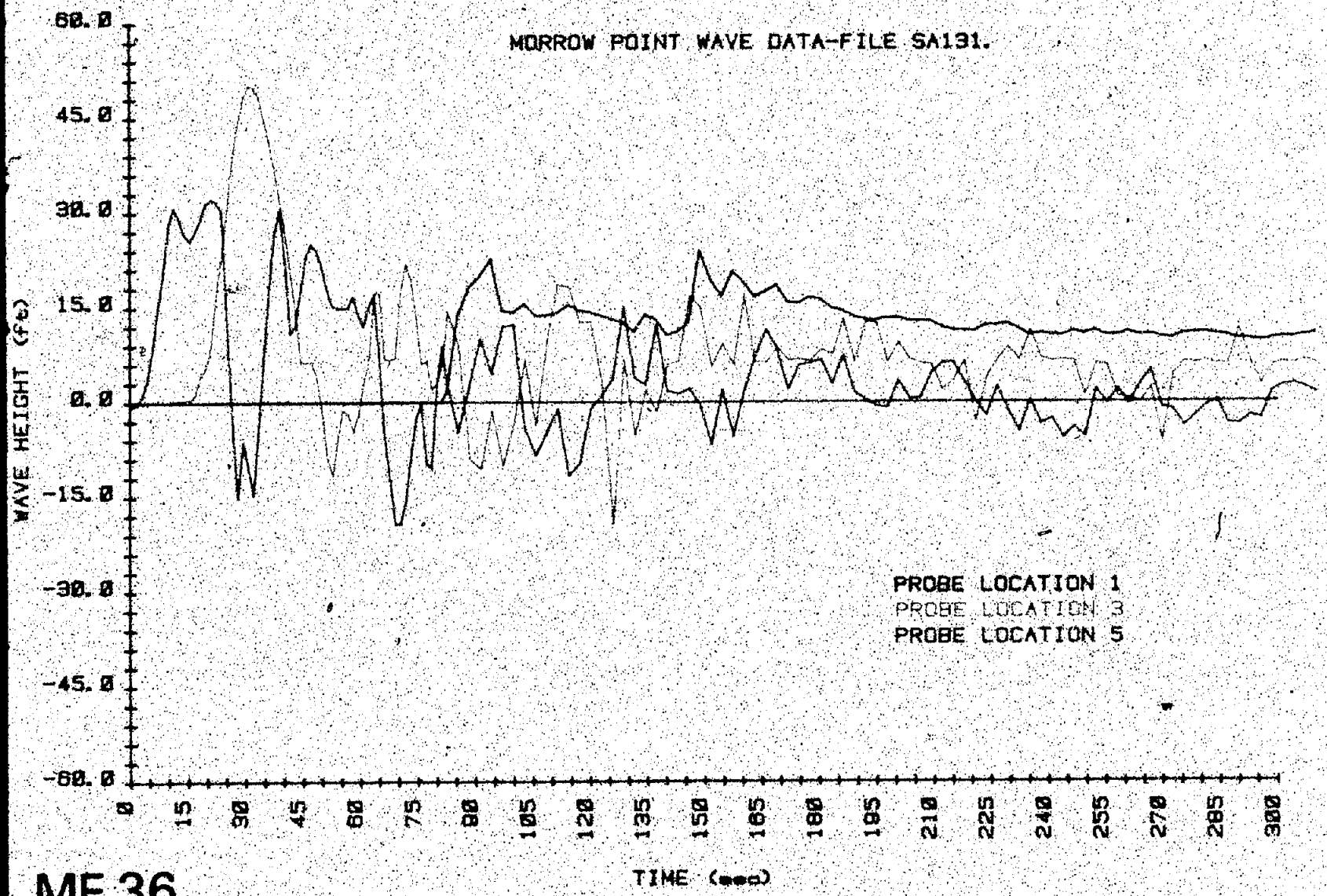

MF 36

Figure B-8.—Wave height versus time — test SA131 (1 of 5).

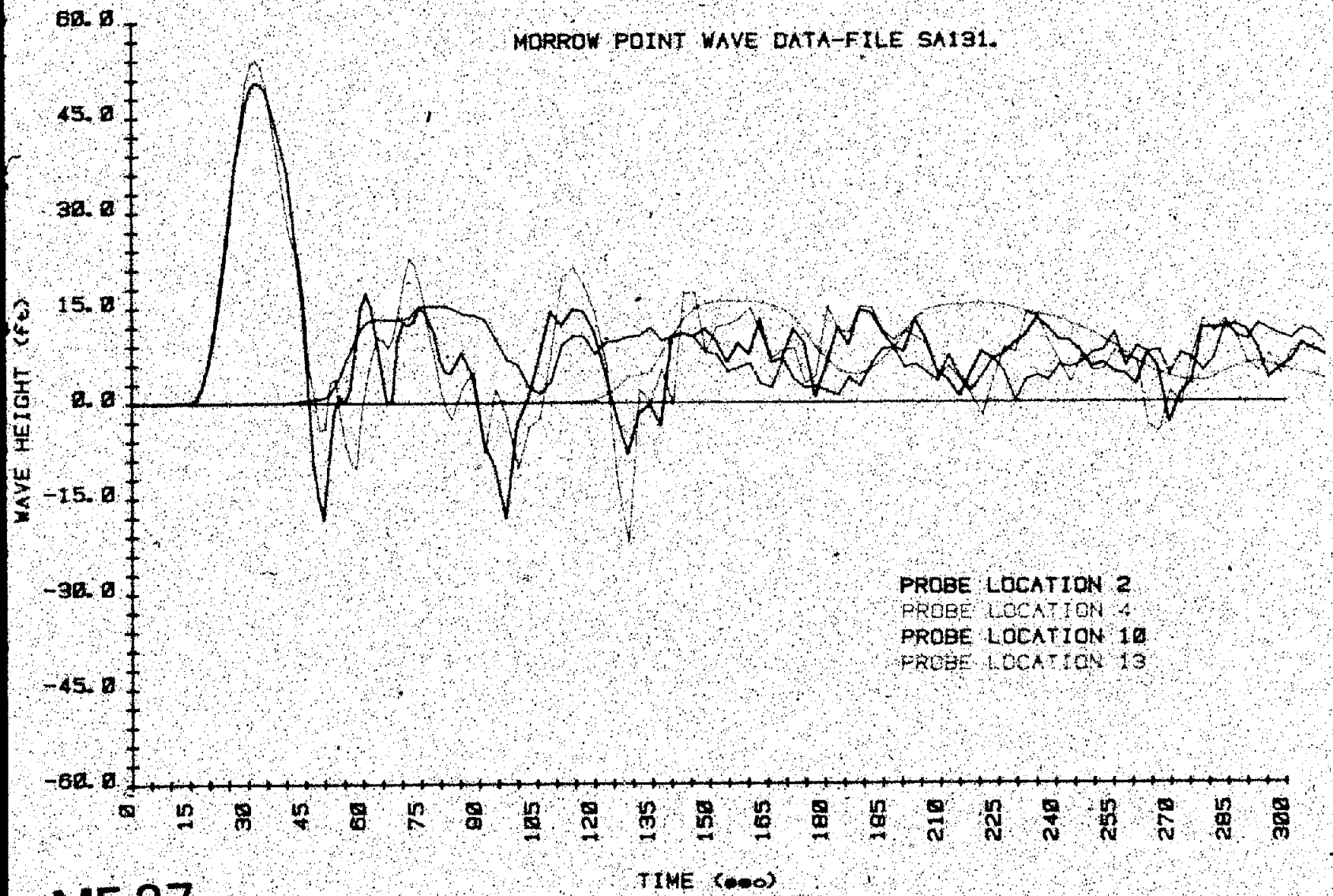

MF 37

Figure B-8.—Wave height versus time — test SA131 (2 of 5).

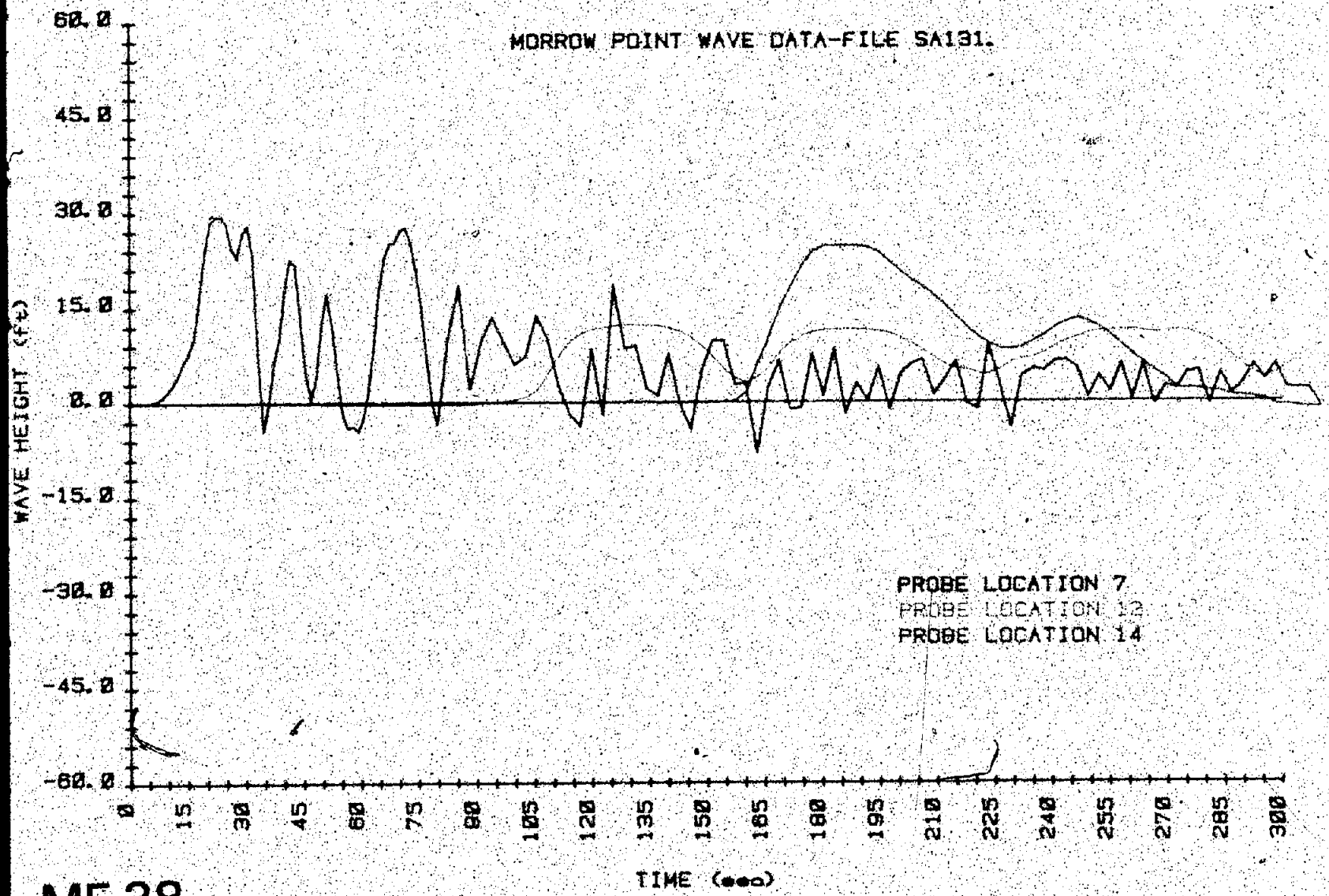

MF 38

Figure B-8.– Wave height versus time – test SA131 (3 of 5)

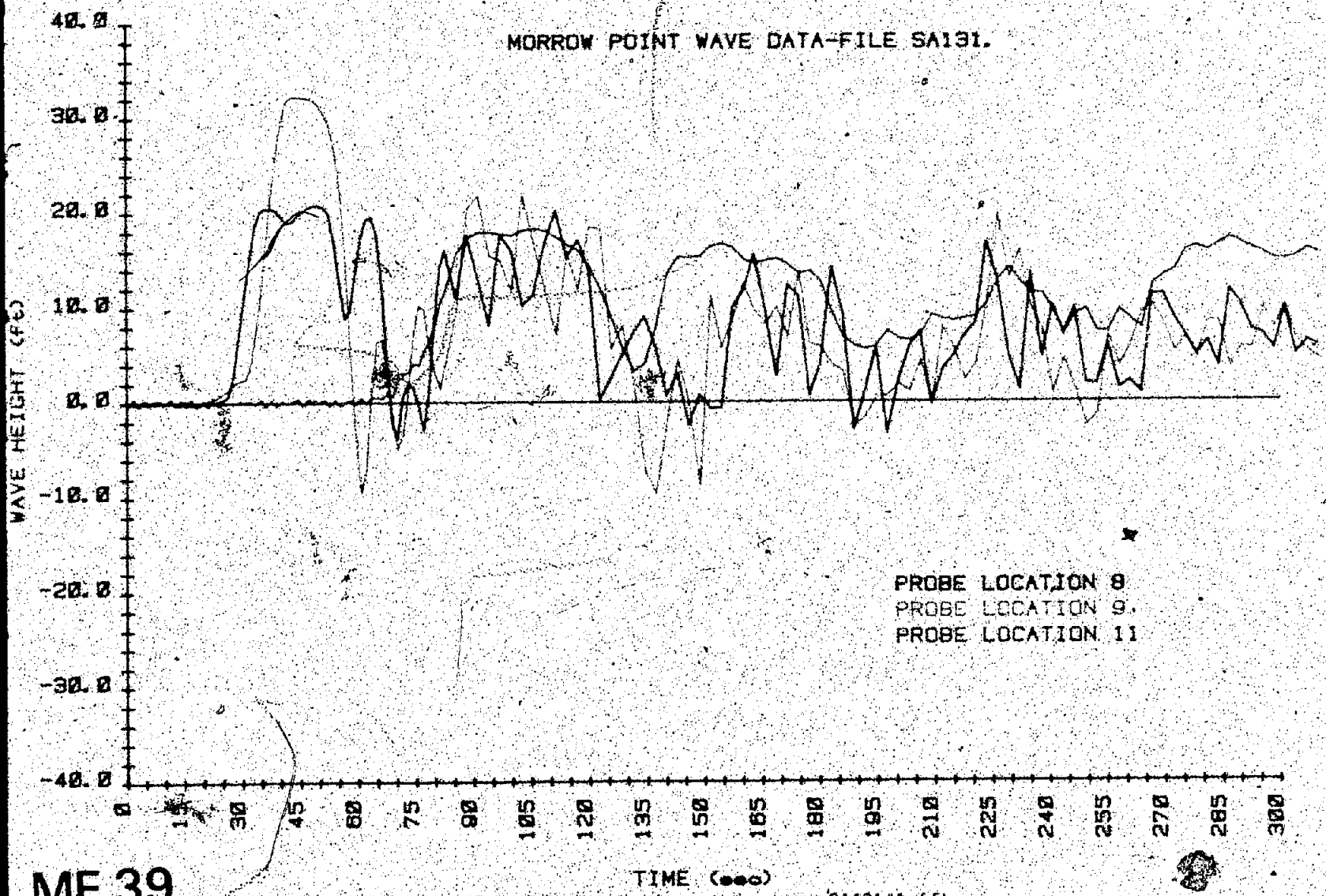

MF 39

Figure B-8 — Wave height versus time — test SA131 (4 of 5)

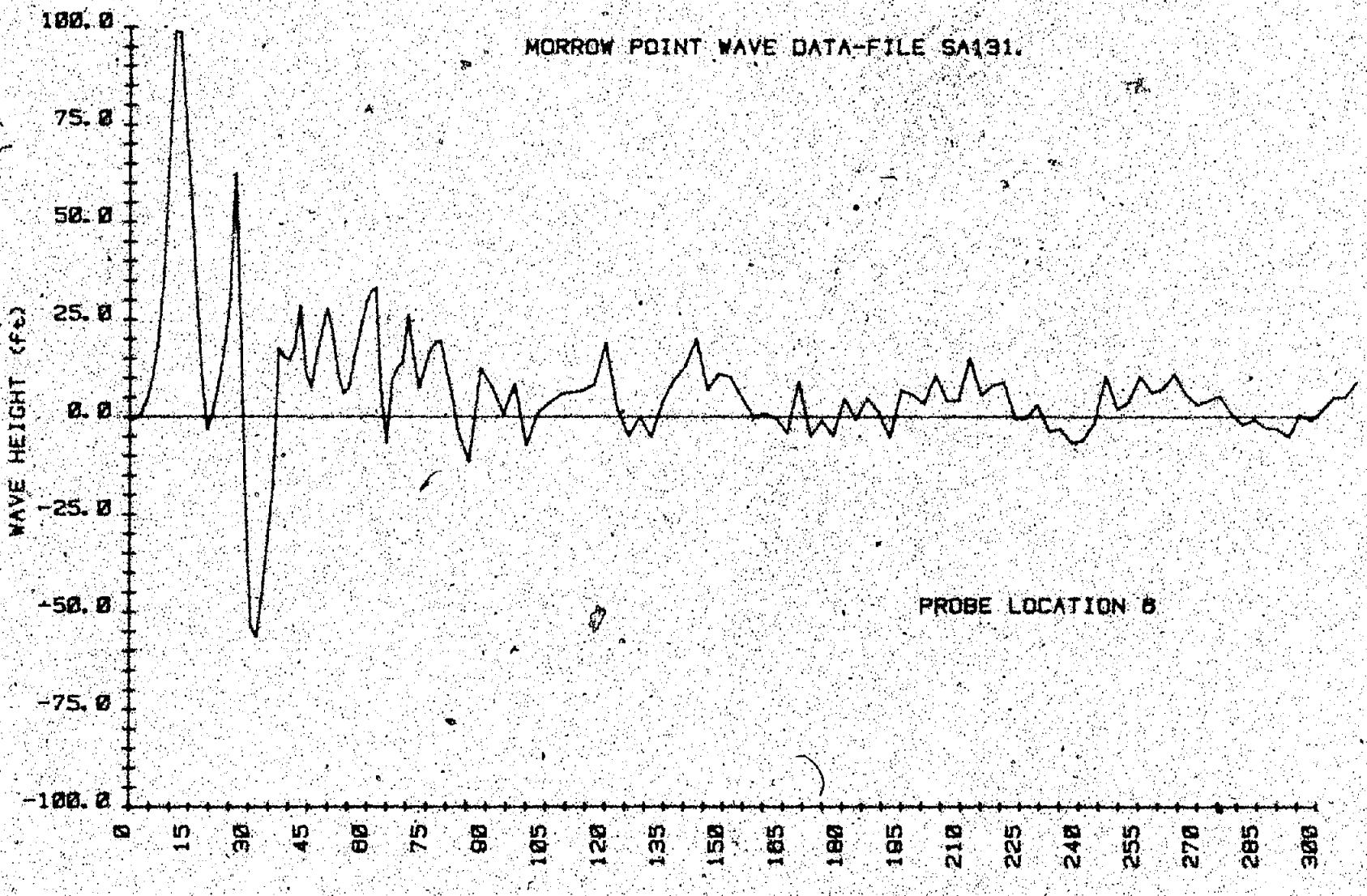

Figure 8-8. – Wave height versus time – test SA131 (5 of 5).

MF 40

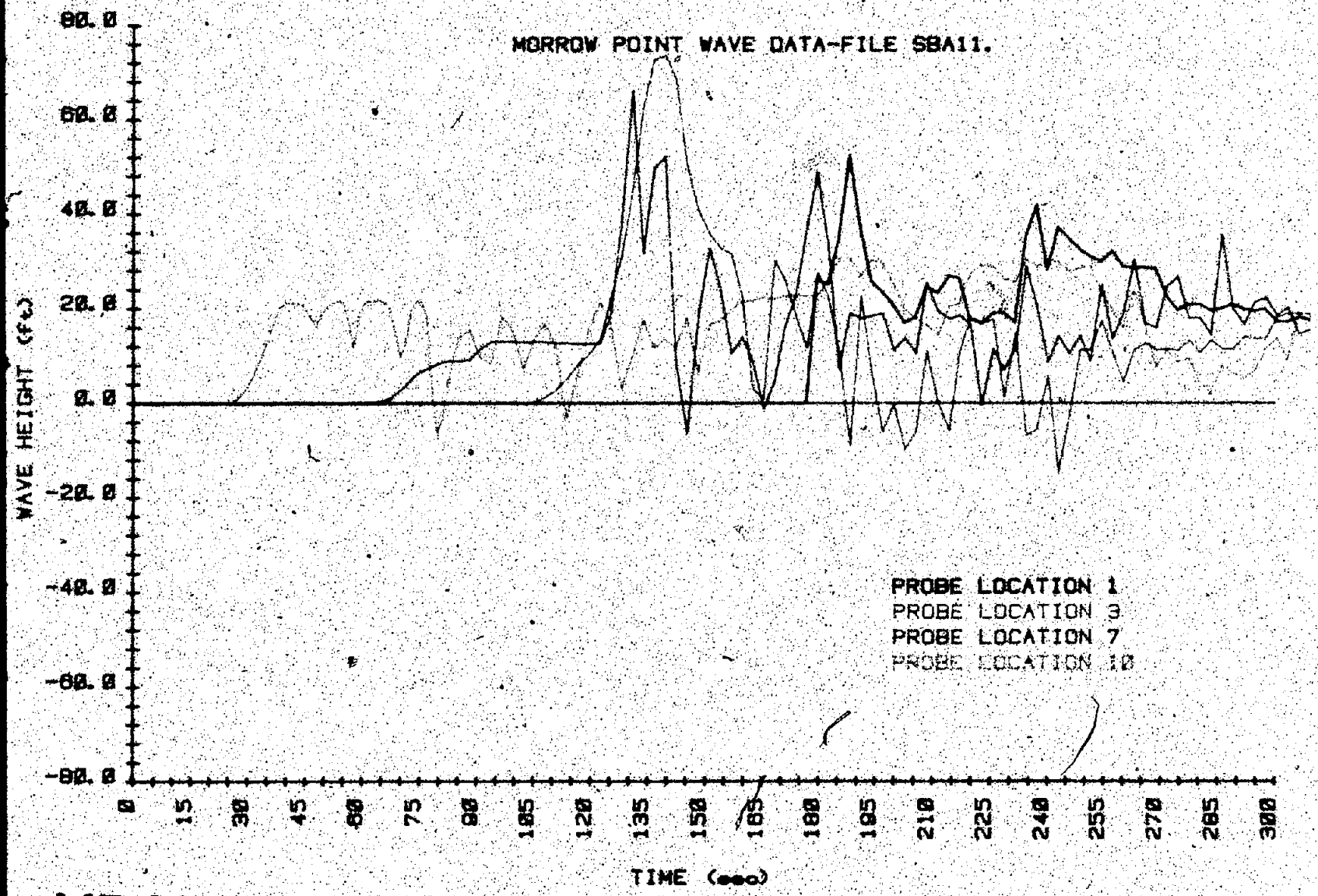

MF 41

Figure B-9. – Wave height versus time – test SBA11 (1 of 5).

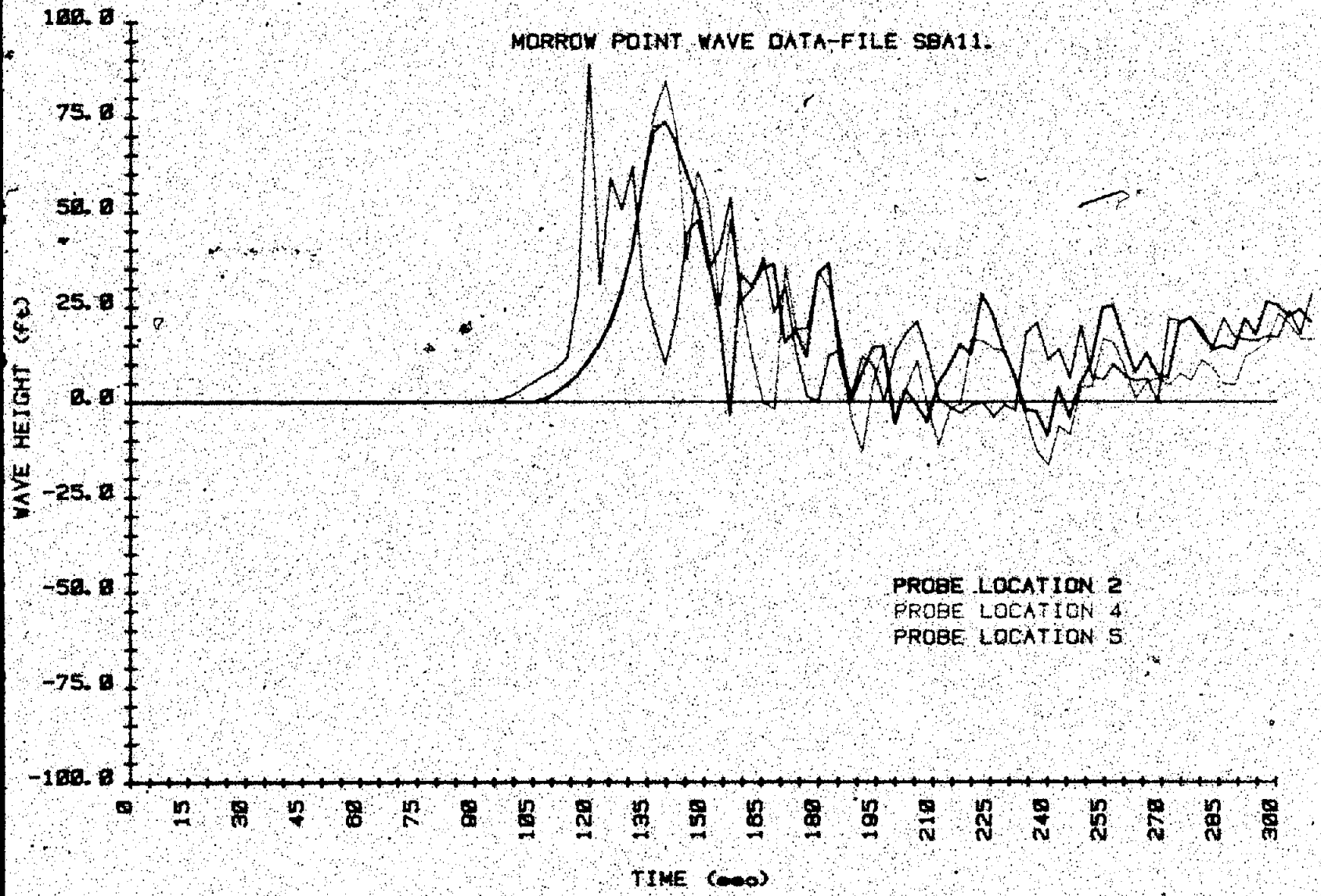

MF 42

Figure B-9.—Wave height versus time — test SBA11 (2 of 5).

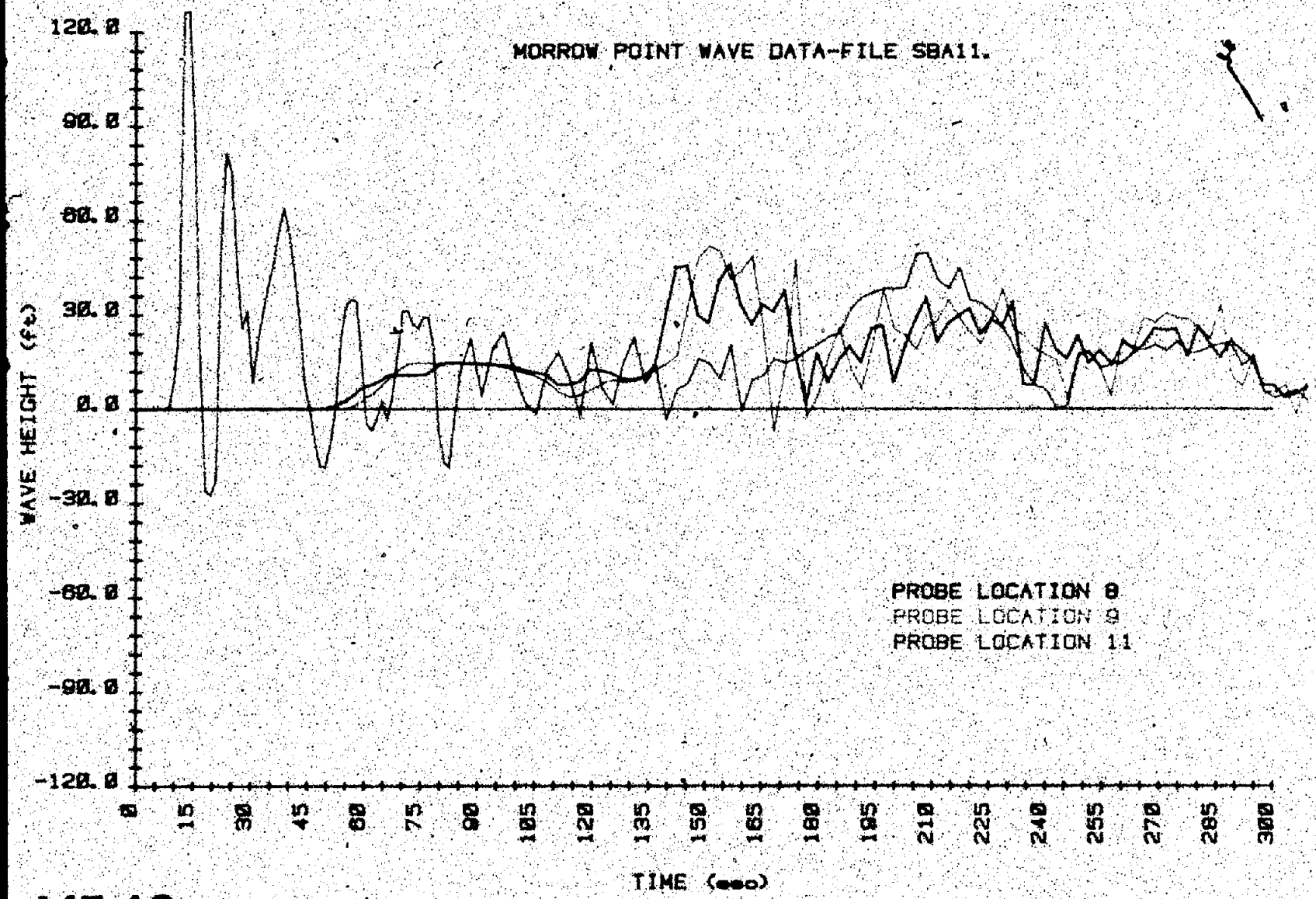

MF 43

Figure B-9. -- Wave height versus time -- test SBA11 (3 of 5)

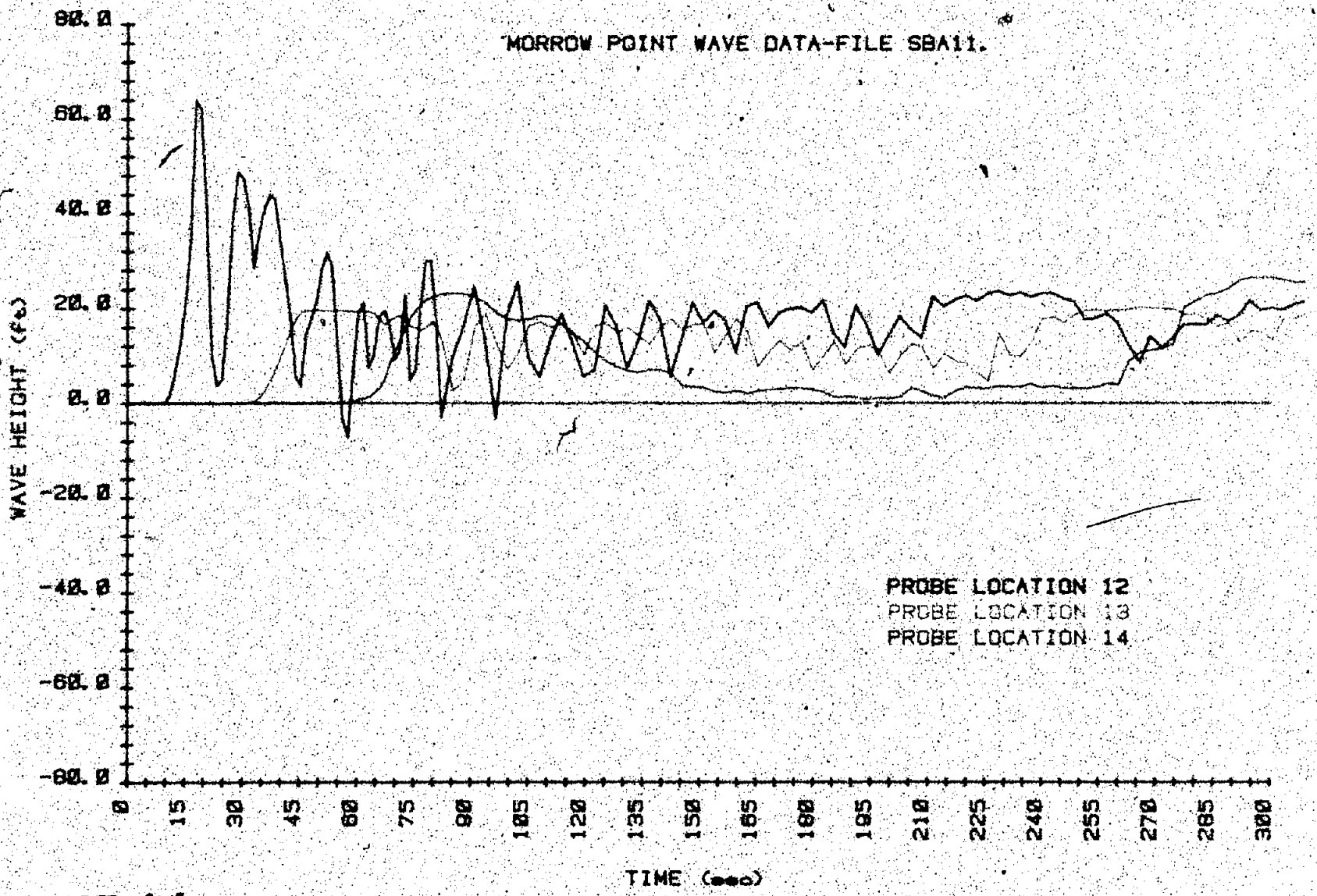

MF 44

Figure B-9. – Wave height versus time – test SBA11 (4 of 5).

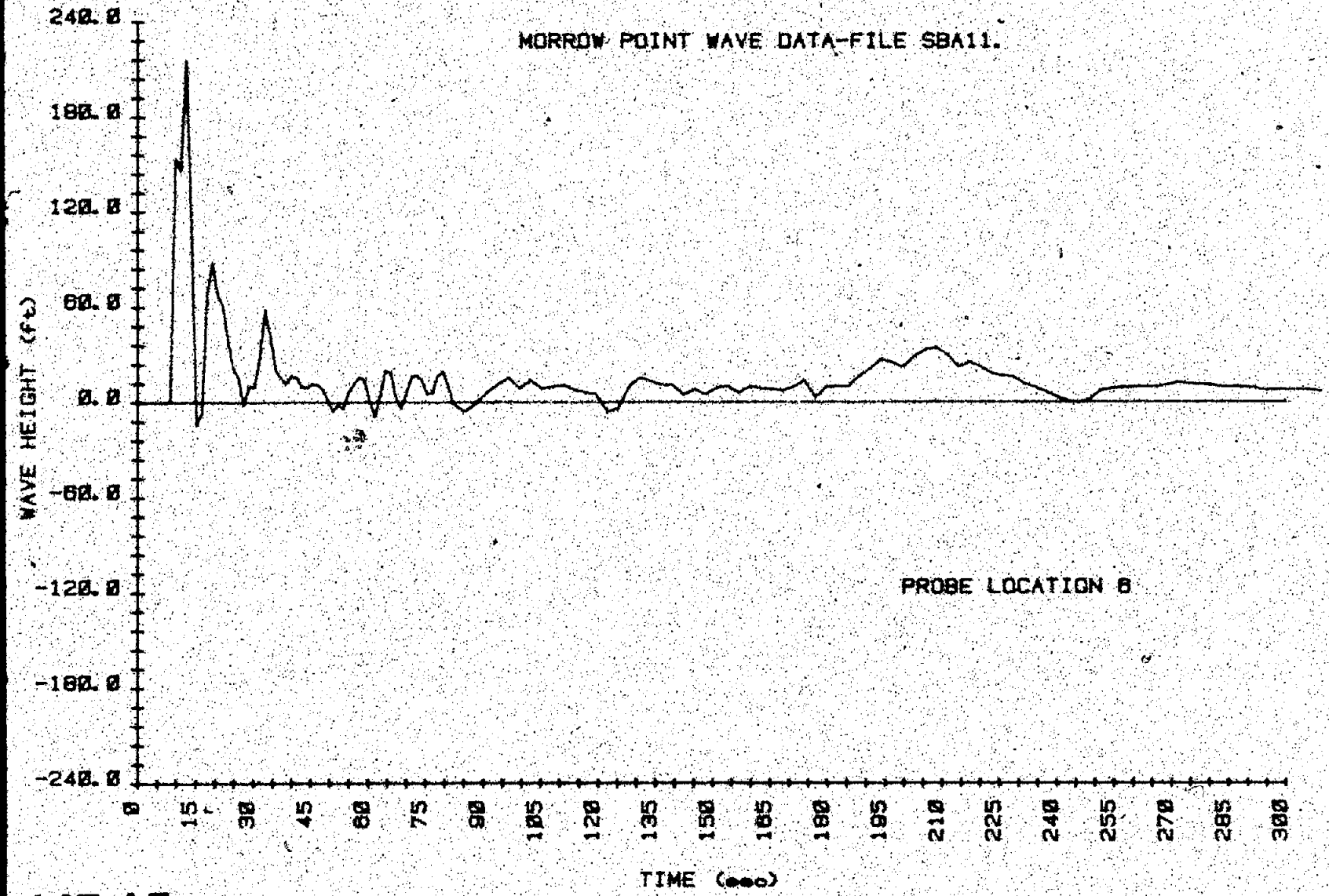

MF 45

Figure B-9. - Wave height versus time -- test SBA11 (5 of 5).

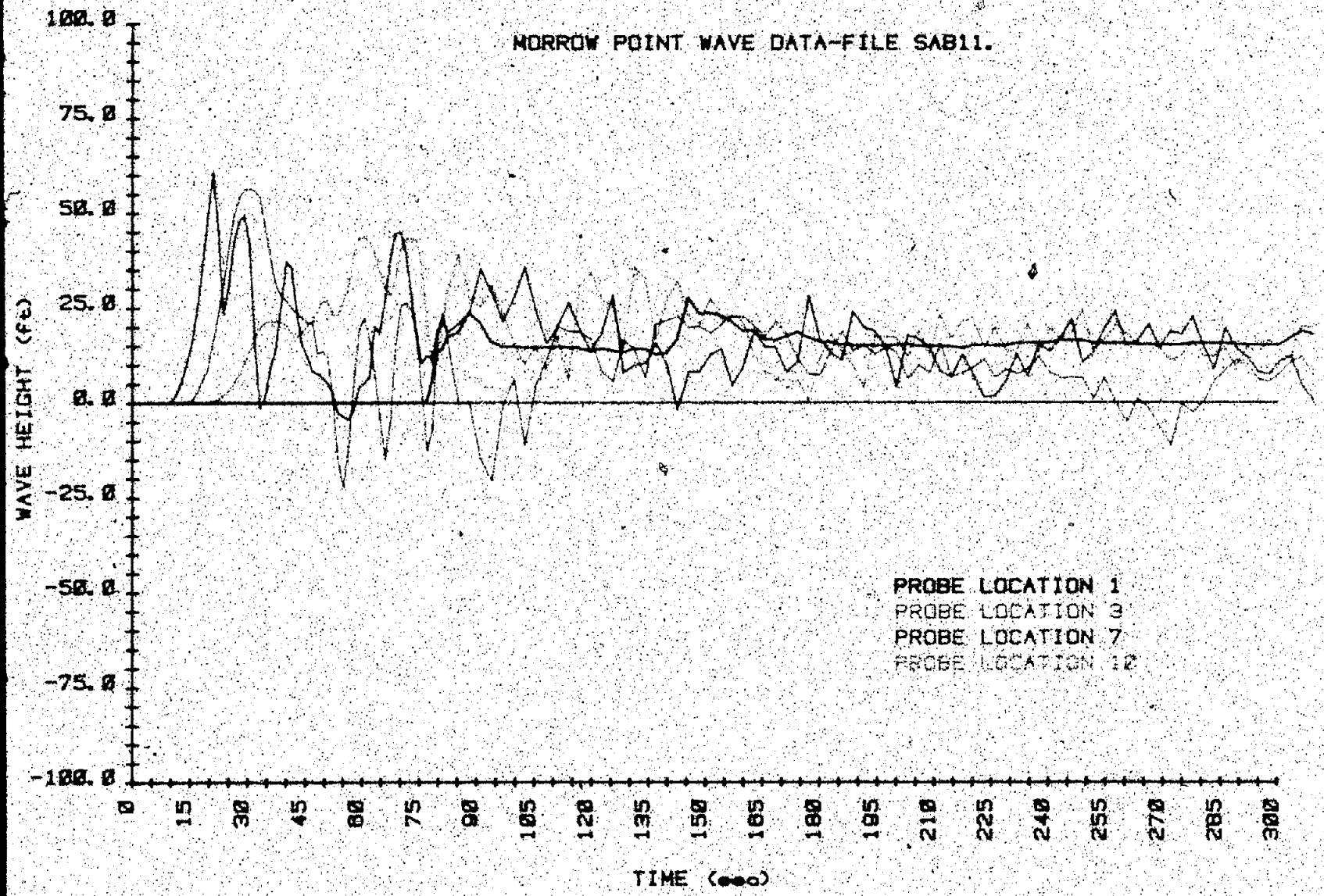

MF 46

Figure B-10.—Wave height versus time — test SAB11 (1 of 5).

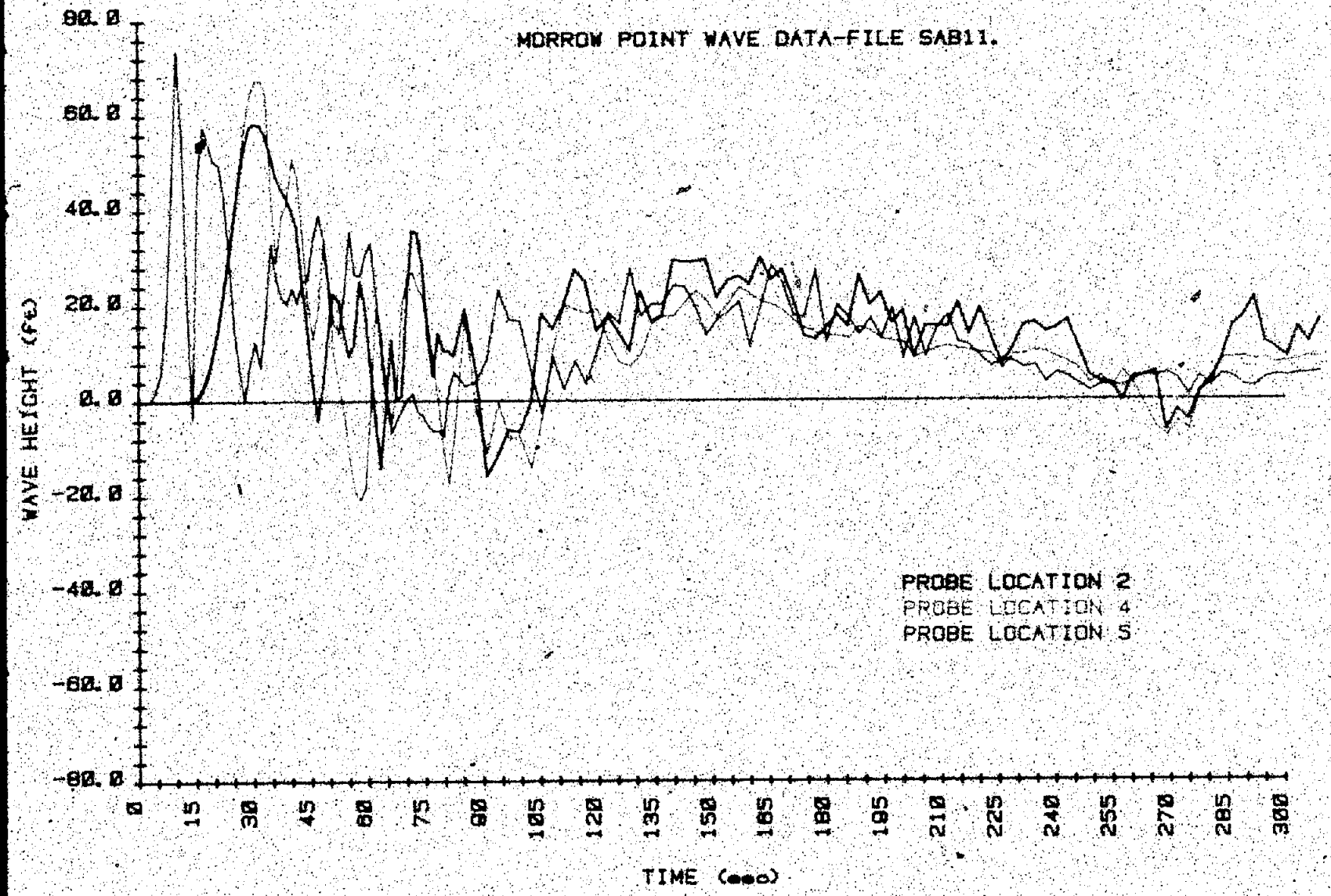

MF 47

Figure 8-10. – Wave height versus time – test SAB11 (2 of 5)

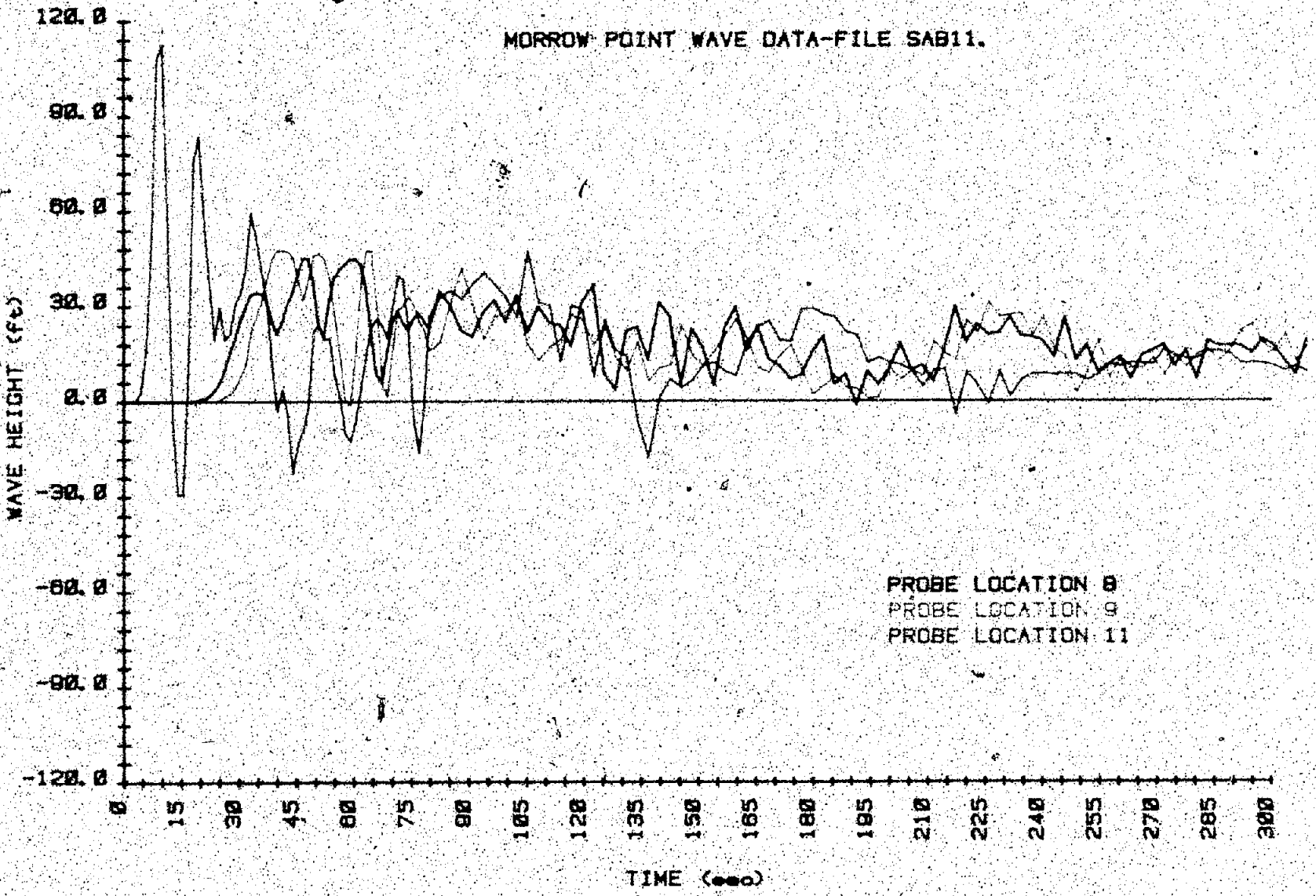

MF 48

Figure B-10 – Wave height versus time – test SAB11 (3 of 5).

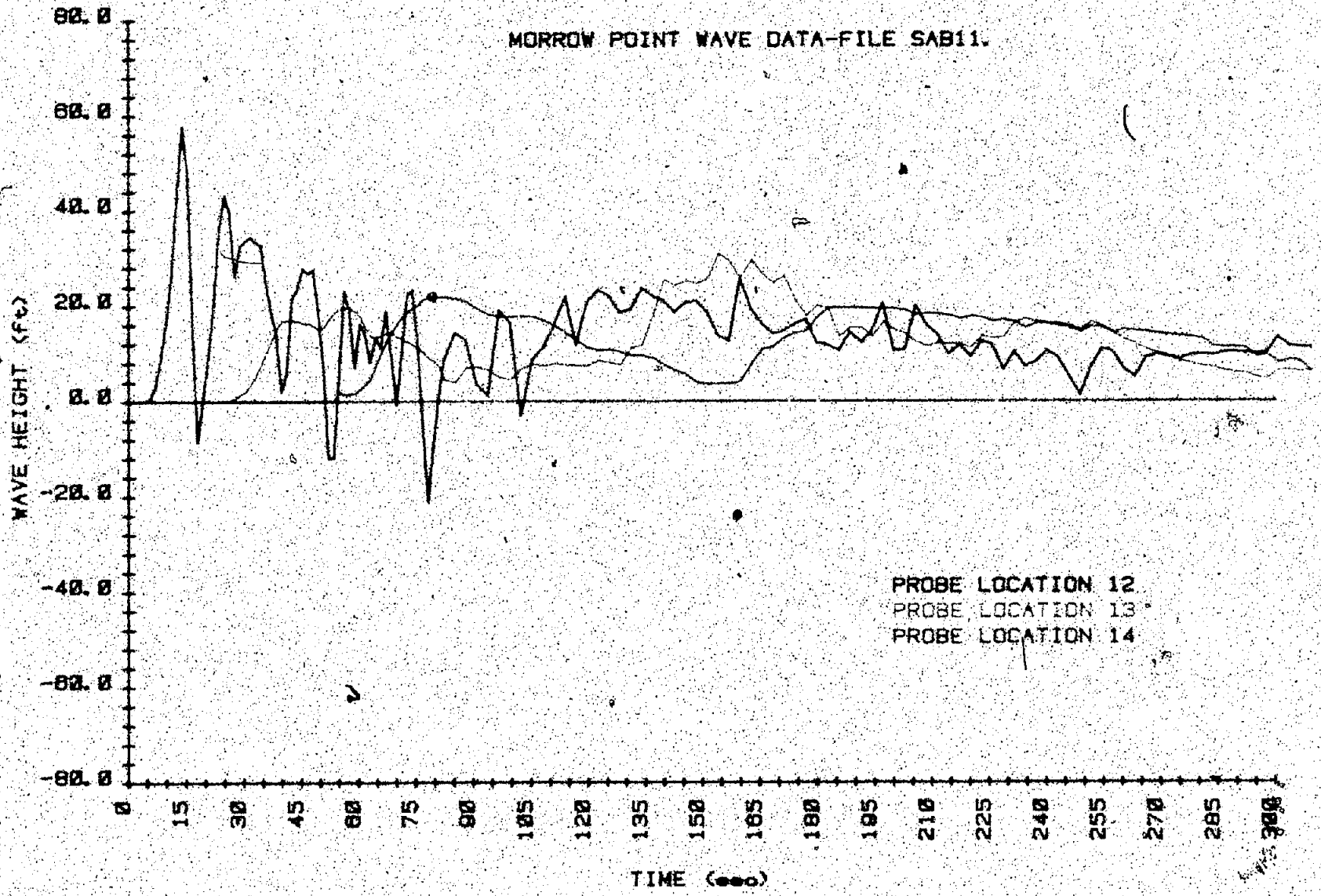

MF 49

Figure B-10. – Wave height versus time – test SAB11 (4 of 5)

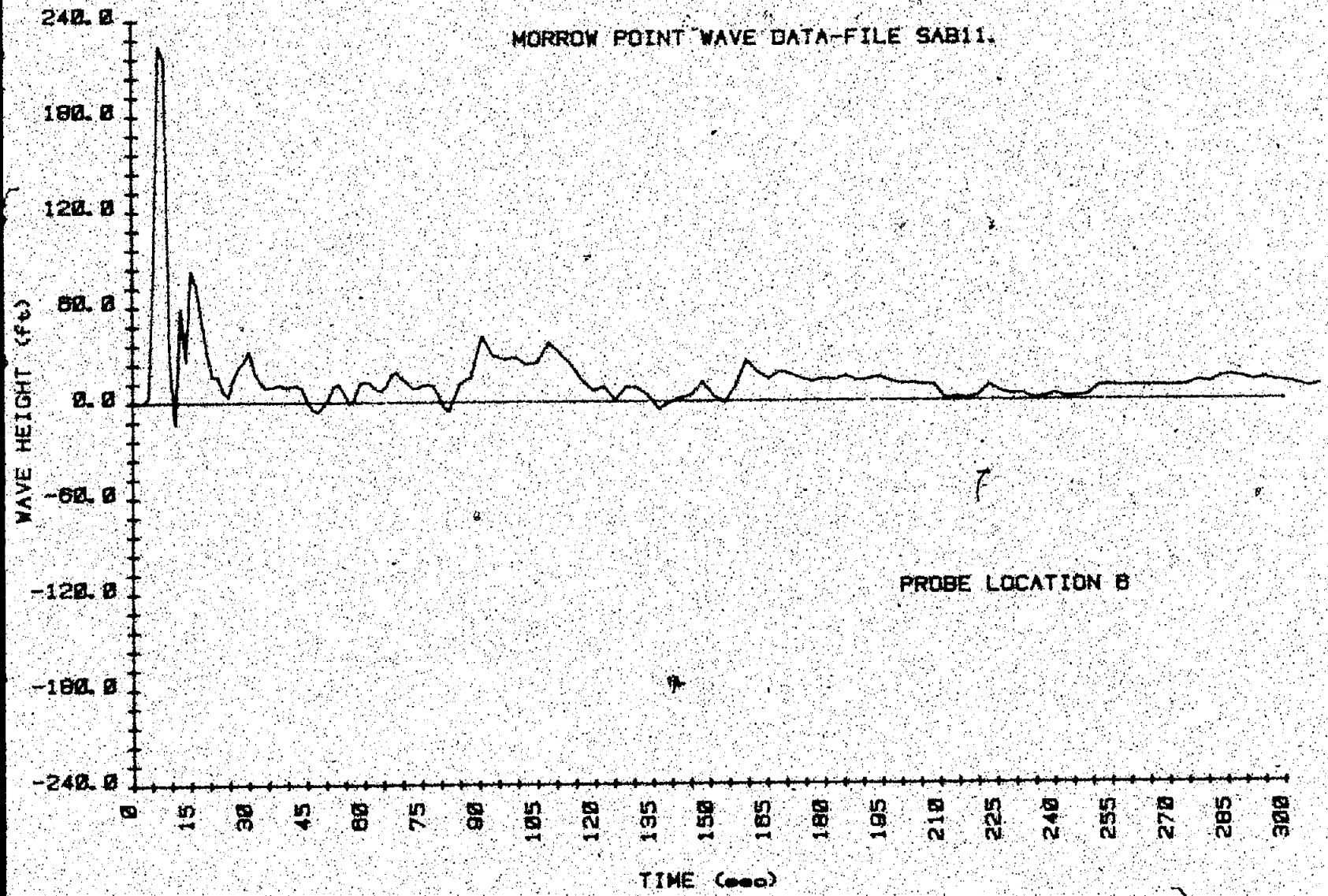

MF 50

Figure B-10.—Wave height versus time — test SAB11 (5 of 5).

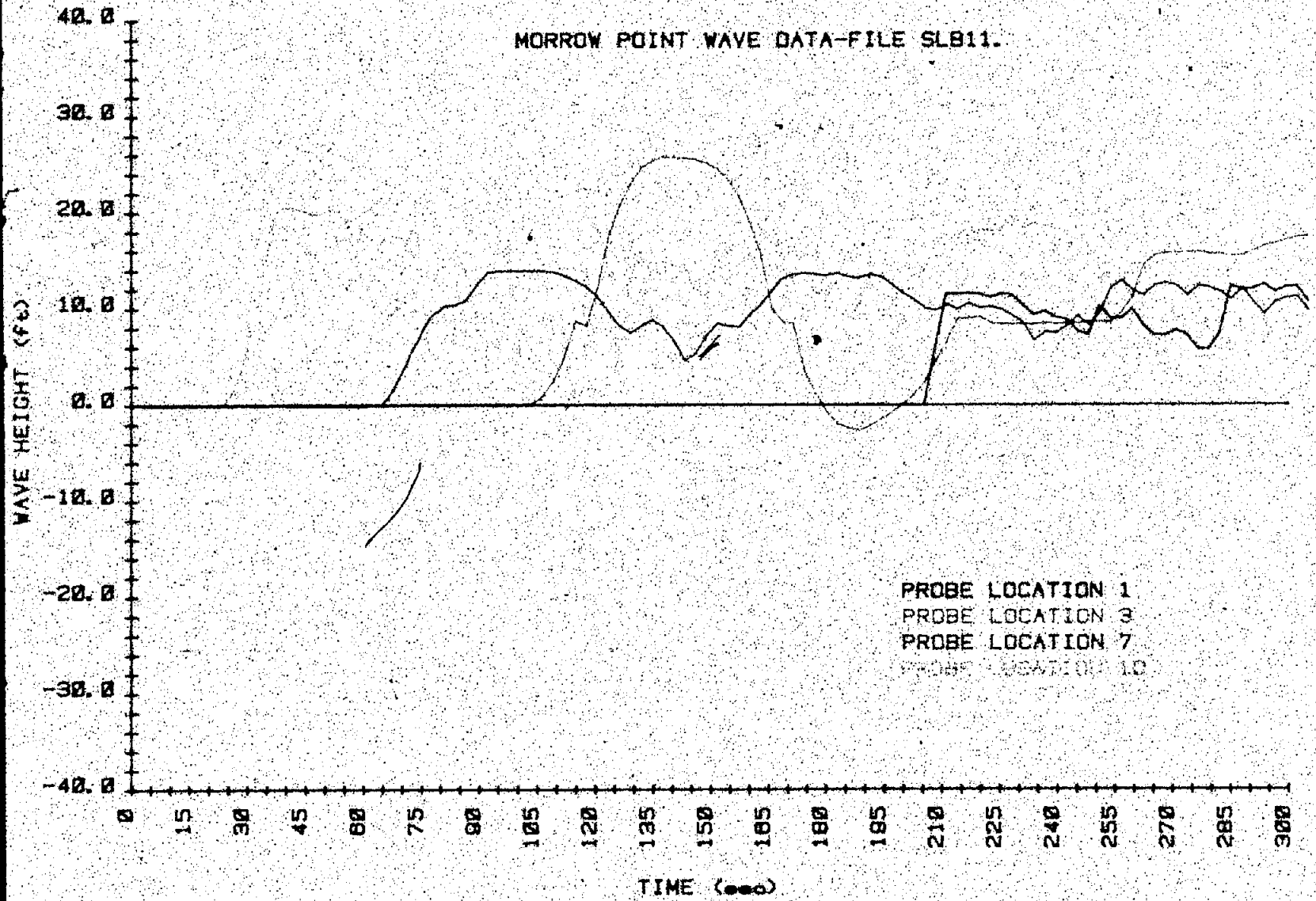

MF 51

Figure B-11.—Wave height versus time — test SLB11 (1 of 4)

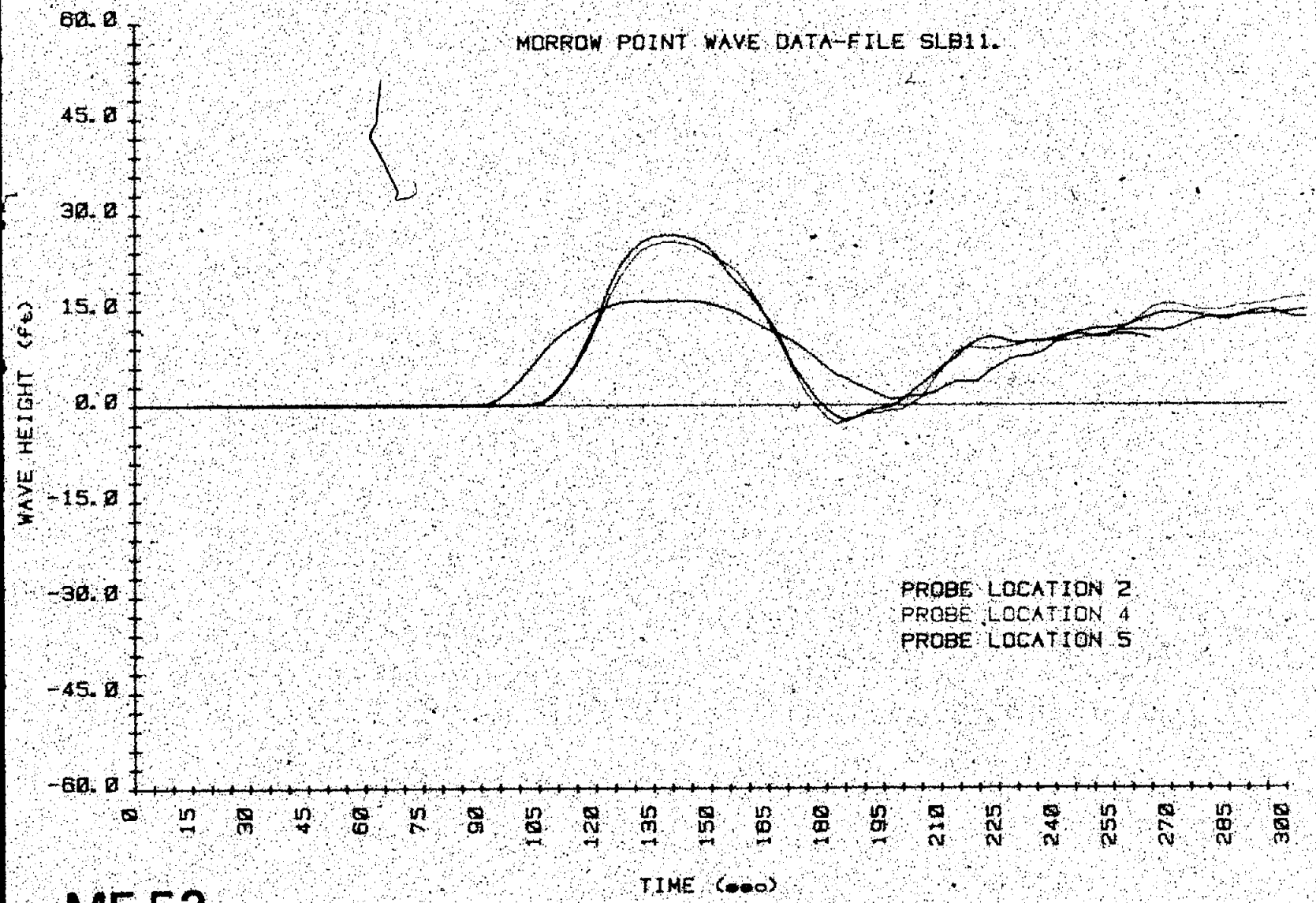

MF 52

Figure B-11.—Wave height versus time — test SLB11 (2 of 4).

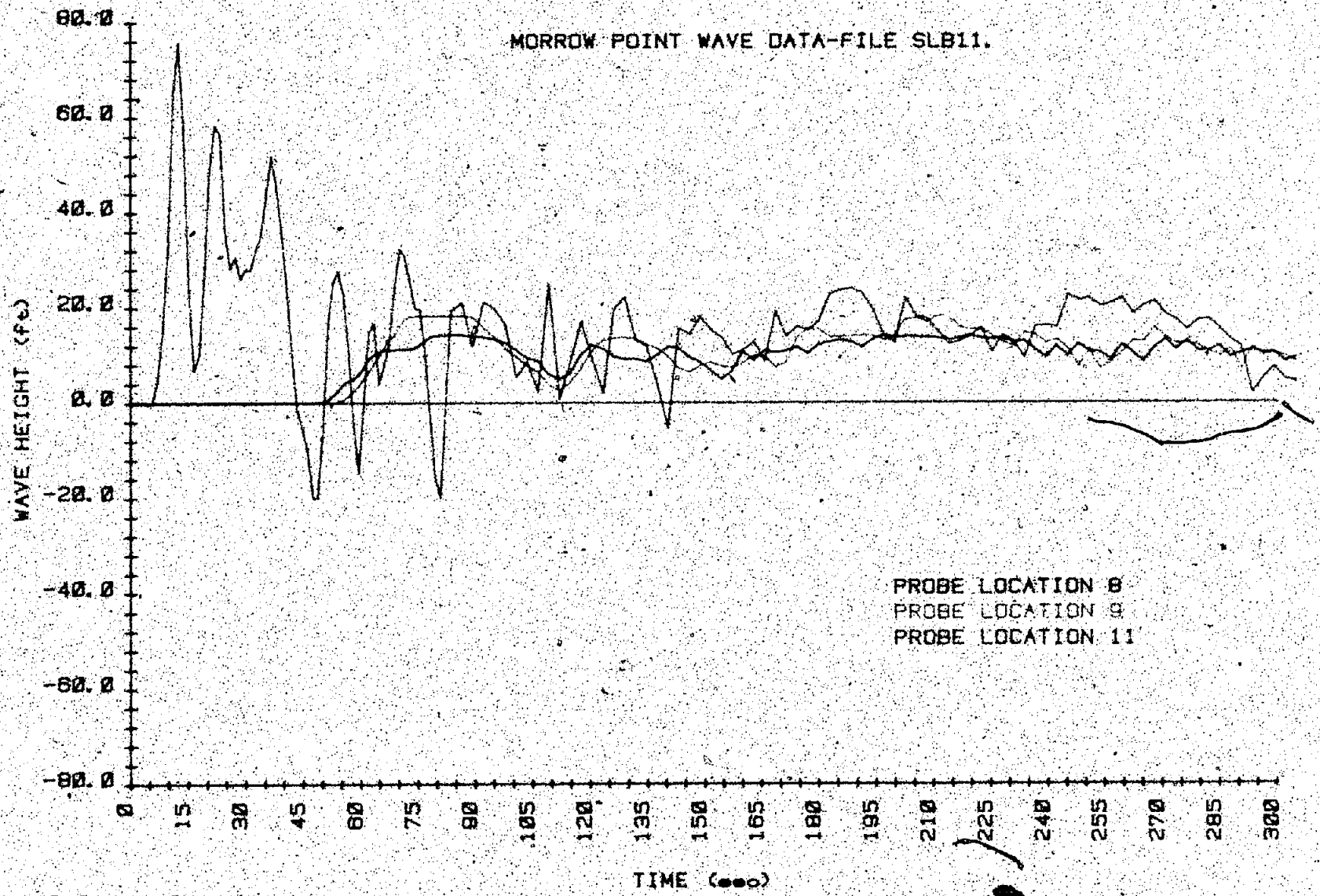

MF 53

Figure B-11. – Wave height versus time – test SLB11 (3 of 4).

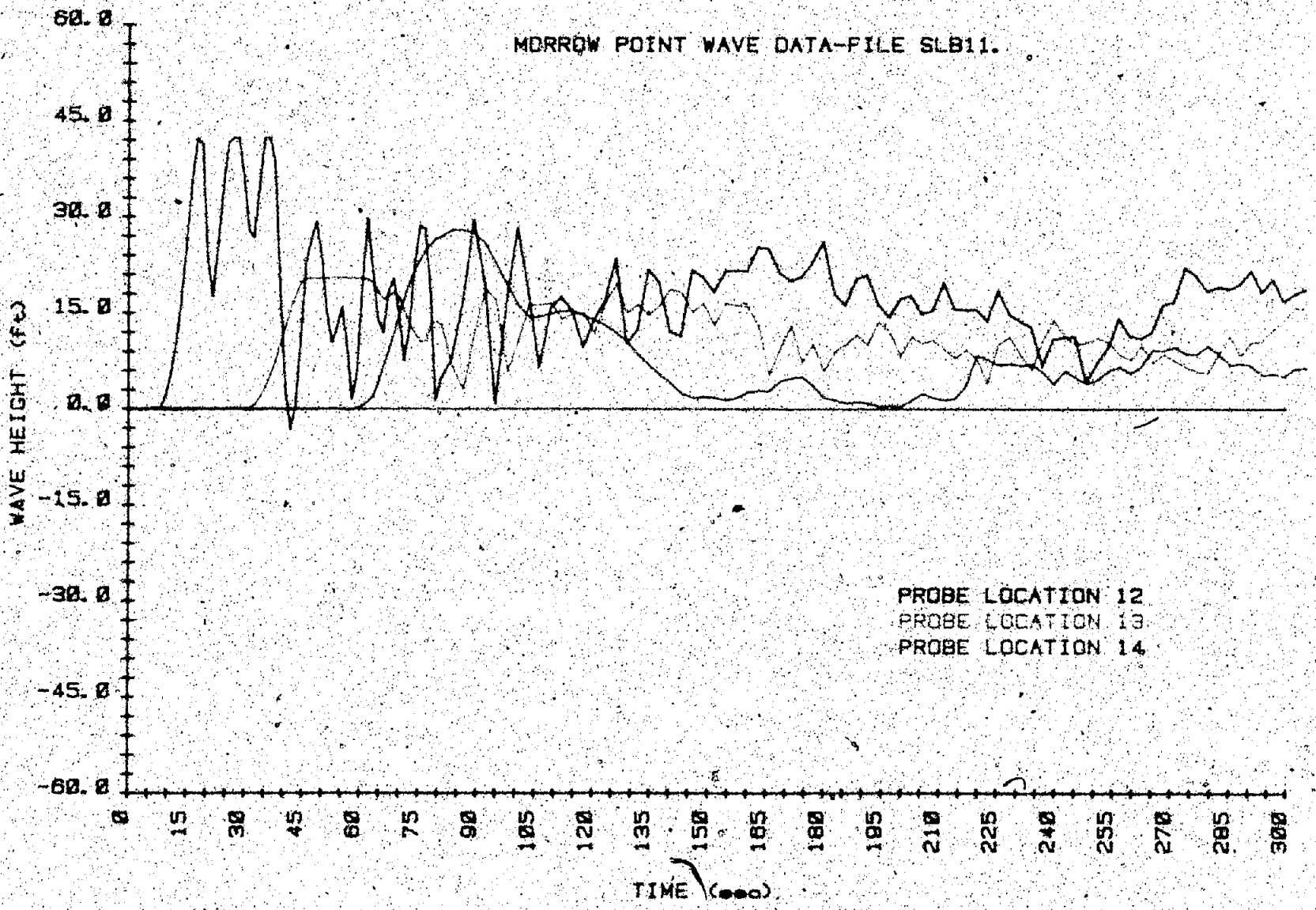

MF 54

Figure B-11.—Wave height versus time — test SLB11 (4 of 4)

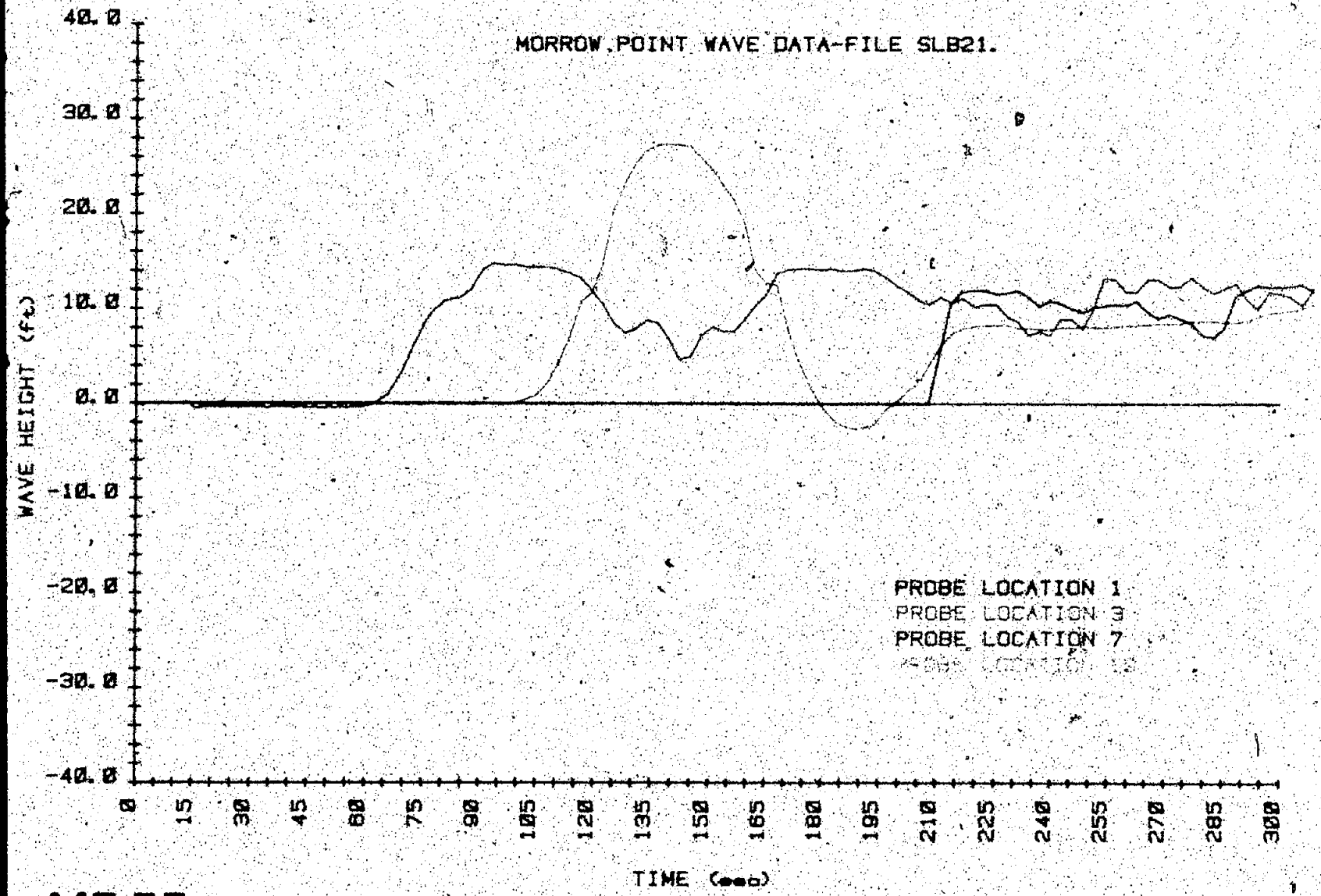

MF 55

Figure B 12. – Wave height versus time – test SLB21 (1 of 5).

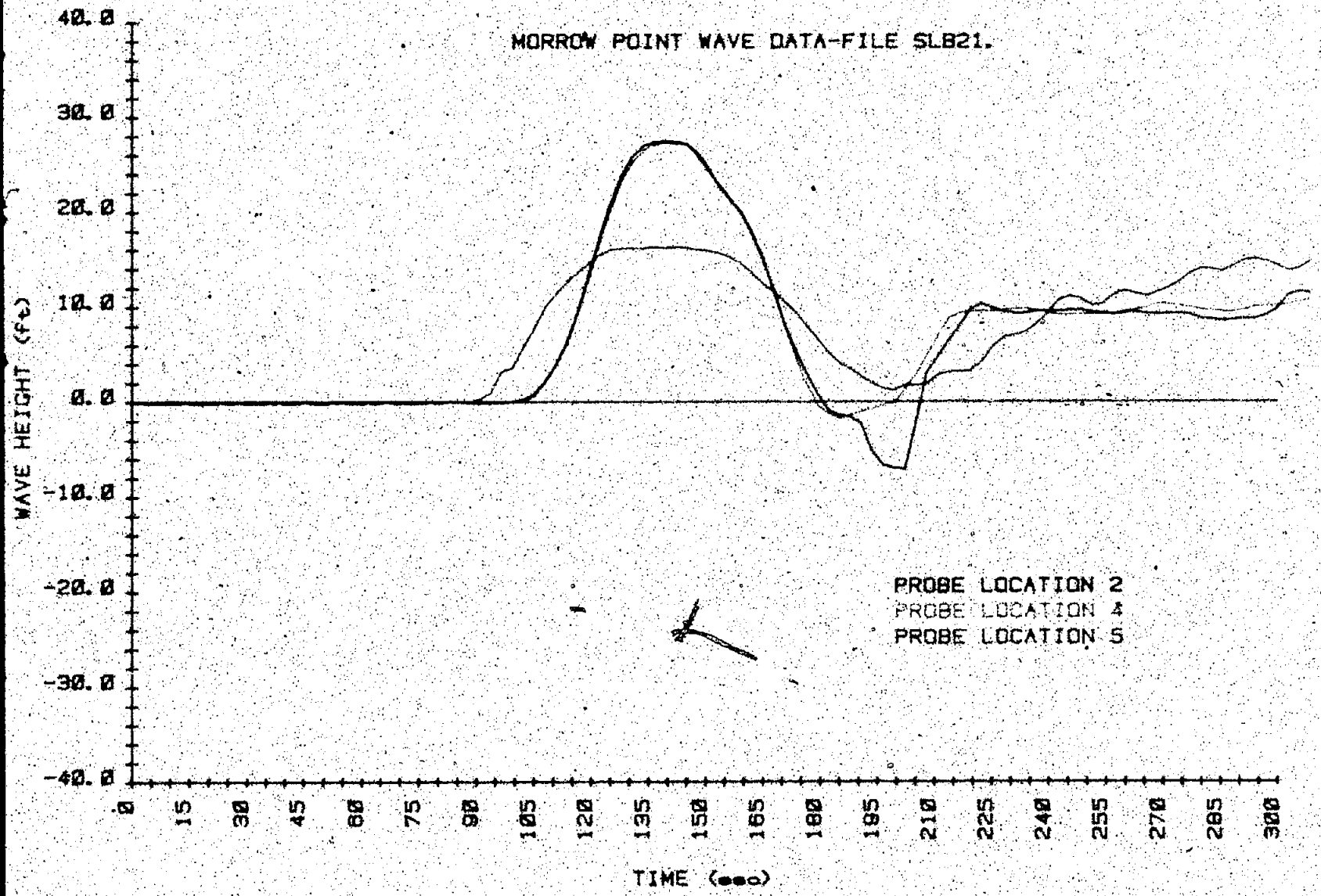

MF 56

Figure B-12.—Wave height versus time — test SLB21 (2 of 5)

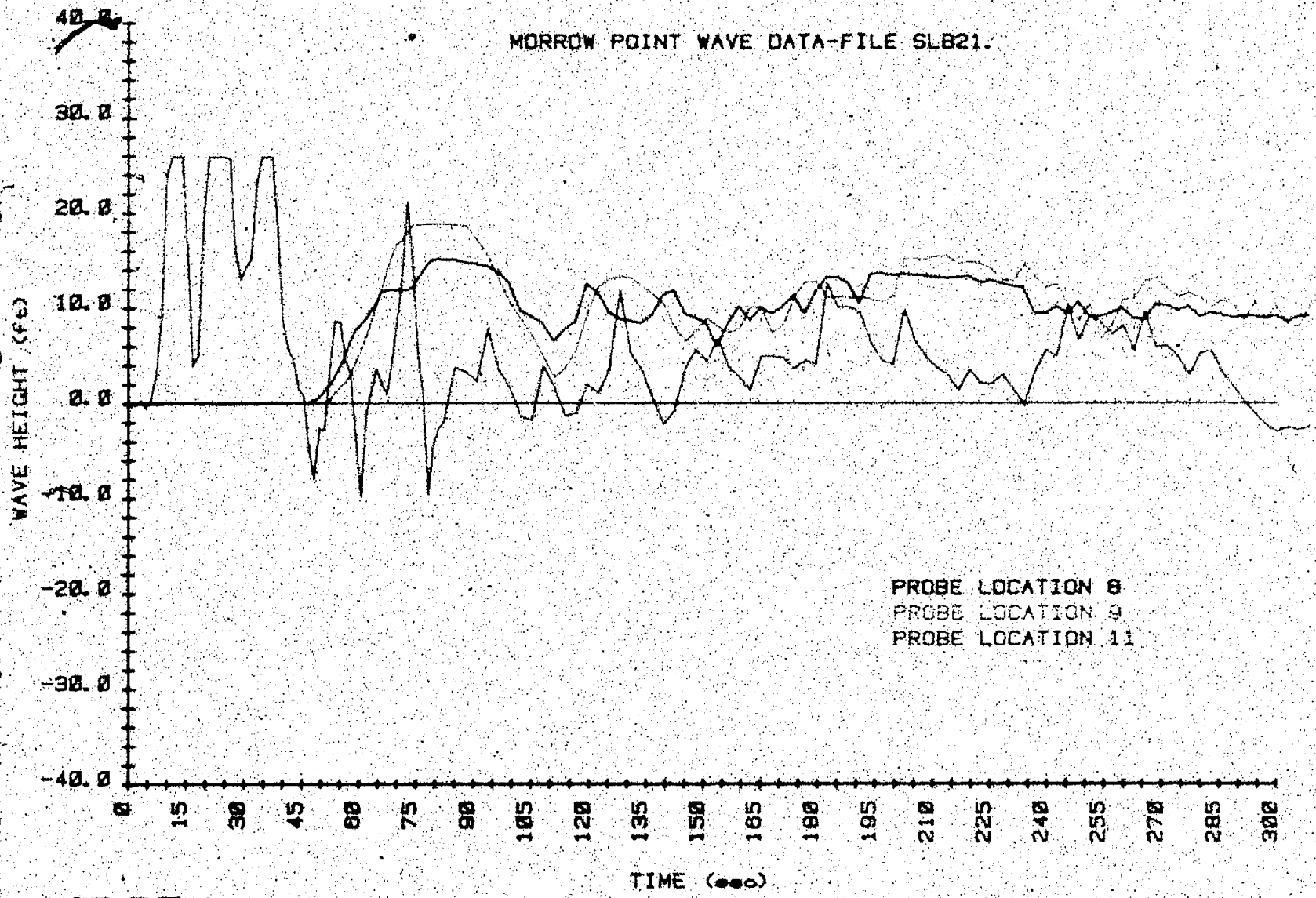

MF 57

Figure B-12. – Wave height versus time — test SLB21 (3 of 5).

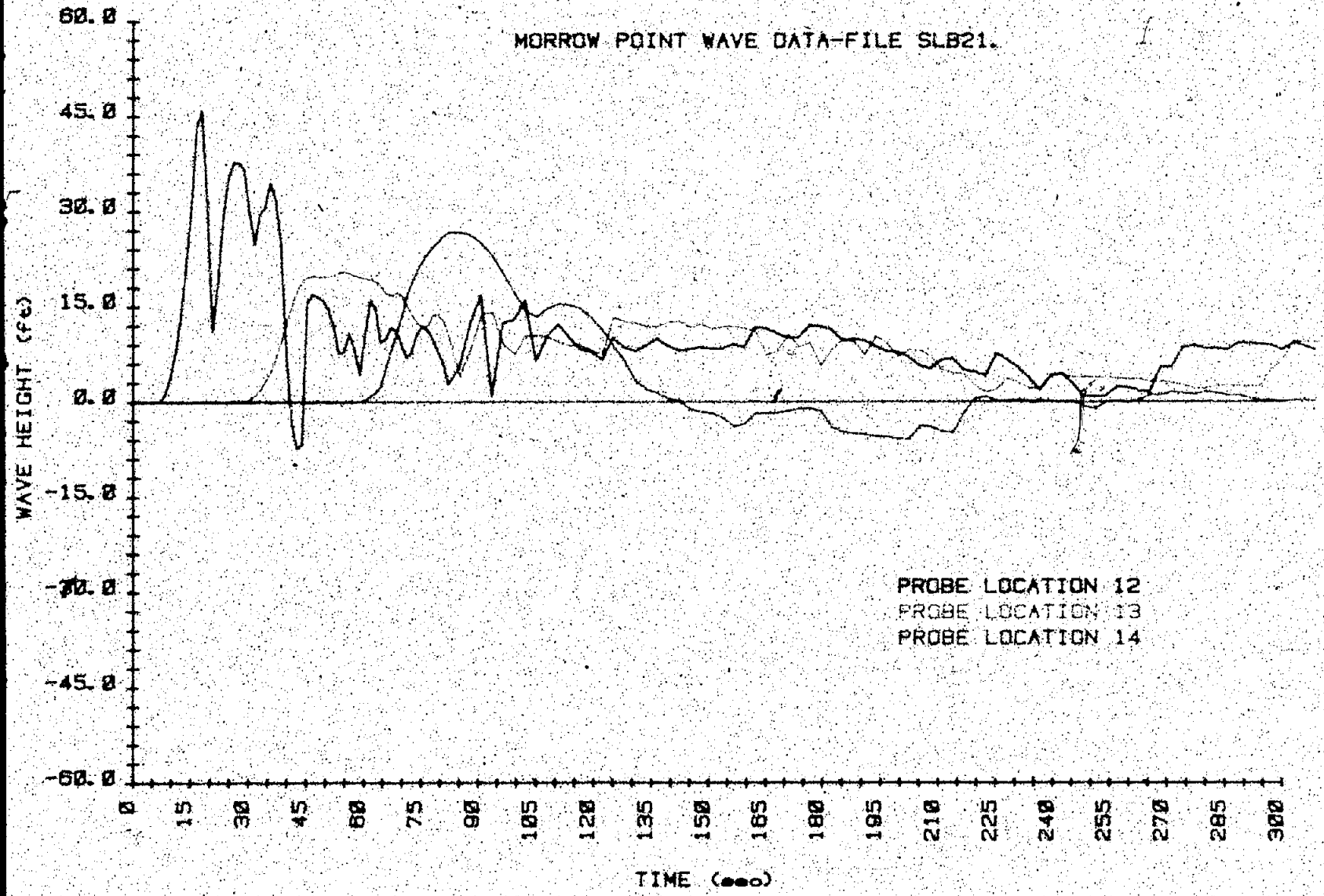

MF 58

Figure B-12.—Wave height versus time — test SLB21 (4 of 5)

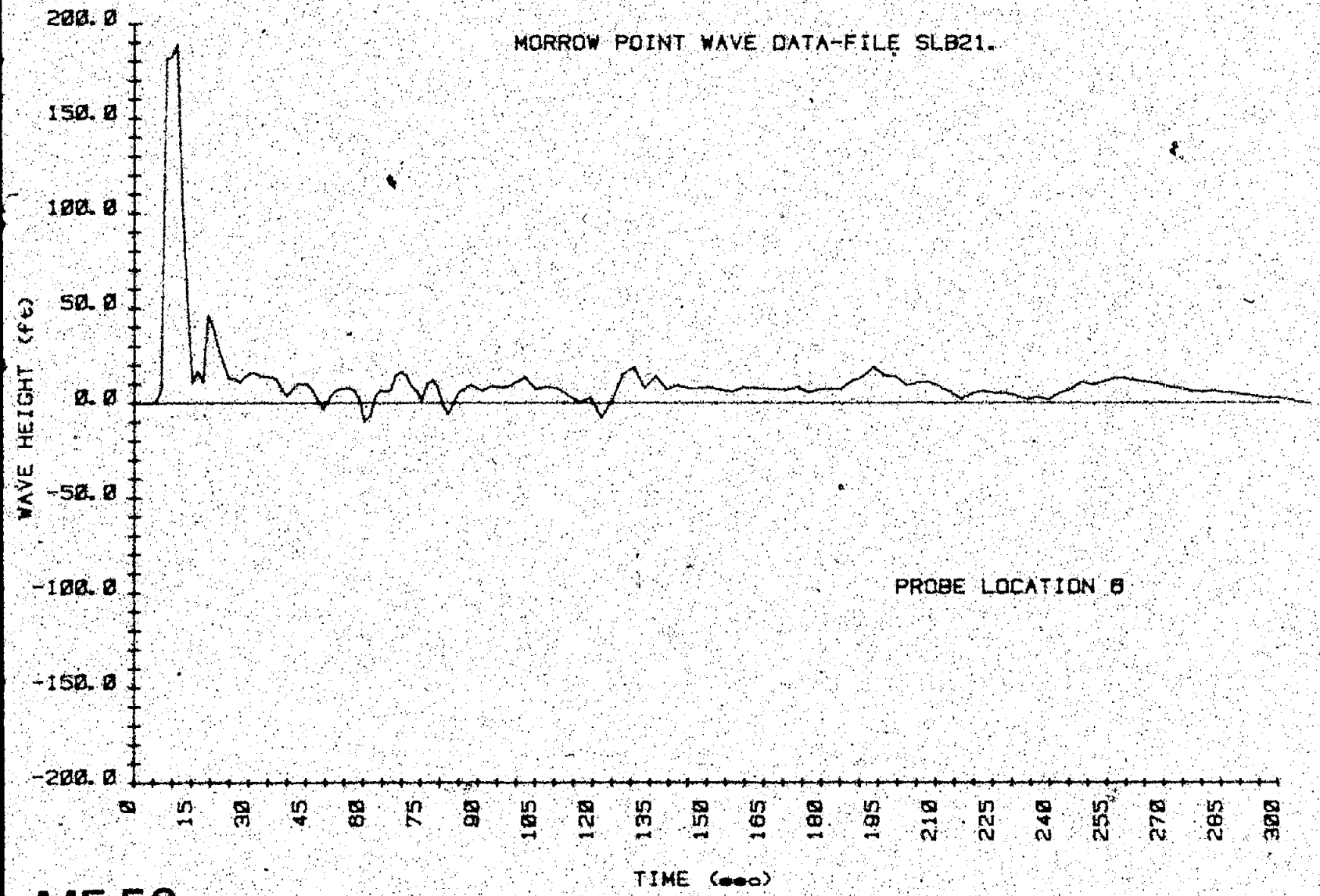

MF 59

Figure B-12. – Wave height versus time – test SLB21 (5 of 5)

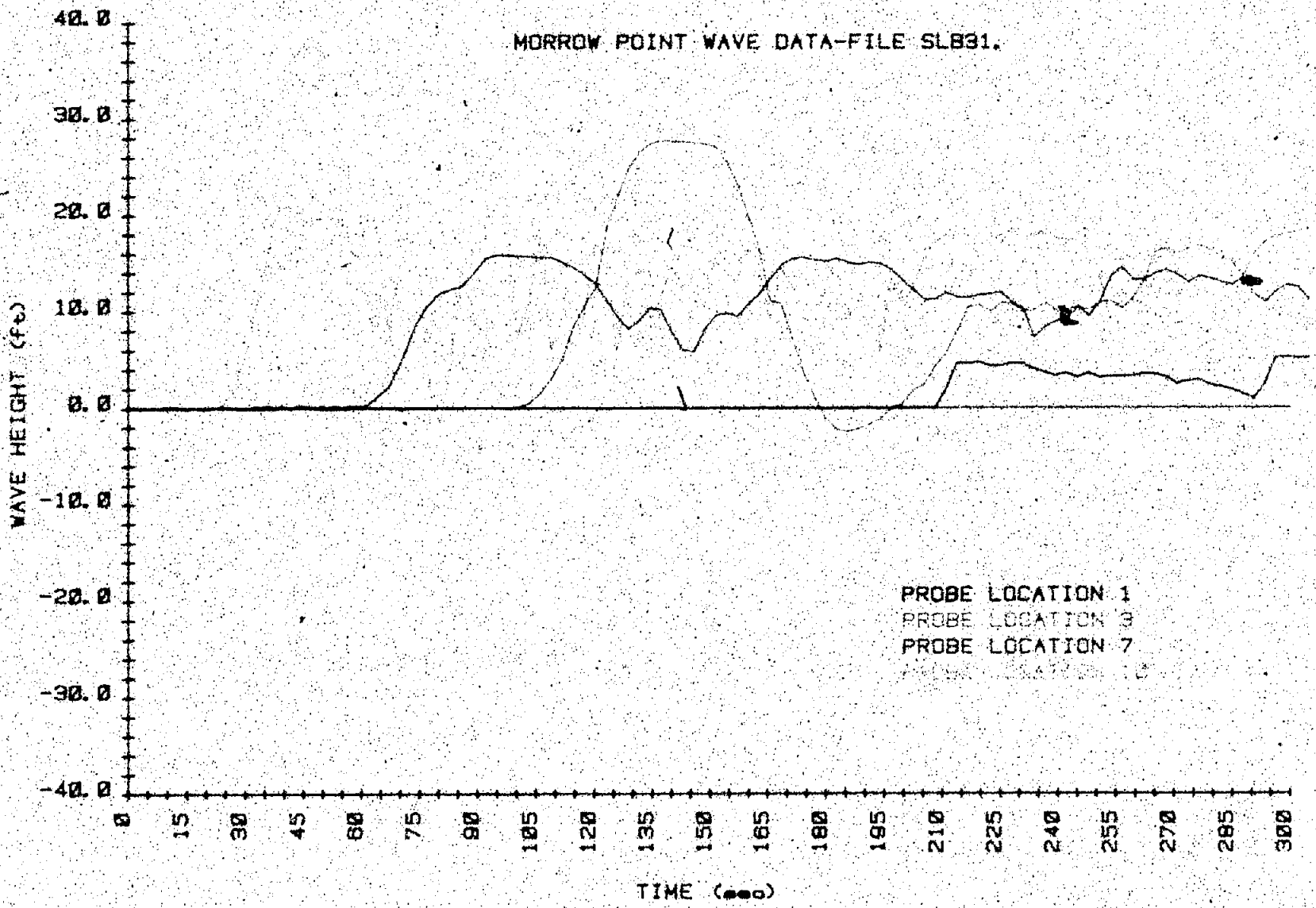

MF 60

Figure B 13.—Wave height versus time — test SLB31 (1 of 5).

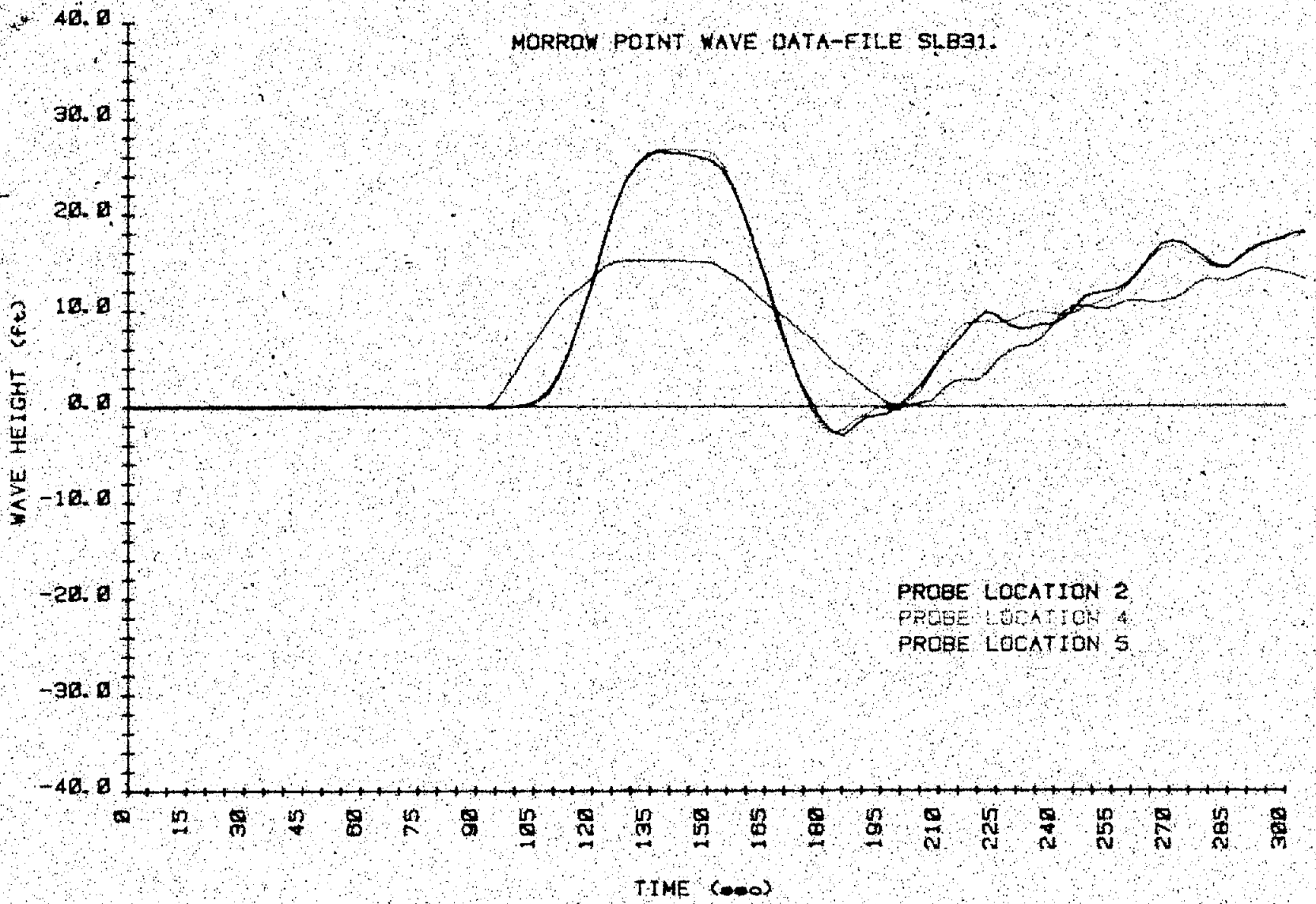

MF 61

Figure B-13.--Wave height versus time.--test SLB31 (2 of 5).

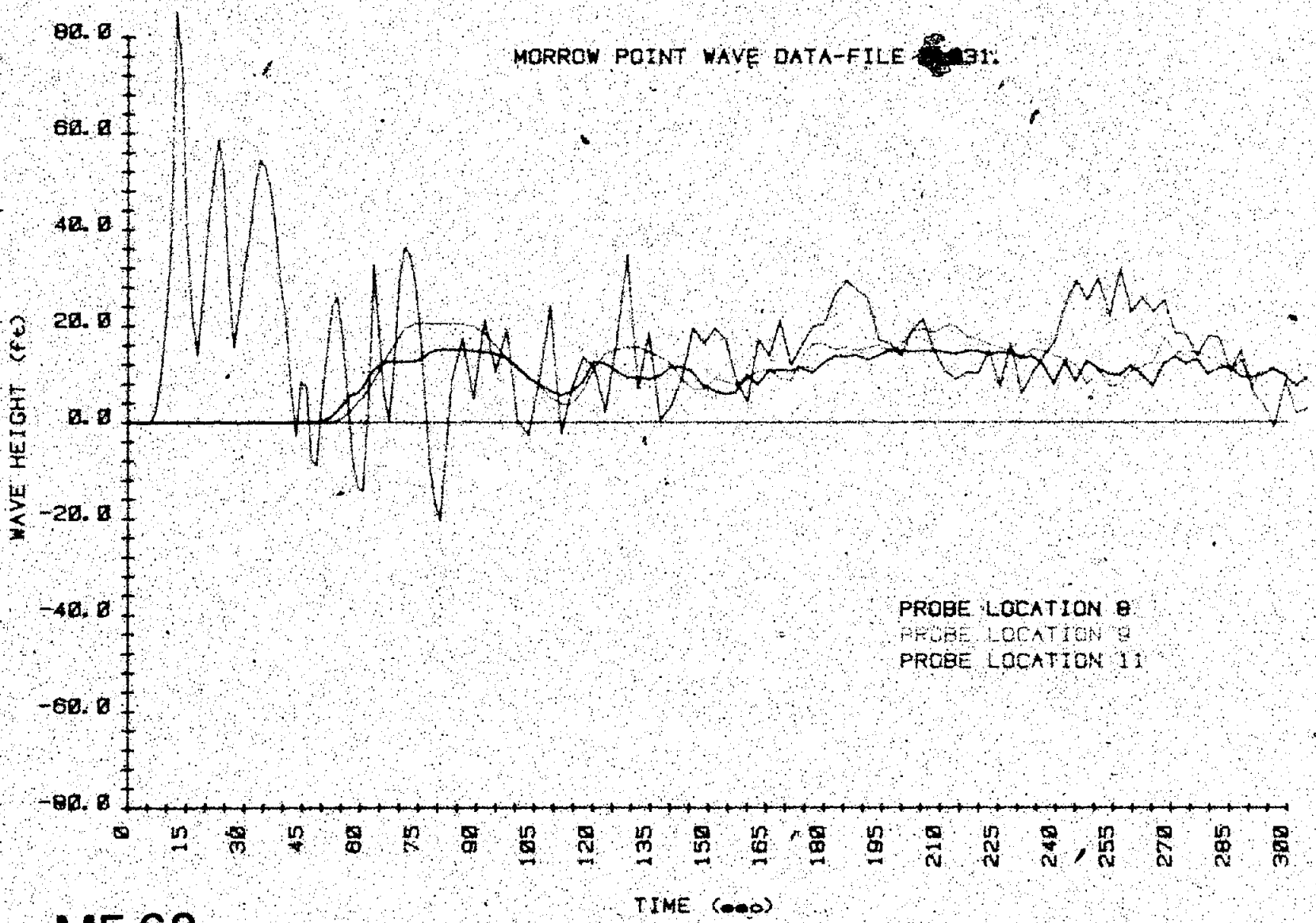

MF 62

Figure B-13.—Wave height versus time—test SLB31 (3 of 5).

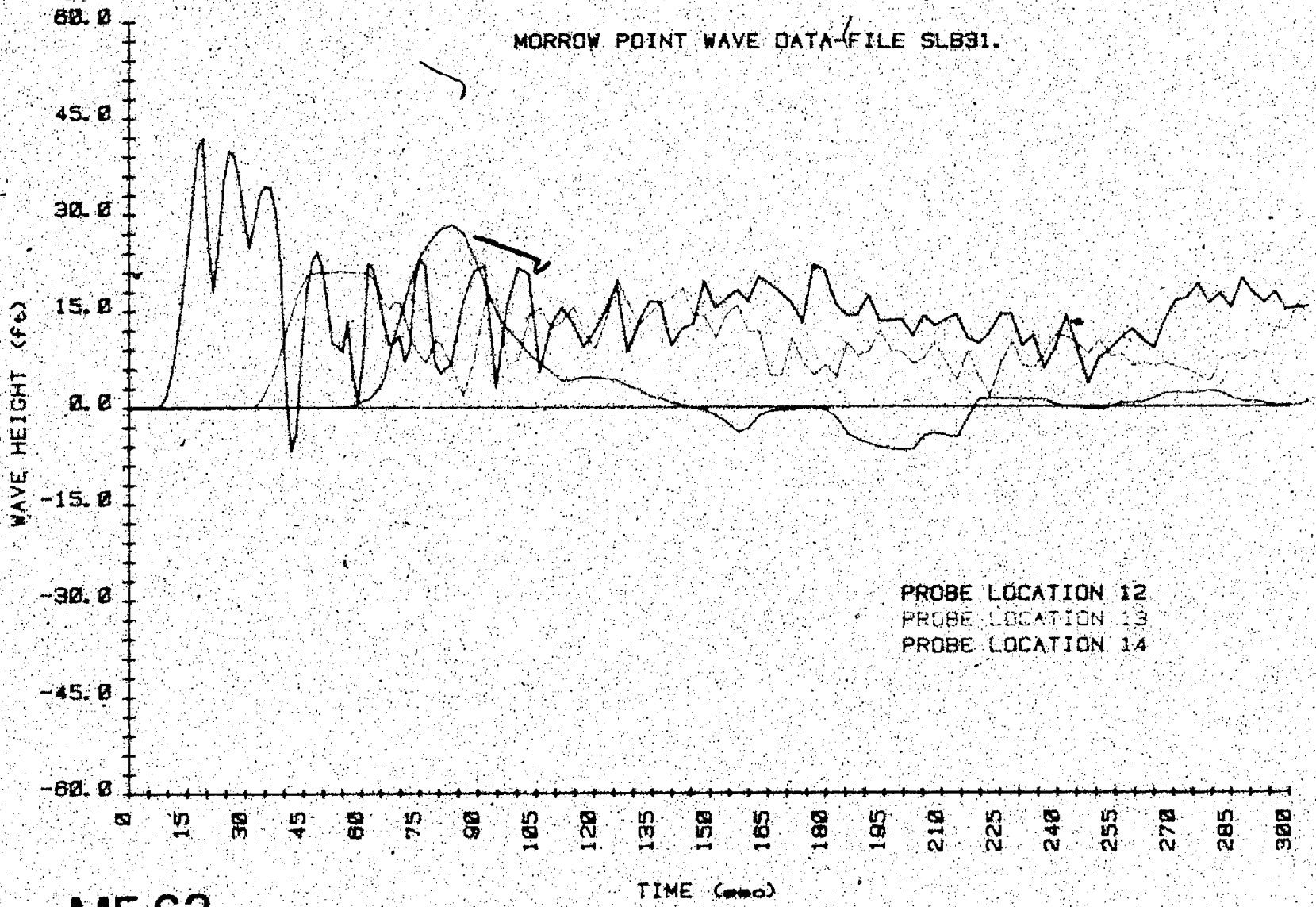

MF 63

Figure B 13. Wave height versus time — test SLB31 (4 of 5)

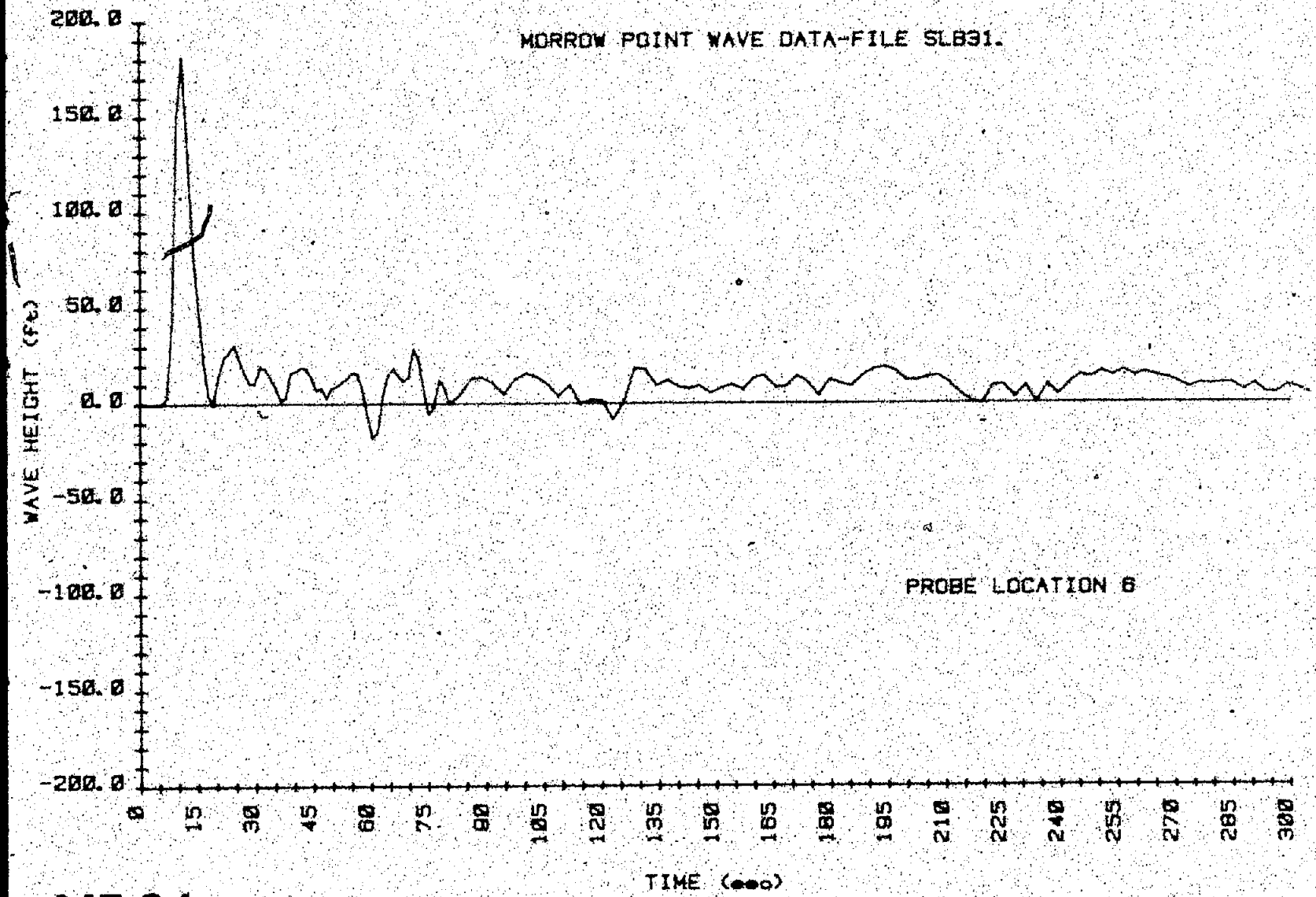

MF 64.

Figure B-13. Wave height versus time -- test SLB31 (5 of 5).

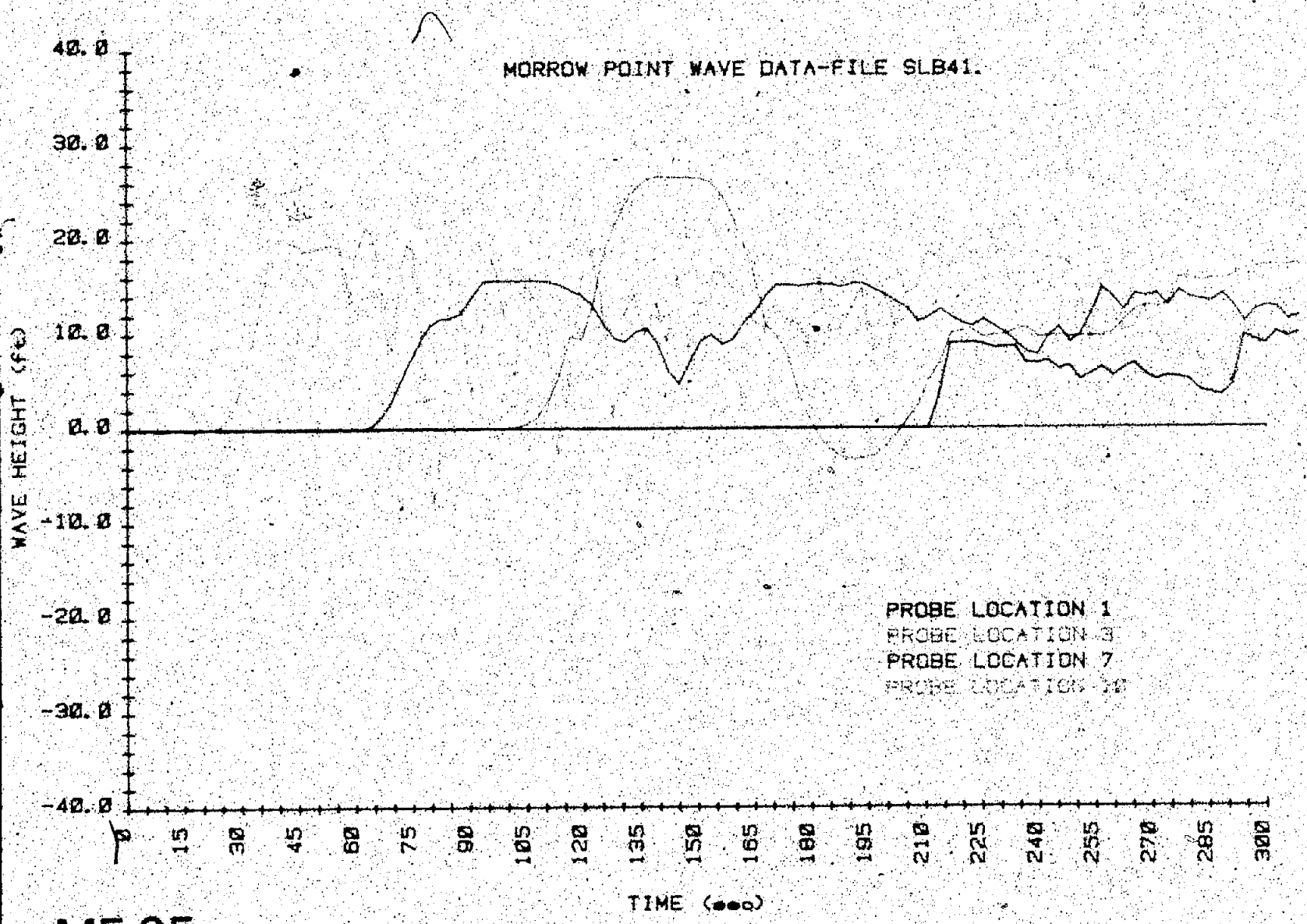

MF 65

Figure B-14. Wave height versus time — test SLB41 (1 of 5).

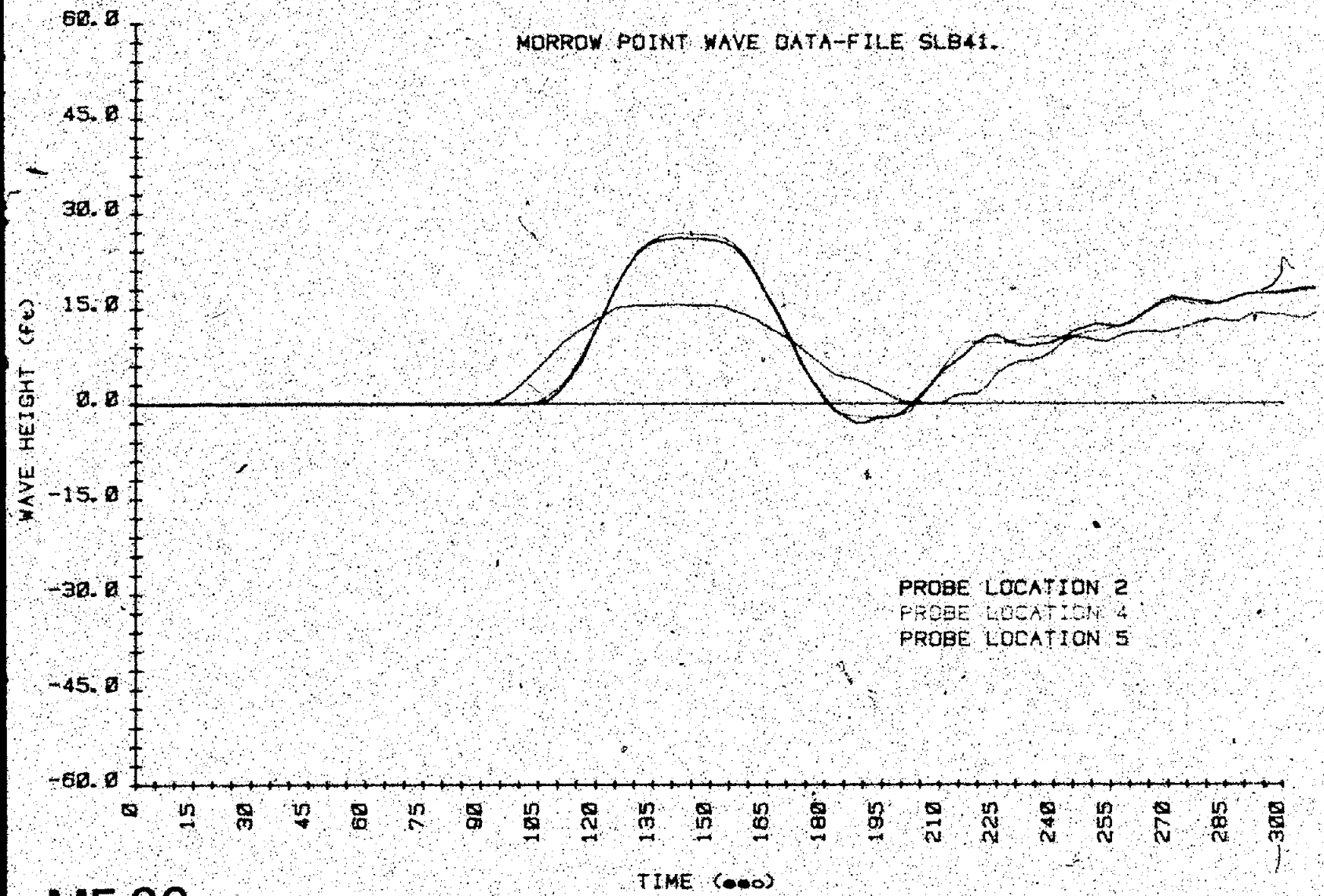

MF 66

Figure B-14.—Wave height versus time — test SLB41 (2 of 5)

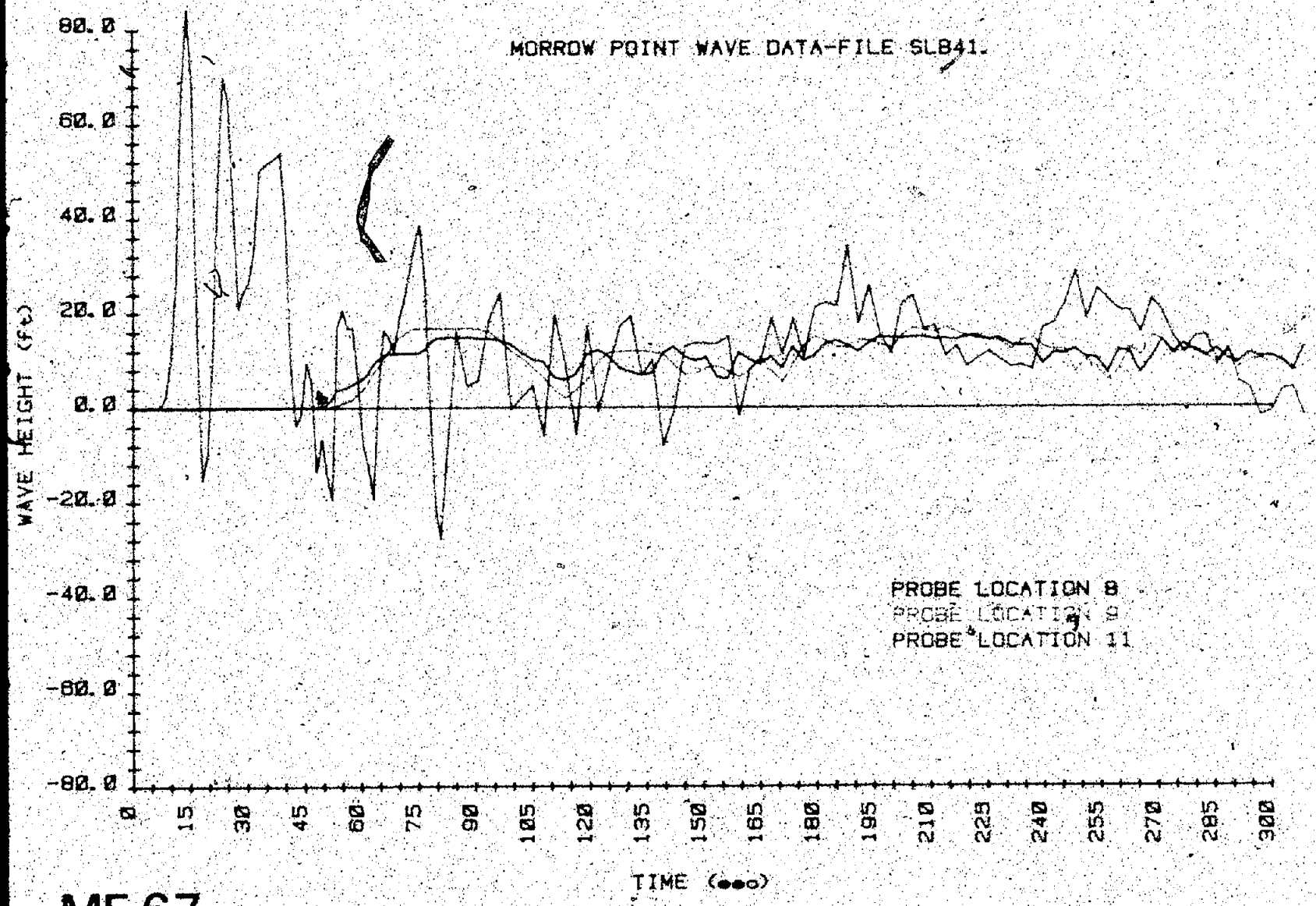

MF 67

Figure 8-14. Wave height versus time – test SLB41 (3 of 5).

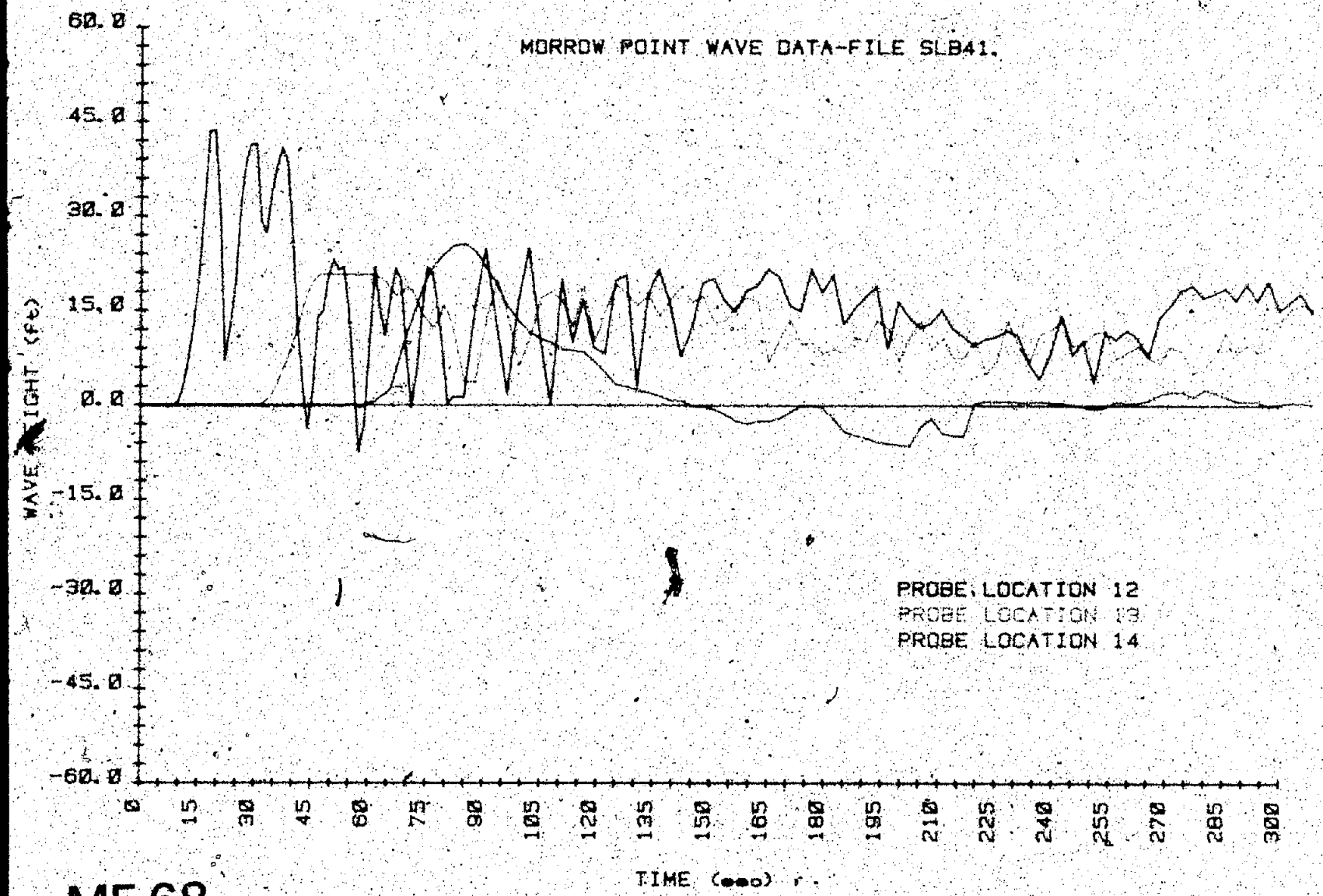

MF 68

Figure B-14. - Wave height versus time - test SLB41 (4 of 5)

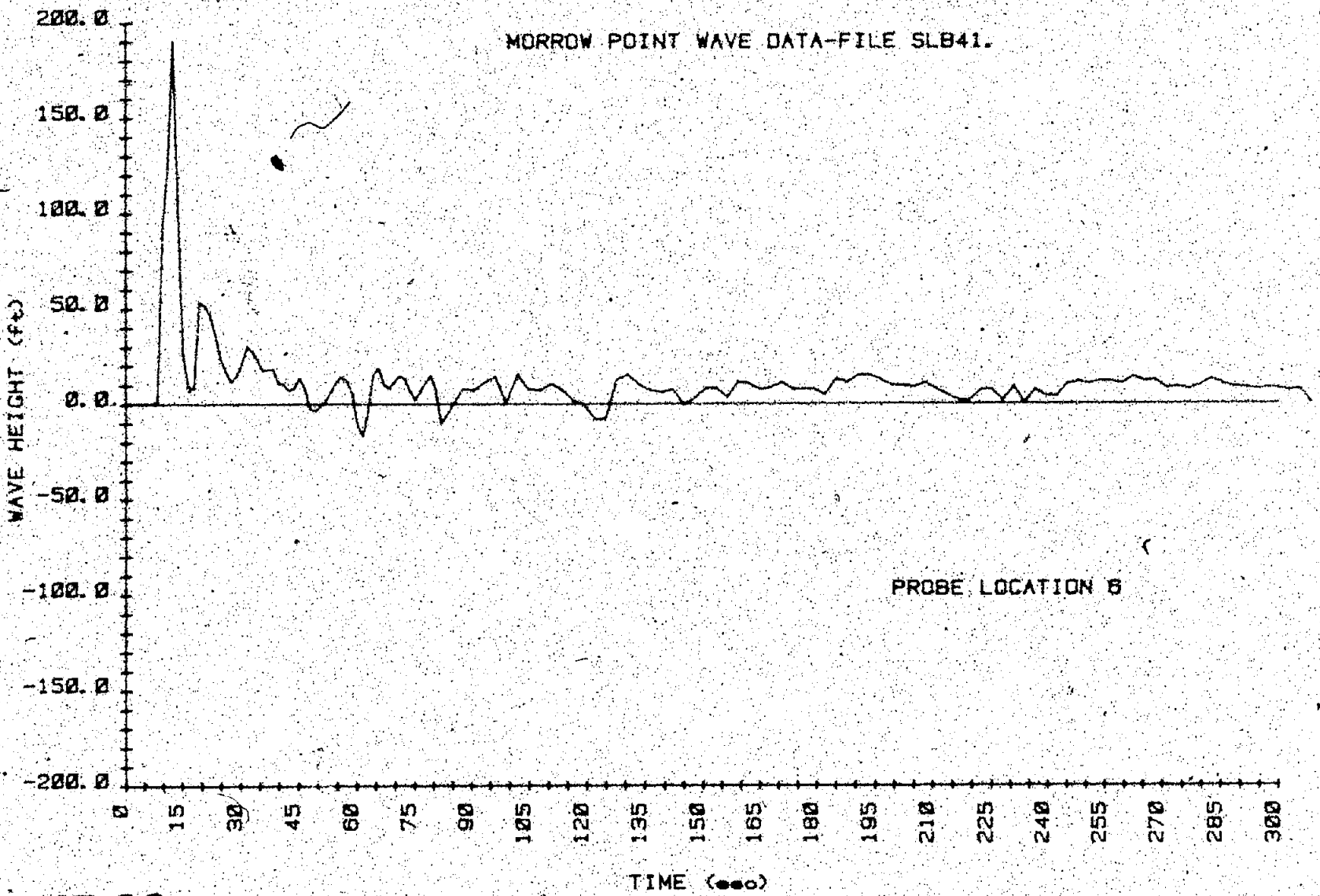

MF 69

Figure B-14. – Wave height versus time – test SLB41 (5 of 5)

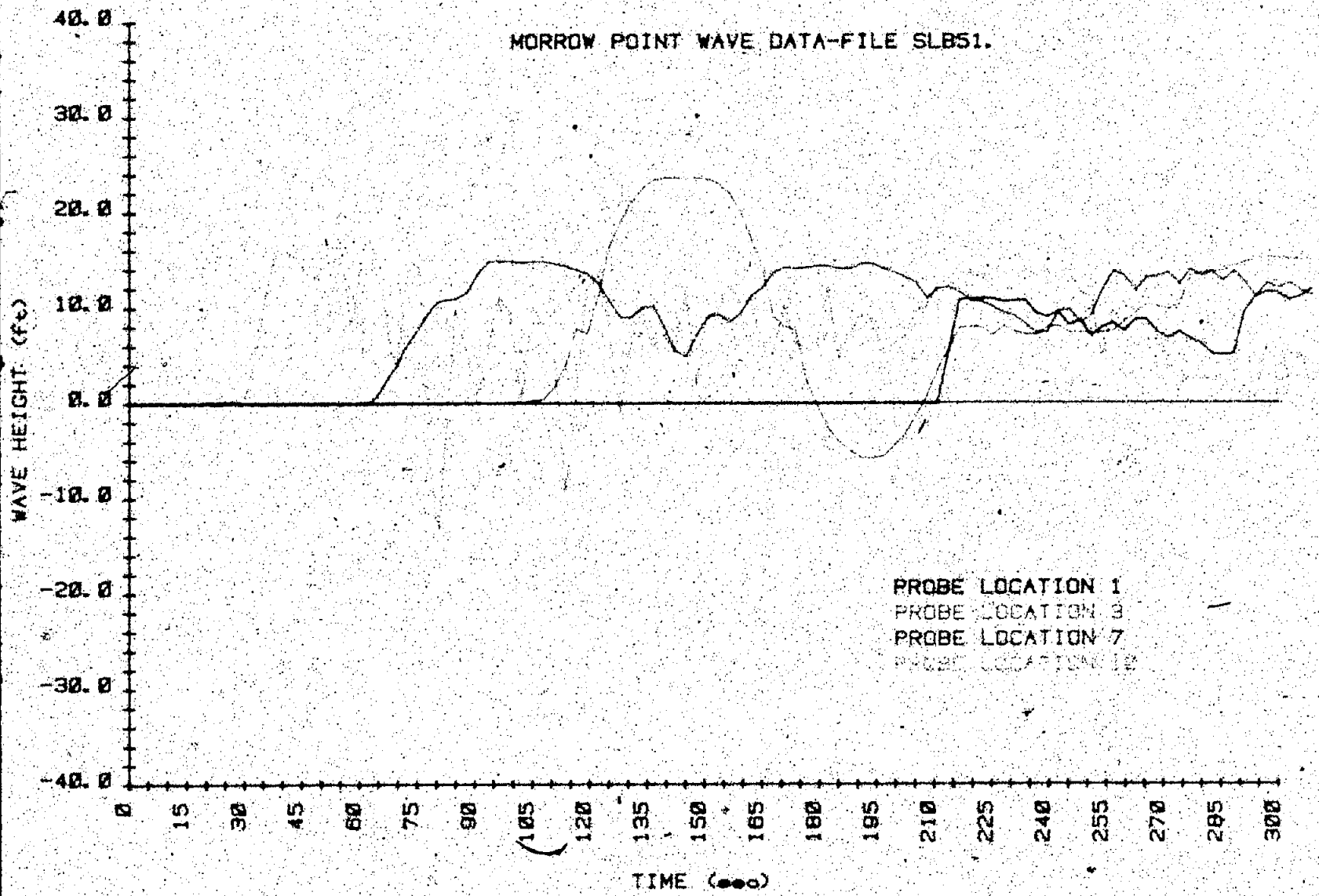

MF 70

Figure B-15. Wave height versus time — test SLB51 (1 of 5)

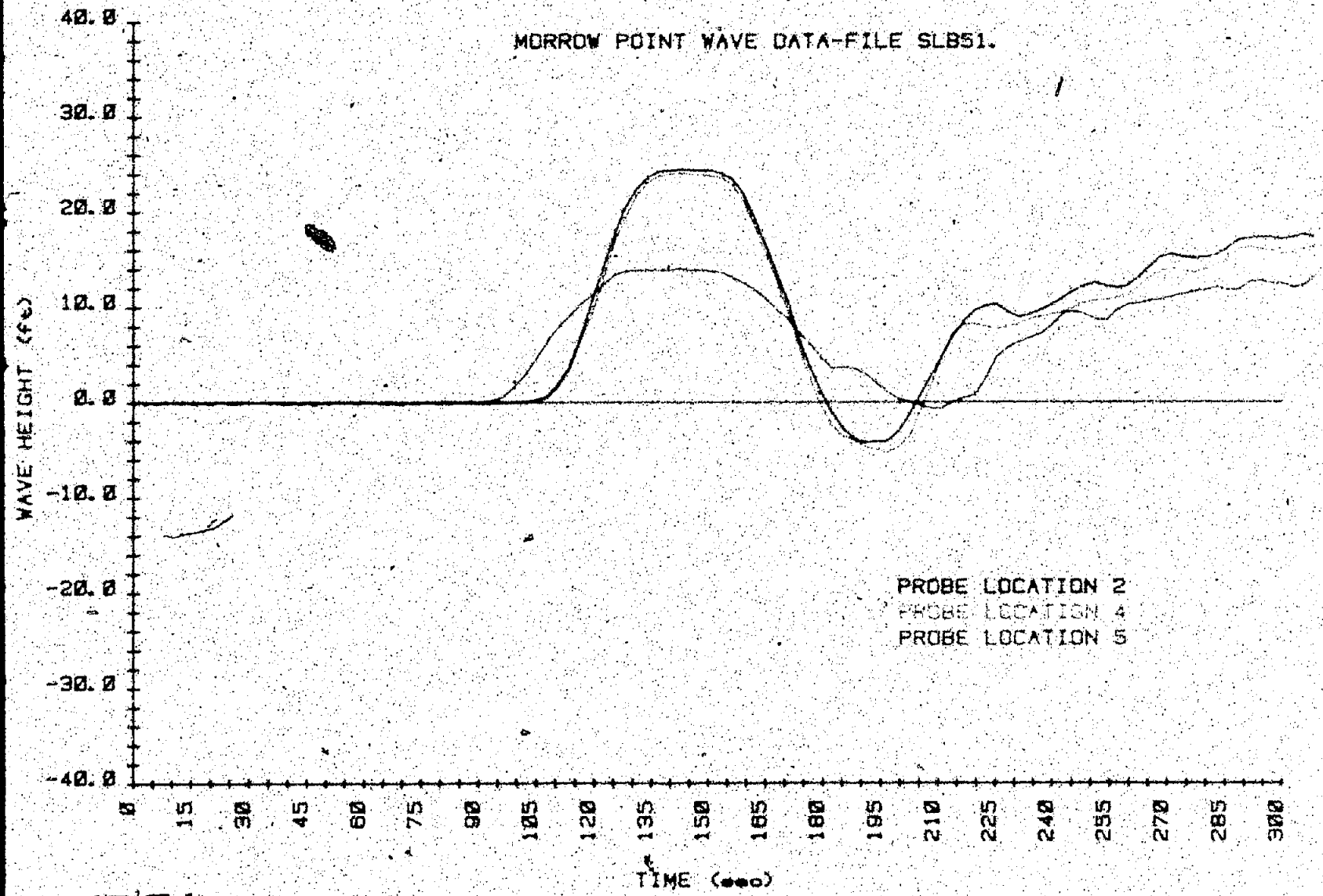

MF 71

Figure B-15 — Wave height versus time — test SLB51 (2 of 3)

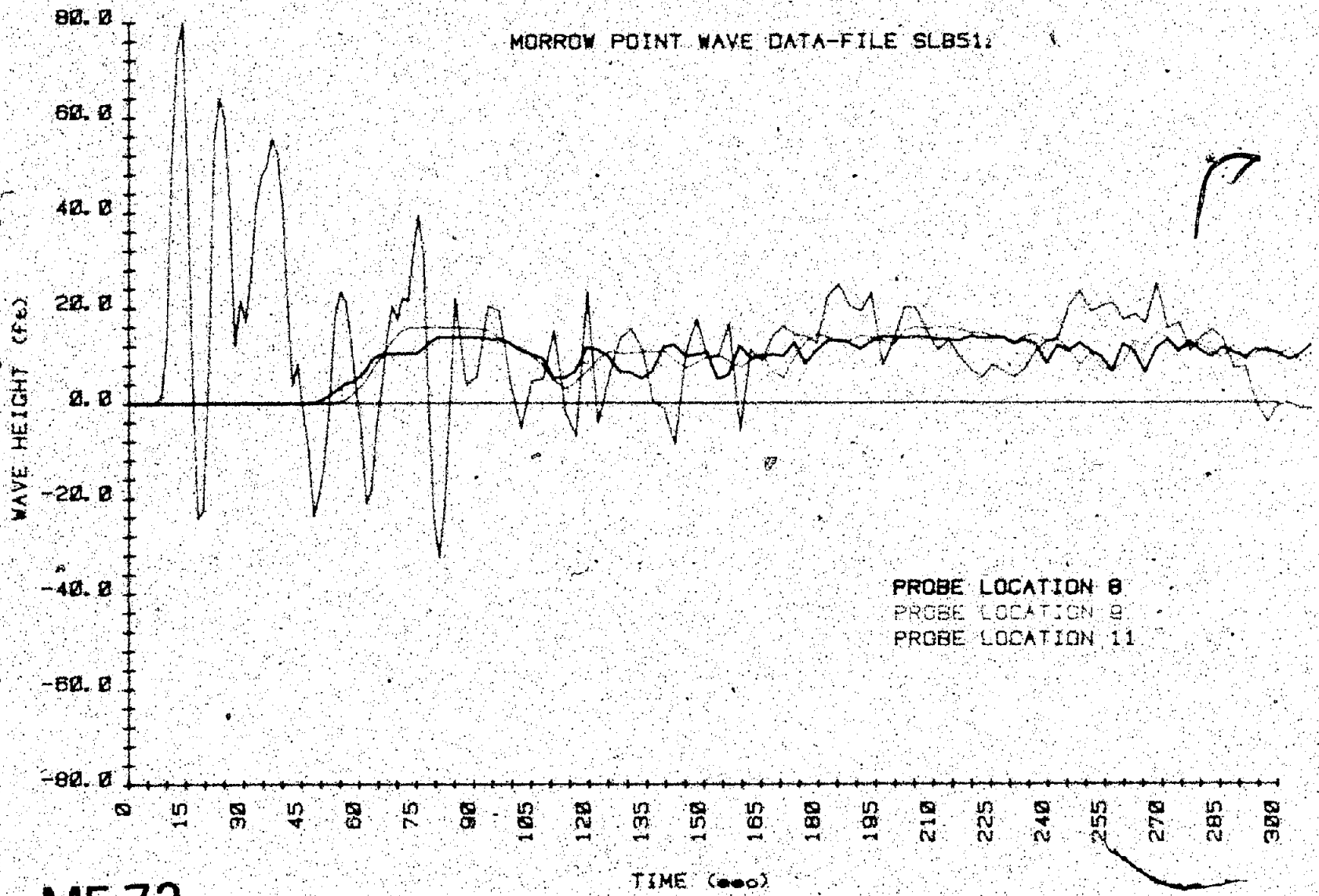

MF 72

Figure B-15 - Wave height versus time - test SL851 (3 of 5)

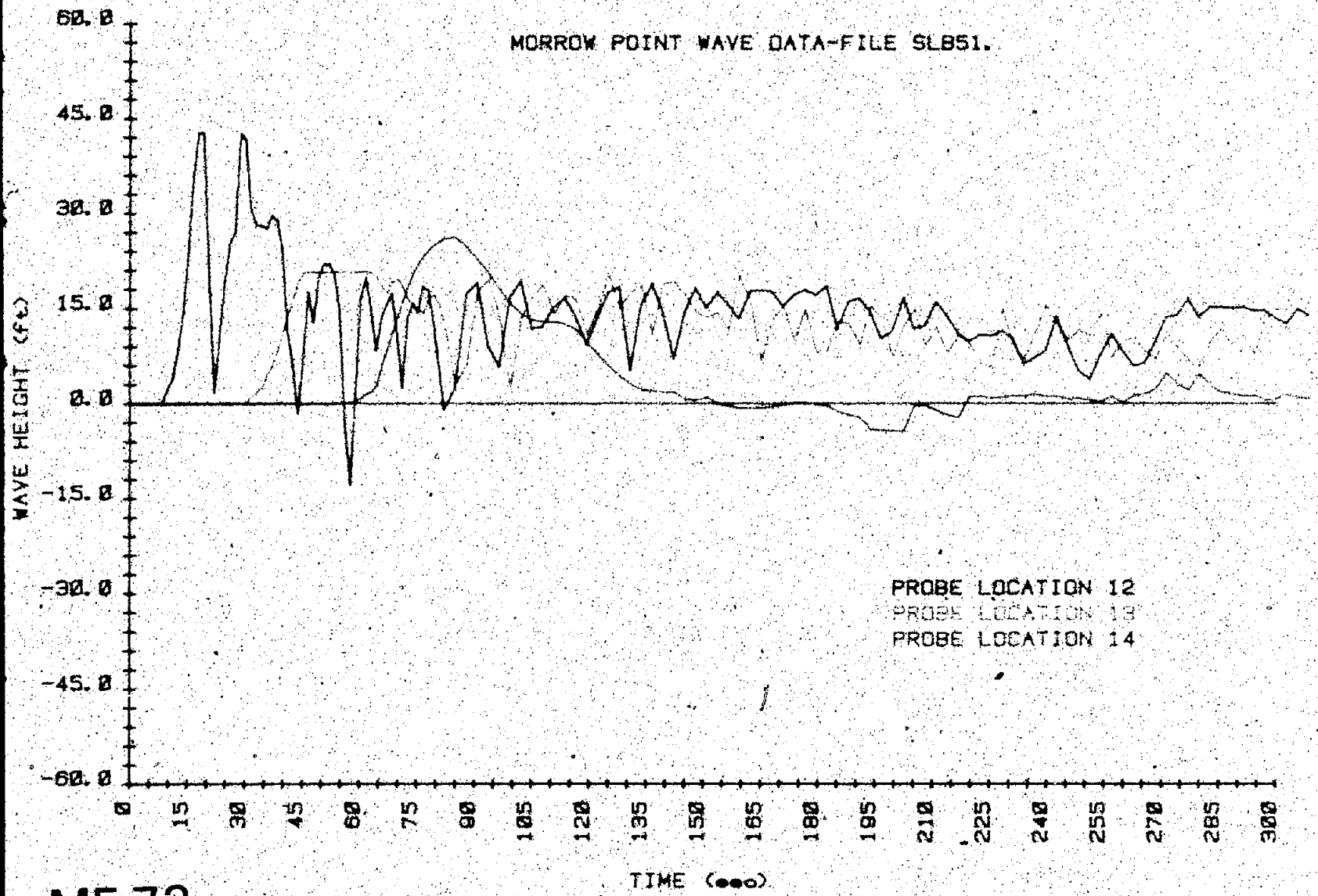

MF 73

Figure B-15. Wave height versus time — test SLB51 (4 of 5)

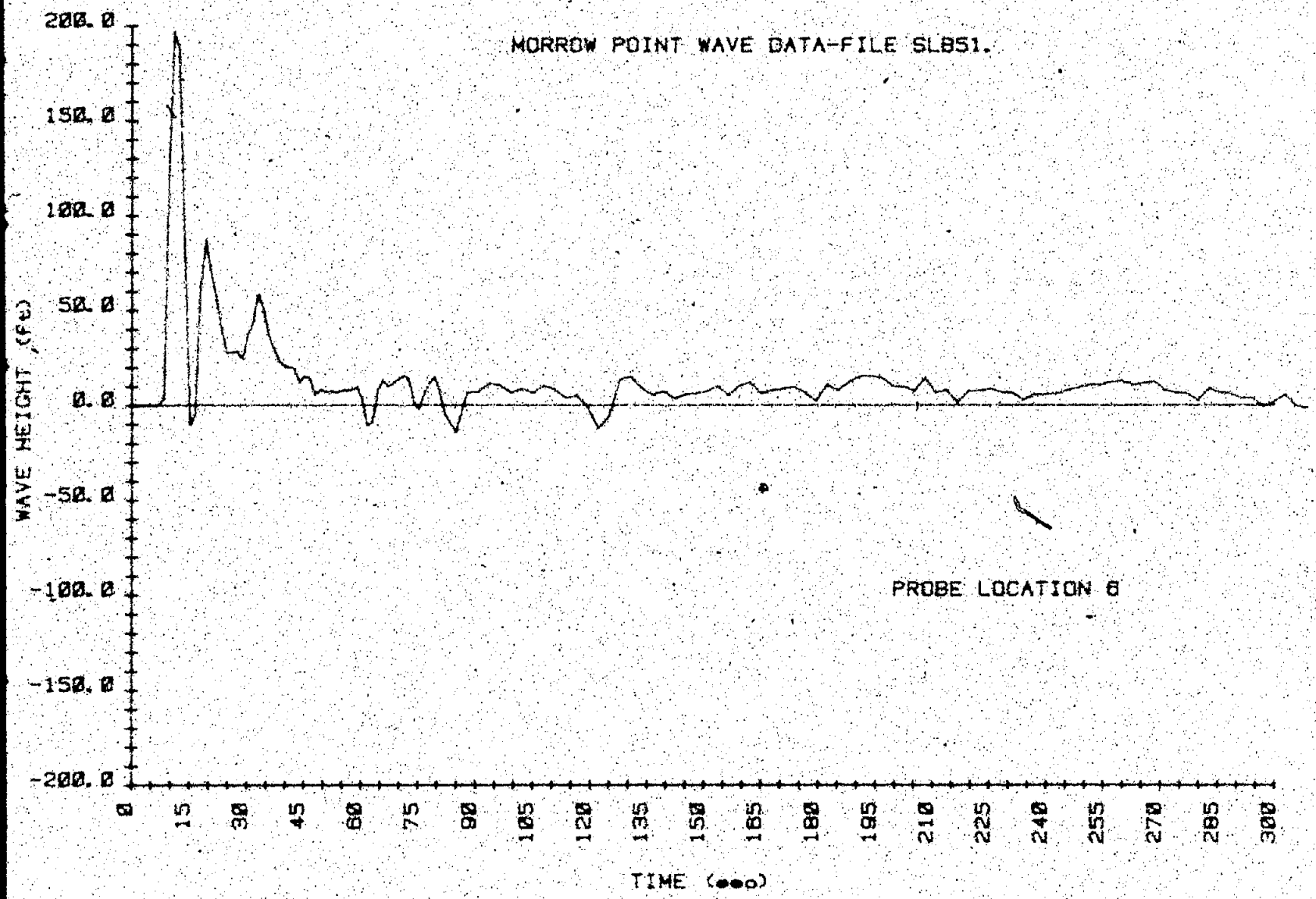

MF 74

Figure B-15. Wave height versus time test SLB51 (5 of 5)

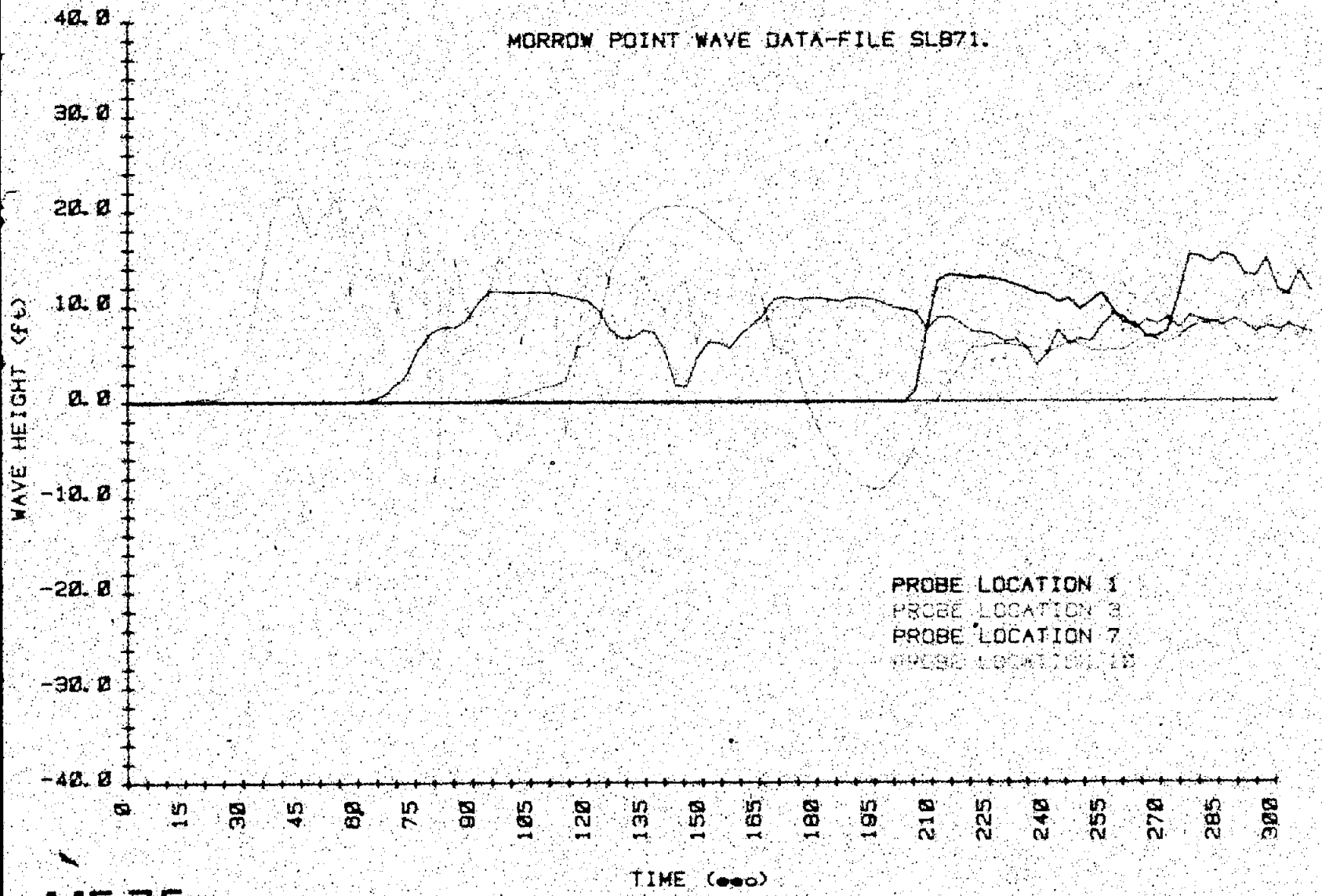

MF 75

Figure B-16. Wave height versus time — test SLB71 (1 of 5).

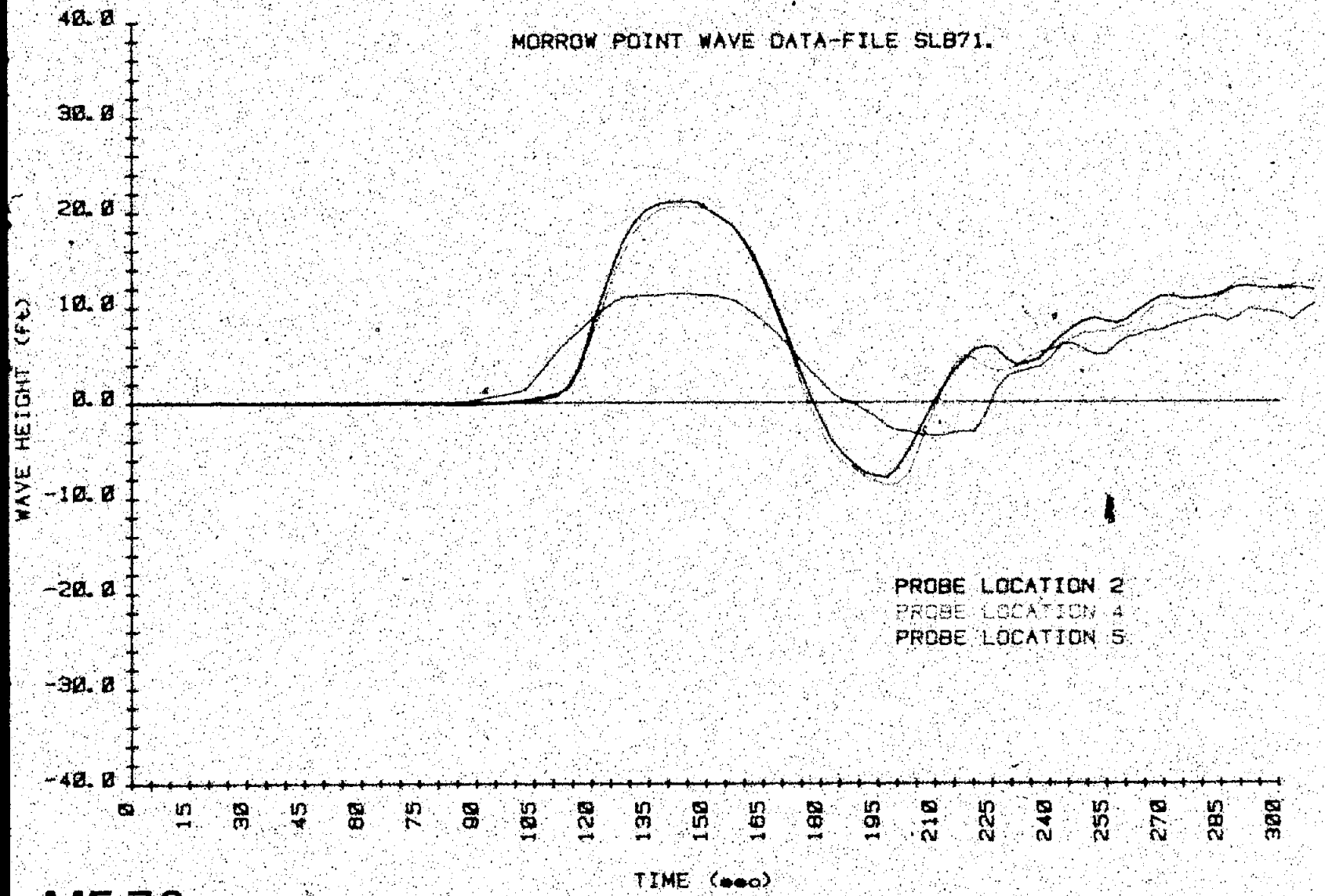

MF 76

Figure B-16. Wave height versus time — test SLB71 (2 of 5)

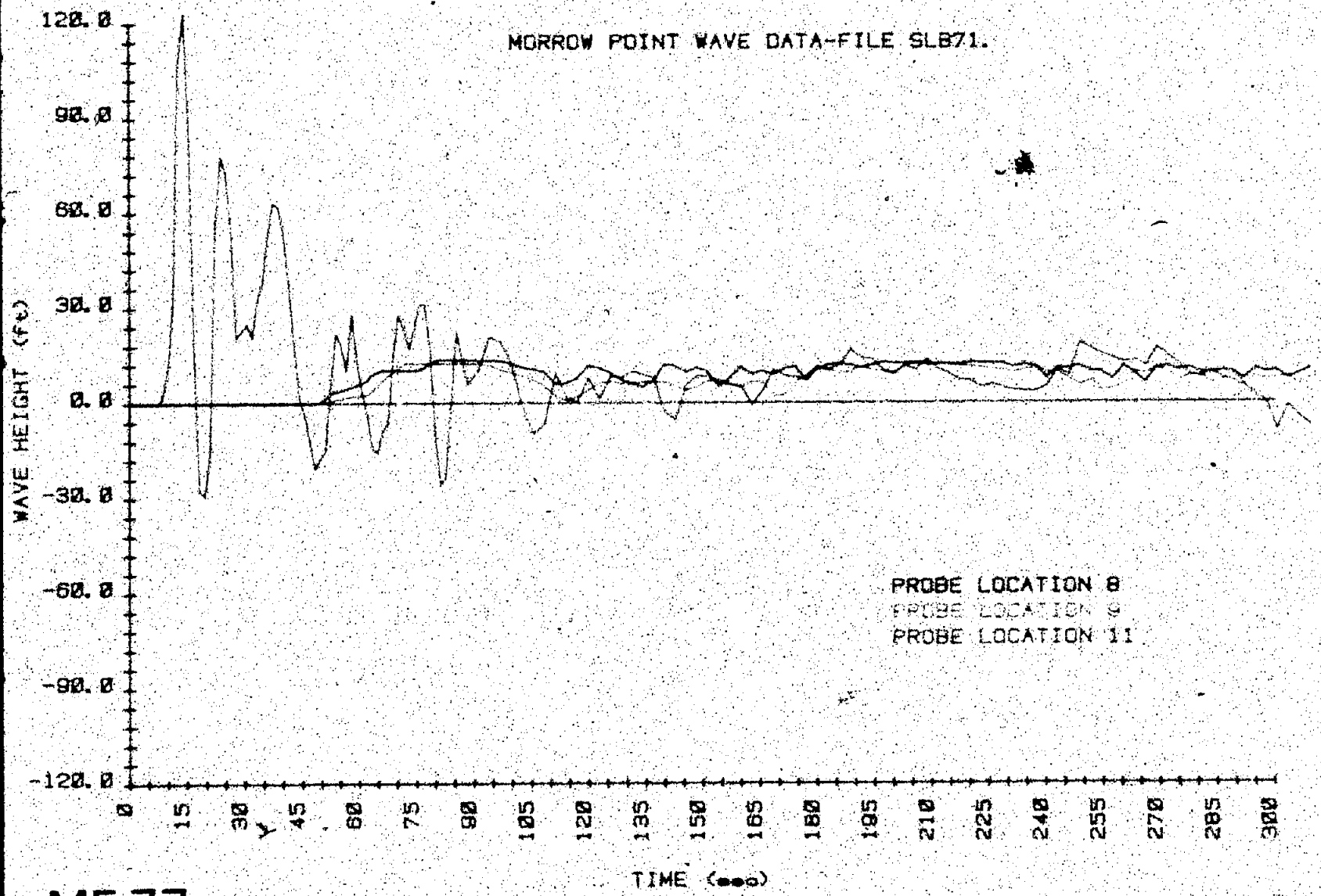

MF 77

Figure B-16 — Wave height versus time — test SLB71 (3 of 5)

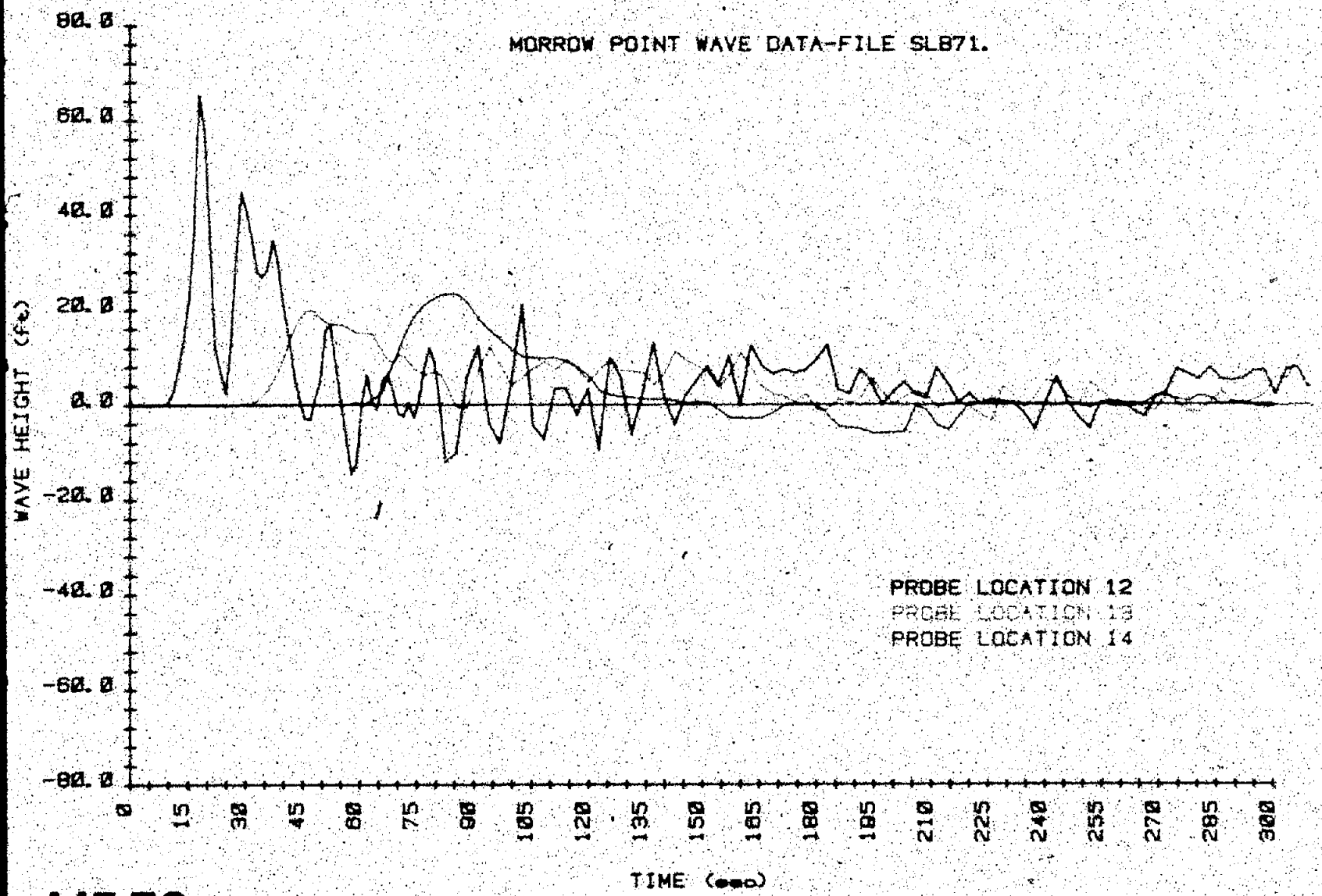

MF 78

Figure B-16 Wave height versus time test SLB71 (4 of 5)

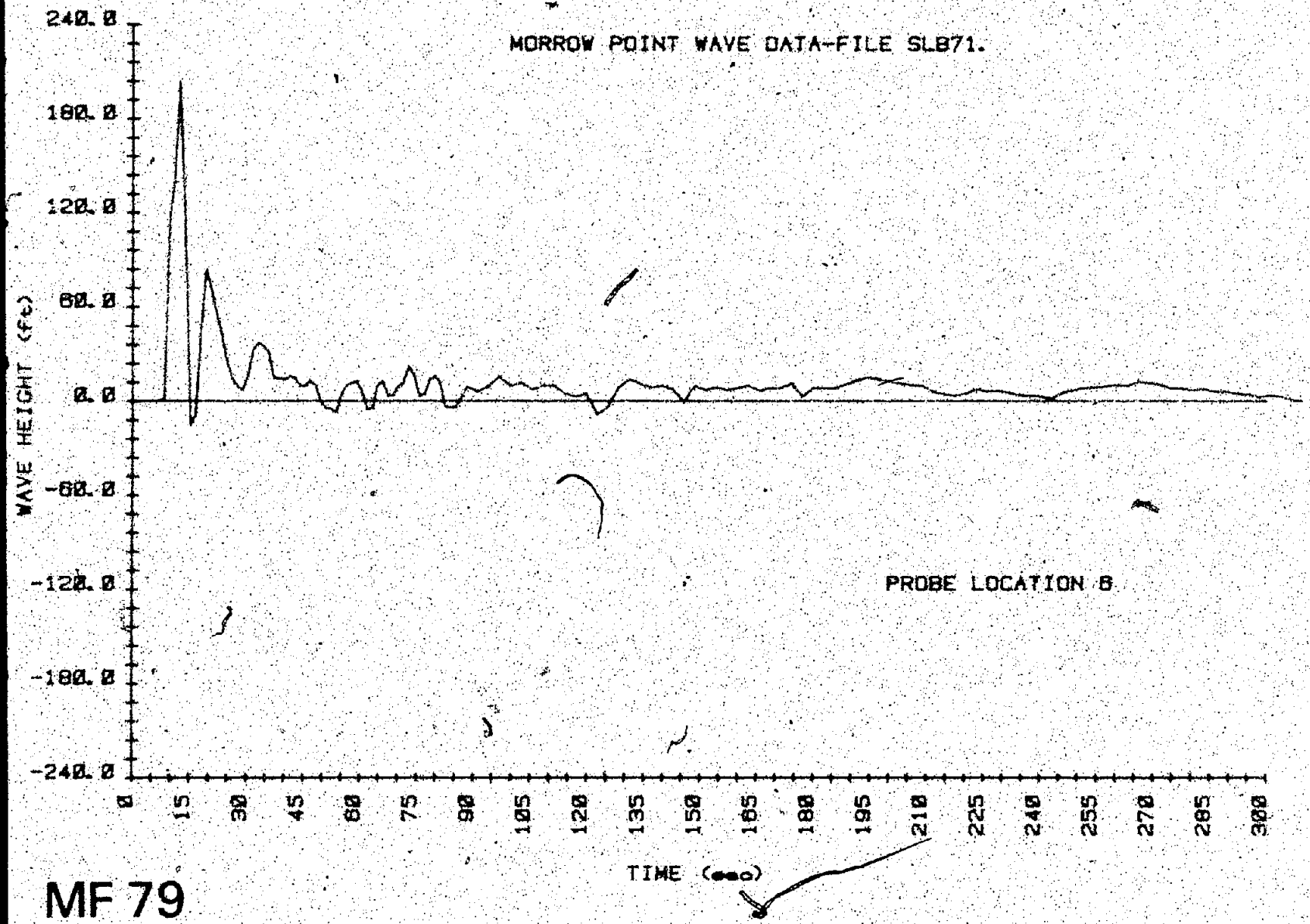

MF 79

Figure B 16. Wave height versus time - test SLB71 (5 of 5)

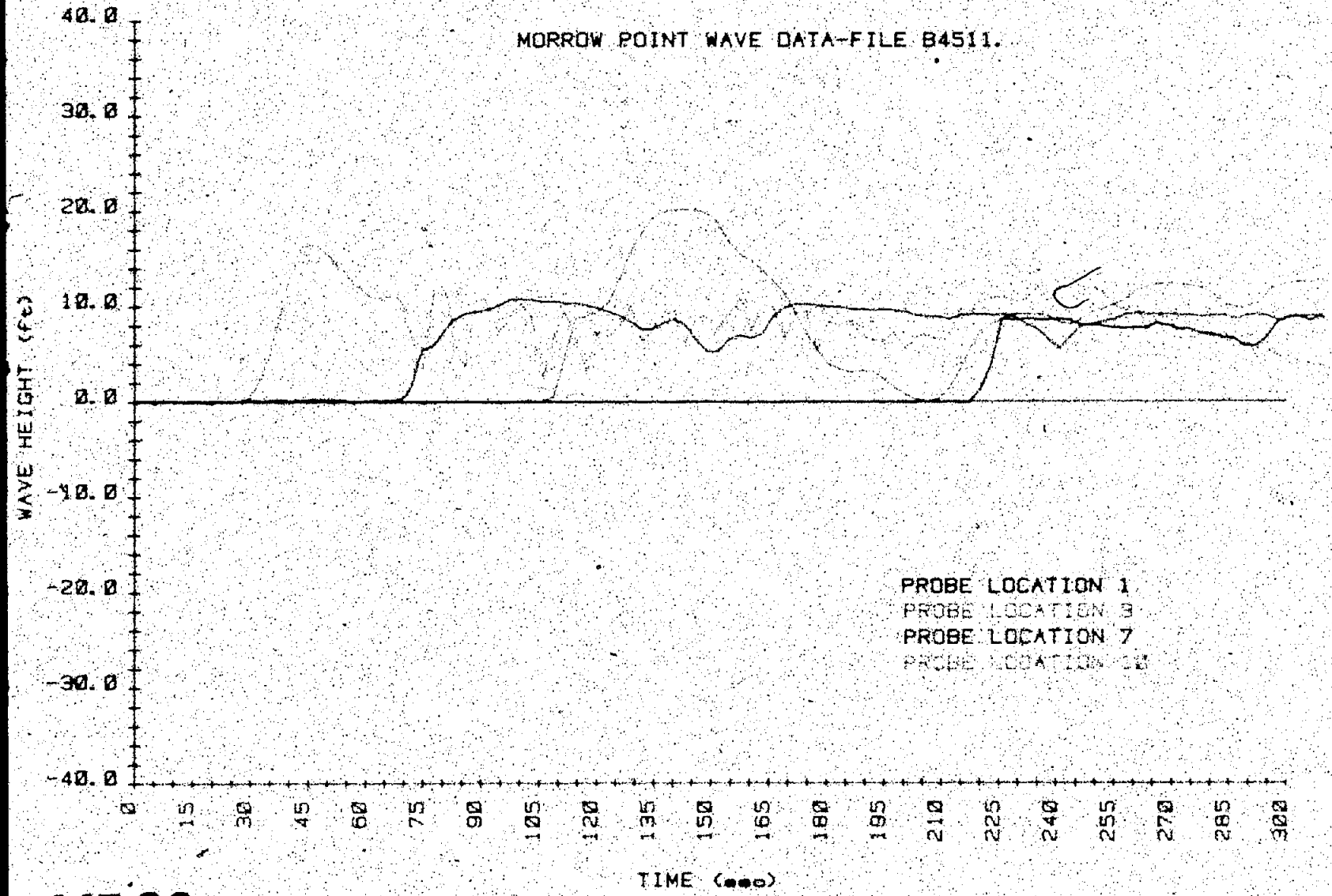

MF 80

Figure B-17. Wave height versus time - test B4511 (1 of 5).

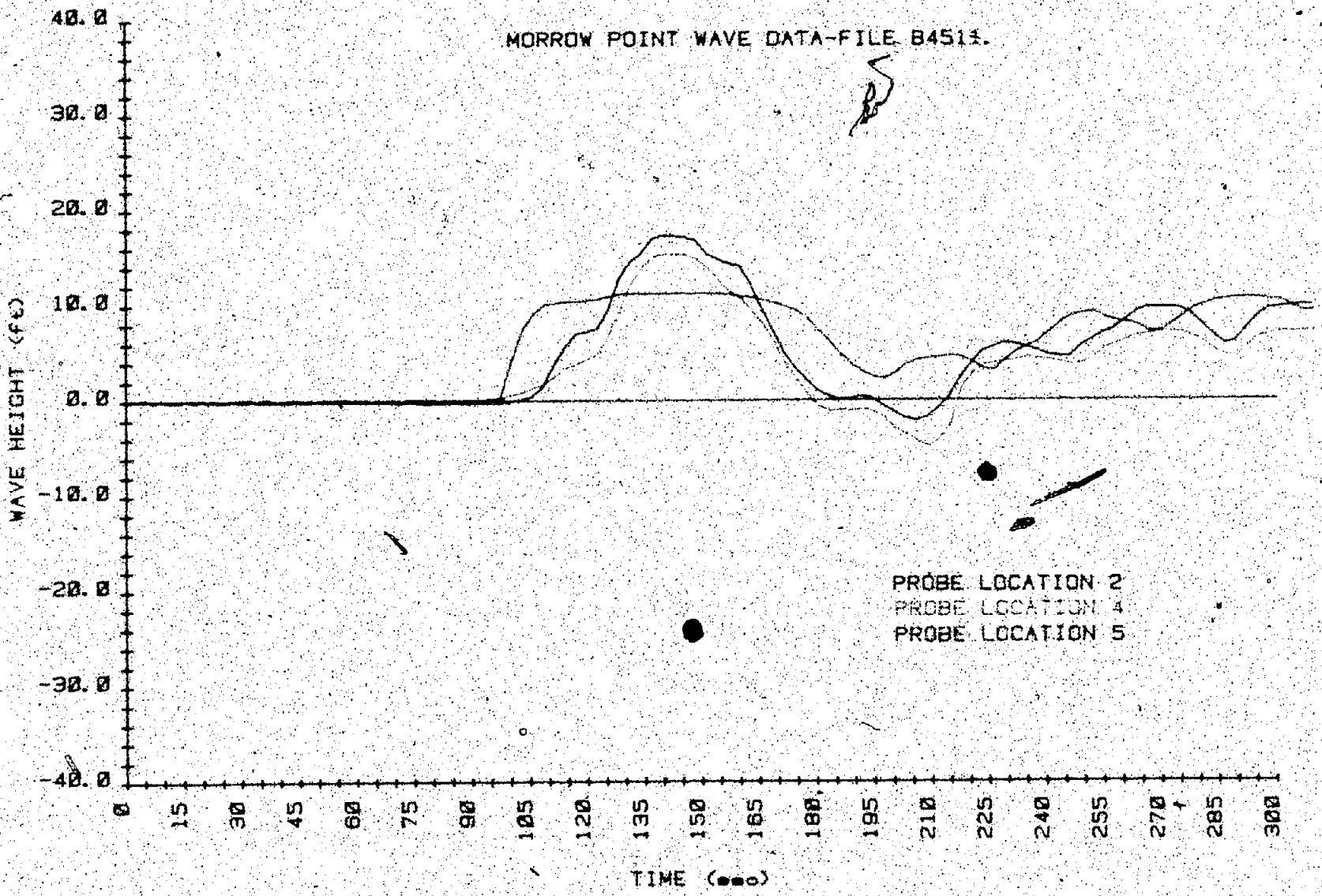

MF 81

Figure B-17. Wave height versus time – test B4511 (2 of 5).

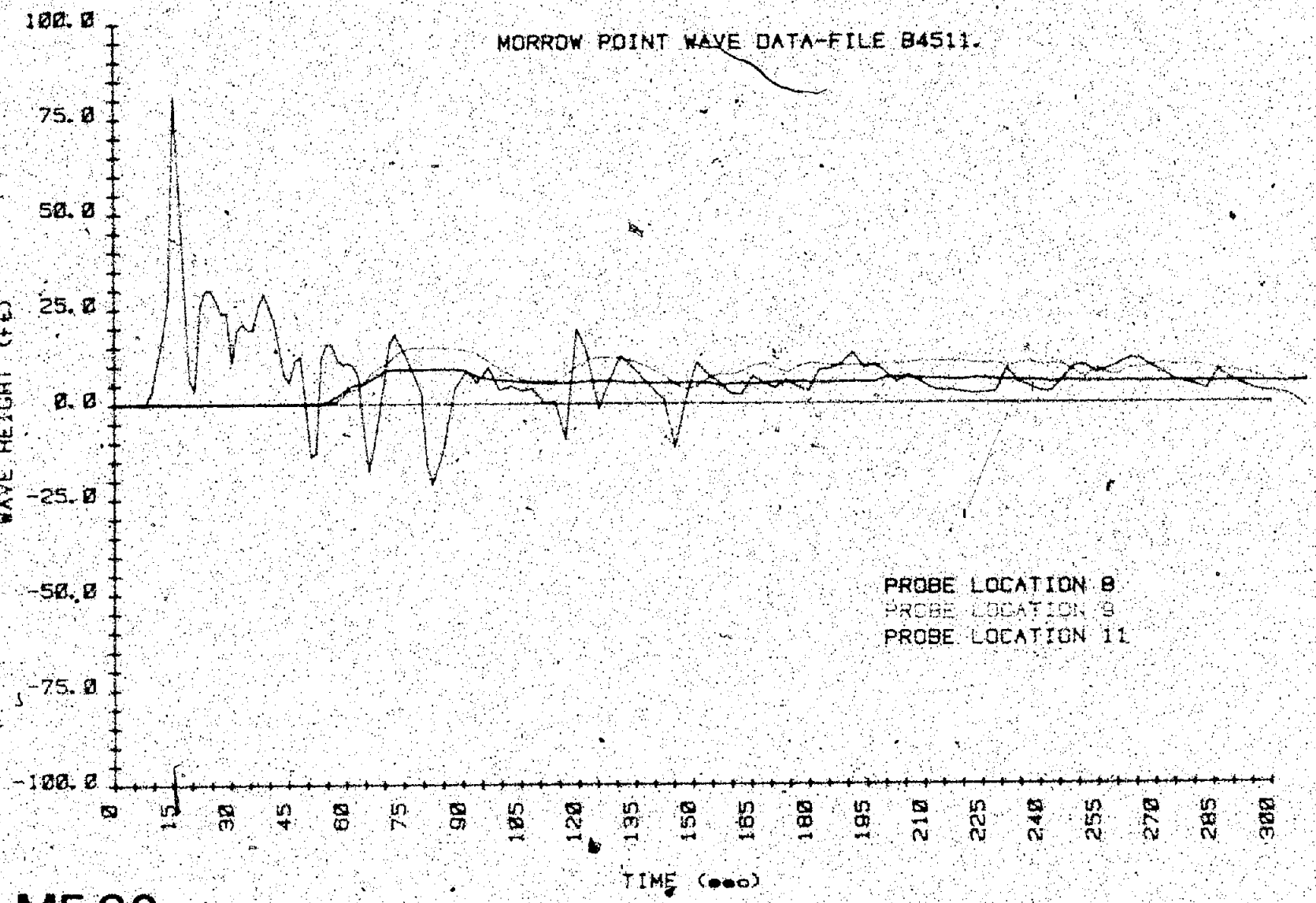

MF 82

Figure B 17 Wave height versus time test B4511 (3 of 5)

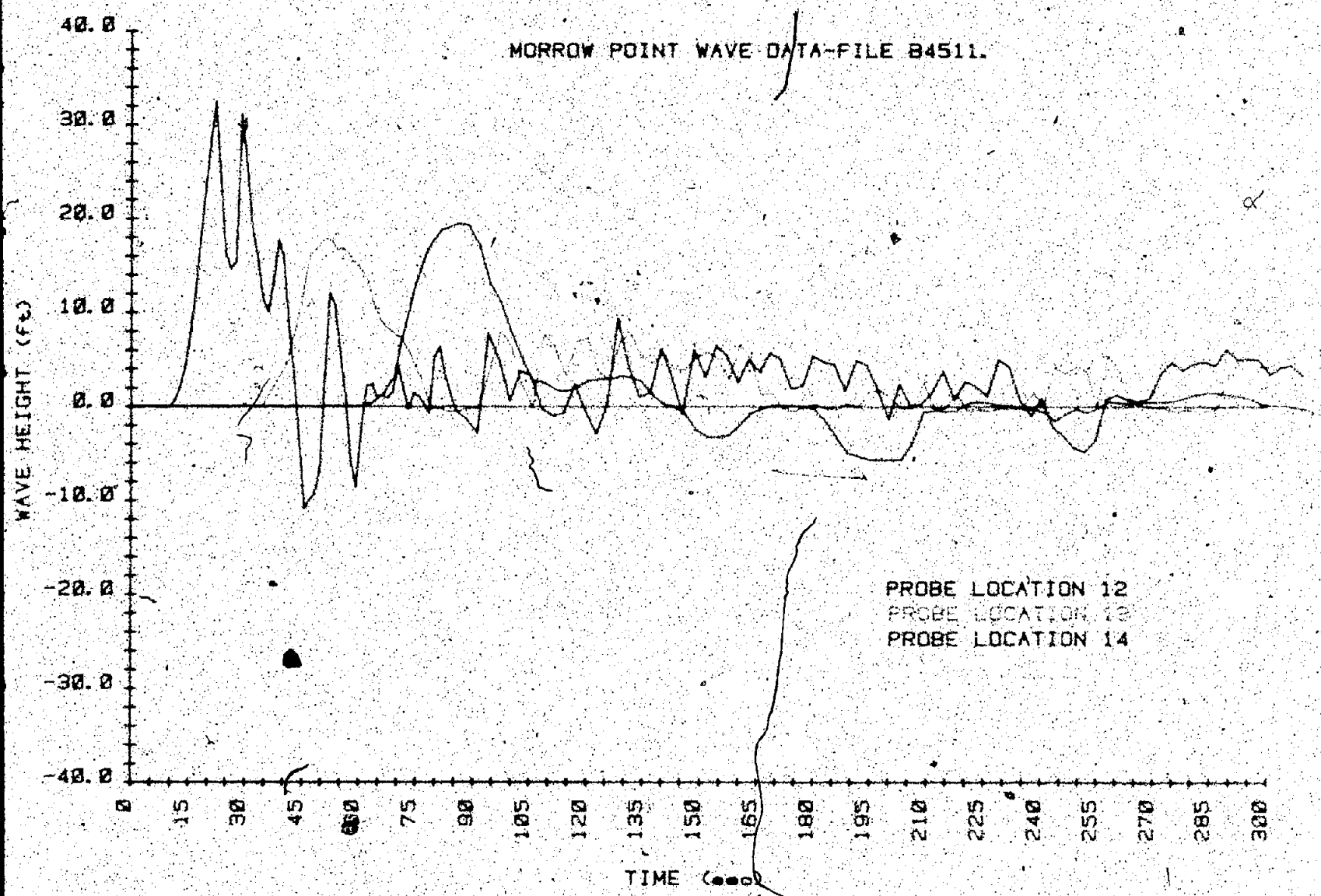

MF 83

Figure B 17. Wave height versus time - test B4511 (4 of 5)

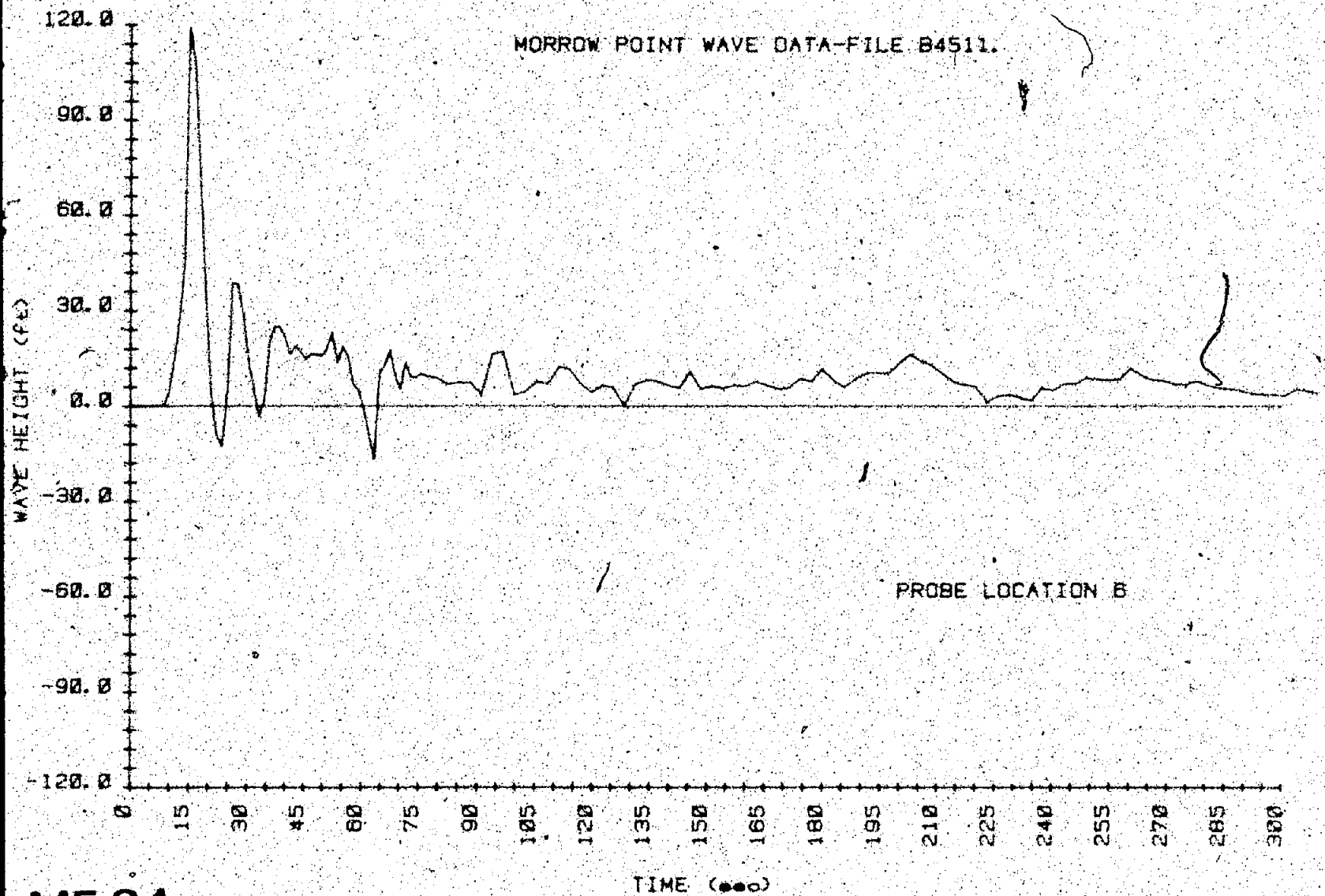

MF 84

Figure B-17. Wave height versus time, test B4511 (5 of 5)

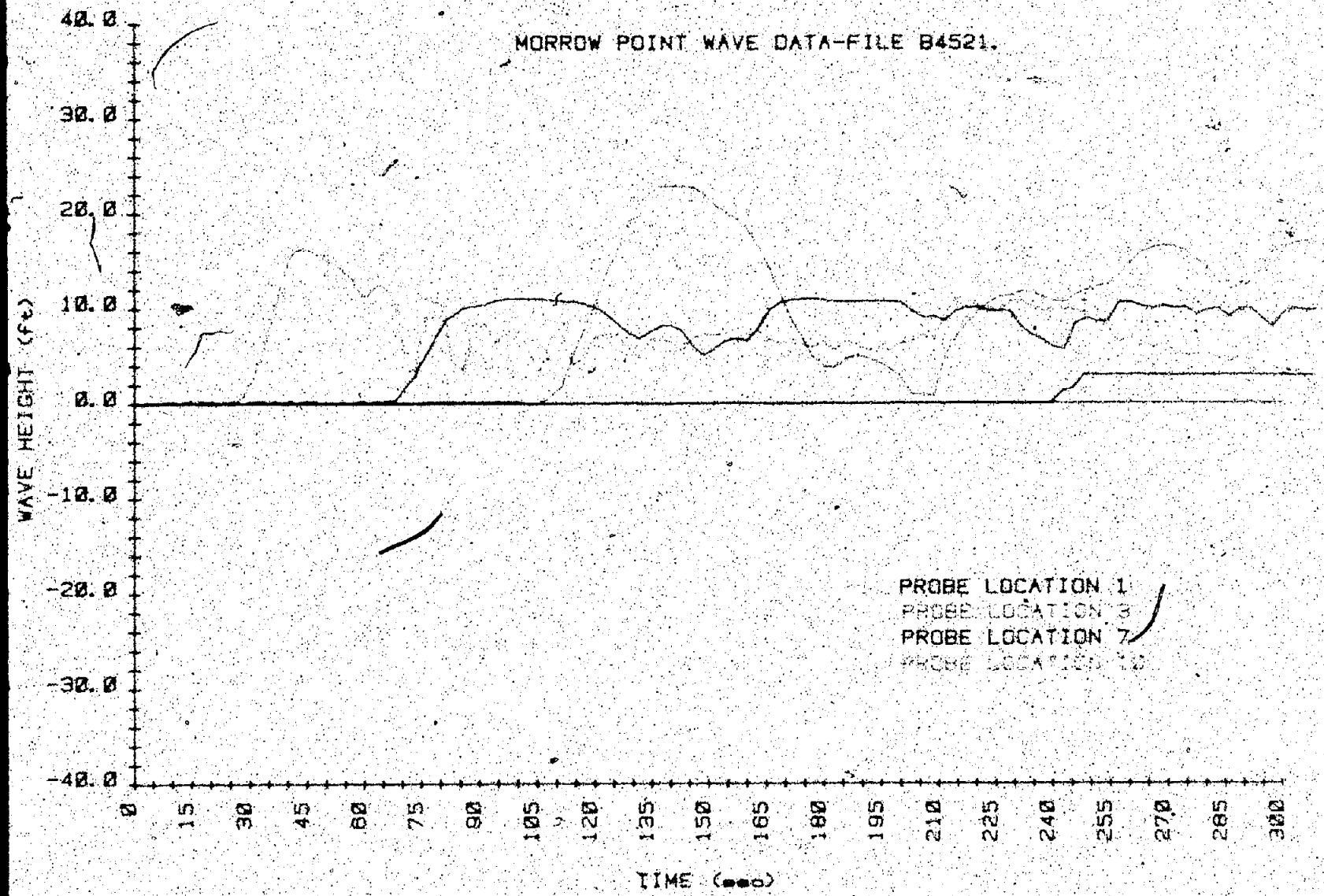

MF 85

Figure B-18. Wave height versus time - test B4521 (1 of 5)

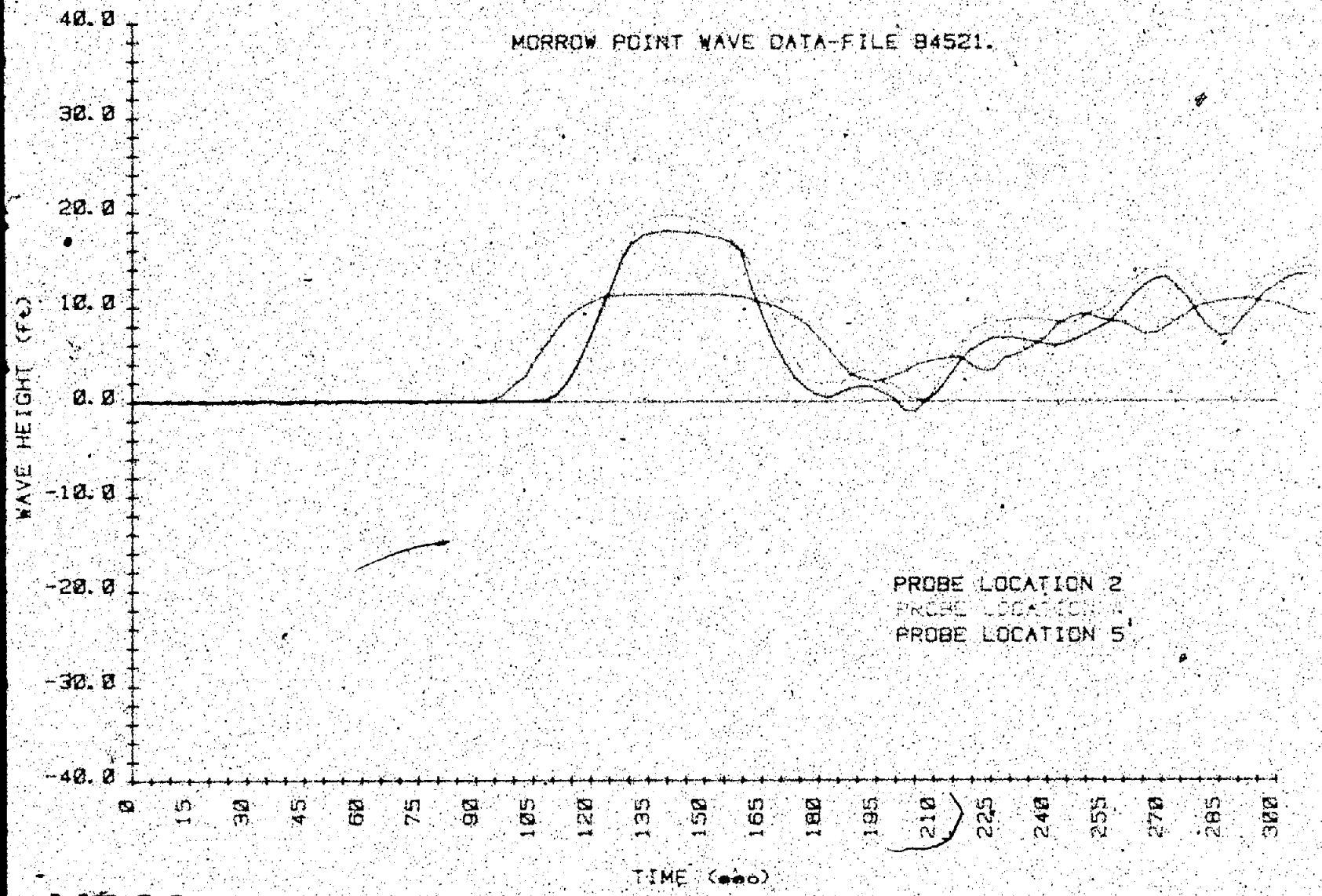

MF 86

Figure B-18 -- Wave height versus time -- test B4521 (2 of 5).

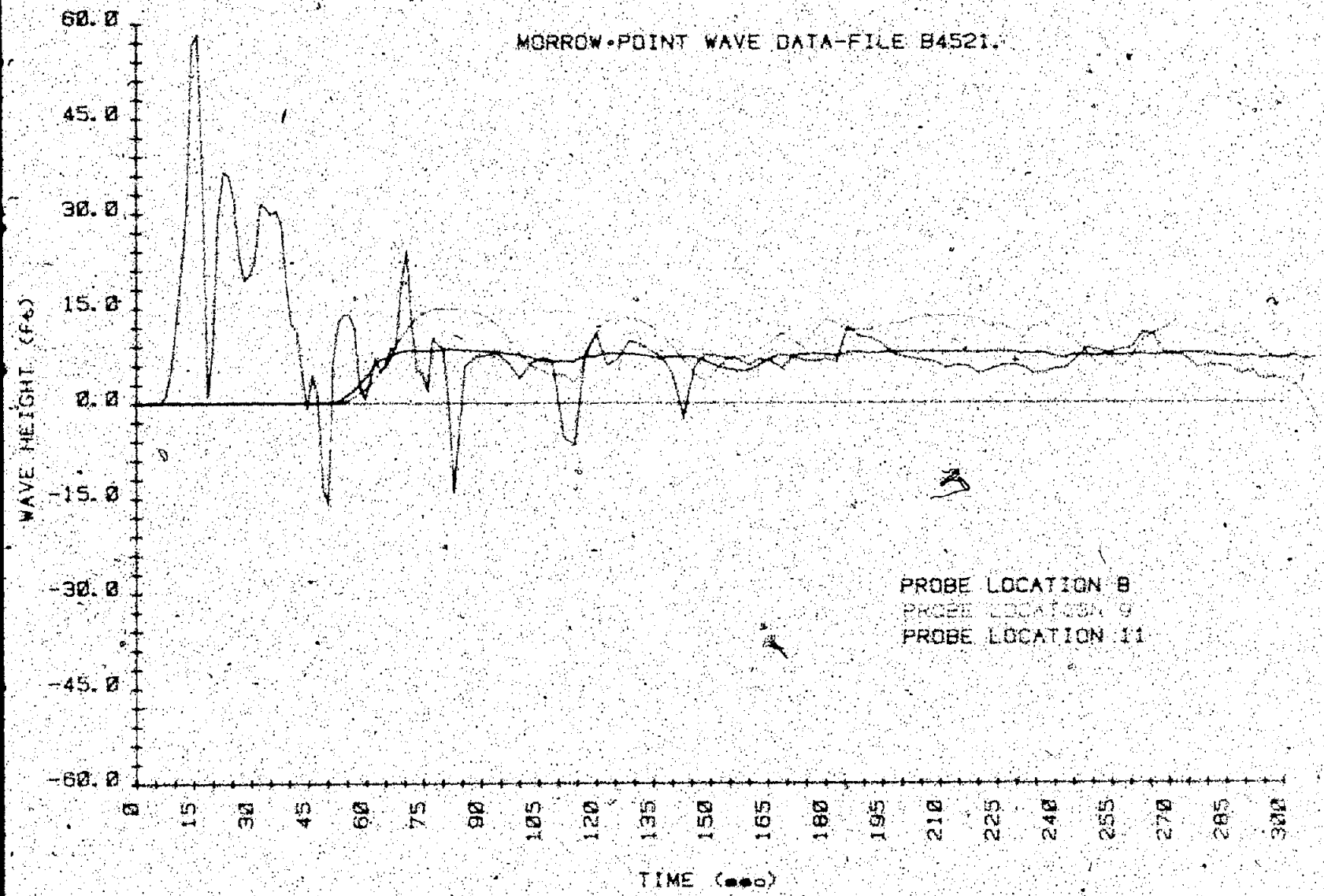

MF 87

Figure B-18 Wave height versus time test B4521 (3 of 5)

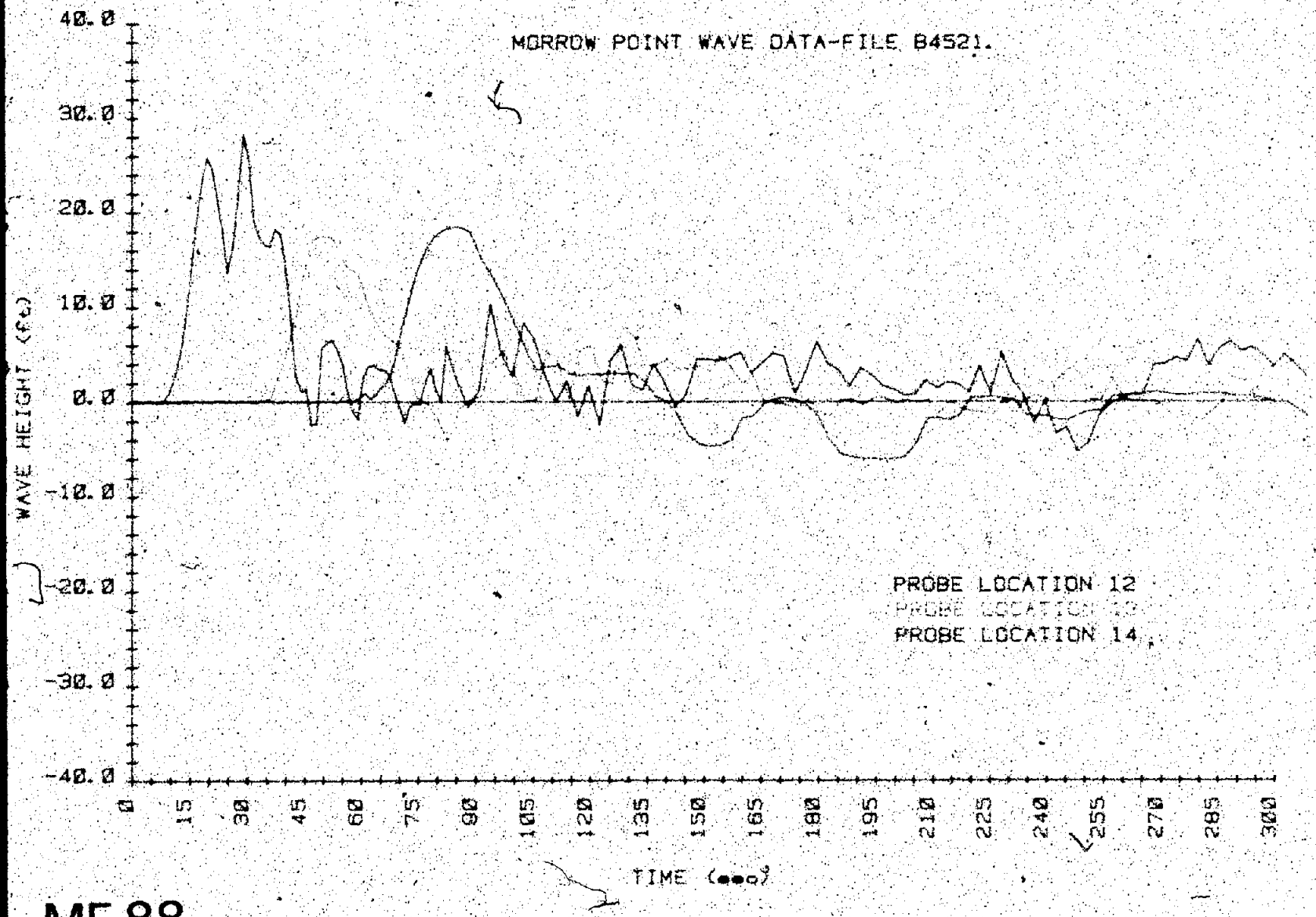

MF 88

Figure B.18. Wave height versus time — test B4521 (4 of 5)

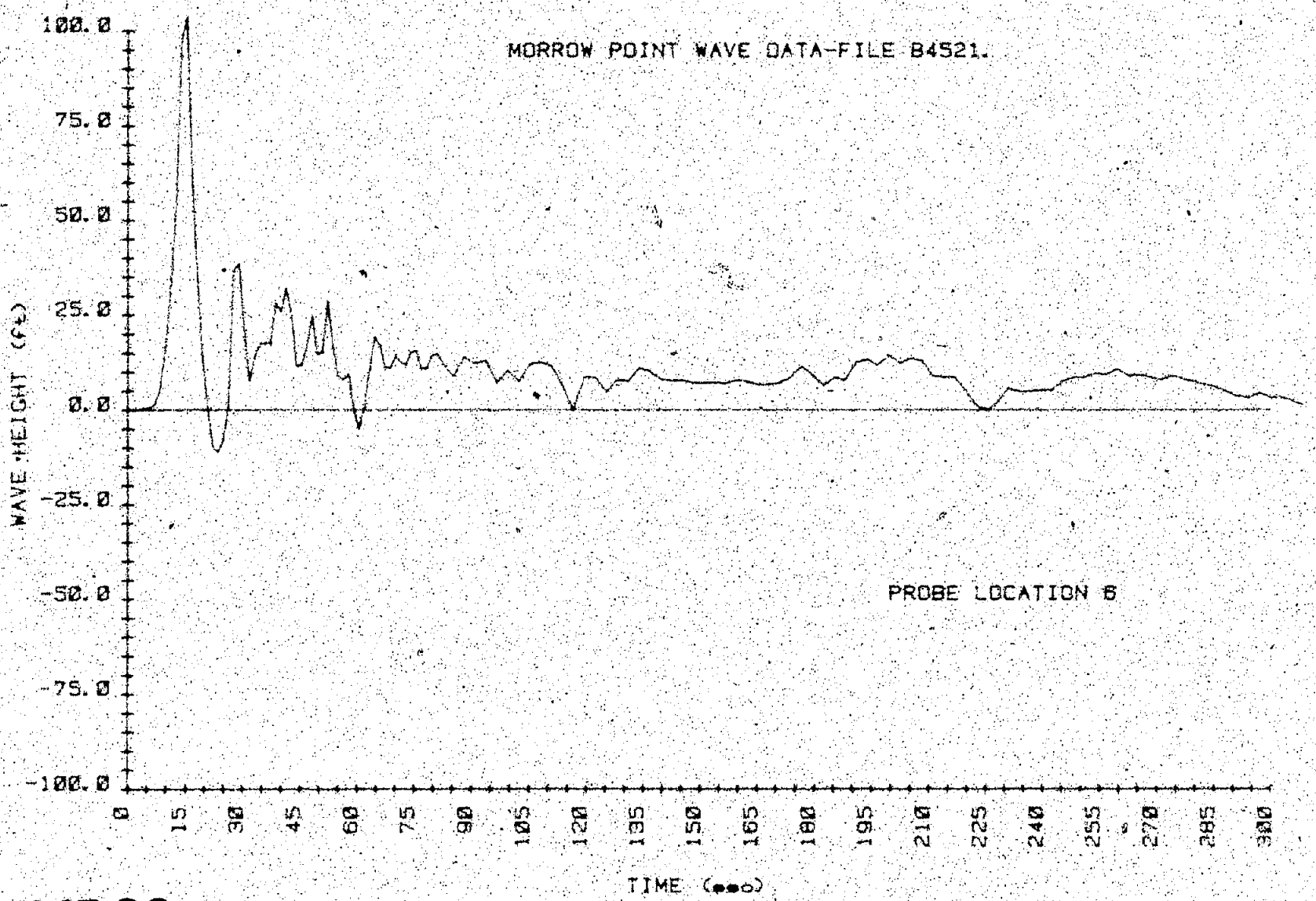

MF 89

Figure B-18. Wave height versus time — test B4521 (5 of 5)

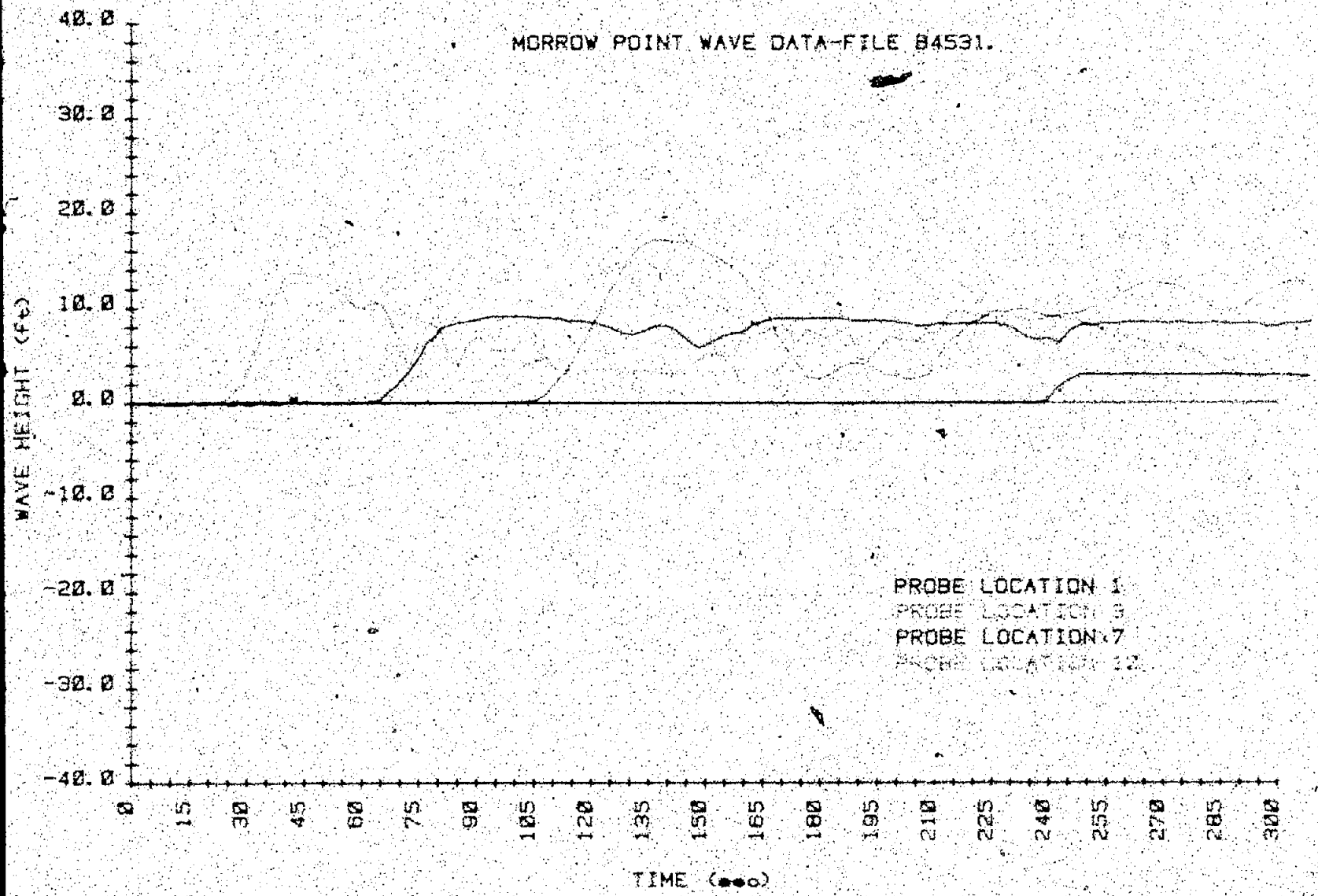

MF 90

Figure B-19. Wave height versus time - test B4531 (1 of 5)

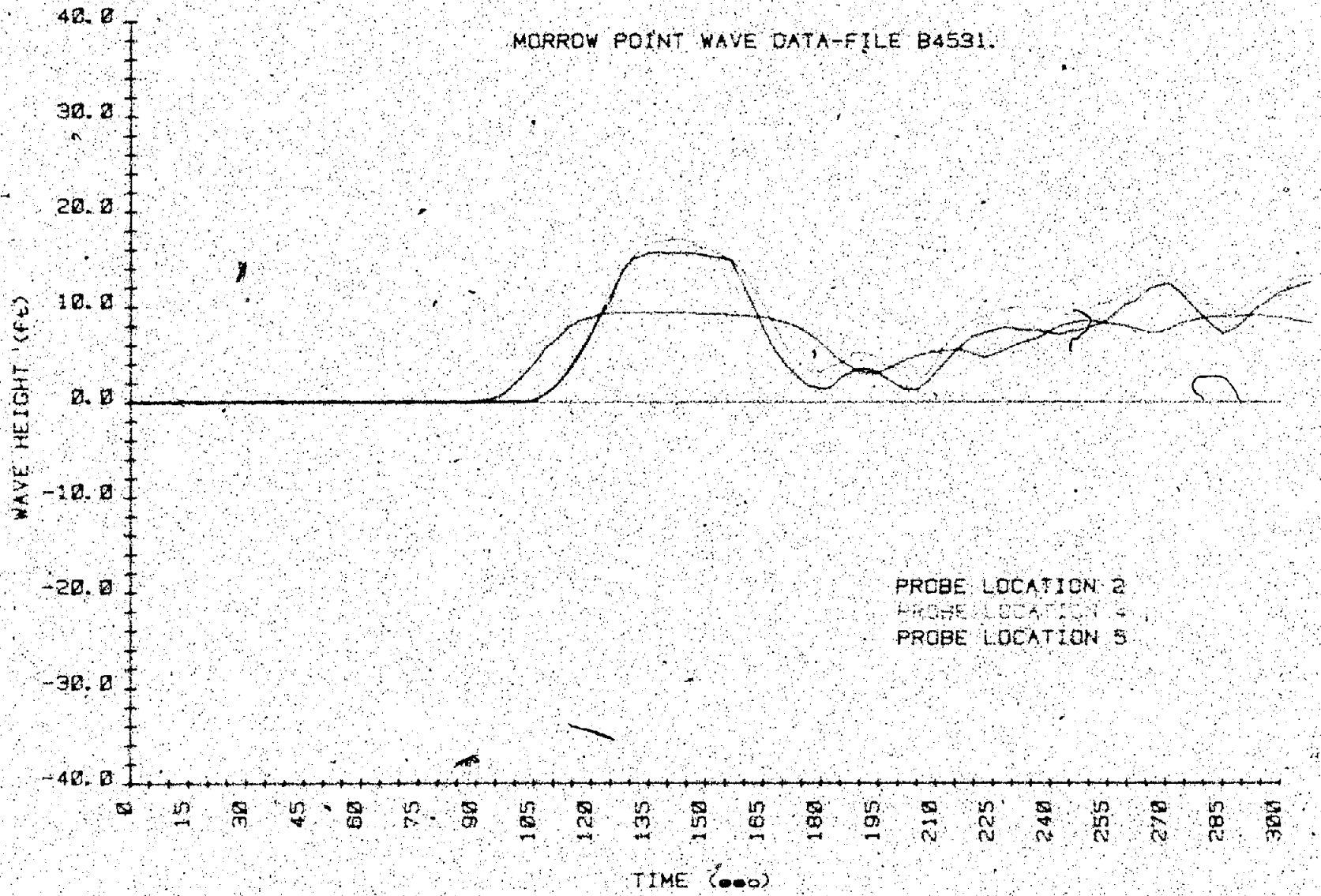

MF 91

Figure B 19. Wave height versus time — test B4531 (2 of 5)

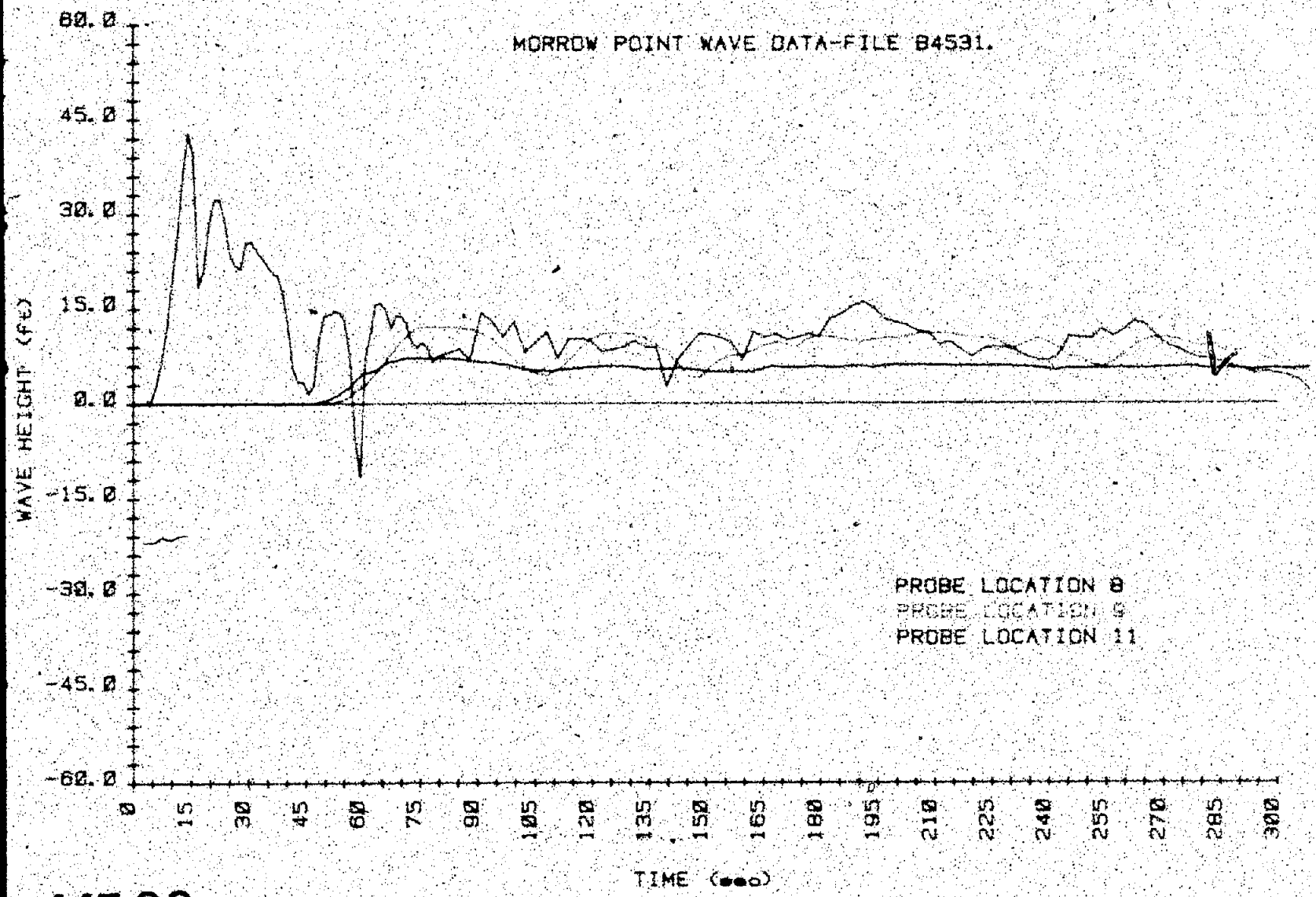

MF 92

Figure B-19 — Wave height versus time — test B4531 (3 of 5)

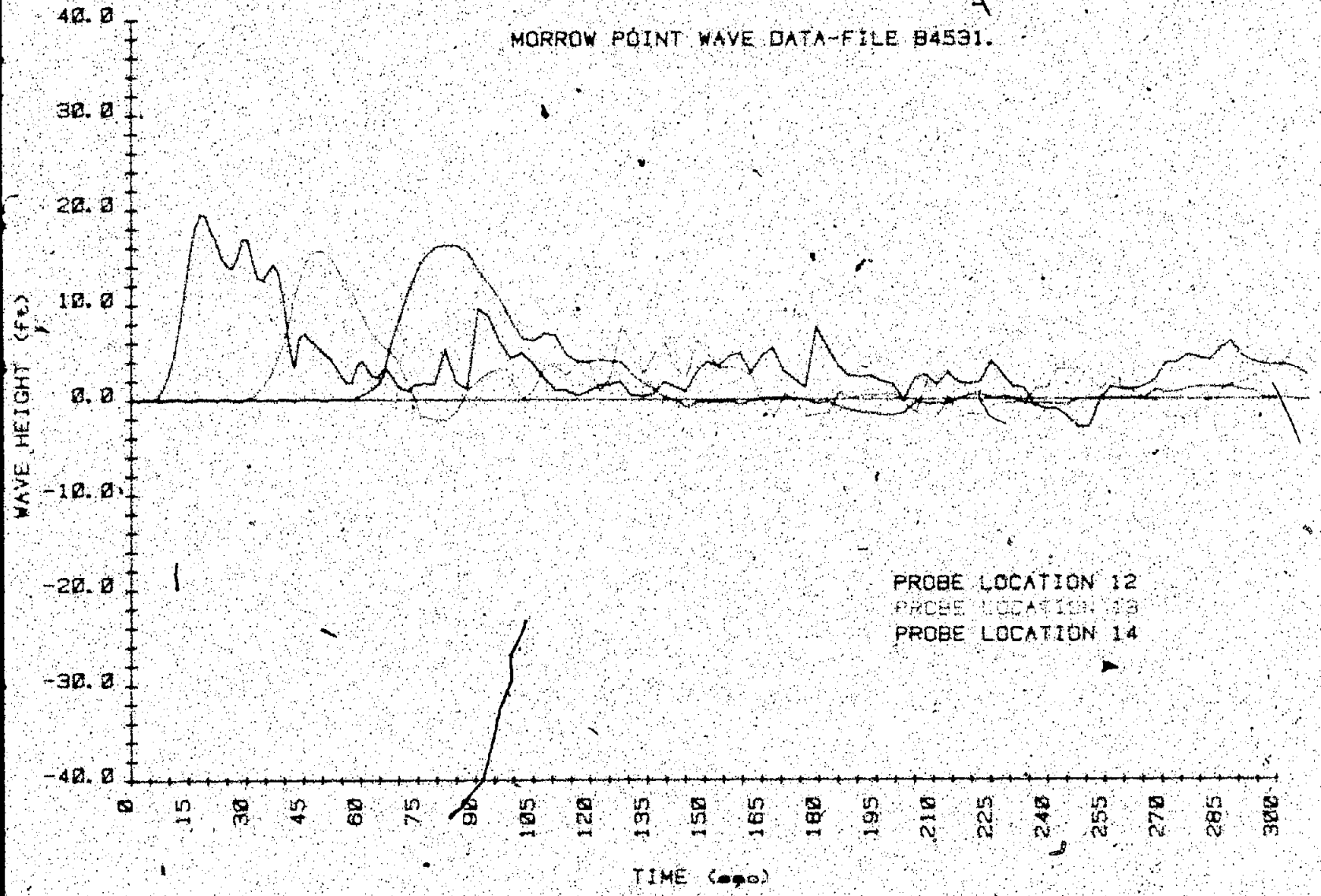

MF 93

Figure B-19 – Wave height versus time – test B4531 (4 of 5).

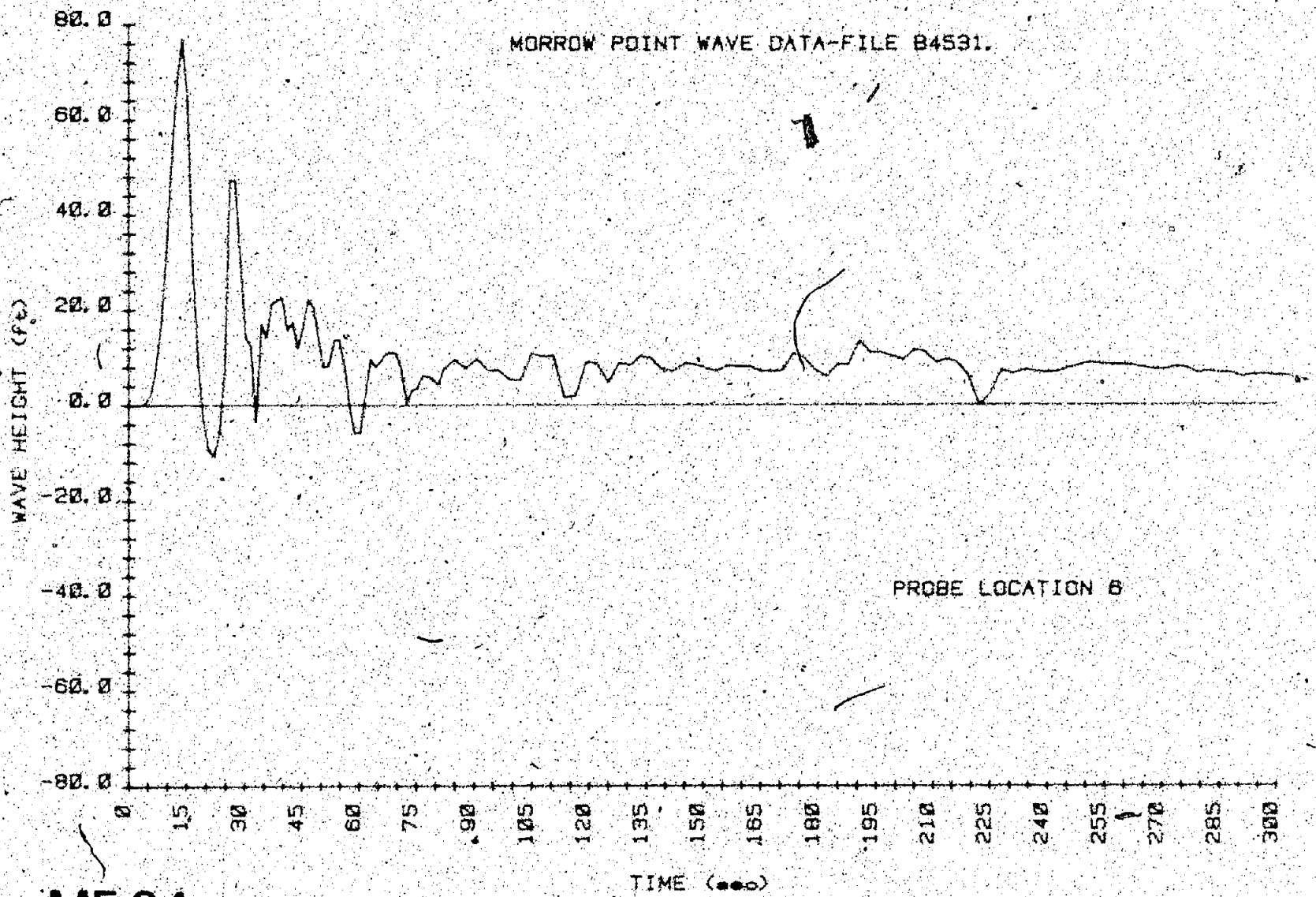

MF 94

Figure B-19. - Wave height versus time - test B4531 (5 of 5).

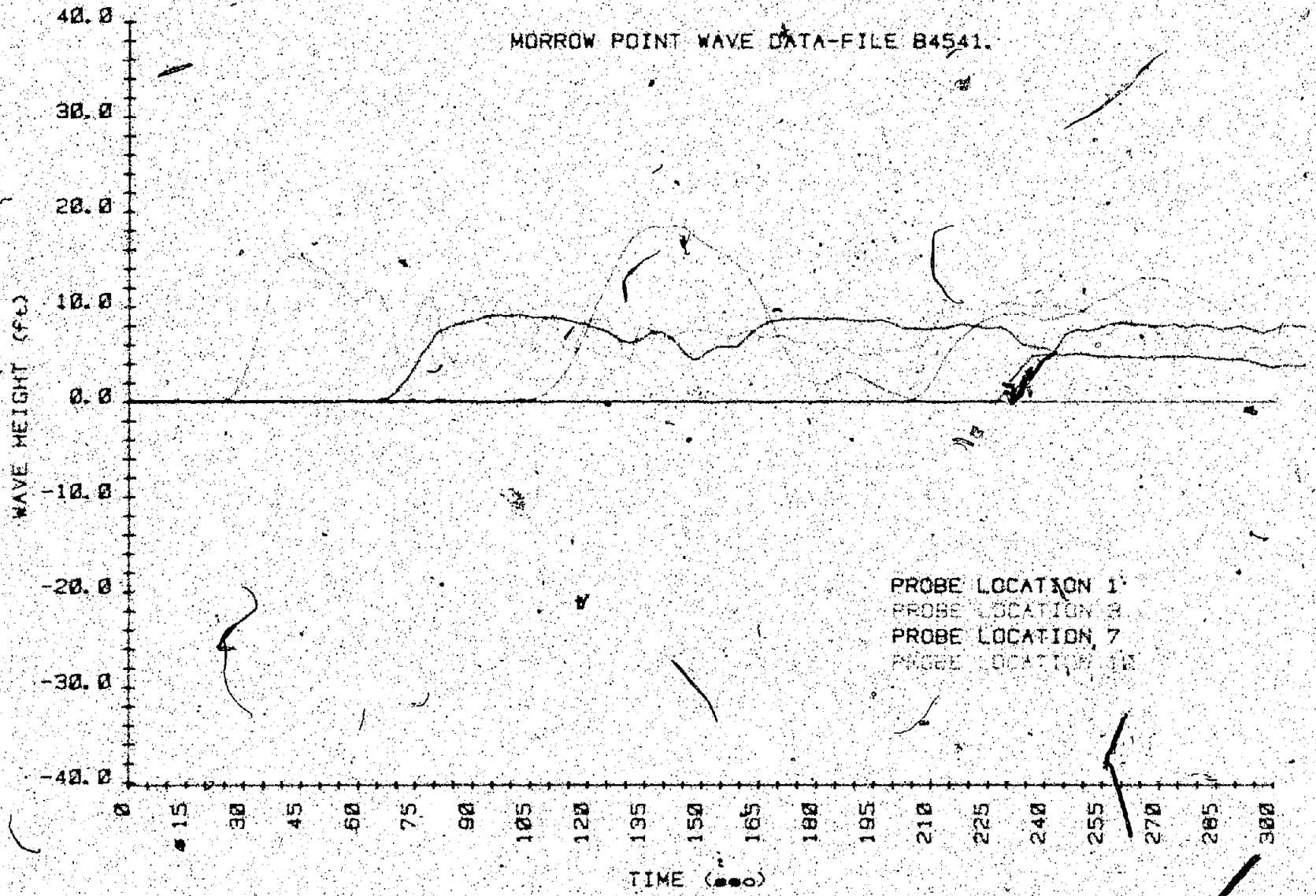

MF 95

Figure 8-20. Wave height versus time - test 84541 (1 of 5)

DEPARTMENT OF THE INTERIOR · MARCH 3, 1849 ·

U.S. DEPARTMENT OF THE INTERIOR

BUREAU OF RECLAMATION

UNITED STATES DEPARTMENT OF THE INTERIOR
Bureau of Reclamation
Engineering and Research Center
P.O. Box 25007
Building 67, Denver Federal Center
Denver, Colorado 80225

THESE ARE REPRODUCTIONS OF RESEARCH REPORTS ISSUED BY THE BUREAU OF RECLAMATION, ENGINEERING AND RESEARCH CENTER. THEY WERE MICROFILMED BY THE MICROGRAPHICS UNIT OF THE E & R CENTER IN A MANNER AND ON MICROFILM WHICH MEETS THE RECOMMENDED REQUIREMENTS OF THE AMERICAN NATIONAL STANDARD INSTITUTE (ANSI) FOR PERMANENT MICROPHOTOGRAPHIC REPRODUCTIONS.

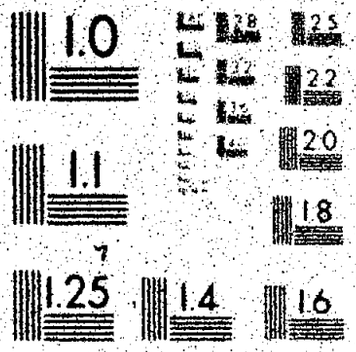

24X

MICROCOPY RESOLUTION TEST CHART
NATIONAL BUREAU OF STANDARDS
STANDARD REFERENCE MATERIAL 10a
ANSI and ISO TEST CHART No. 2

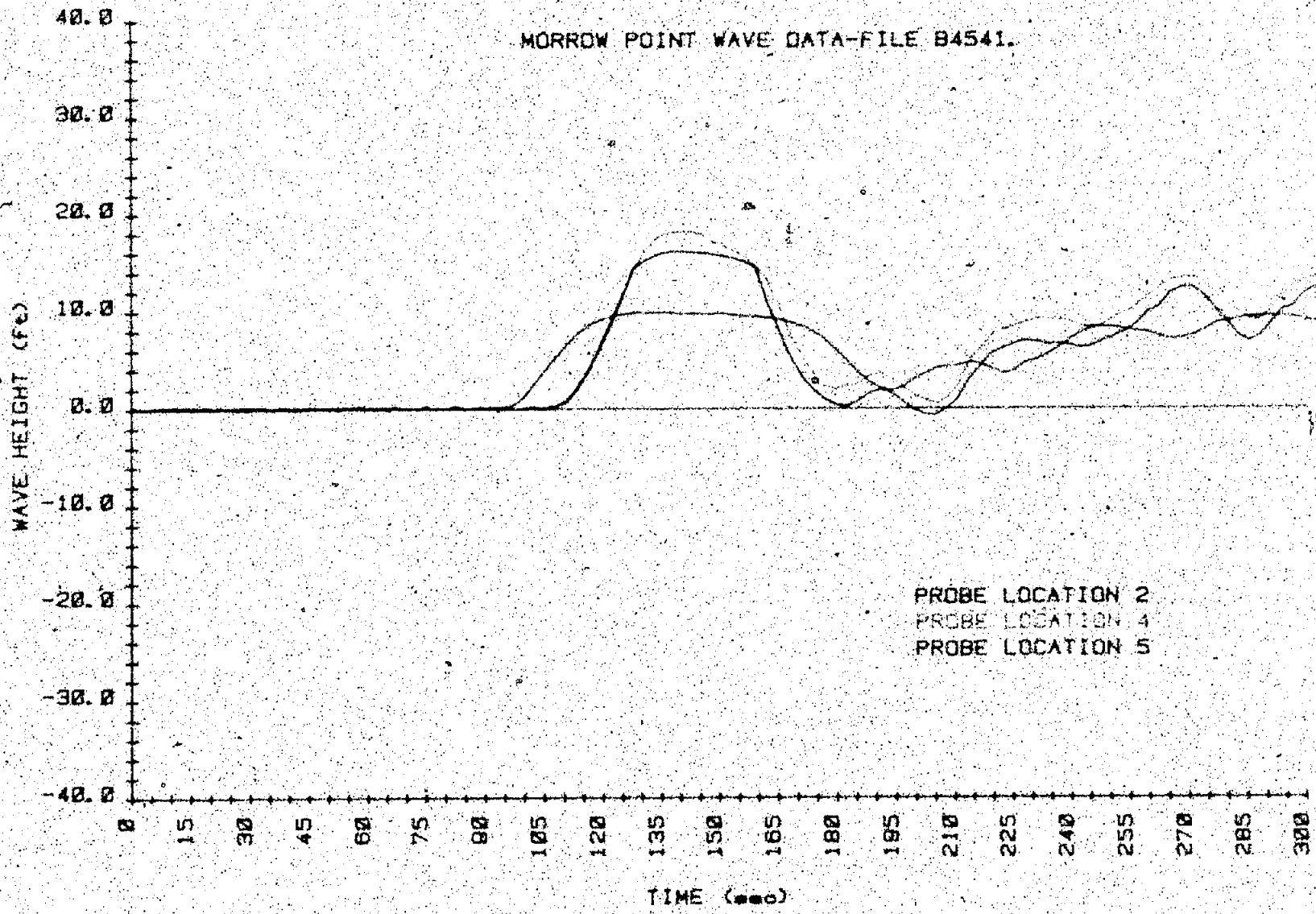

MF 96

Figure B 20. Wave height versus time — test B4541 (2 of 5)

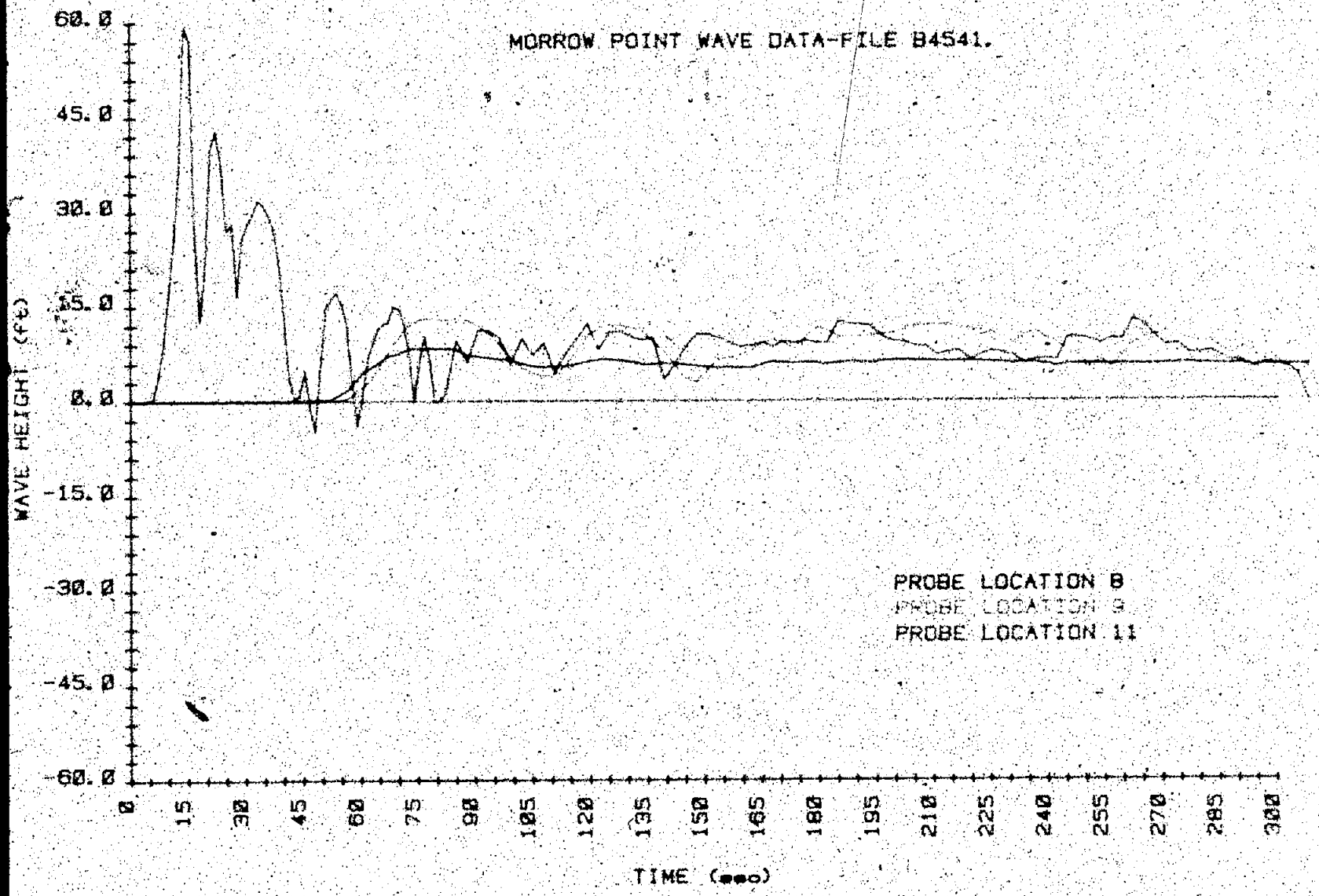

MF 97

Figure B-20. Wave height versus time — test B4541 (3 of 5)

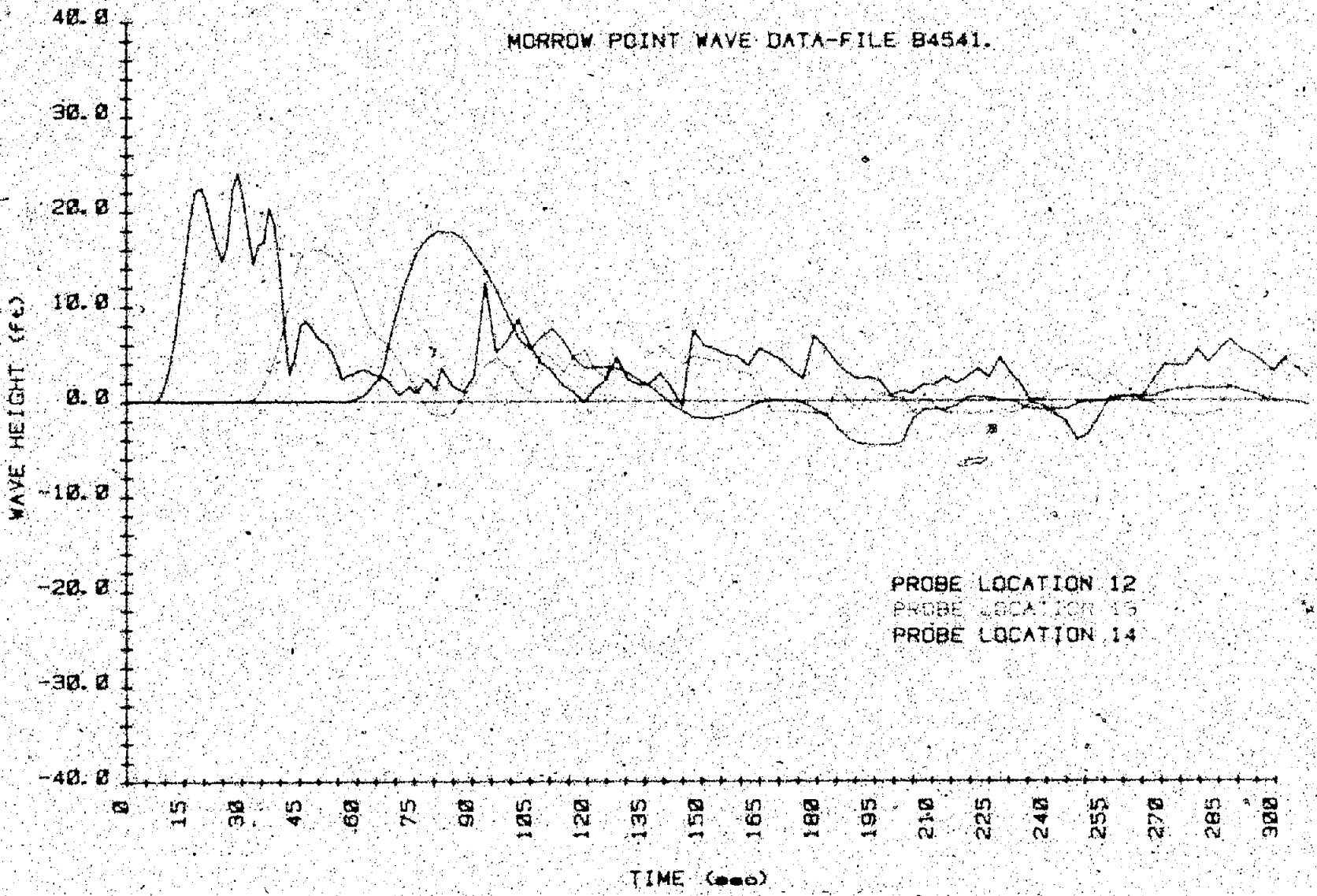

MF 98

Figure B.20 Wave height versus time test B4541 (4 of 5)

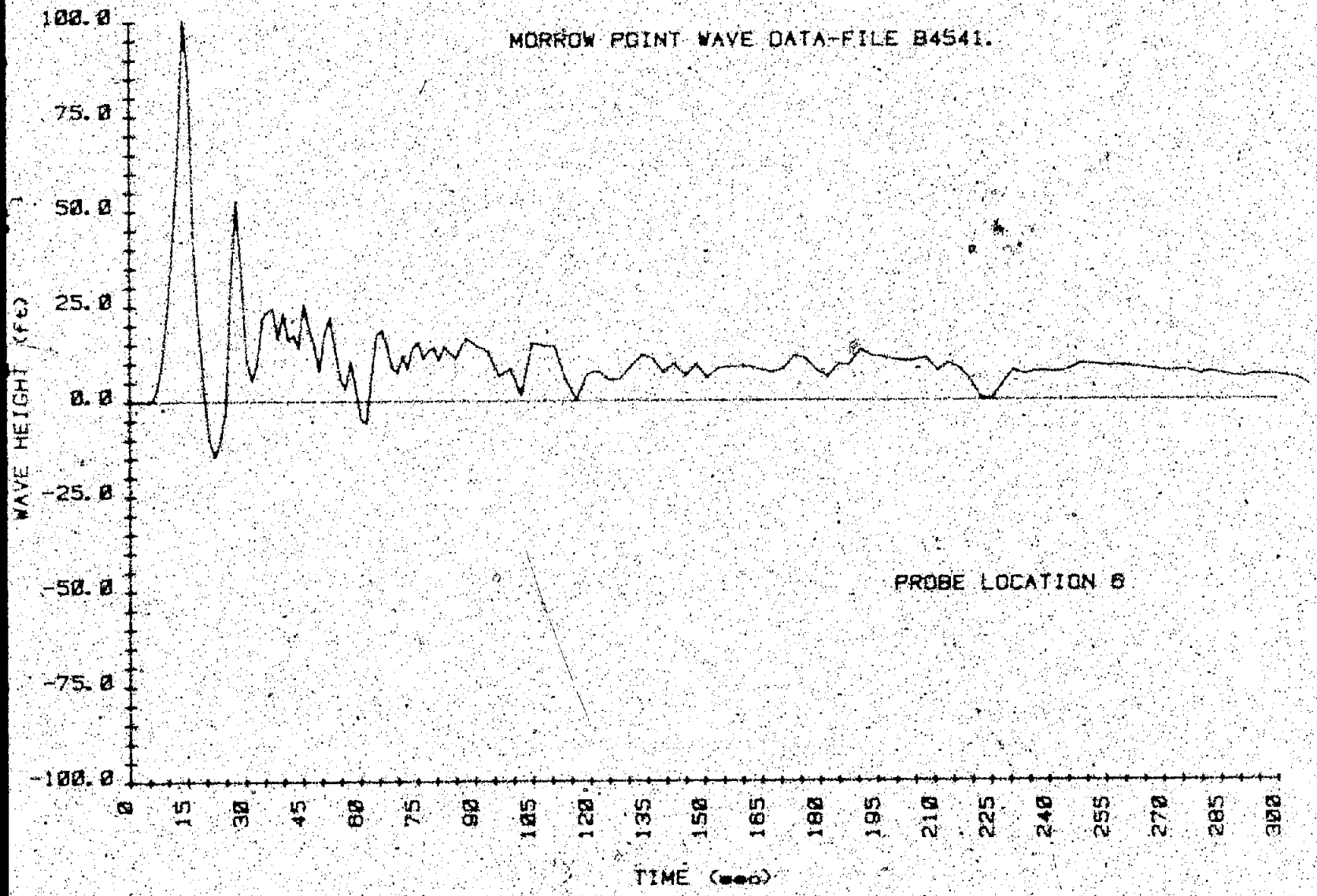

MF 99

Figure B.20. – Wave height versus time – test B4541 (5 of 5).

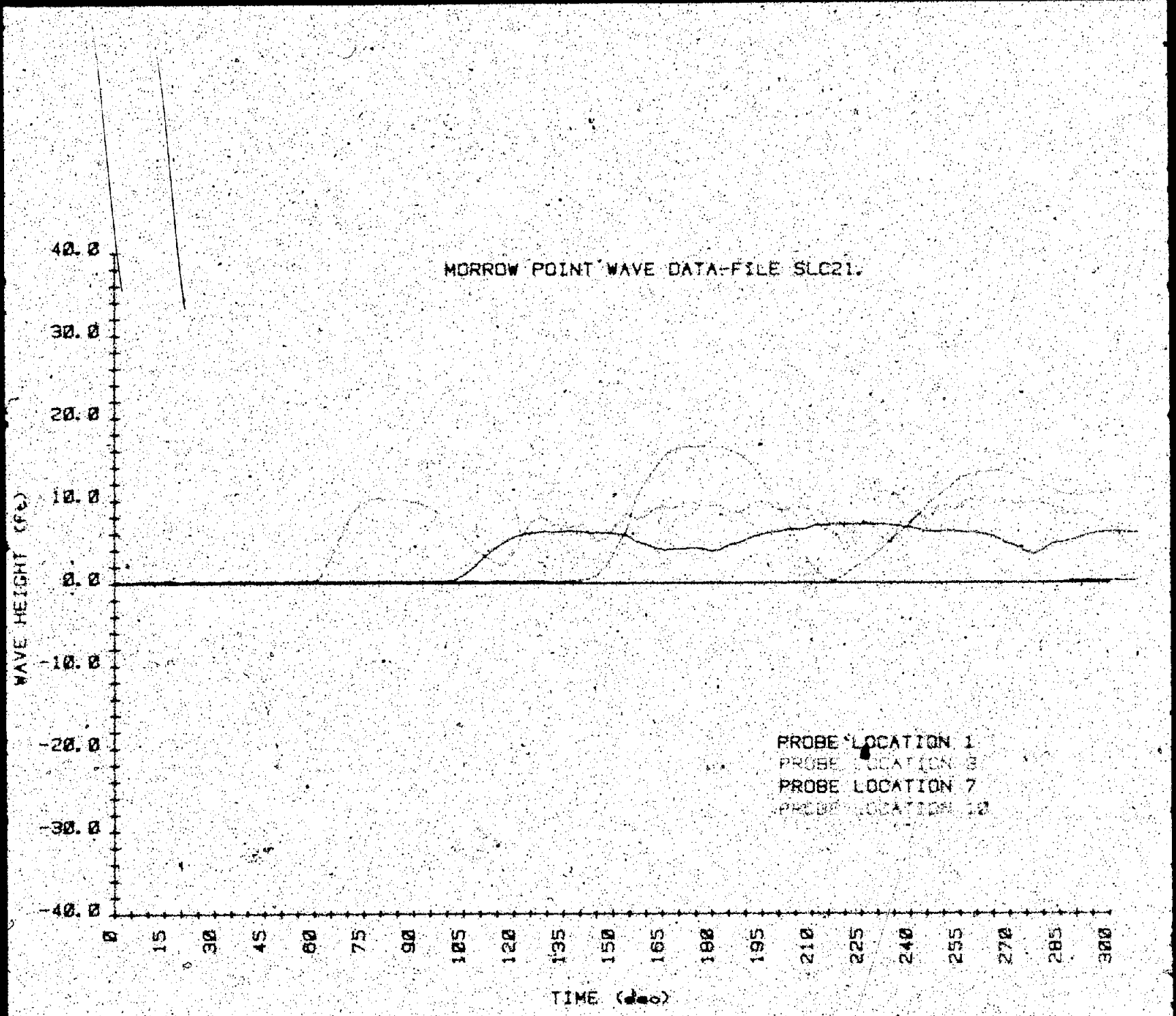

MF 100

Figure B 21. – Wave height versus time – test SLC21 (1 of 5)

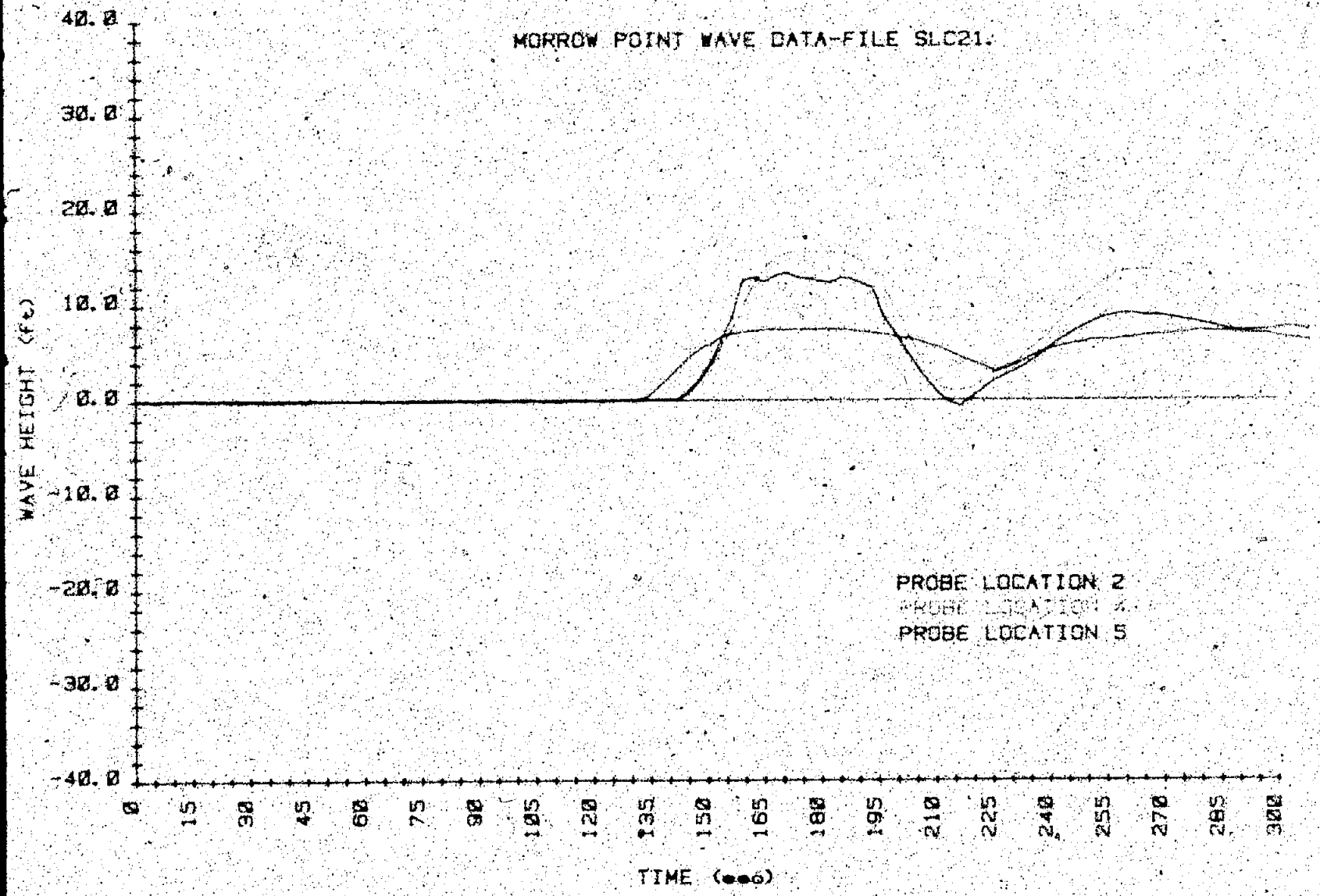

MF 101

Figure B 21 Wave height versus time - test SLC21 (2 of 5)

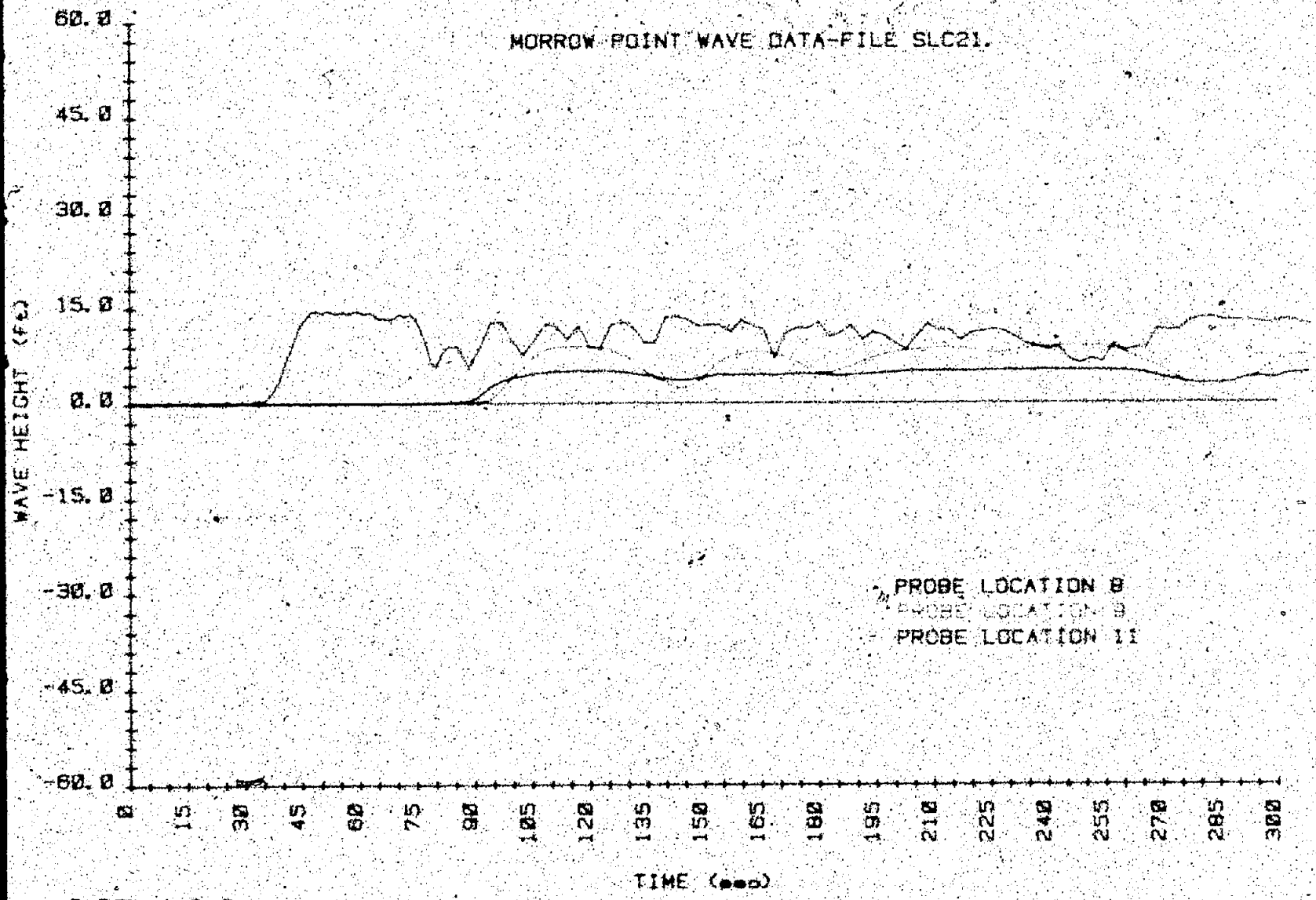

MF 102

Figure B-21. - Wave height versus time - test SLC21 (3 of 5)

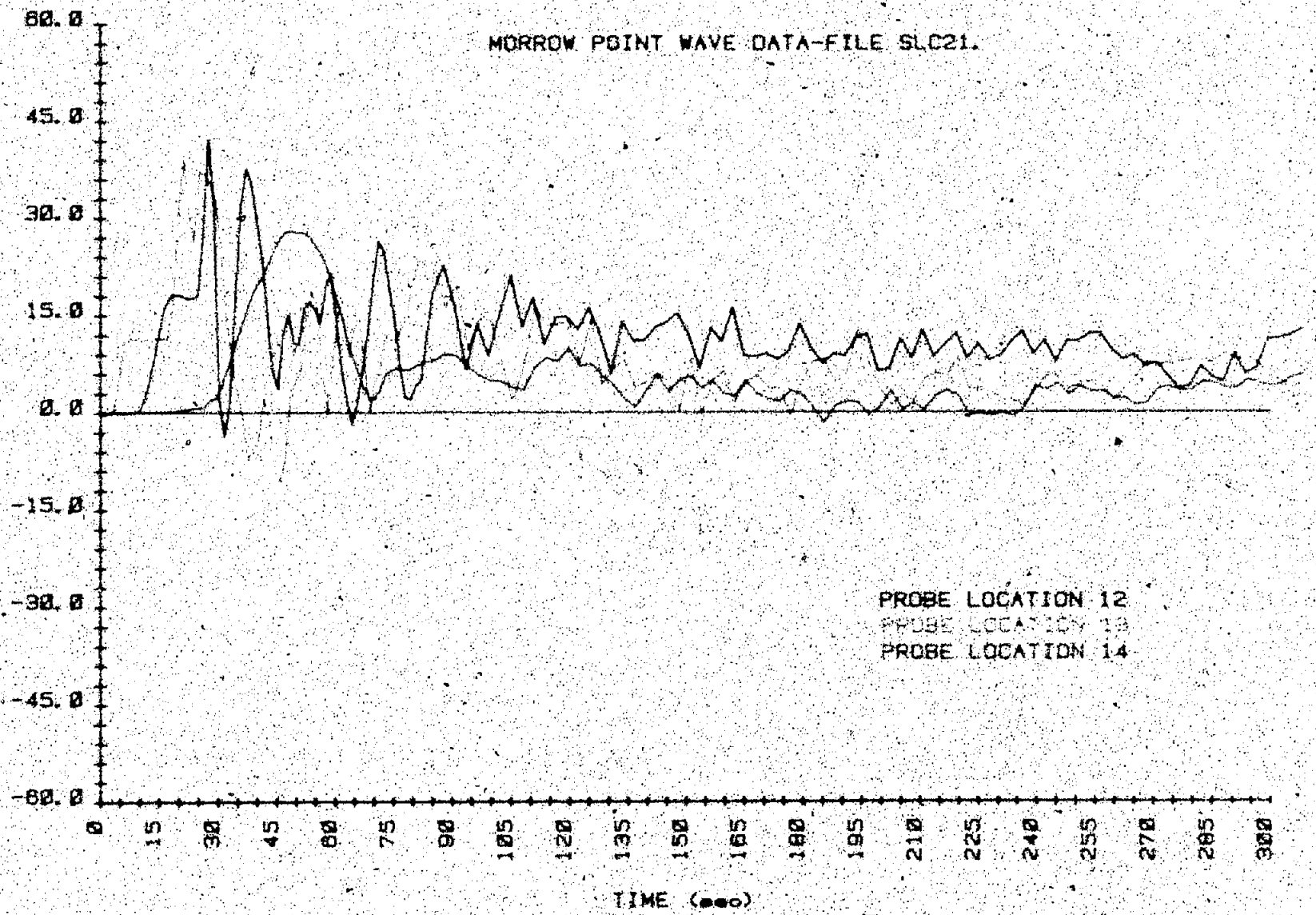

MF 103

Figure B-21. Wave height versus time — test SLC21 (4 of 5)

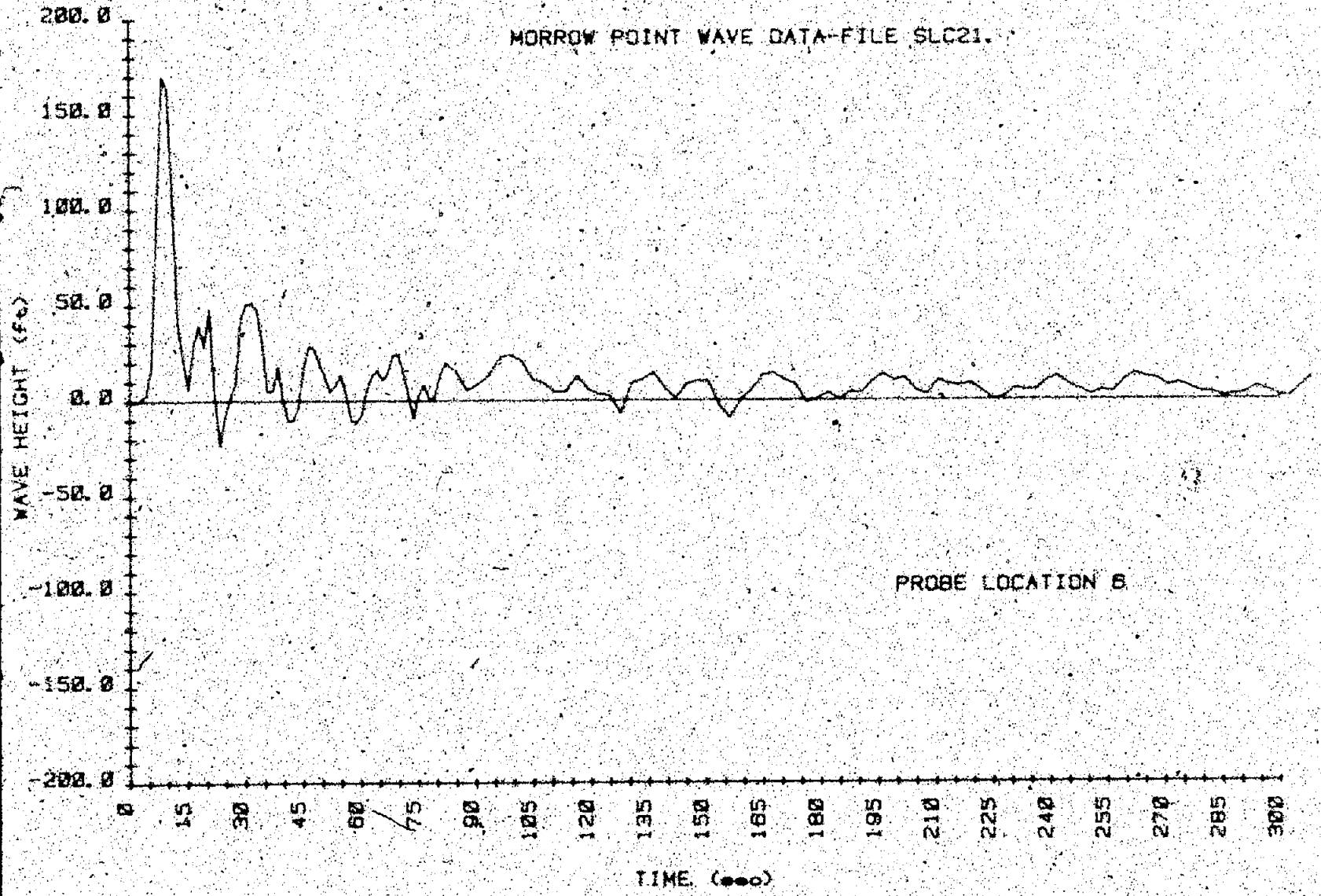

MF 104

Figure B-21. Wave height versus time test SLC21 (5 of 5)

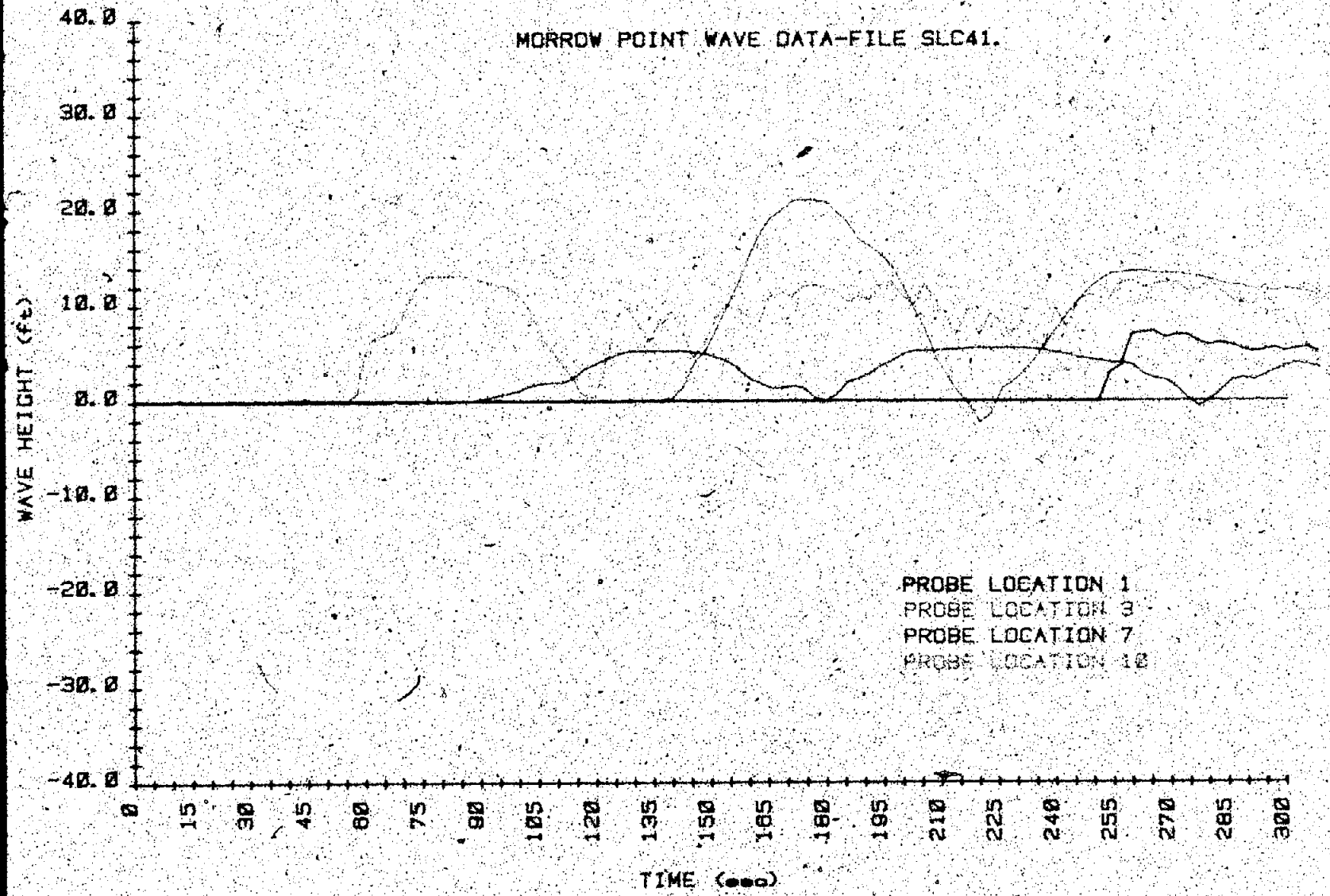

MF 105

Figure B-22.—Wave height versus time — test SLC41 (1 of 5)

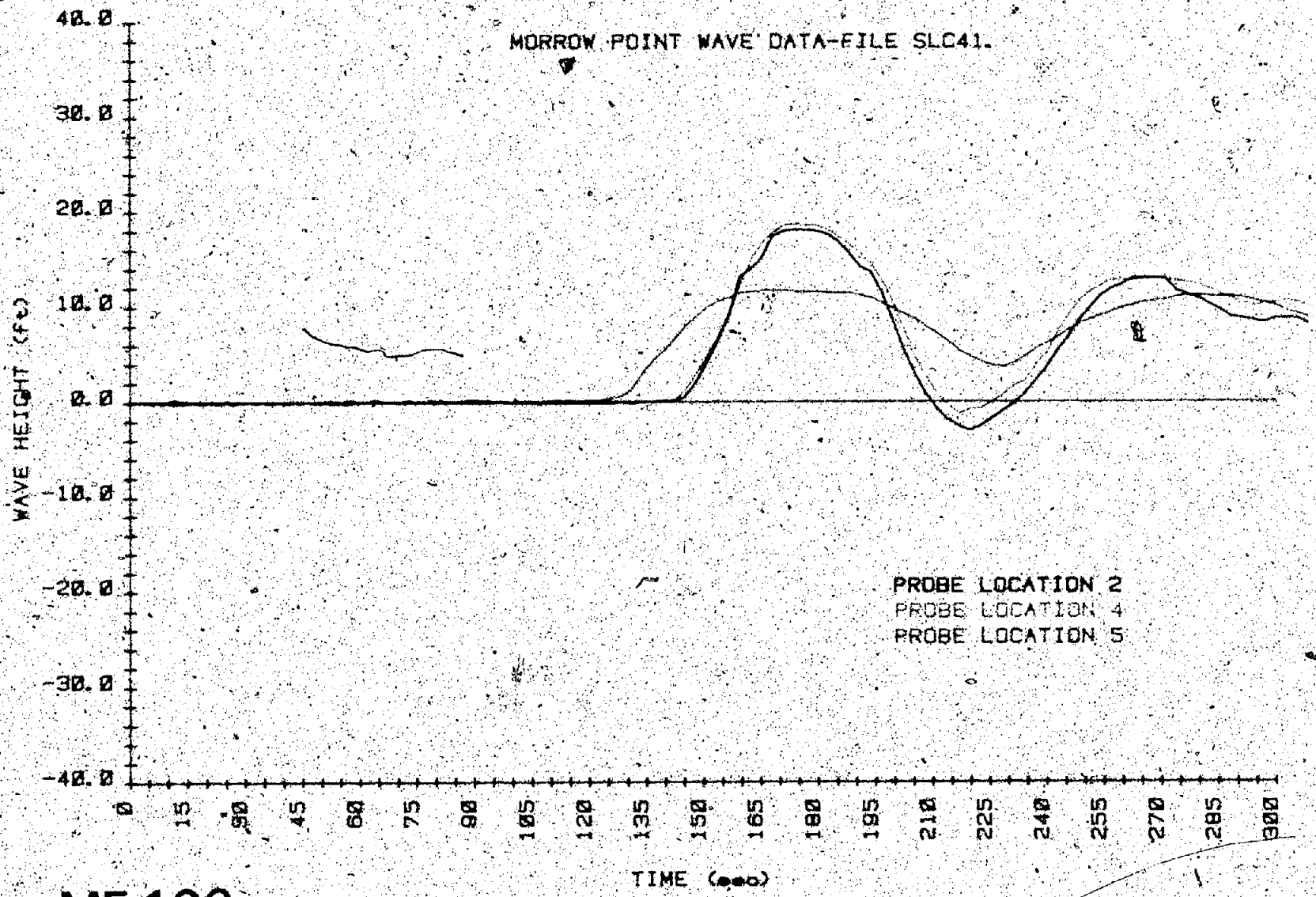

MF 106

Figure B 22. Wave height versus time — test SLC41 (2 of 5)

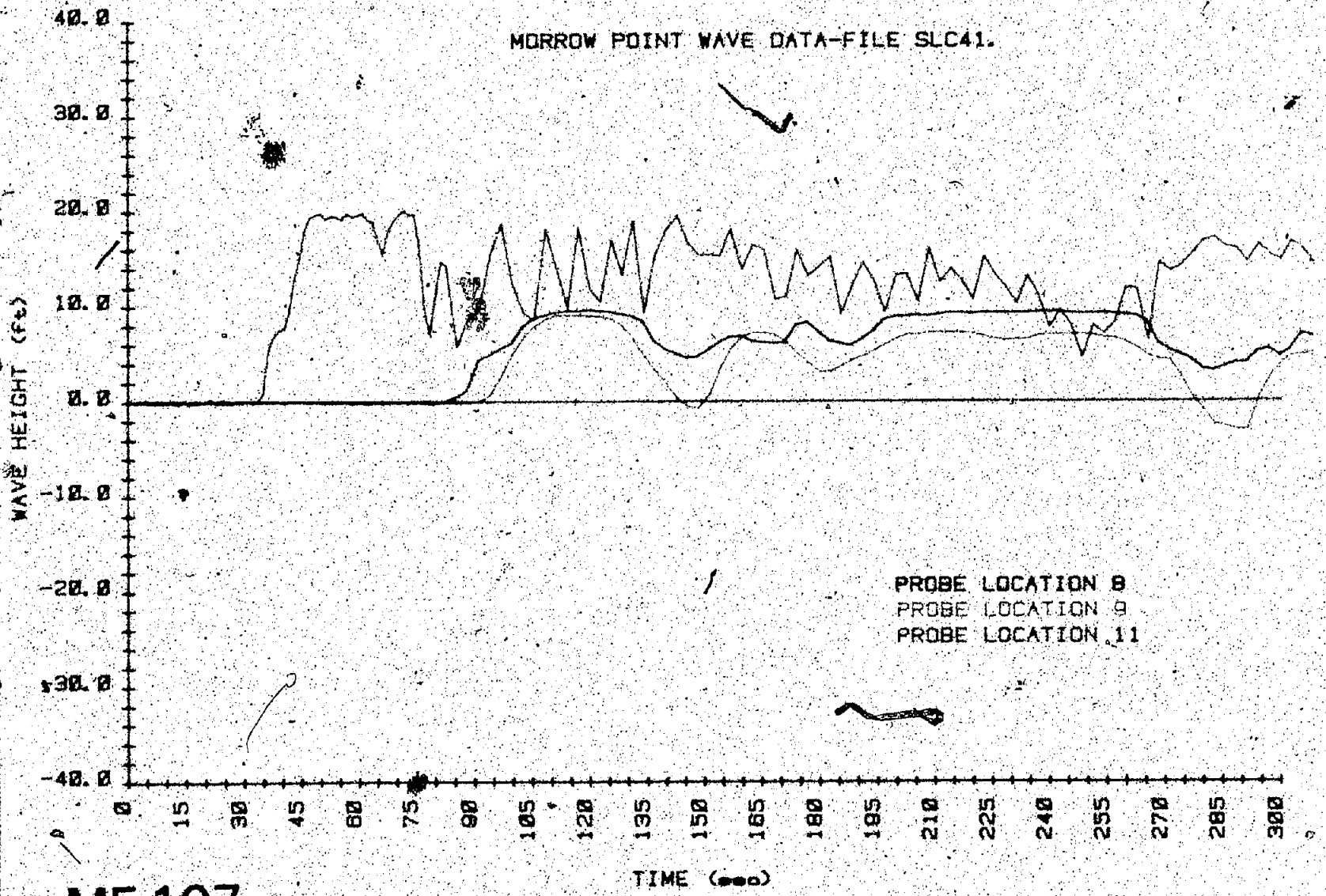

MF 107

Figure B-22.—Wave height versus time — test SLC41 (3 of 5).

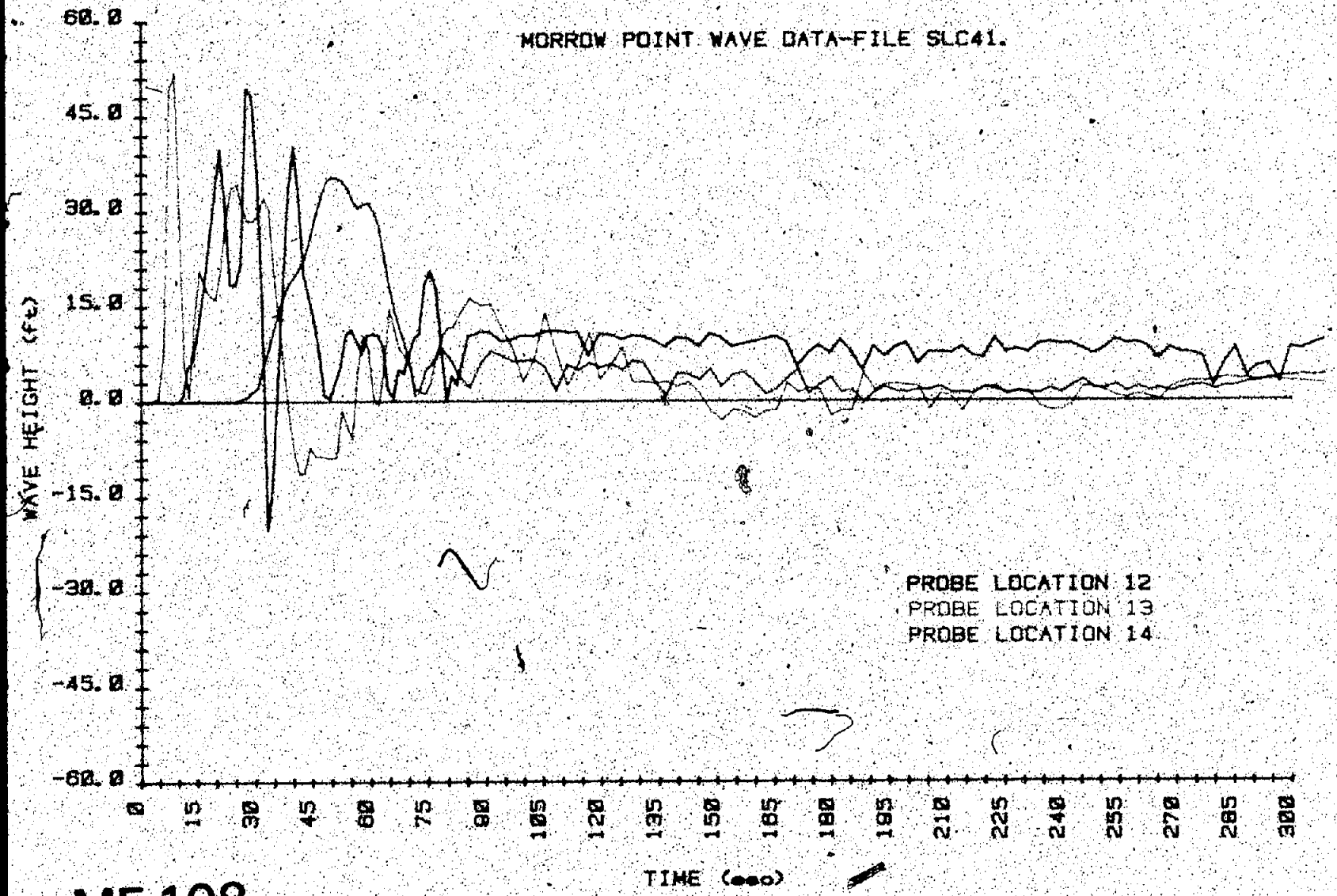

MF 108

Figure B-22. – Wave height versus time – test SLC41 (4 of 5).

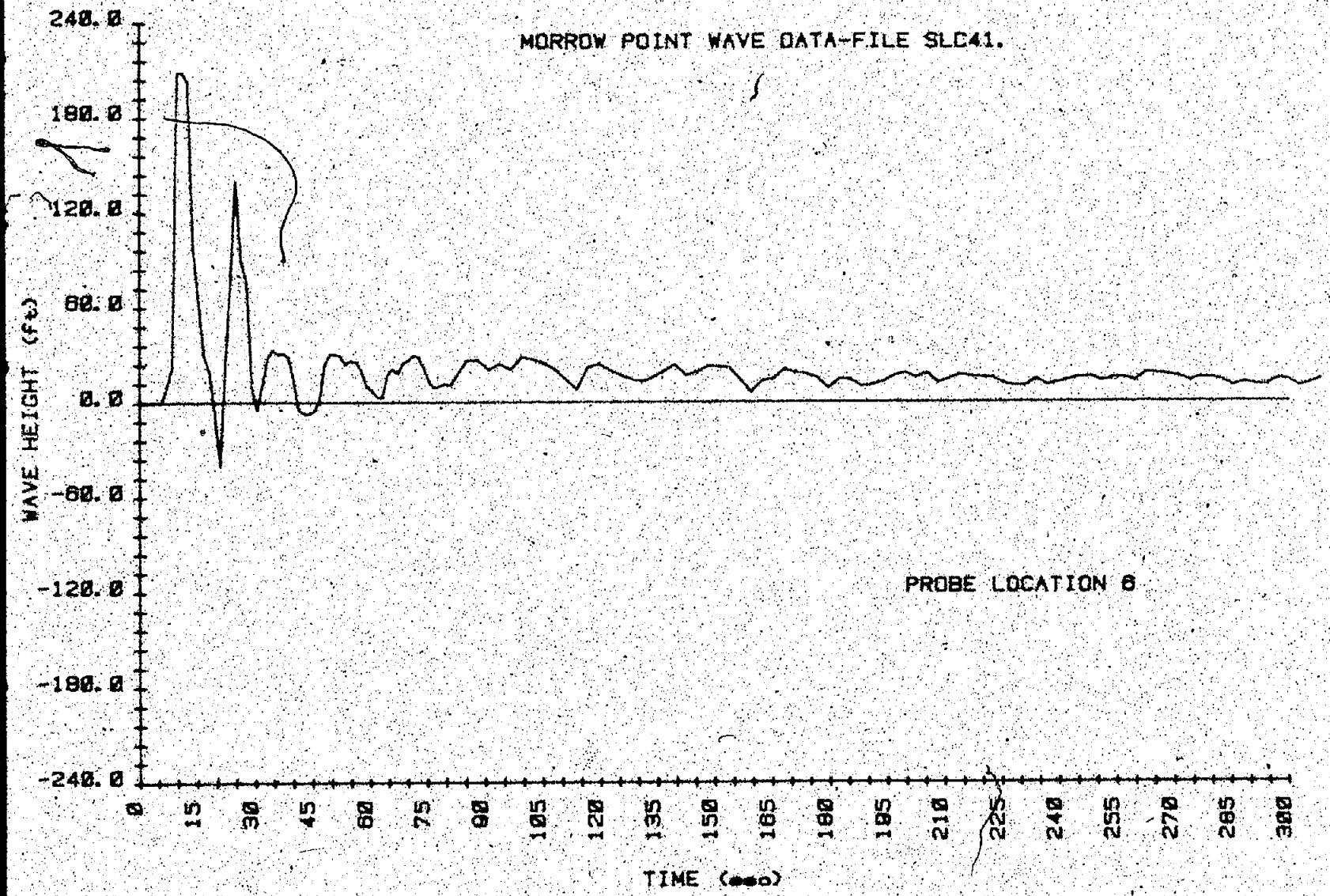

MF 109

Figure B-22 — Wave height versus time — test SLC41 (5 of 5).

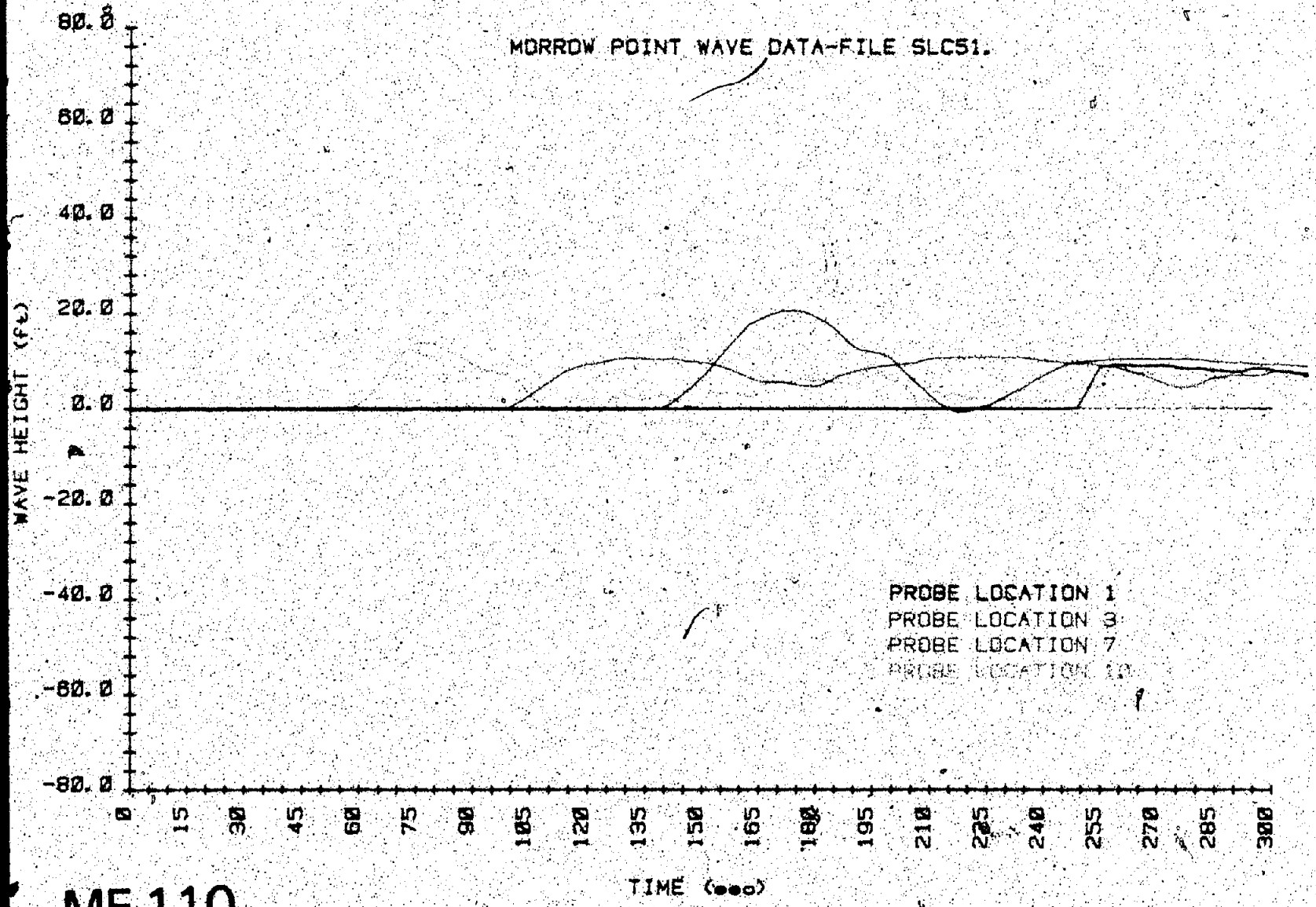

MF 110

Figure 8-23. – Wave height versus time – test SLC51 (1 of 6)

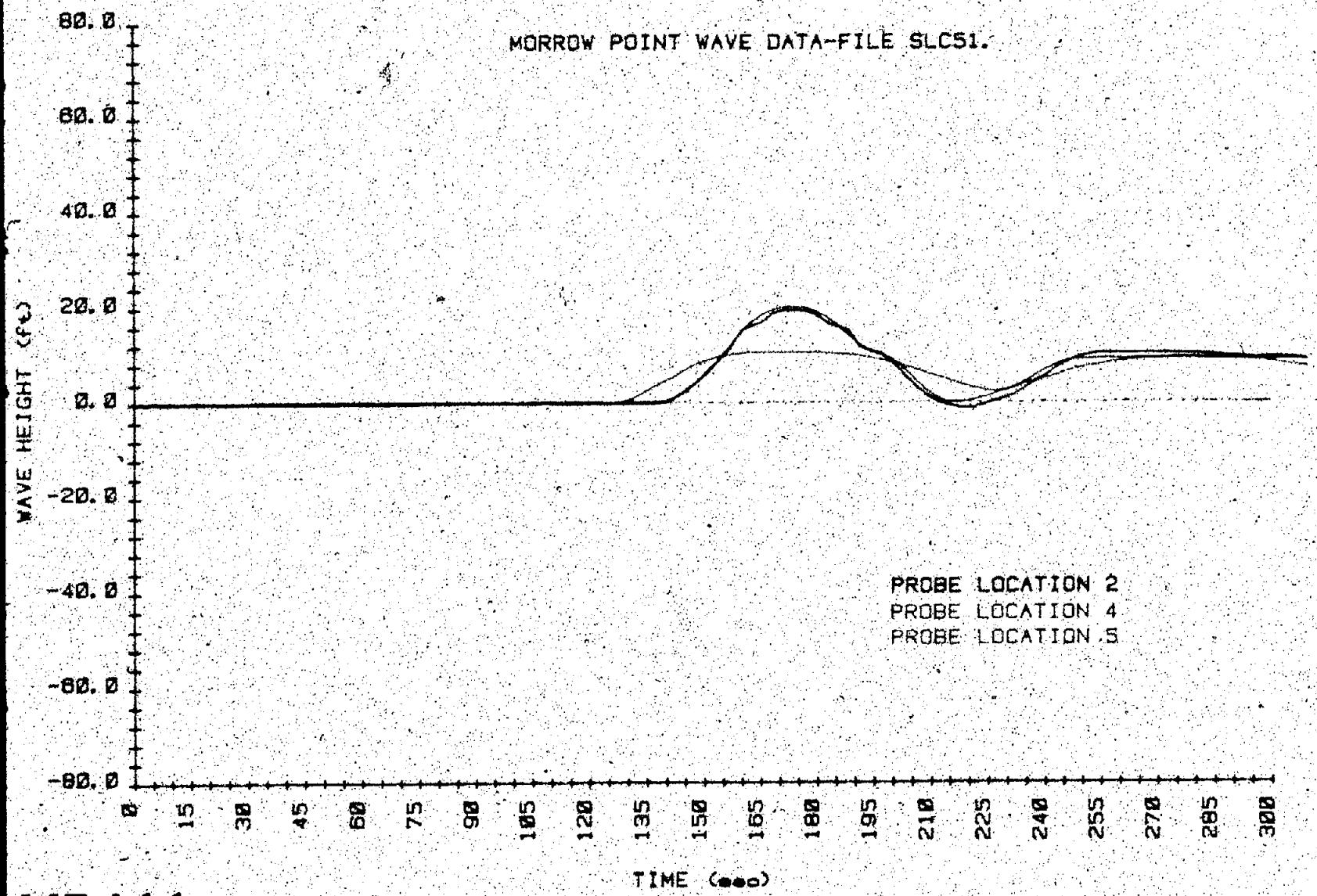

MF 111

Figure B 23. Wave height versus time — test SLC51 (2 of 5)

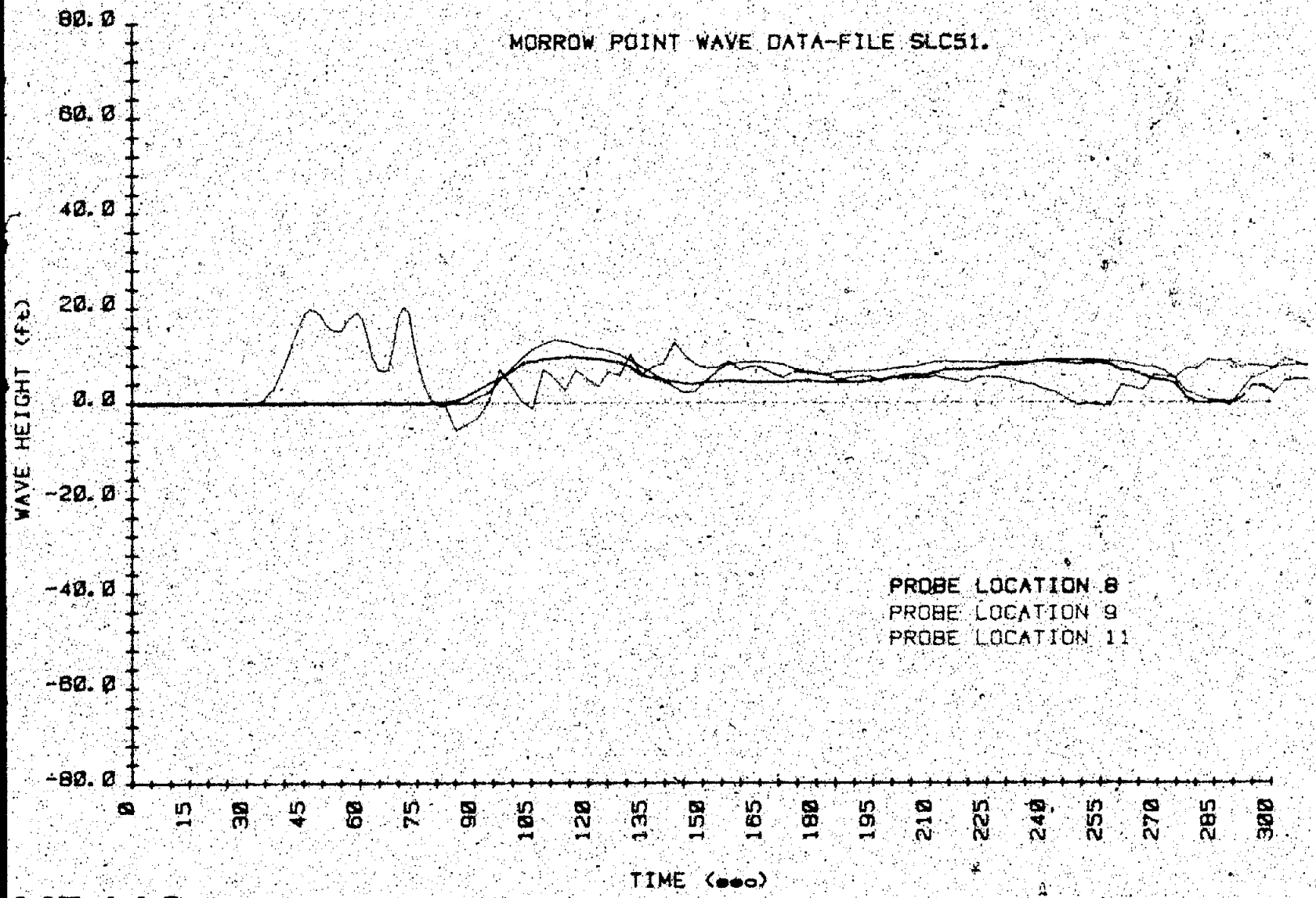

MF 112

Figure 8-23. Wave height versus time – test SLC51 (3 of 5).

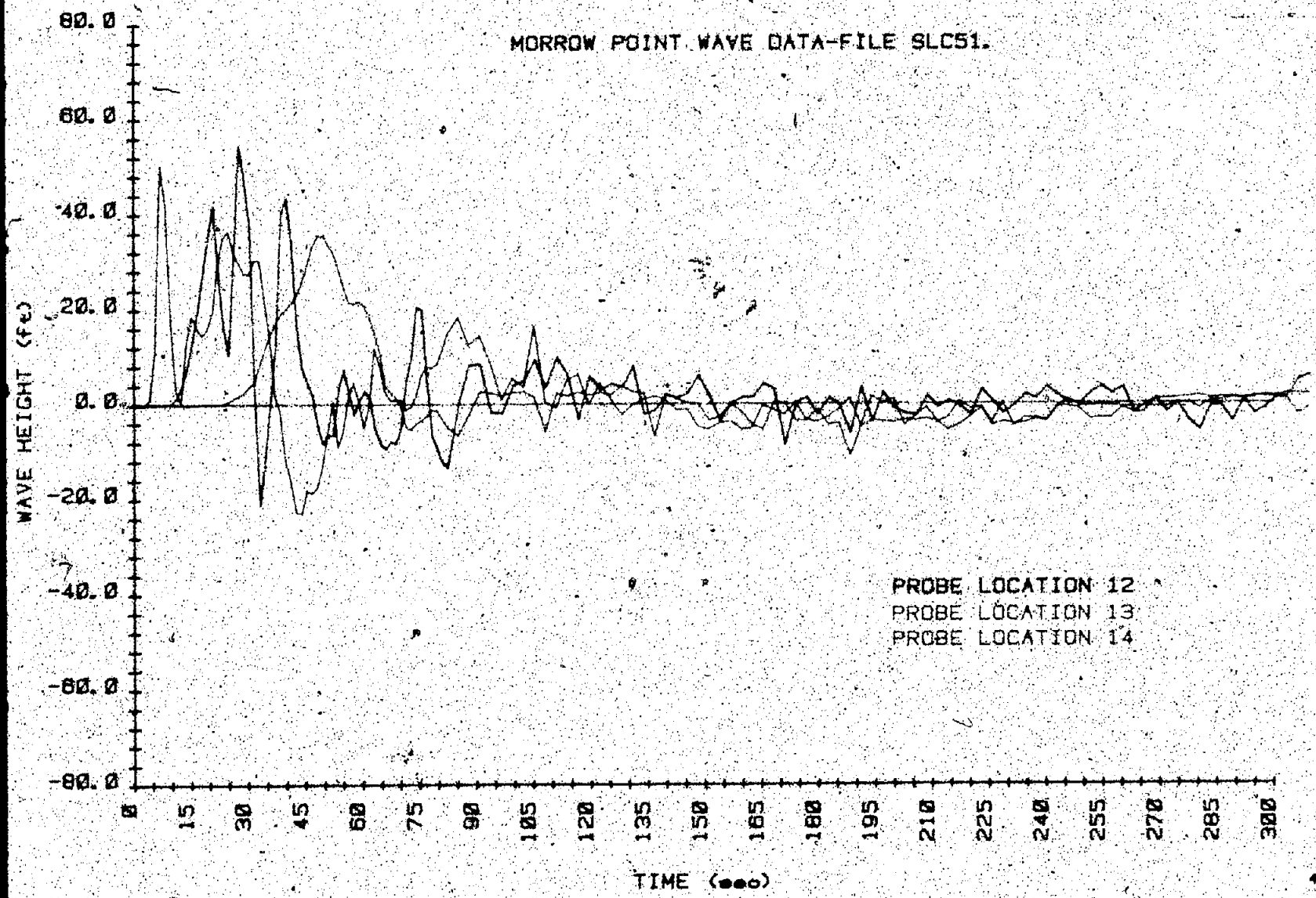

MF 113

Figure B-23. Wave height versus time — test SLC51 (4 of 5).

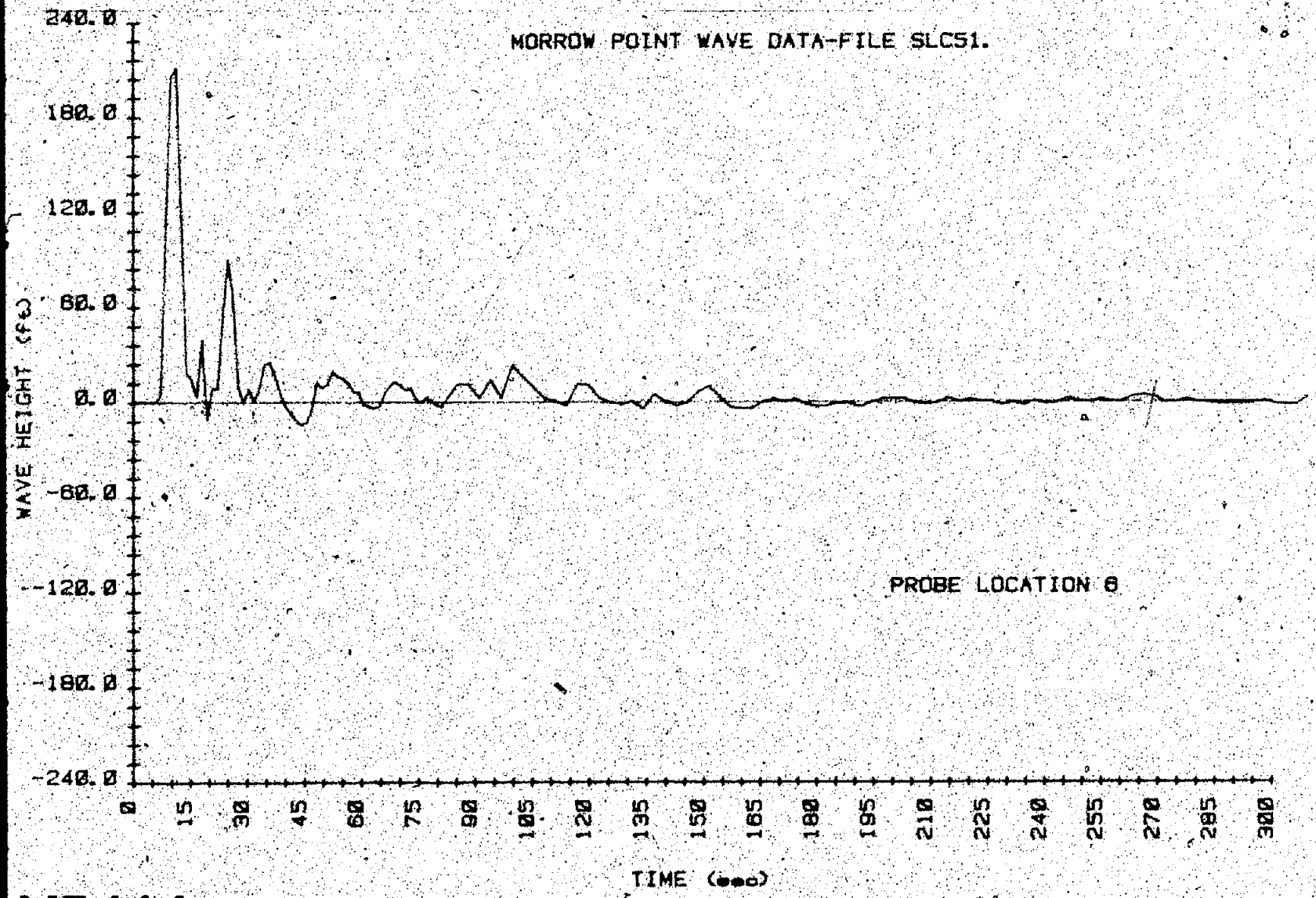

MF 114

Figure 8-23.—Wave height versus time — test SLCS1 (5 of 5).

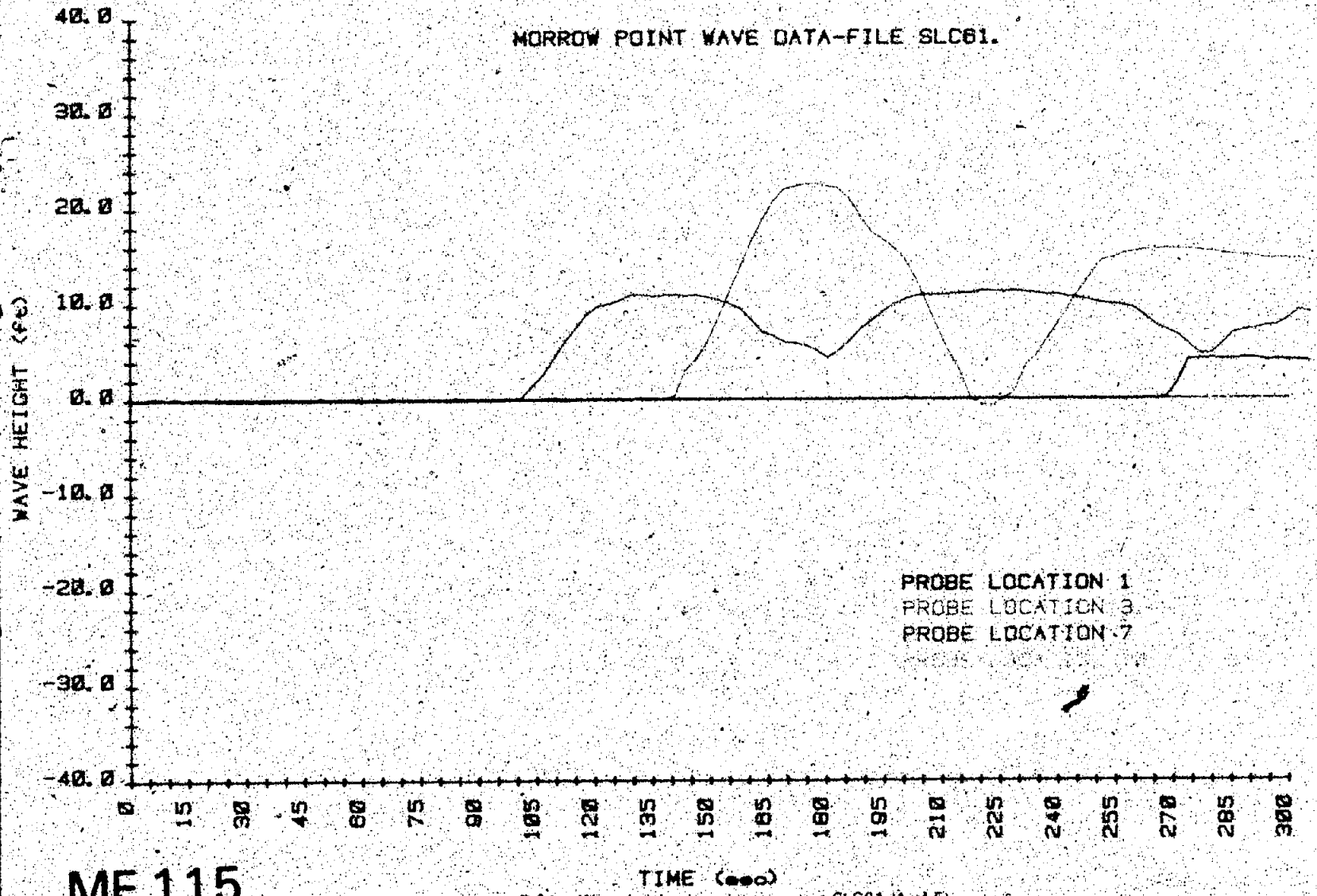

MF 115

Figure B-24.—Wave height versus time — test SLC61 (1 of 5).

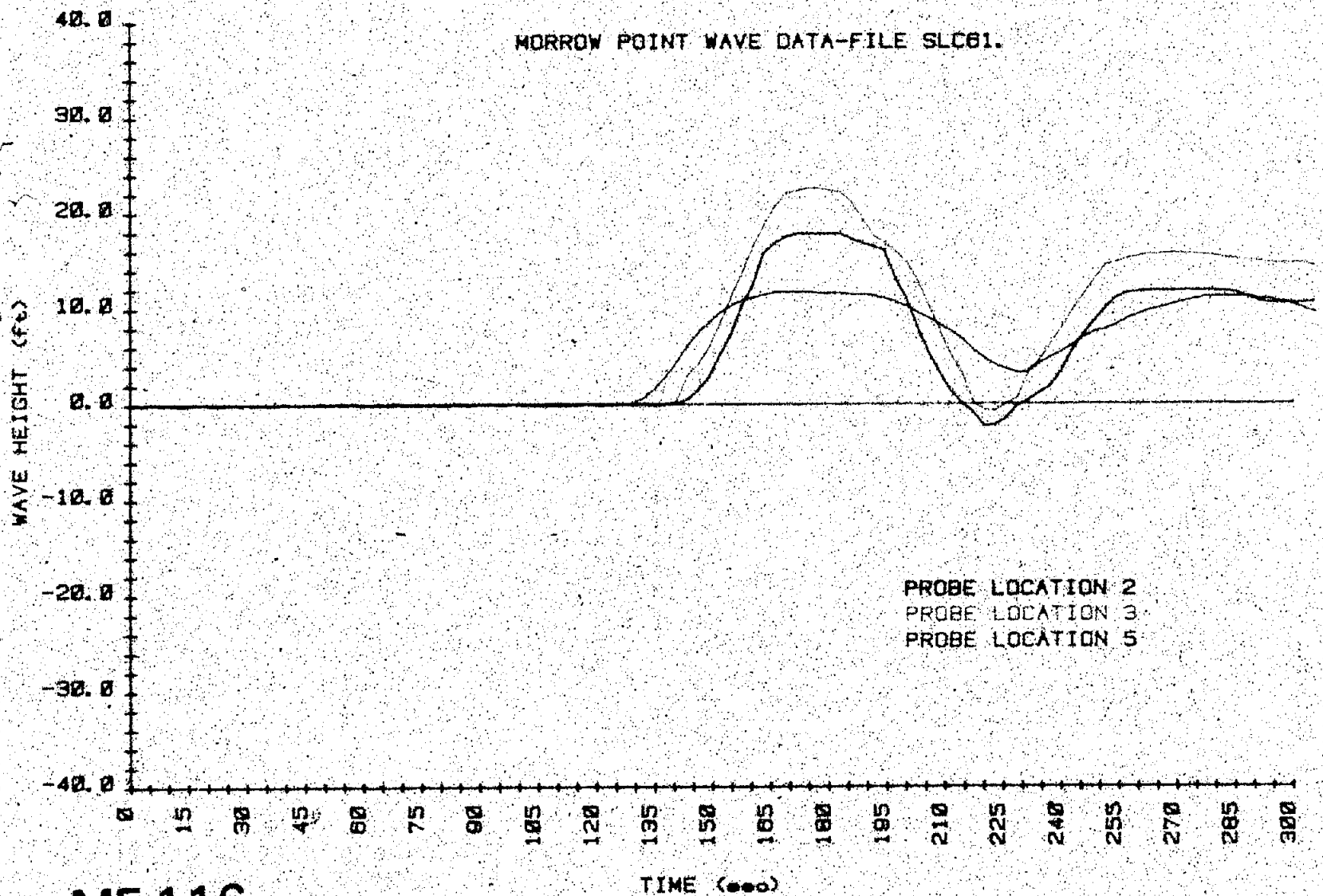

MF 116

Figure B-24.—Wave height versus time — test SLC61 (2 of 5).

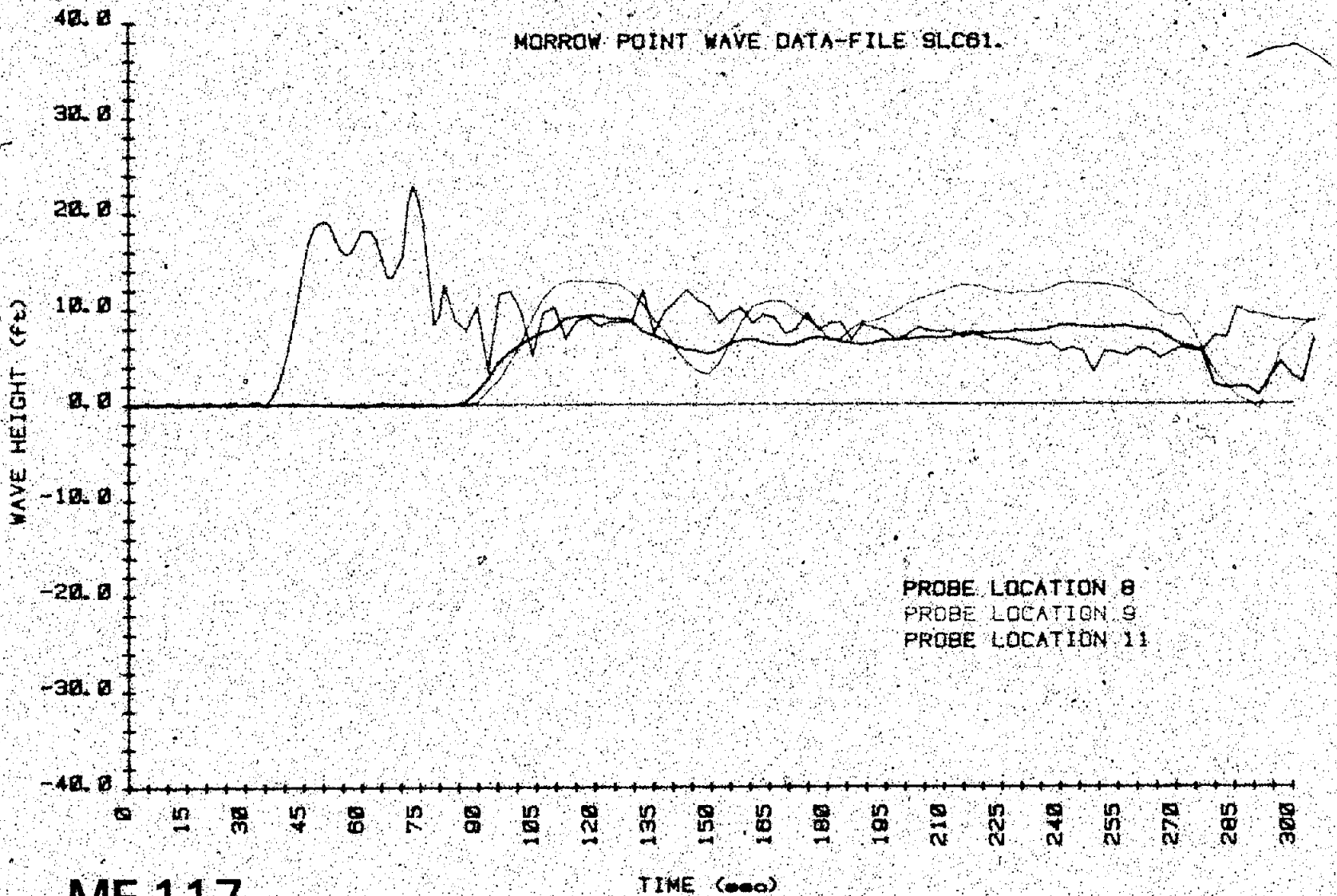

MF 117

Figure B-24. – Wave height versus time – test SLC61 (3 of 5).

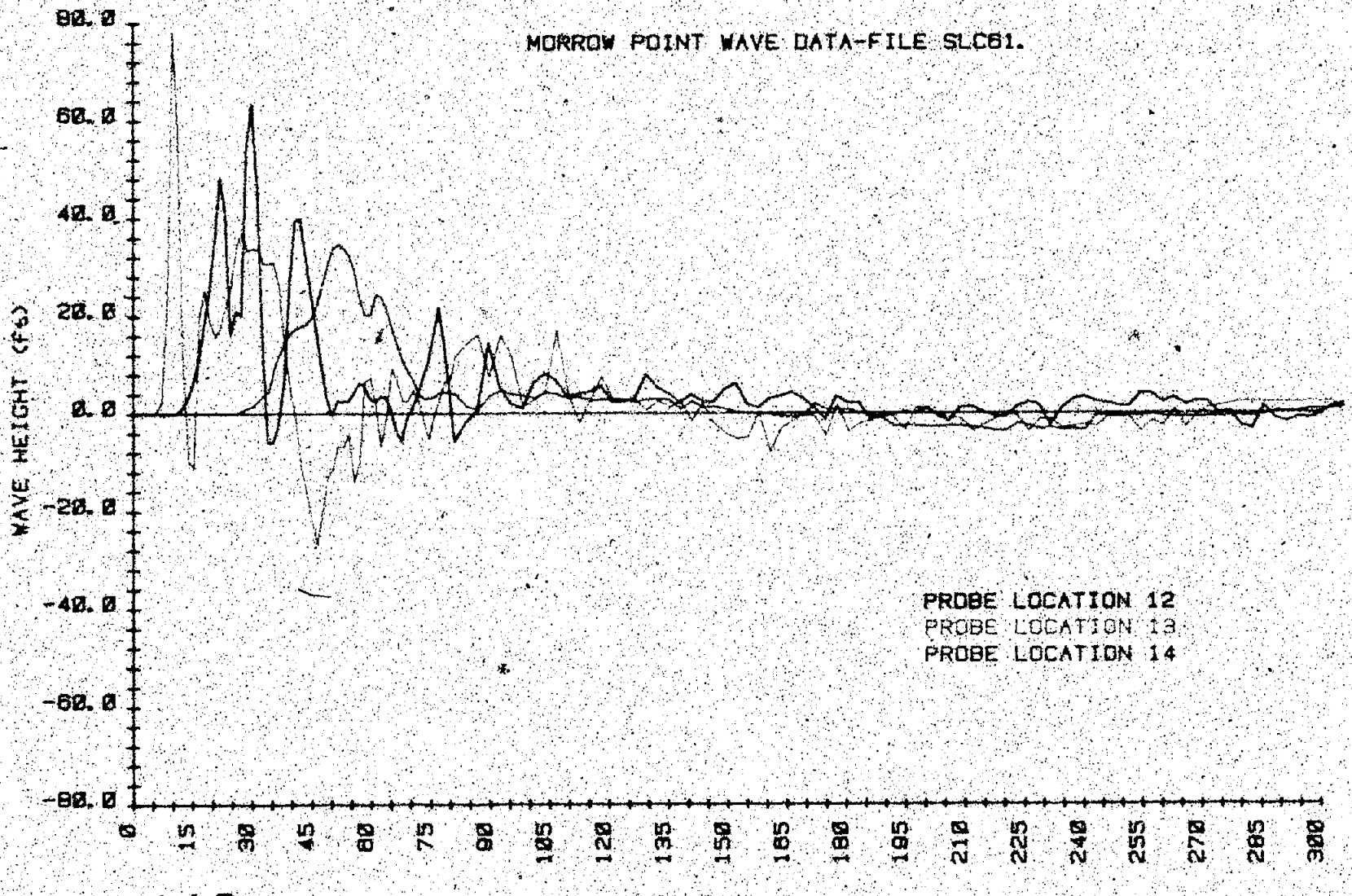

MF 118

Figure B-24.—Wave height versus time — test SLC61 (4 of 5).

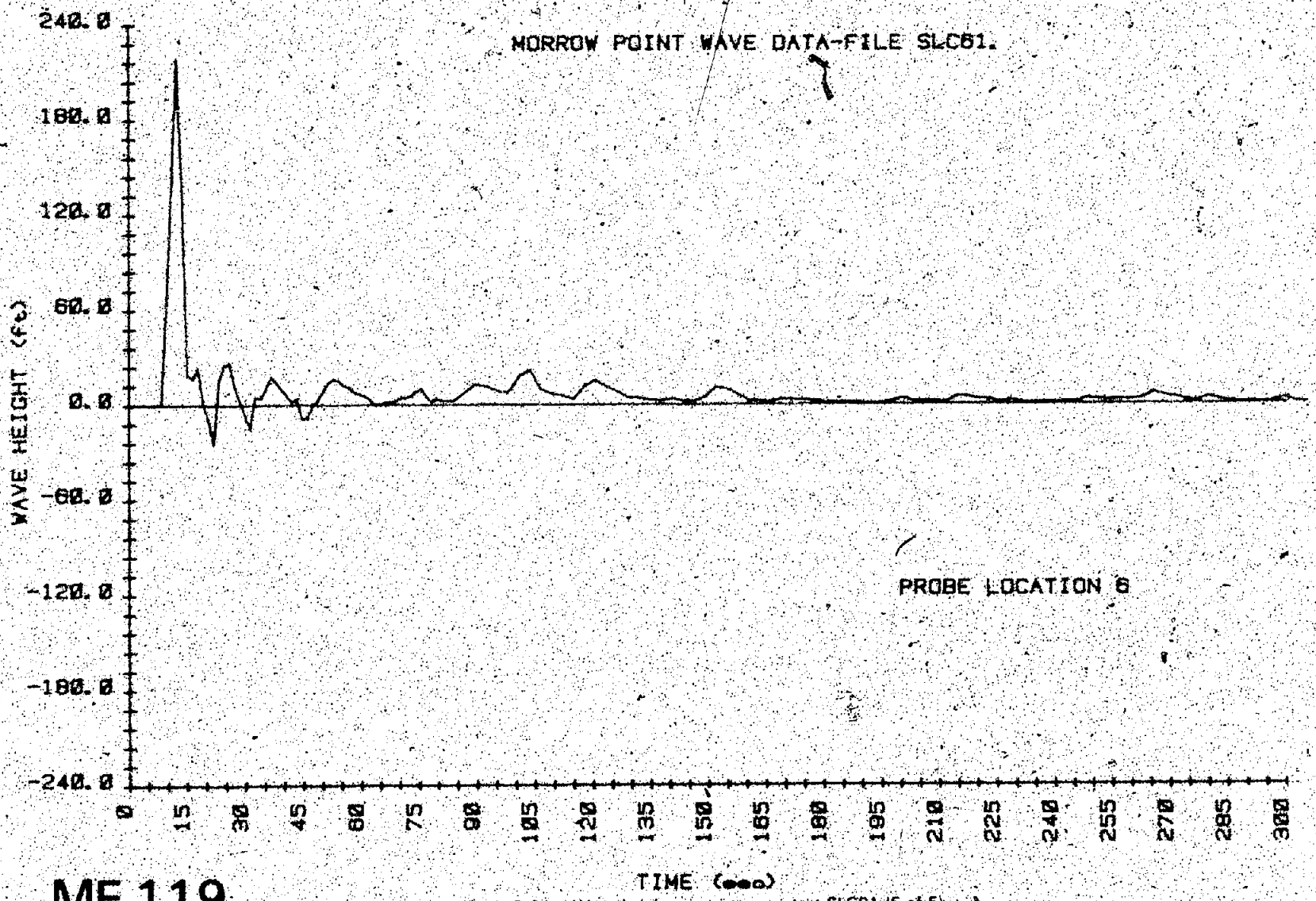

MF 119

Figure B-24. – Wave height versus time – test SLC61 (5 of 5).

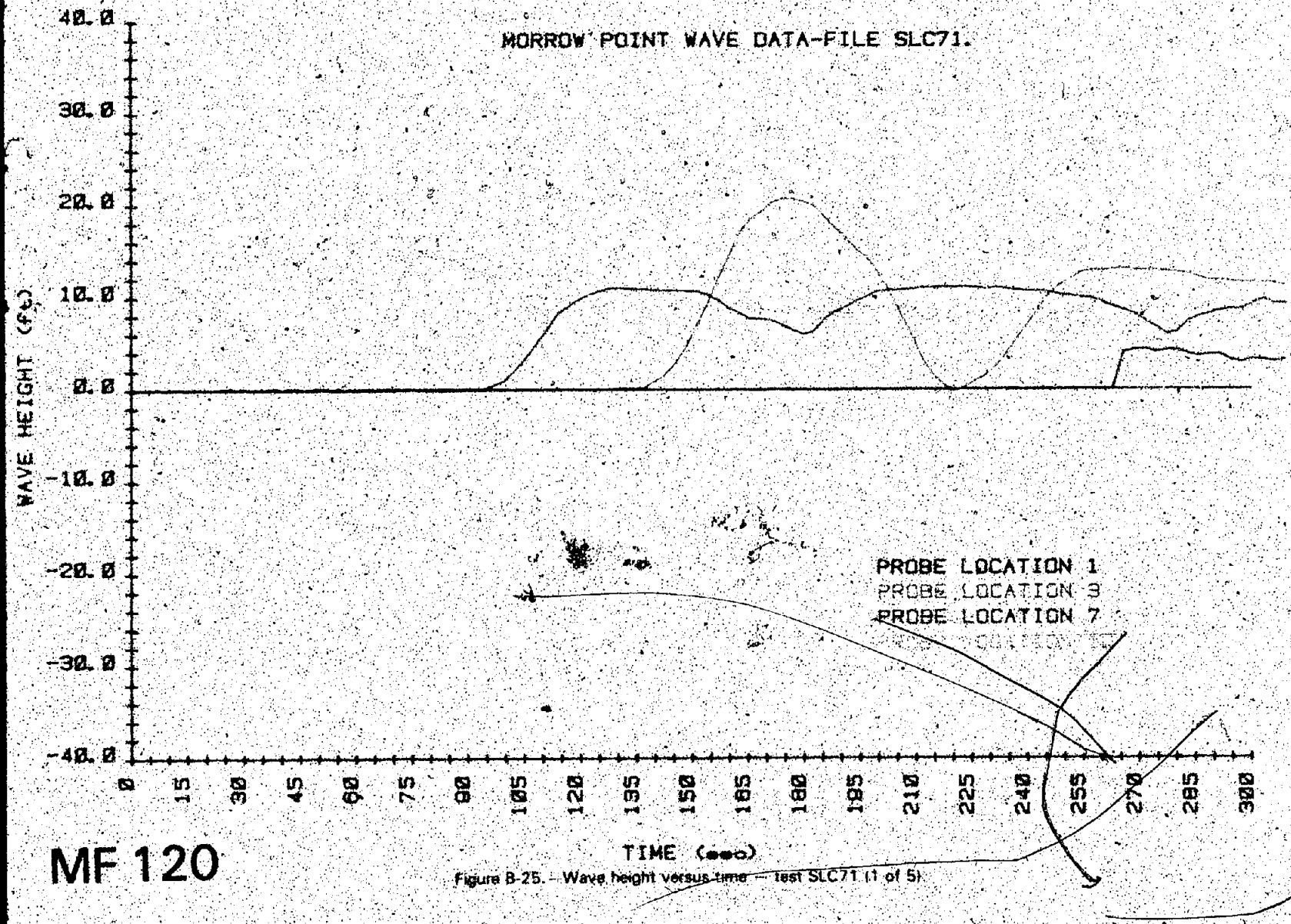

MF 120

Figure B-25.– Wave height versus time — test SLC71 (1 of 5)

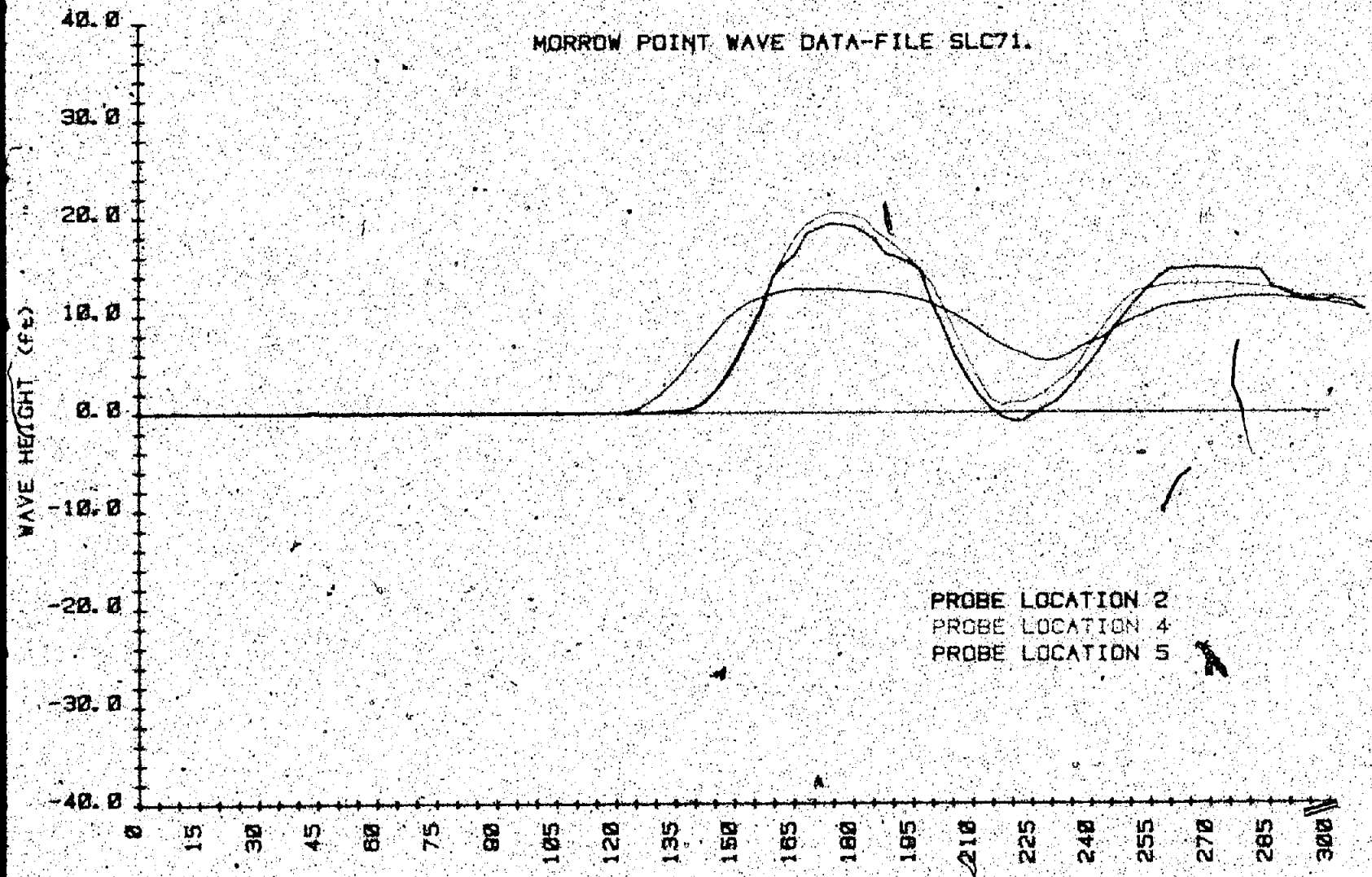

MF 121

Figure B-25. –Wave height versus time – test SLC71 (2 of 5).

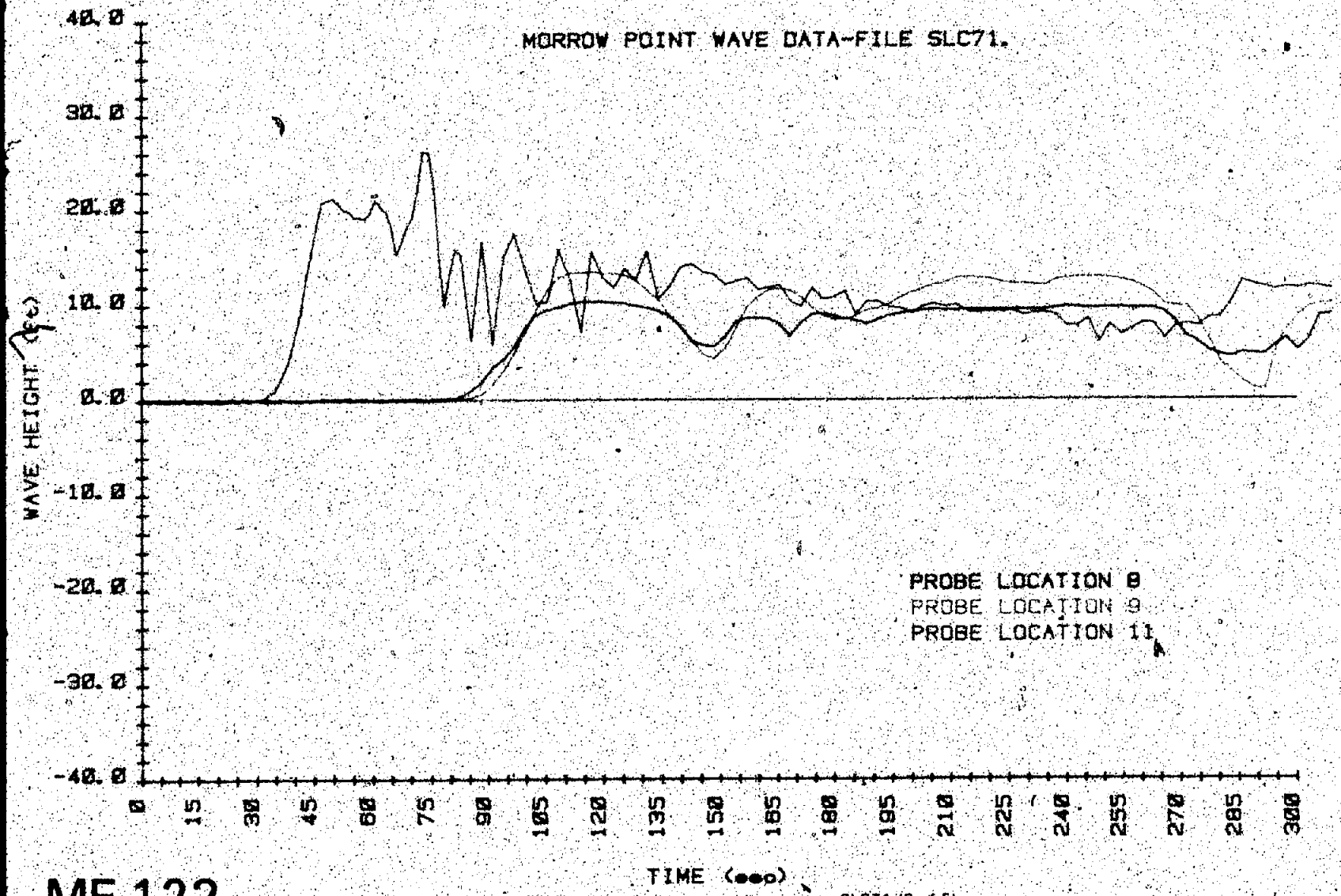

MF 122

Figure B.25. - Wave height versus time - test SLC71 (3 of 5).

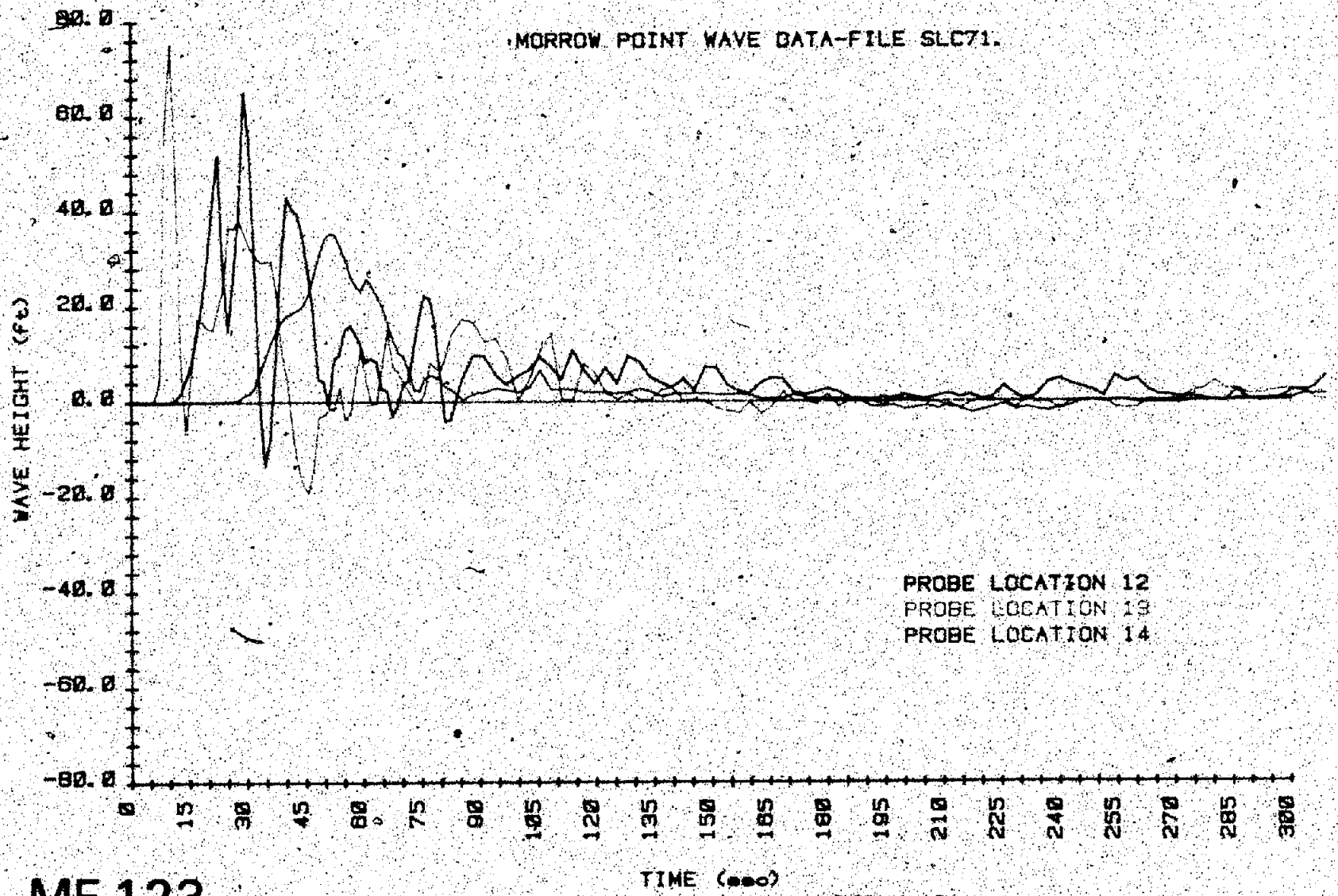

MF 123

Figure B-25. – Wave height versus time – test SLC71 (4 of 5).

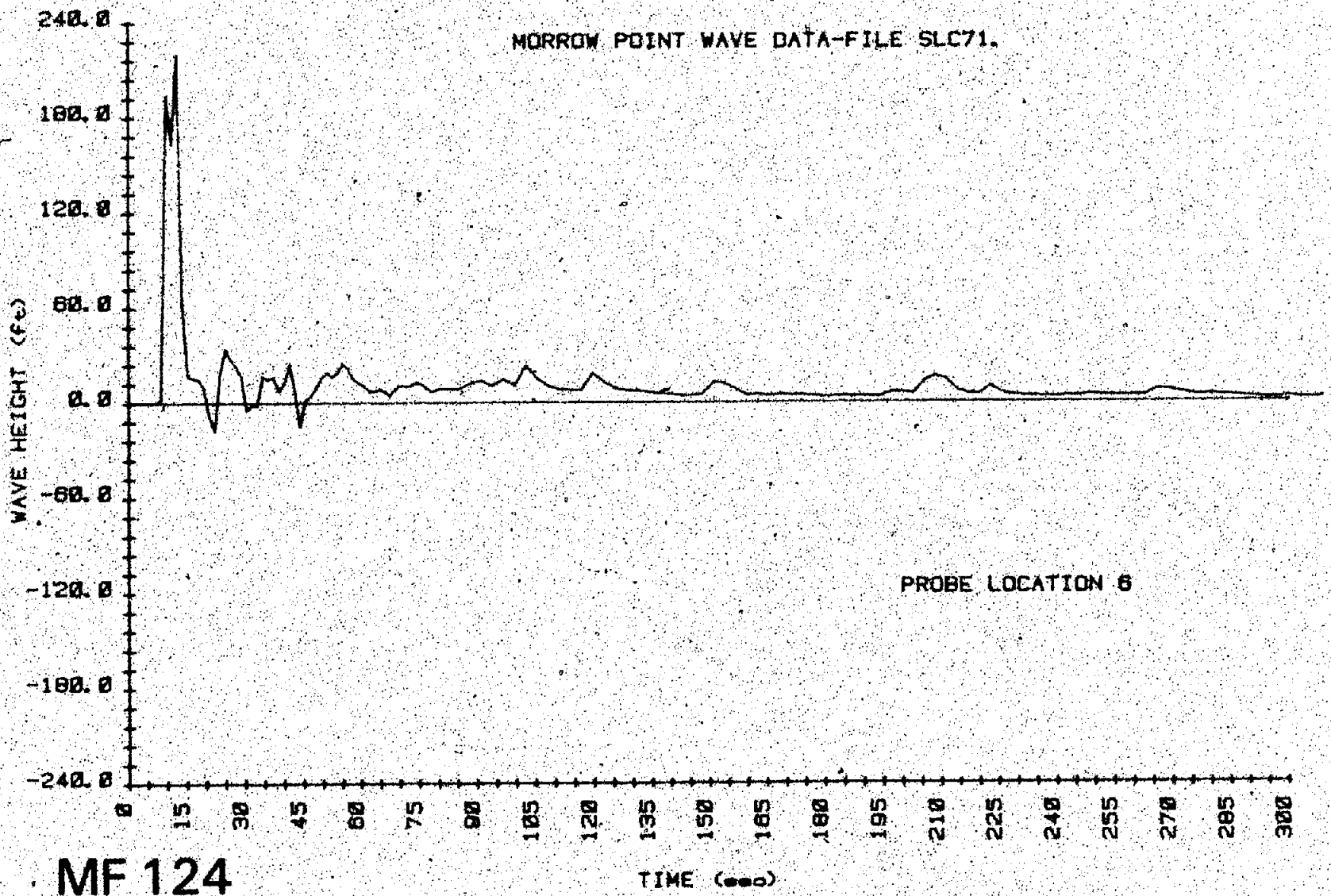

MF 124

Figure B-25. – Wave height versus time — test SLC71 (5 of 5).

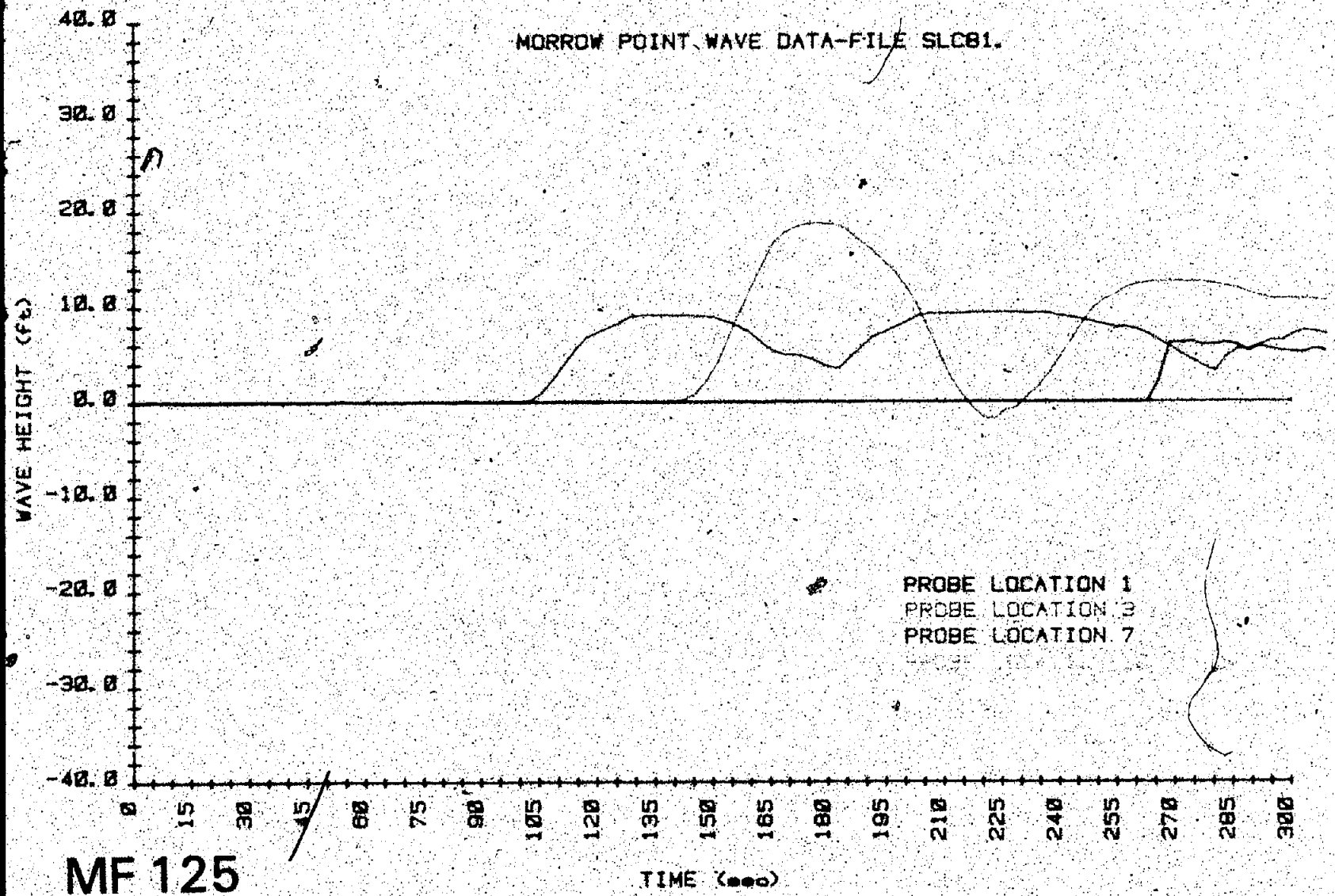

MF 125

Figure B-26. – Wave height versus time – test SLC81 (1 of 5)

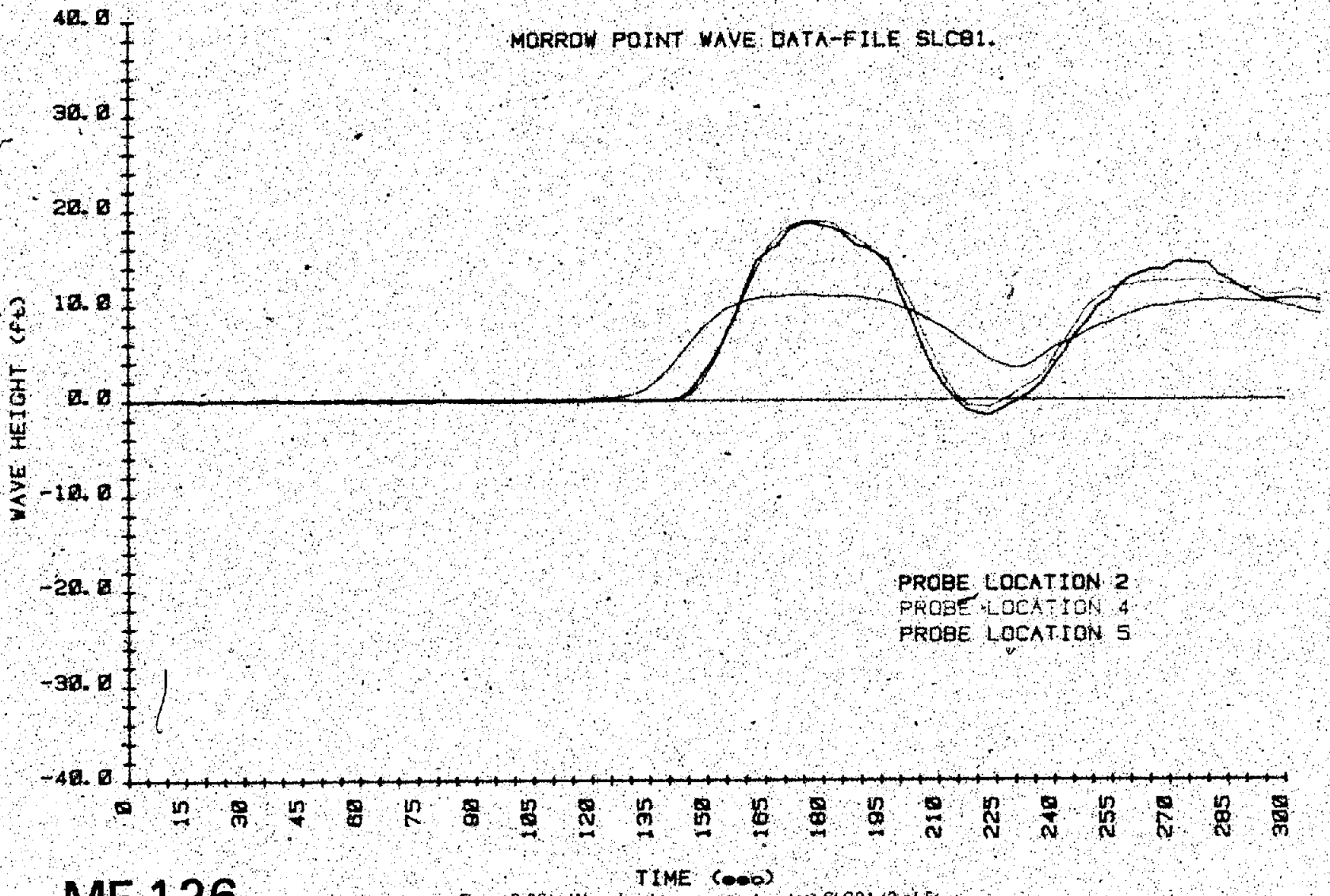

MF 126

Figure B-26. - Waveheight versus time - test SLC81 (2 of 5).

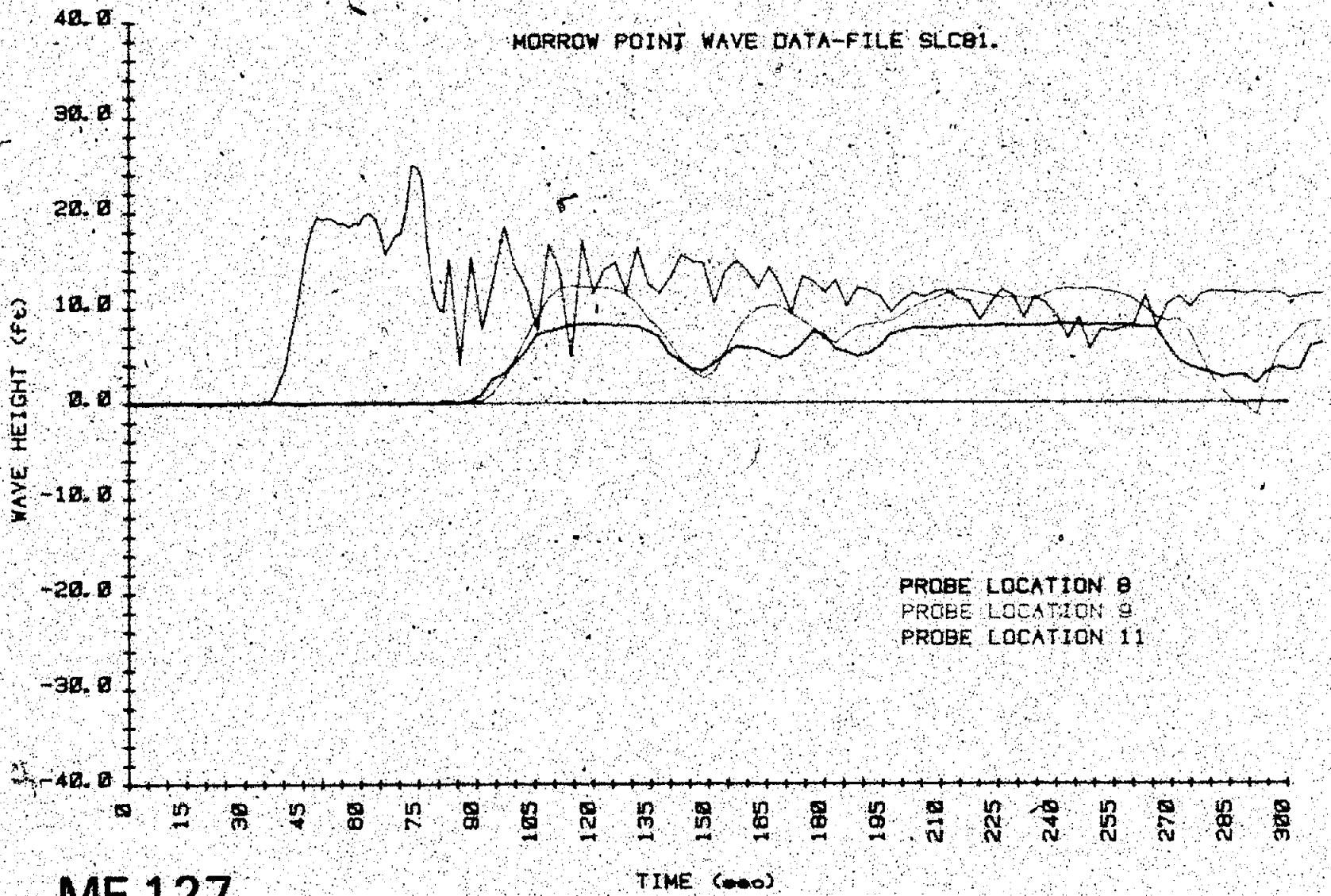

MF 127

Figure B-26. Wave height versus time — test SLC81 (3 of 5).

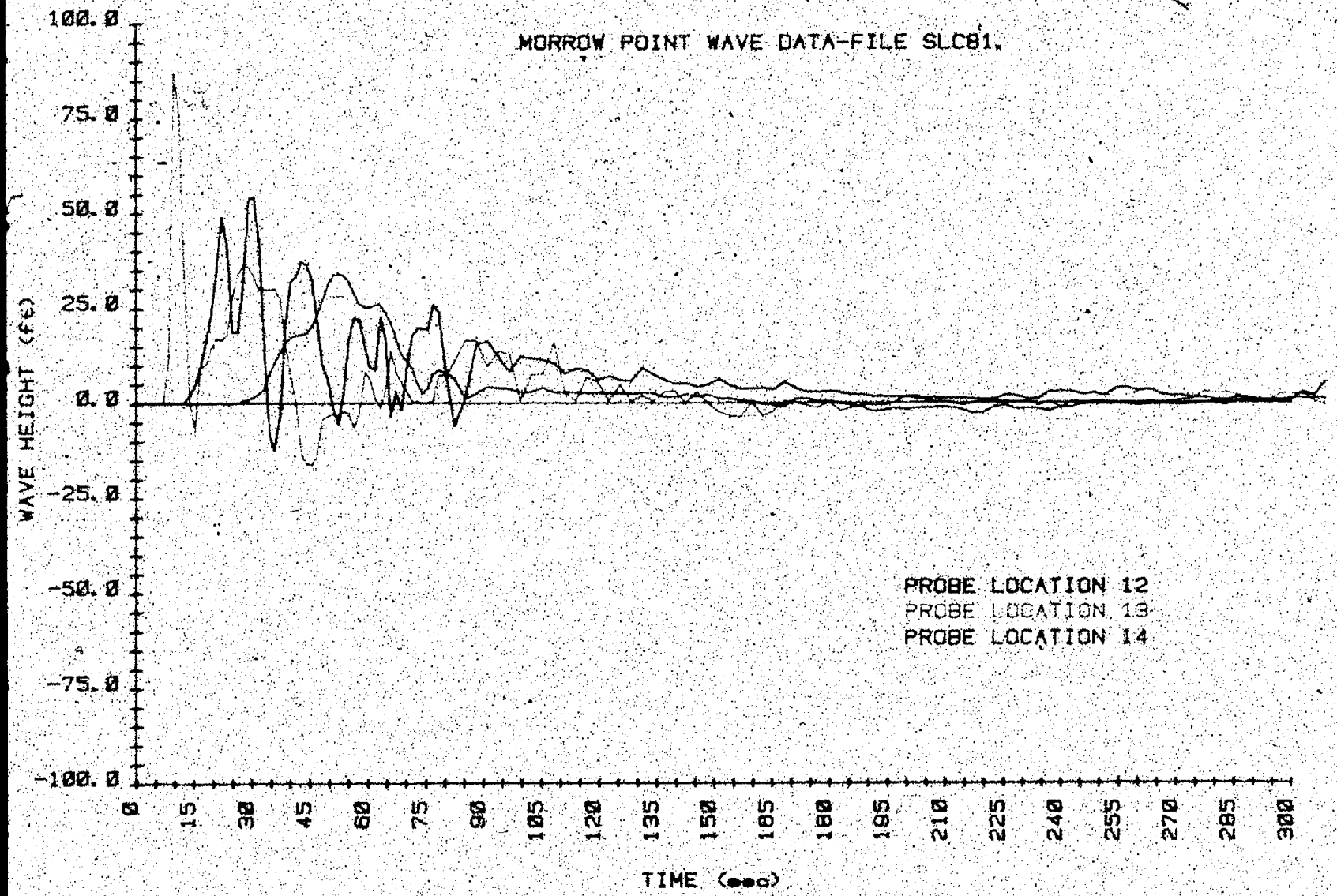

MF 128

Figure B-26.—Wave height versus time — test SLC81 (4 of 5).

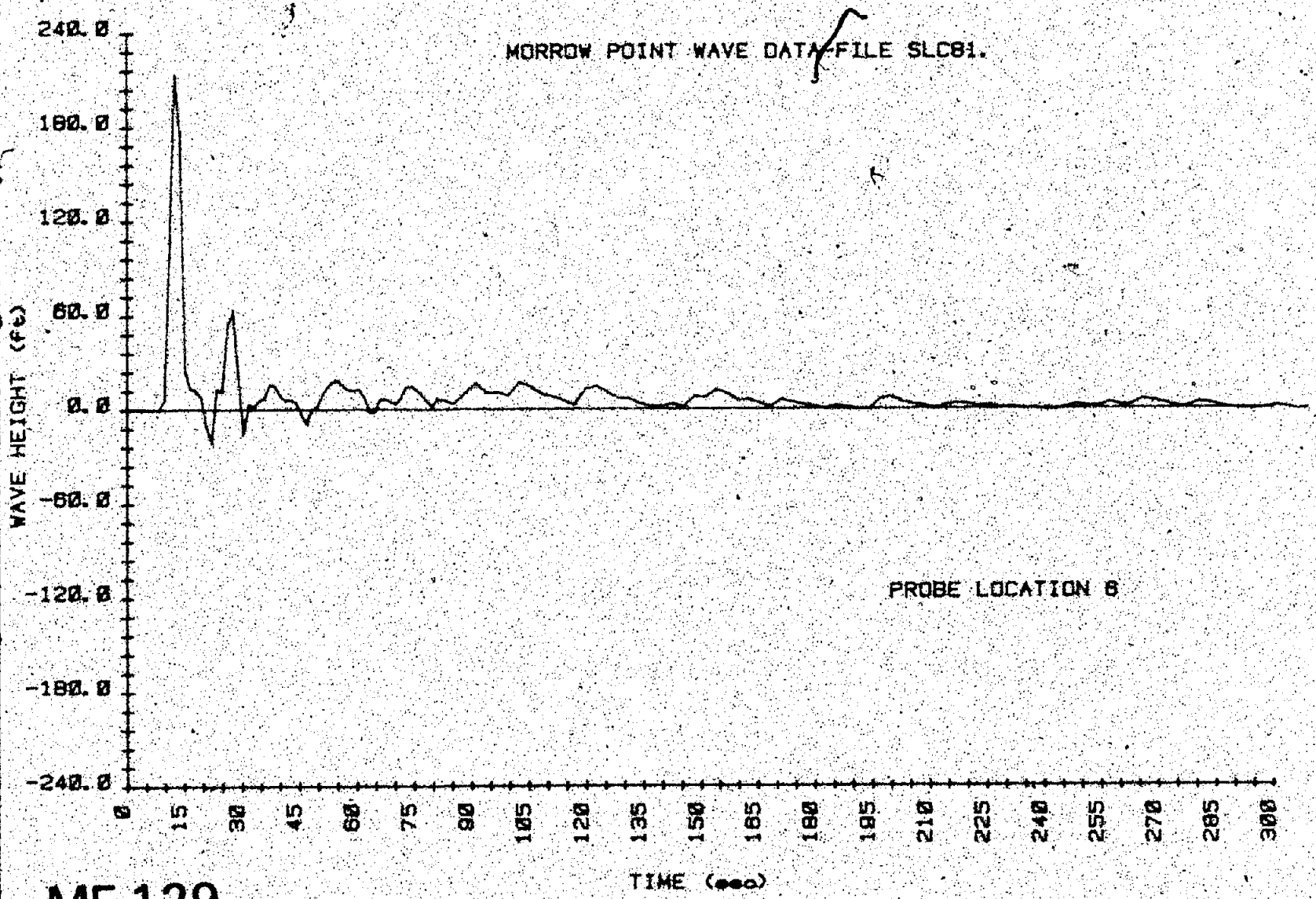

MF 129

Figure B-26. - Wave height versus time. — test SLC81 (5 of 5).

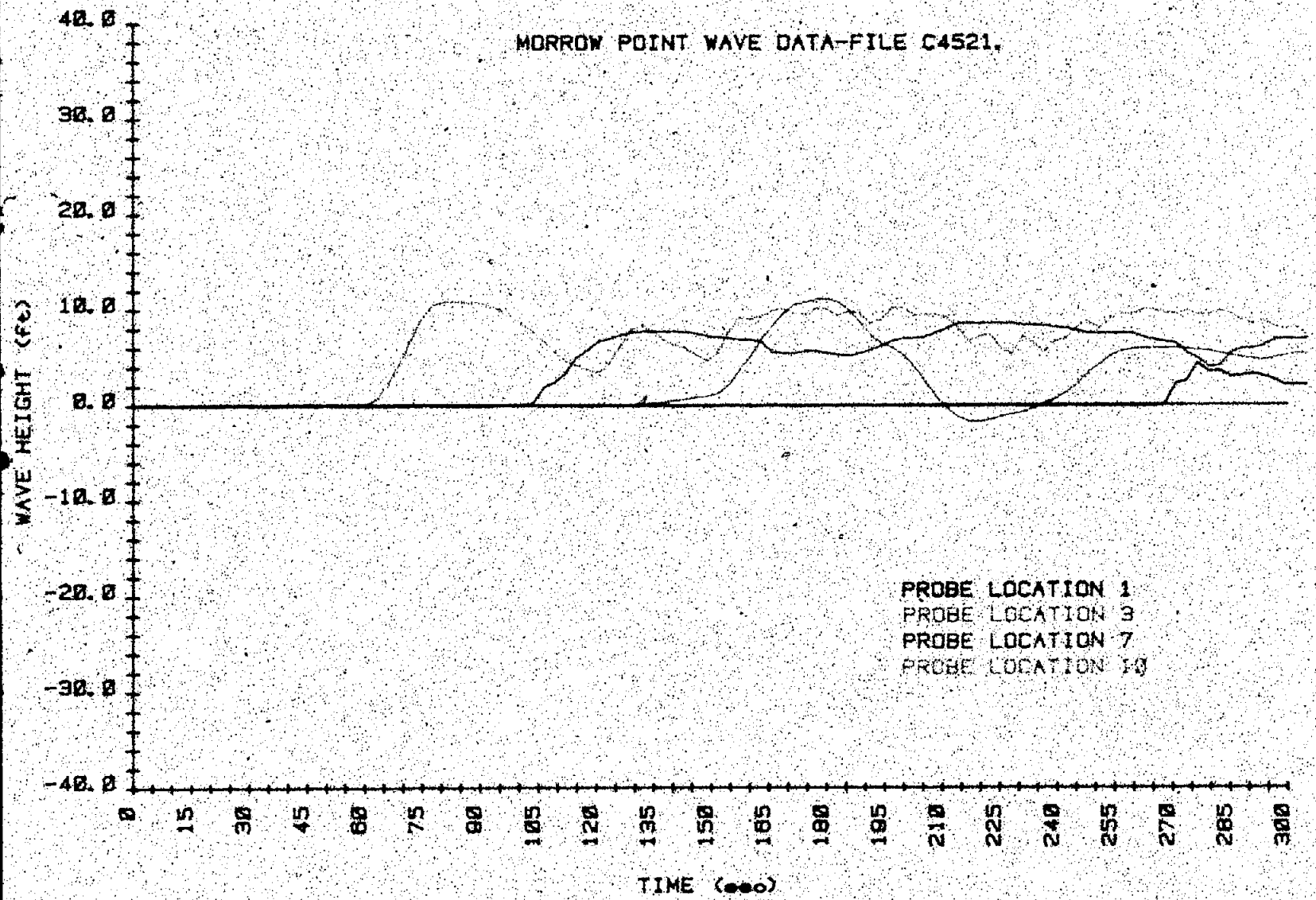

MF 130

Figure B-27. – Wave height versus time – test C4521 (1 of 4).

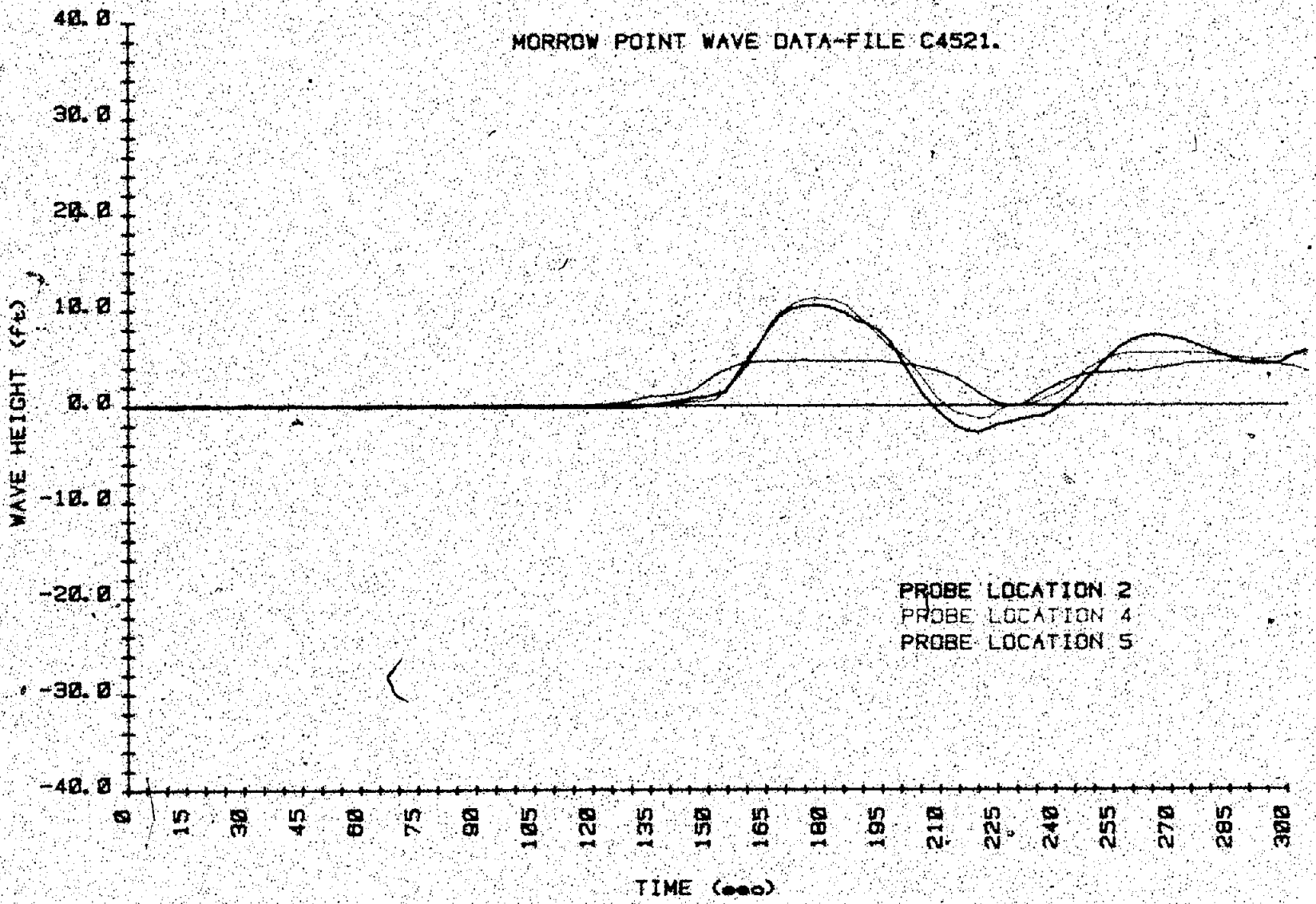

MF 131

Figure B-27.--Wave height versus time -- test C4521 (2 of 4).

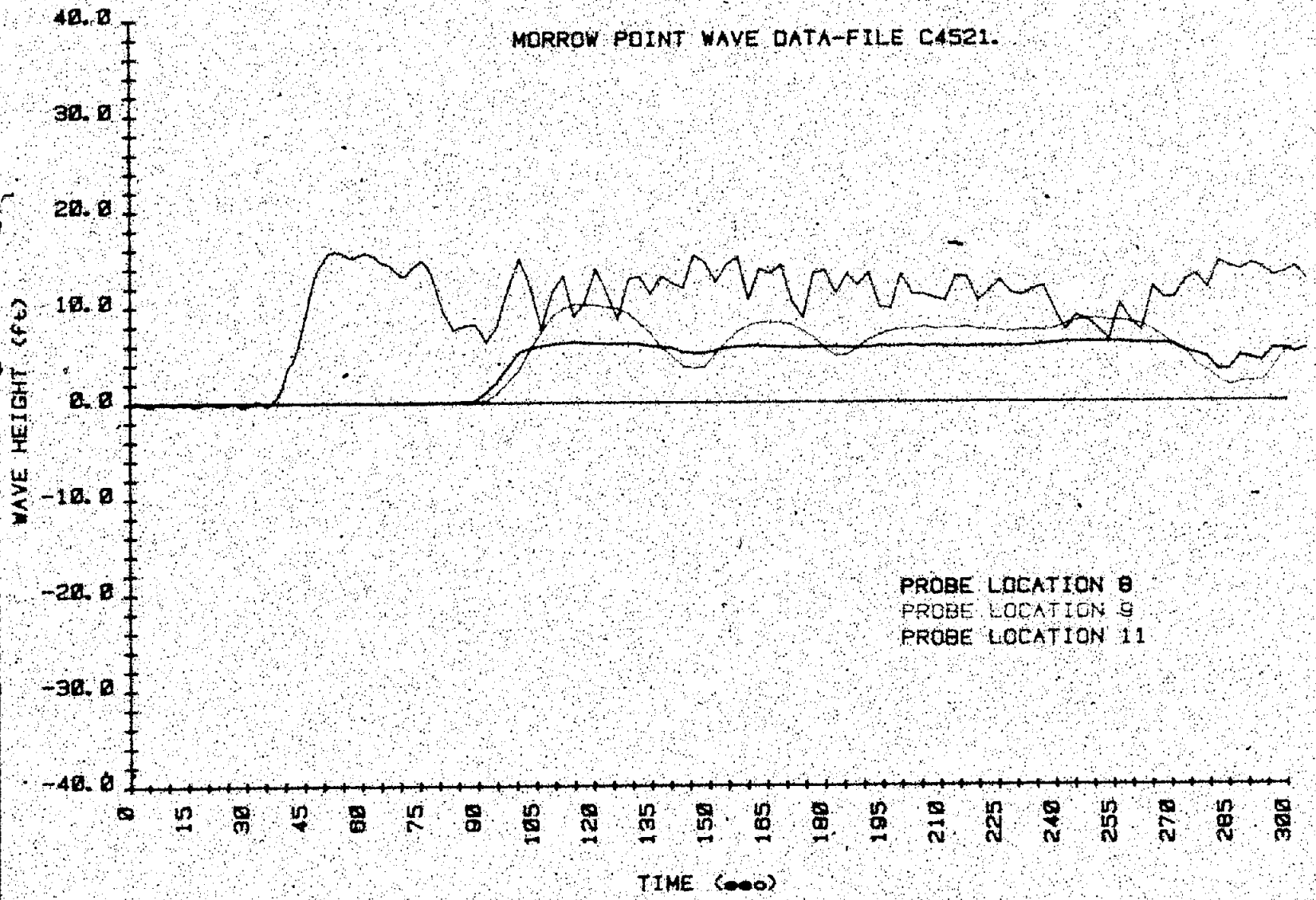

MF 132

Figure B-27. - Wave height versus time - test C4521 (3 of 4).

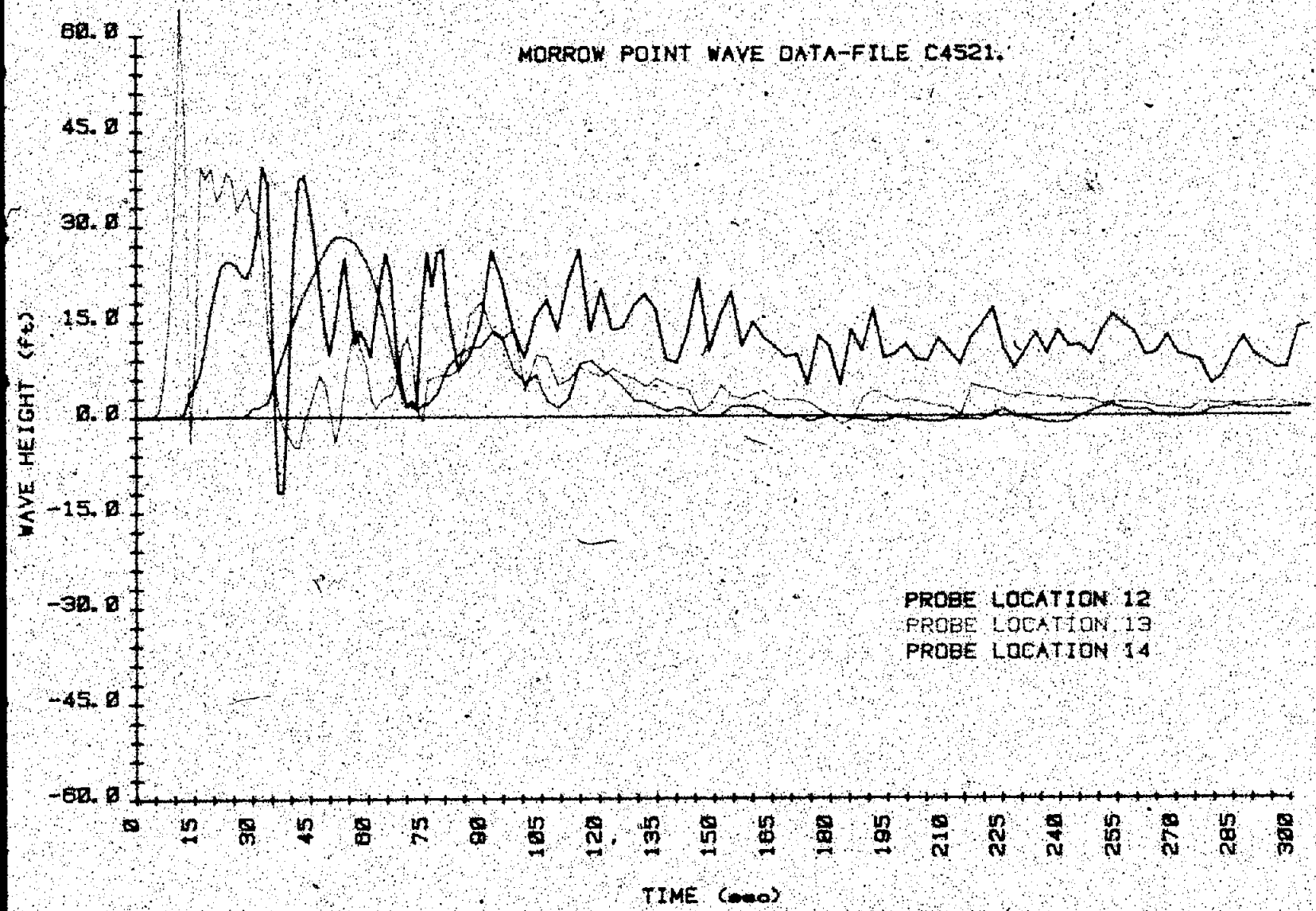

MF 133

Figure B-27. – Wave height versus time – test C4521 (4 of 4).

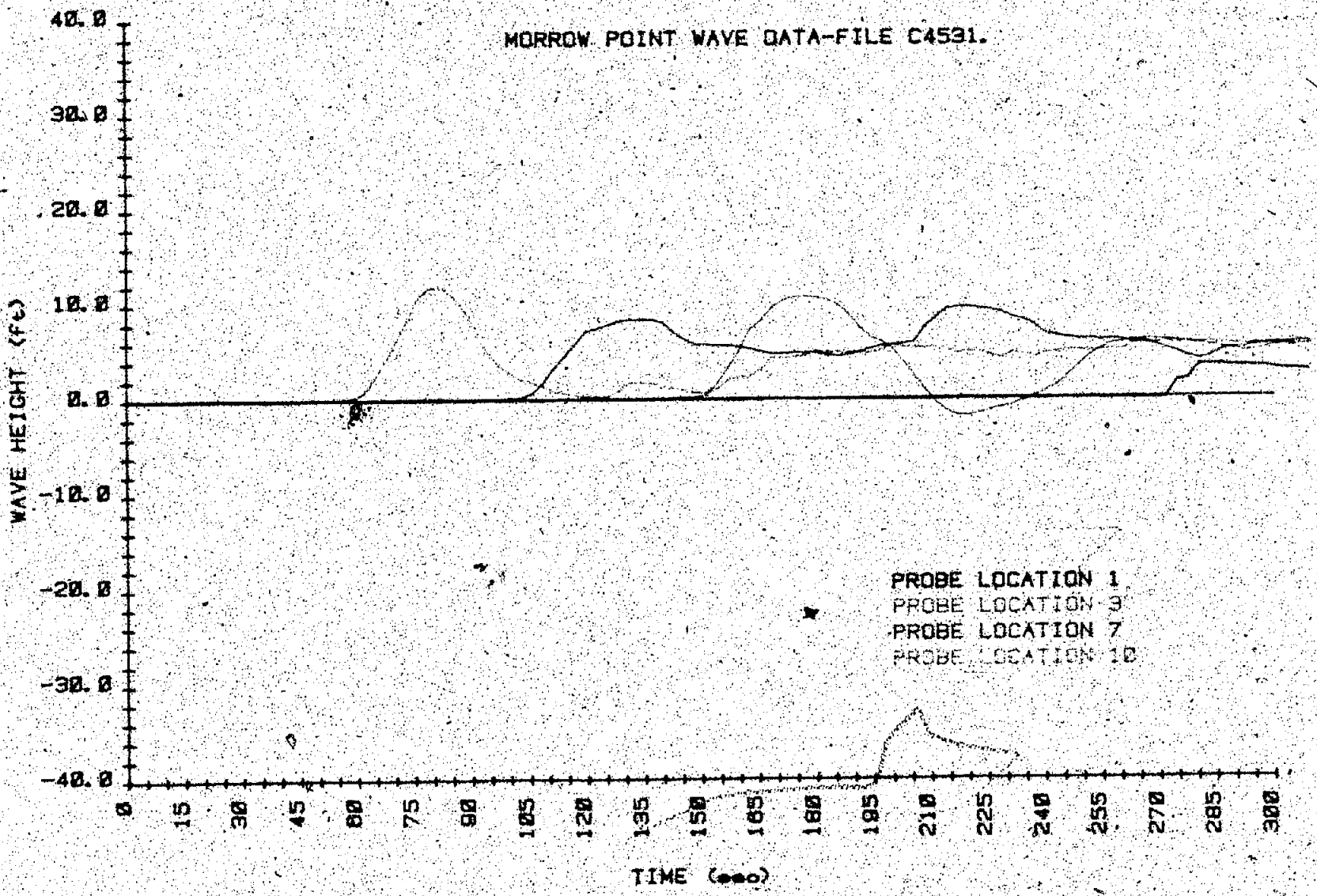

MF 134

Figure B-28. – Wave height versus time — test C4531 (1 of 4).

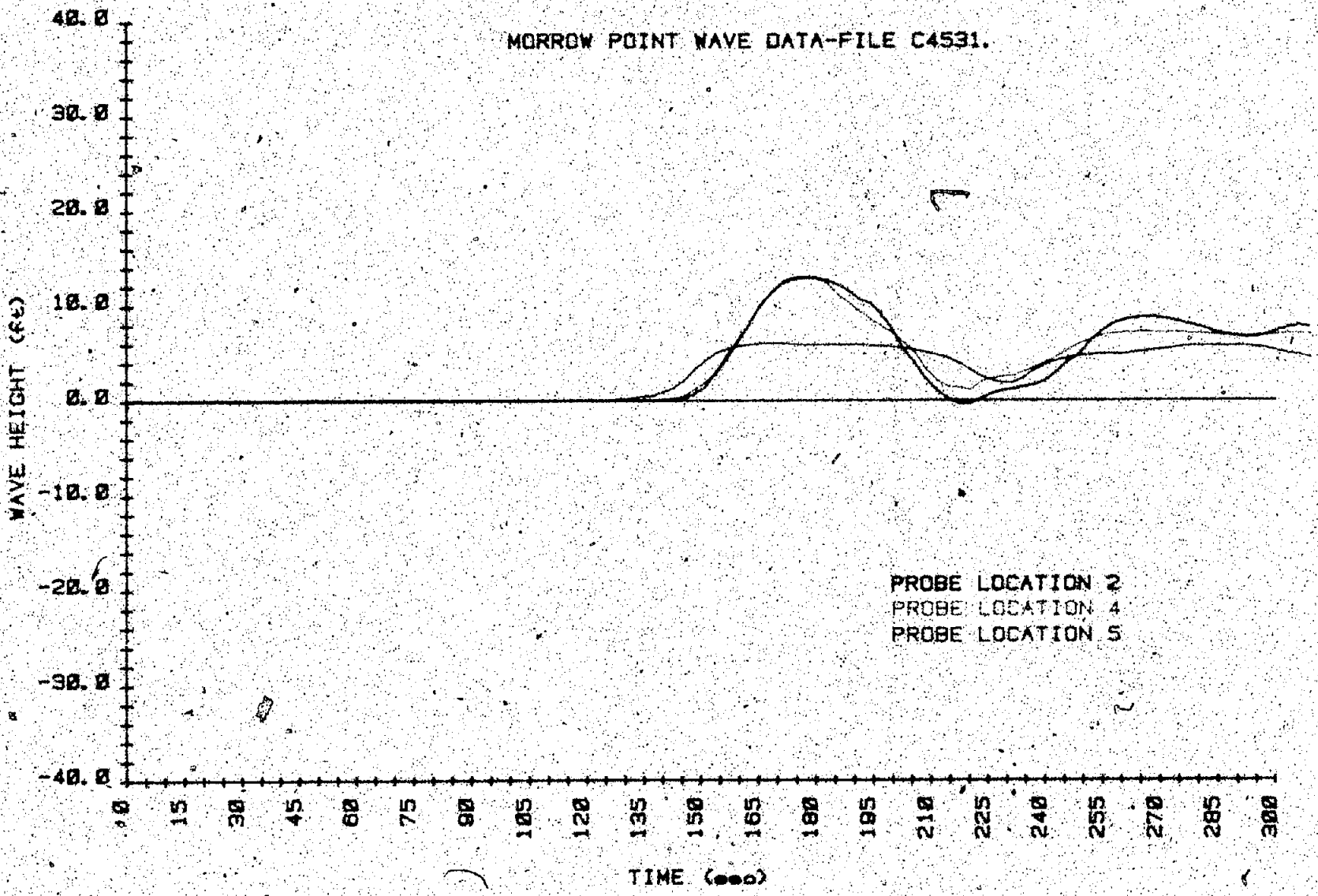

MF 135

Figure B-28. – Wave height versus time – test C4531 (2 of 4)

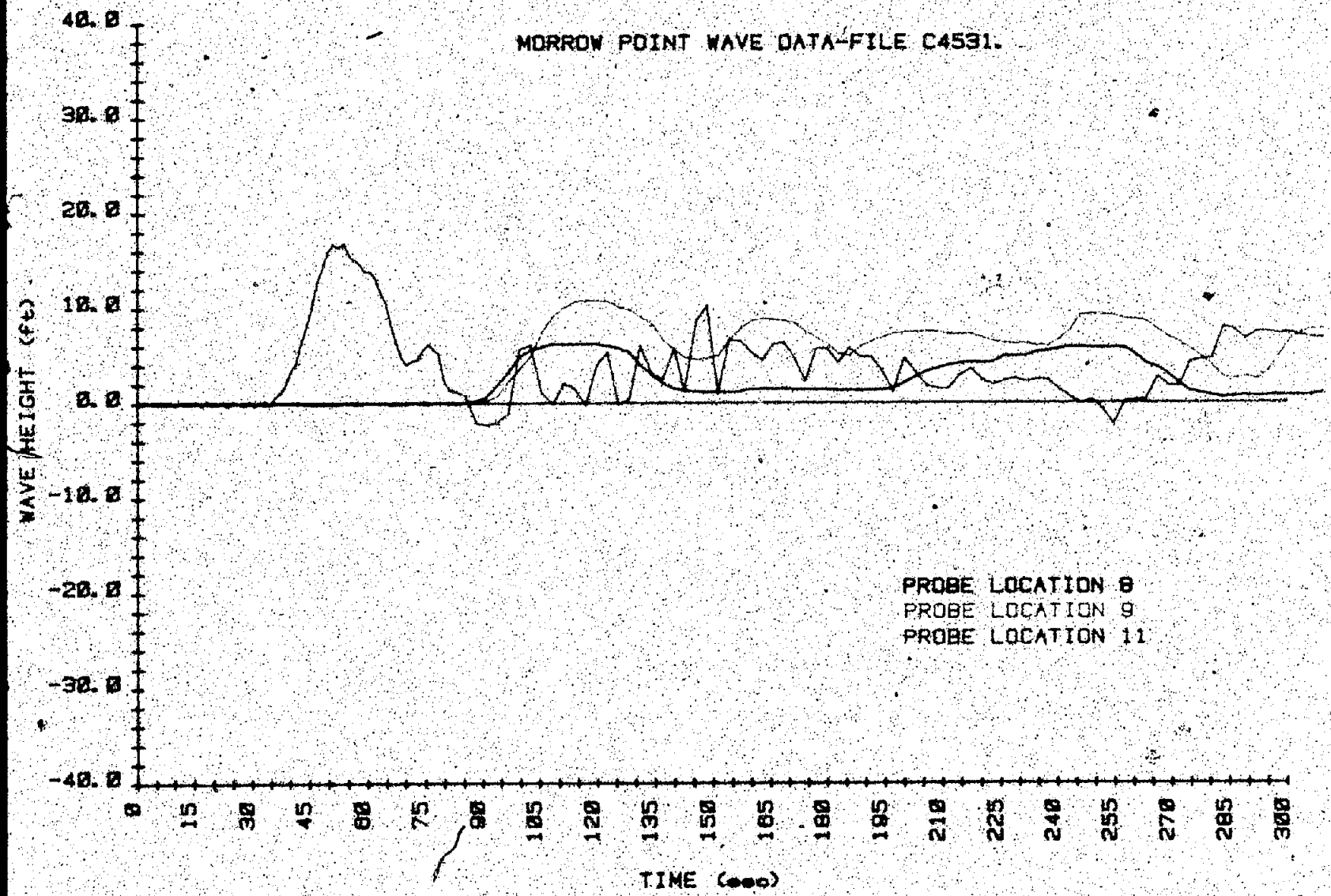

MF 136

Figure B-28. Wave height versus time — test C4531 (3 of 4)

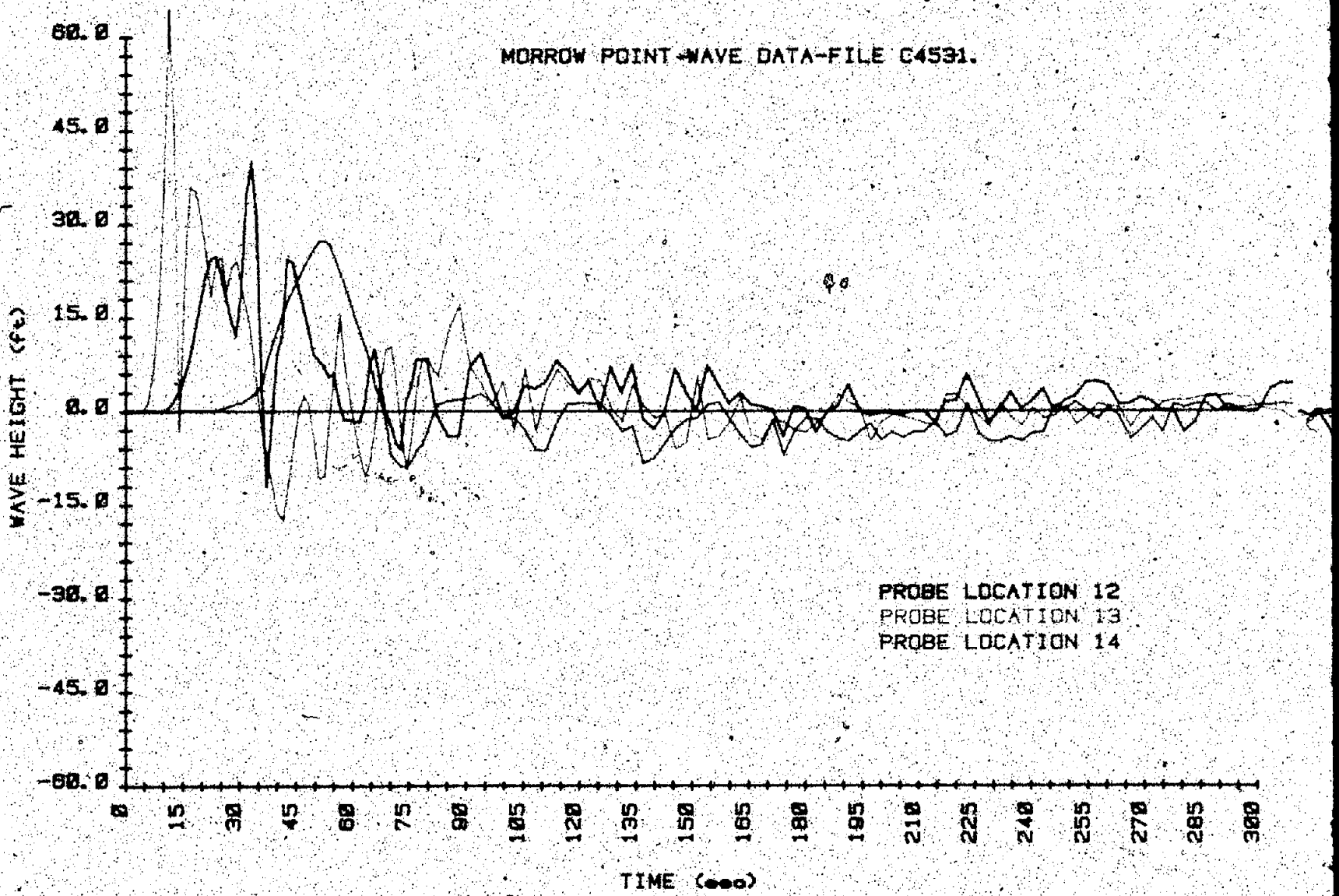

MF 137

Figure 8-28.—Wave height versus time — test C4531 (4 of 4).

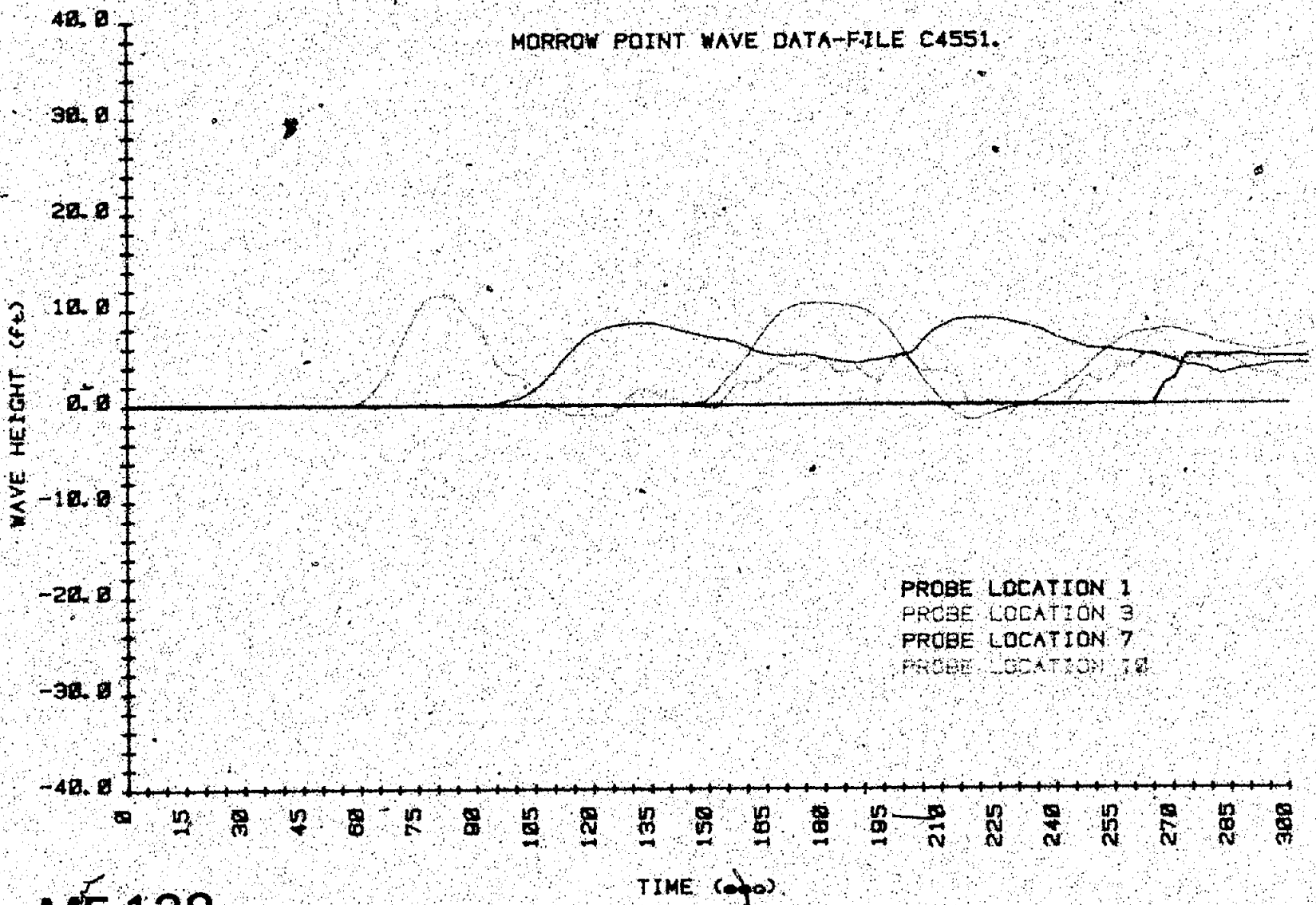

MF 138

Figure B-29. – Wave height versus time – test C4551 (1 of 5).

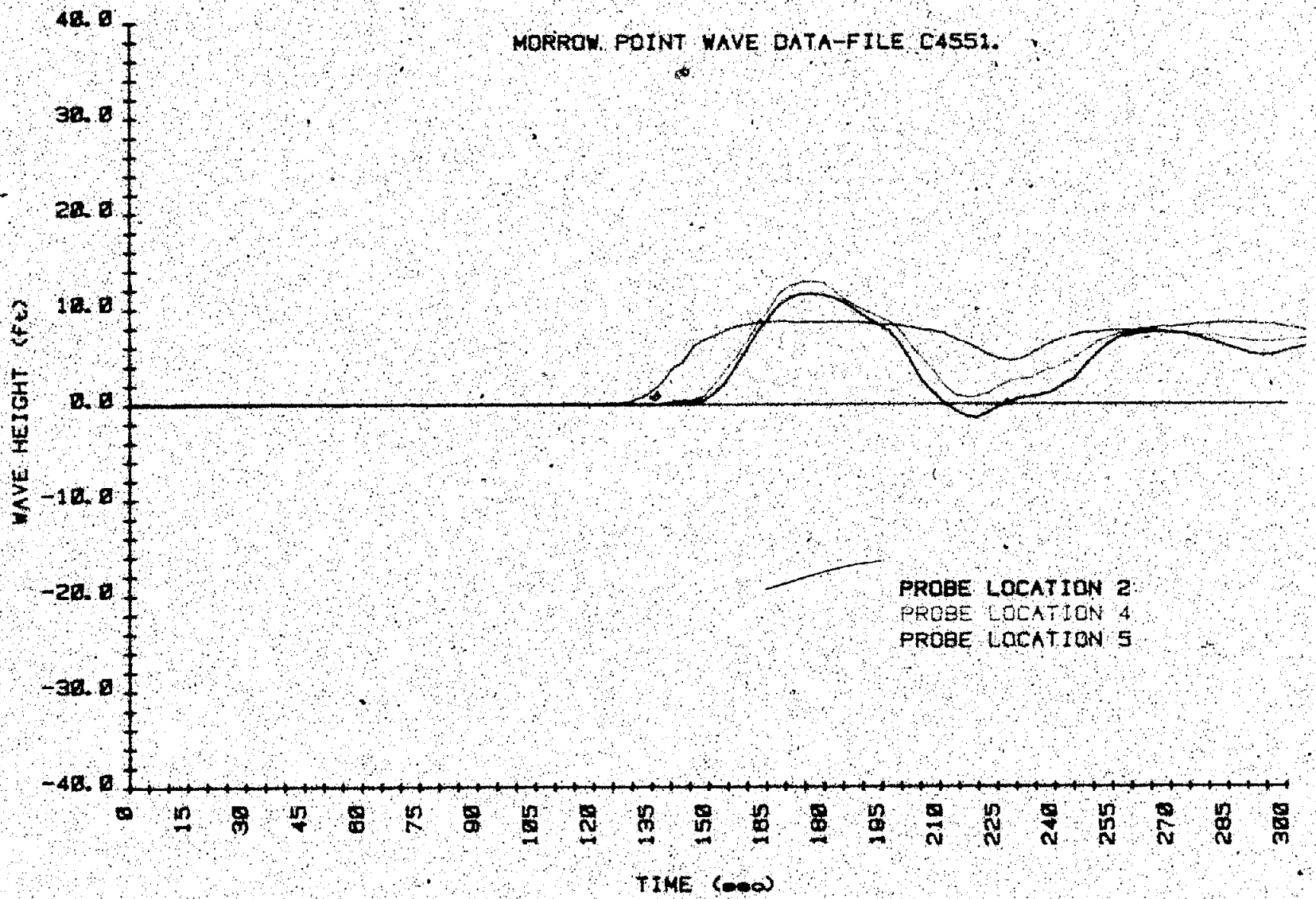

MF 139

Figure B-29.—Wave height versus time — test C4551 (2 of 5).

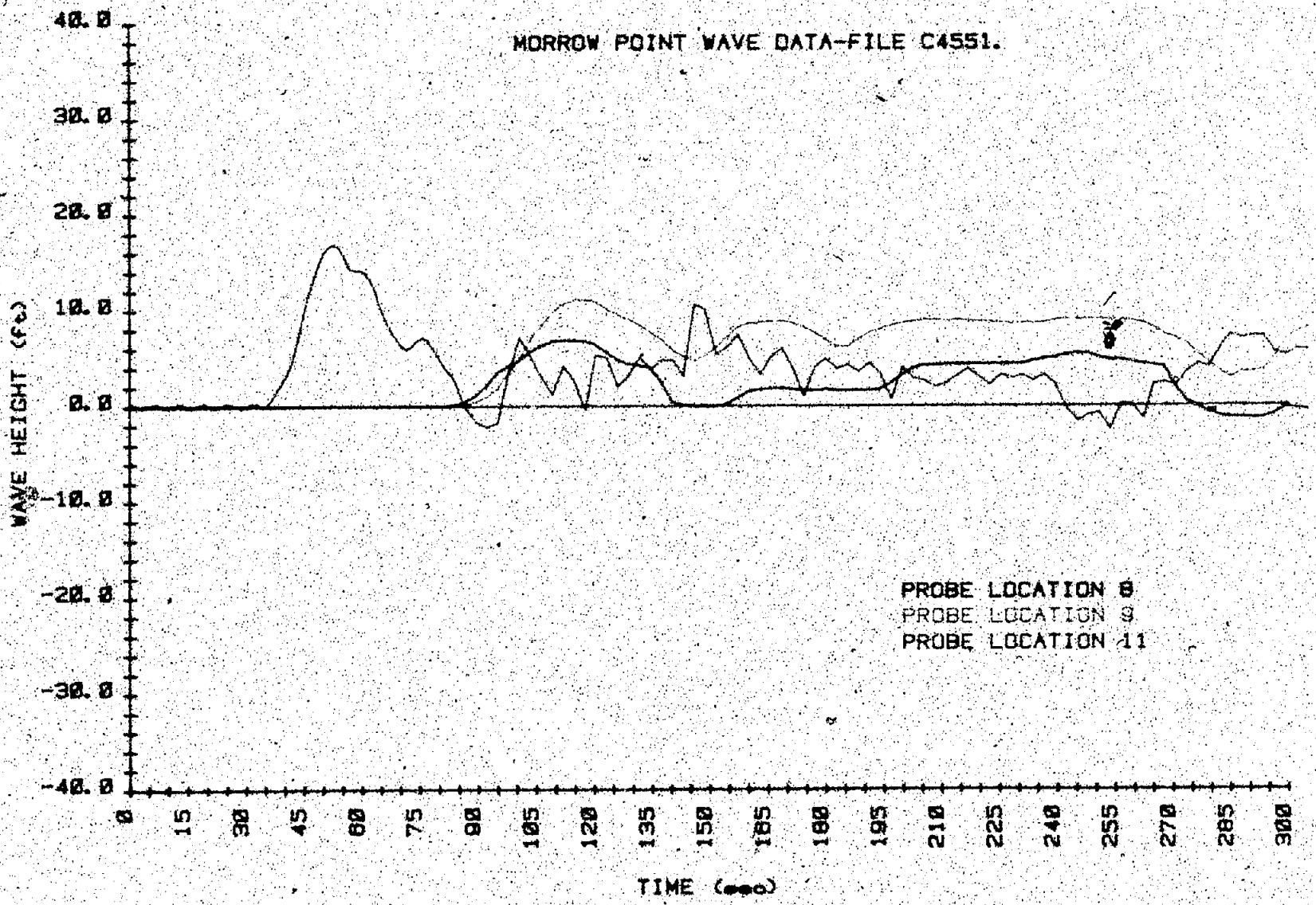

MF 140

Figure B-29. – Wave height versus time – test C4551 (3 of 5)

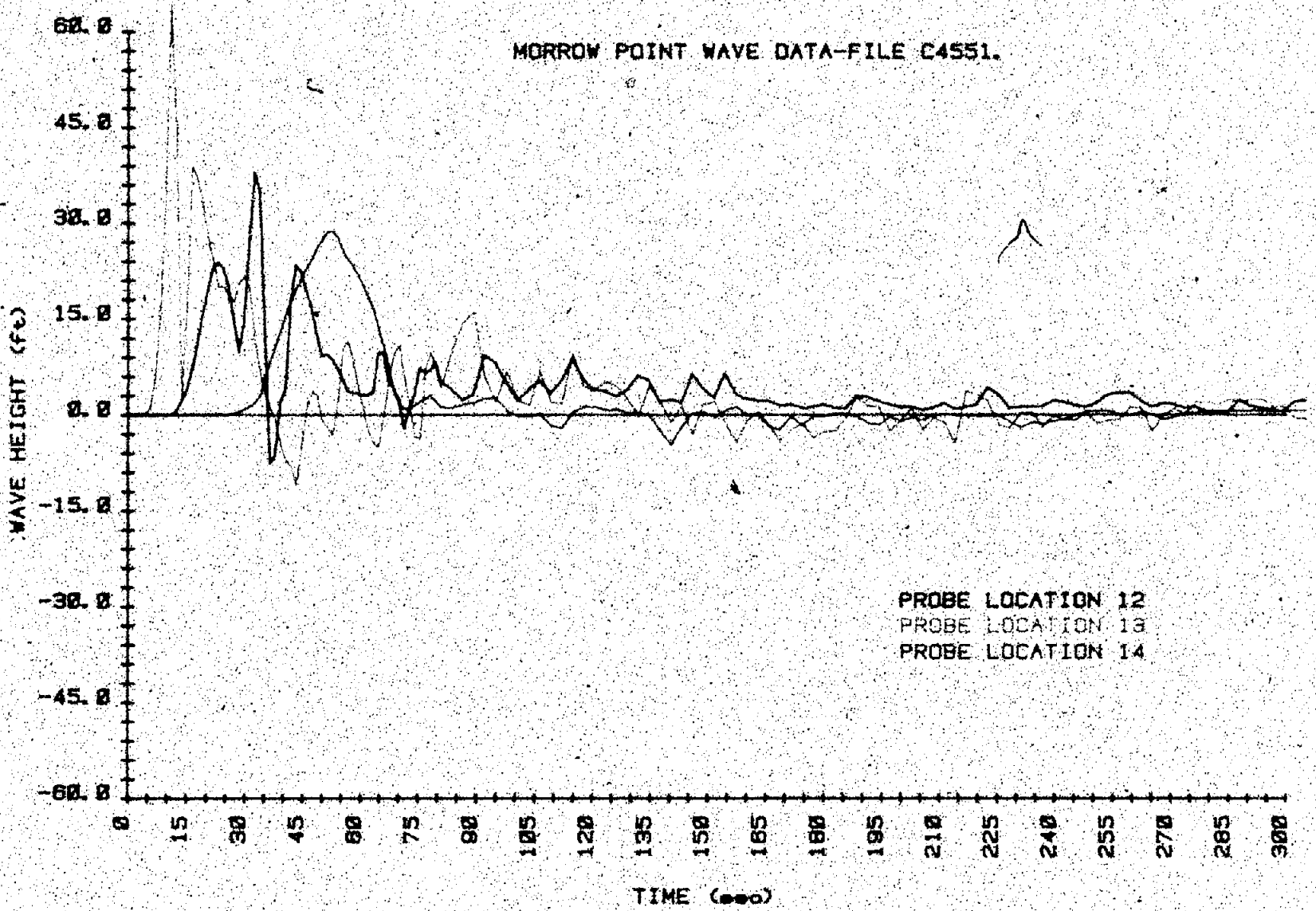

MF 141

Figure B-29.—Wave height versus time — test C4551 (4 of 5).

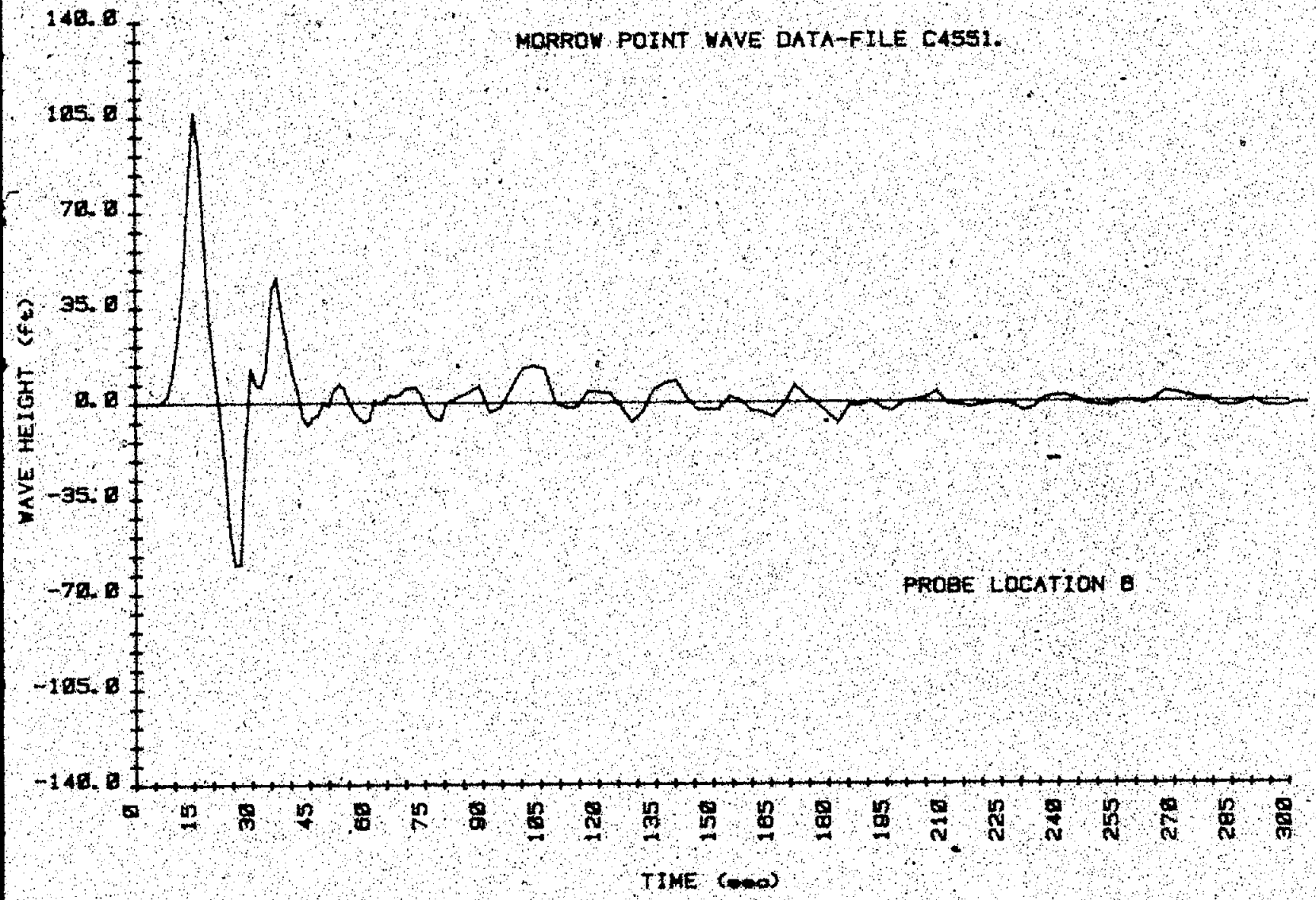

MF 142

Figure 8-29. – Wave height versus time — test C4551 (5 of 5).

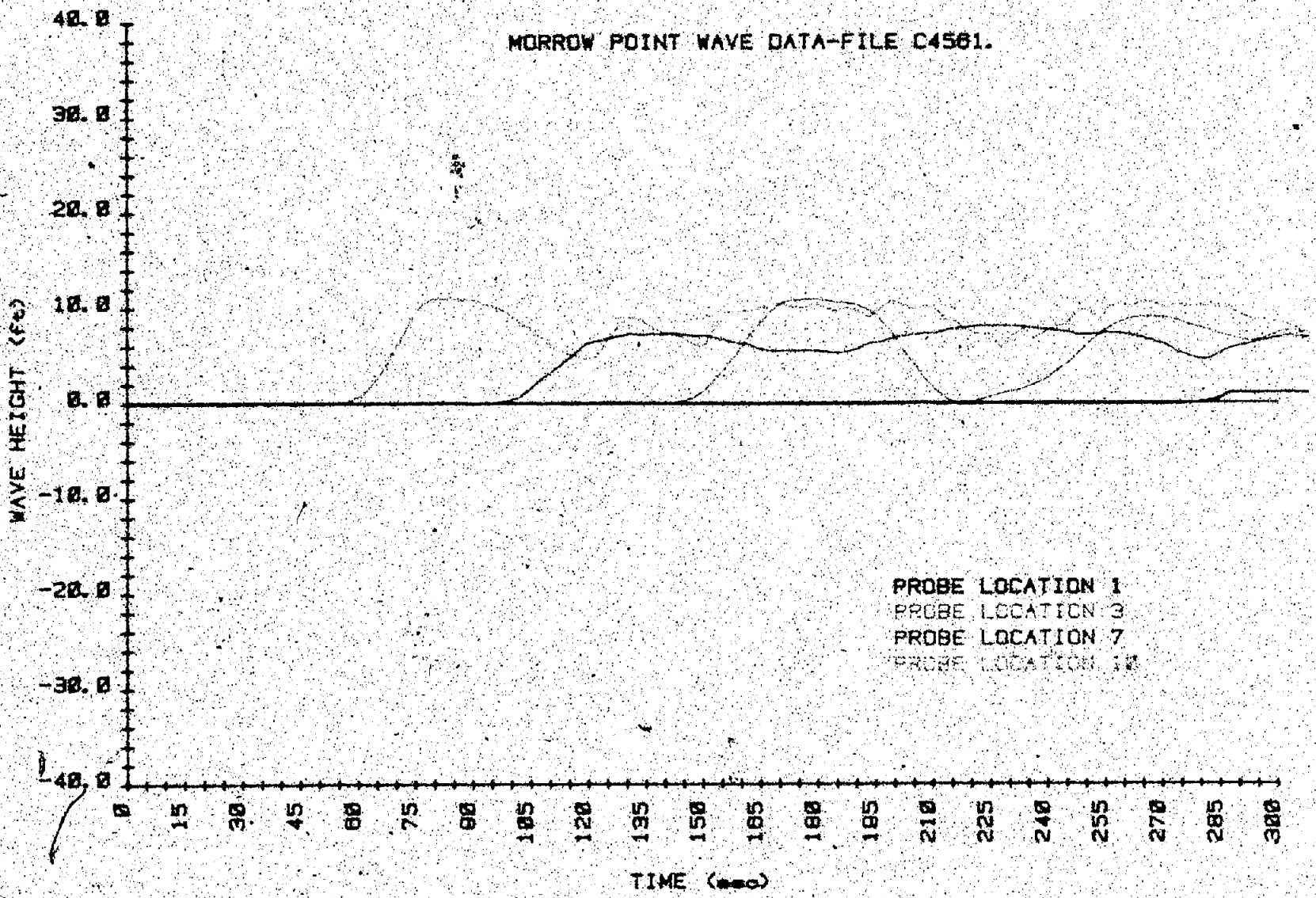

MF 143

Figure B-30. (Wave height versus time — test C4561 (1 of 5)

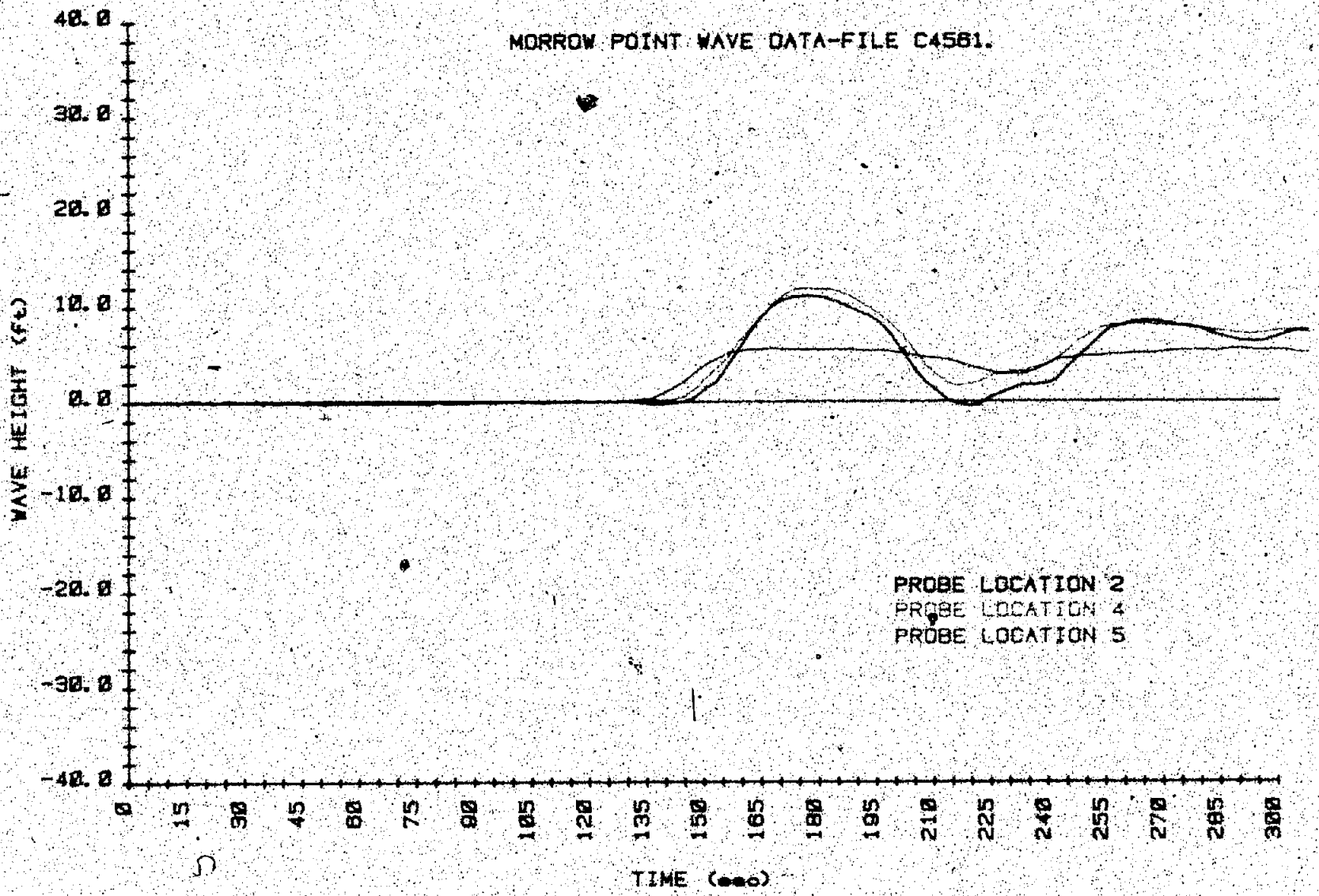

MF 144

Figure B-30. Wave height versus time – test C4561 (2 of 6)

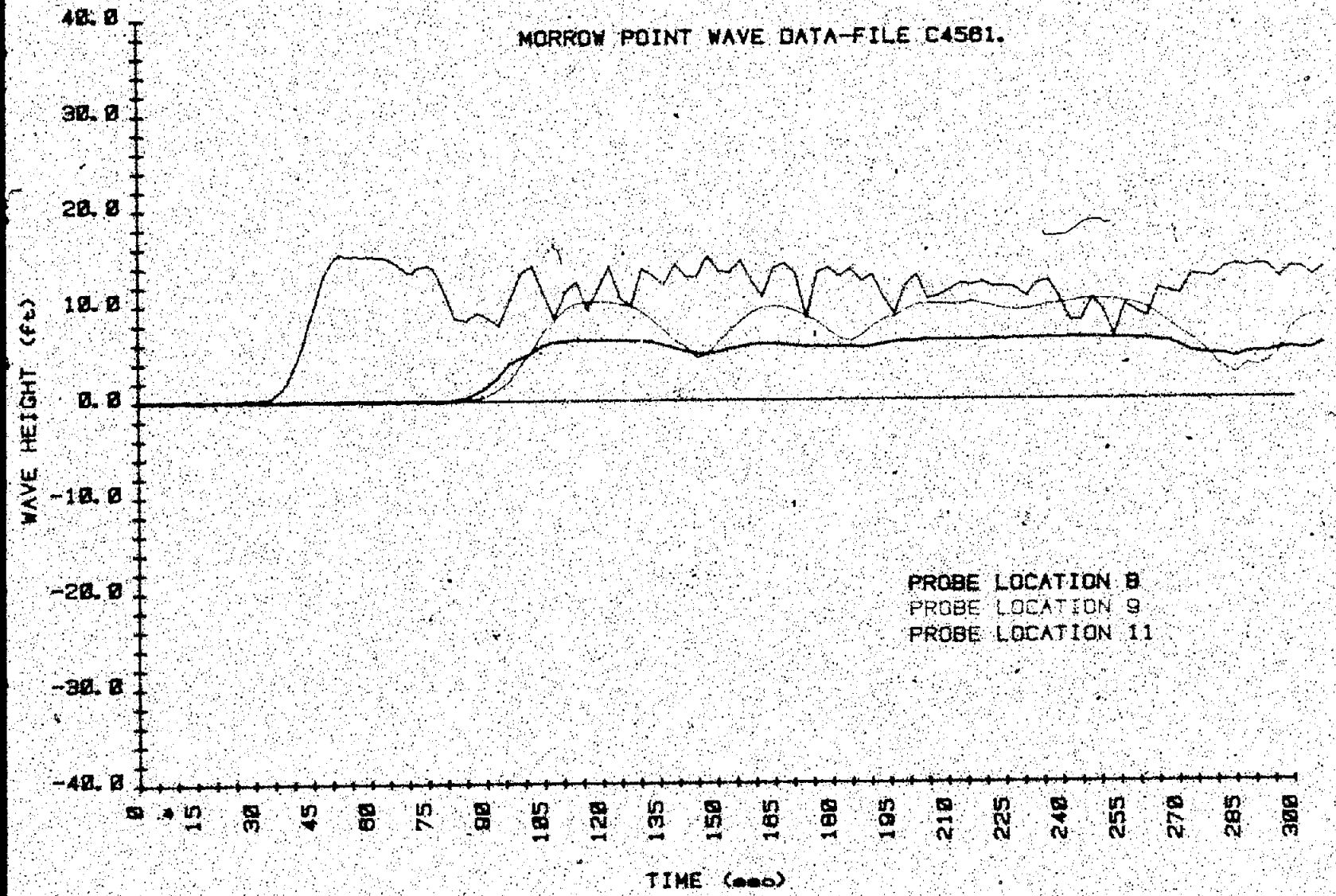

MF 145

Figure B-30. – Wave height versus time – test C4561 (3 of 5).

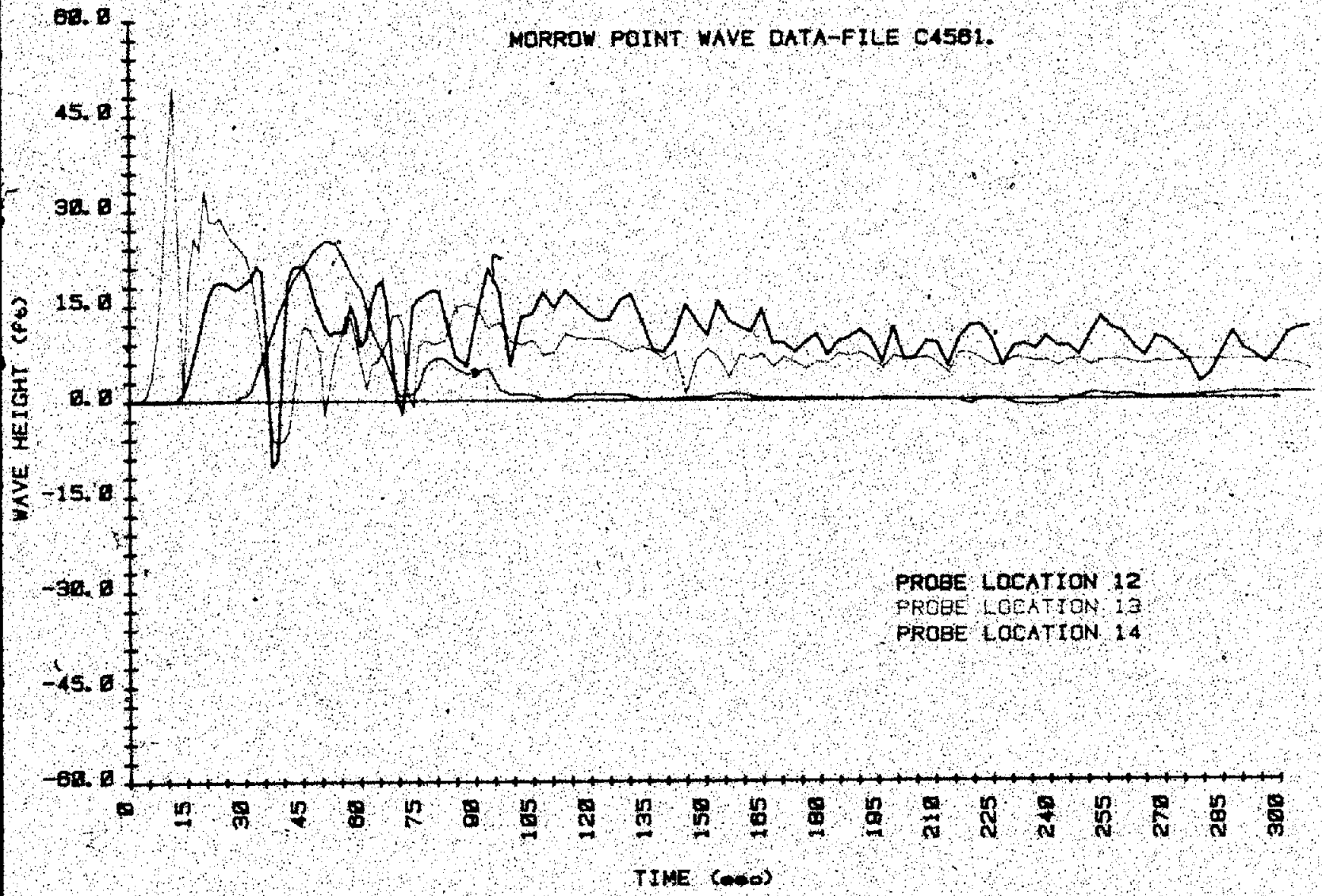

MF 146

Figure 8-30.—Wave height versus time — test C4561 (4 of 5).

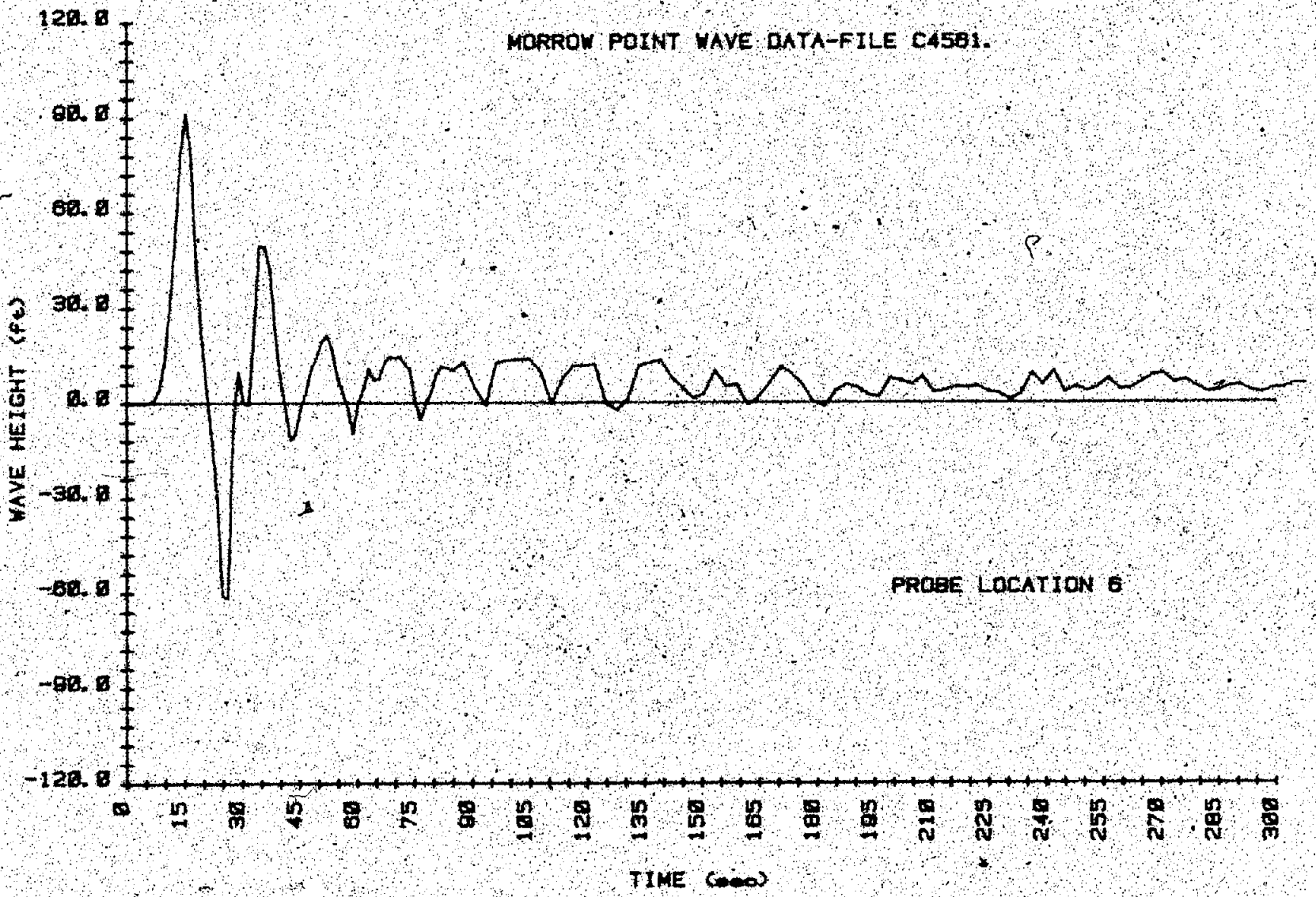

MF 147

Figure B-30. – Wave height versus time – test C4561 (5 of 6).

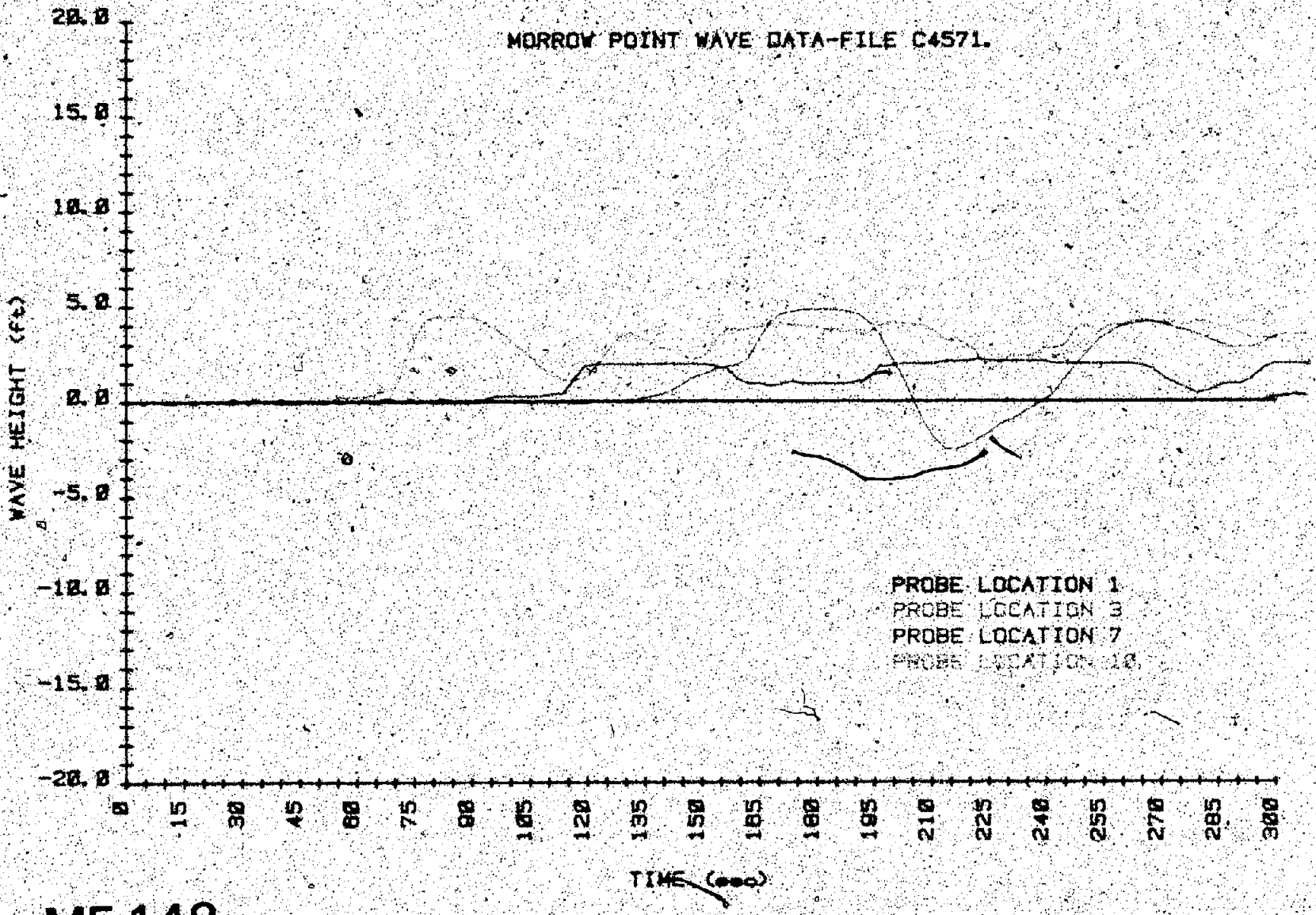

MF 148

Figure B-31.—Wave height versus time — test C4571 (1 of 5).

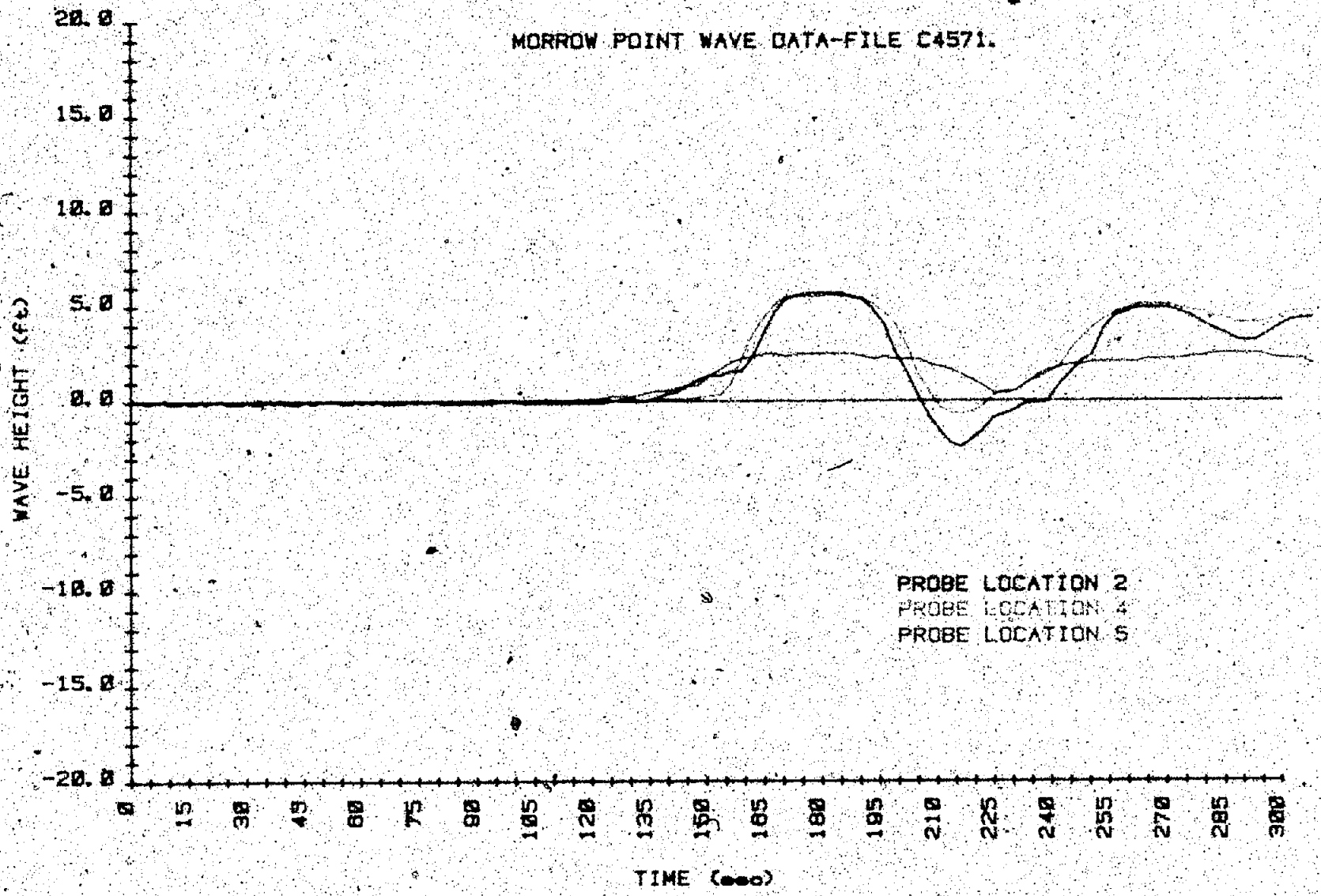

MF 149

Figure B-31. Wave height versus time – test C4571 (2 of 5).

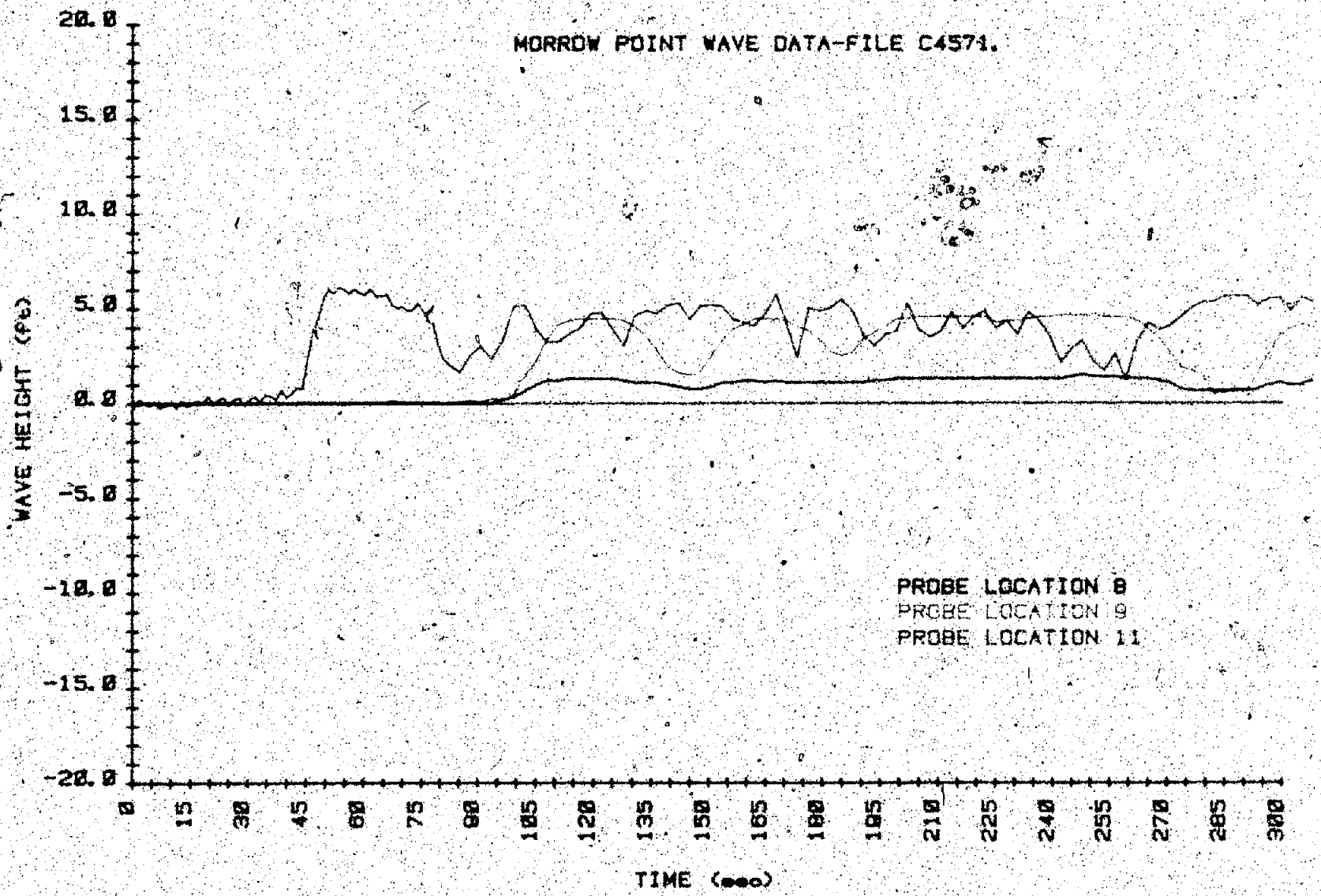

MF 150

Figure B-31.—Wave height versus time — test C4571 (3 of 5).

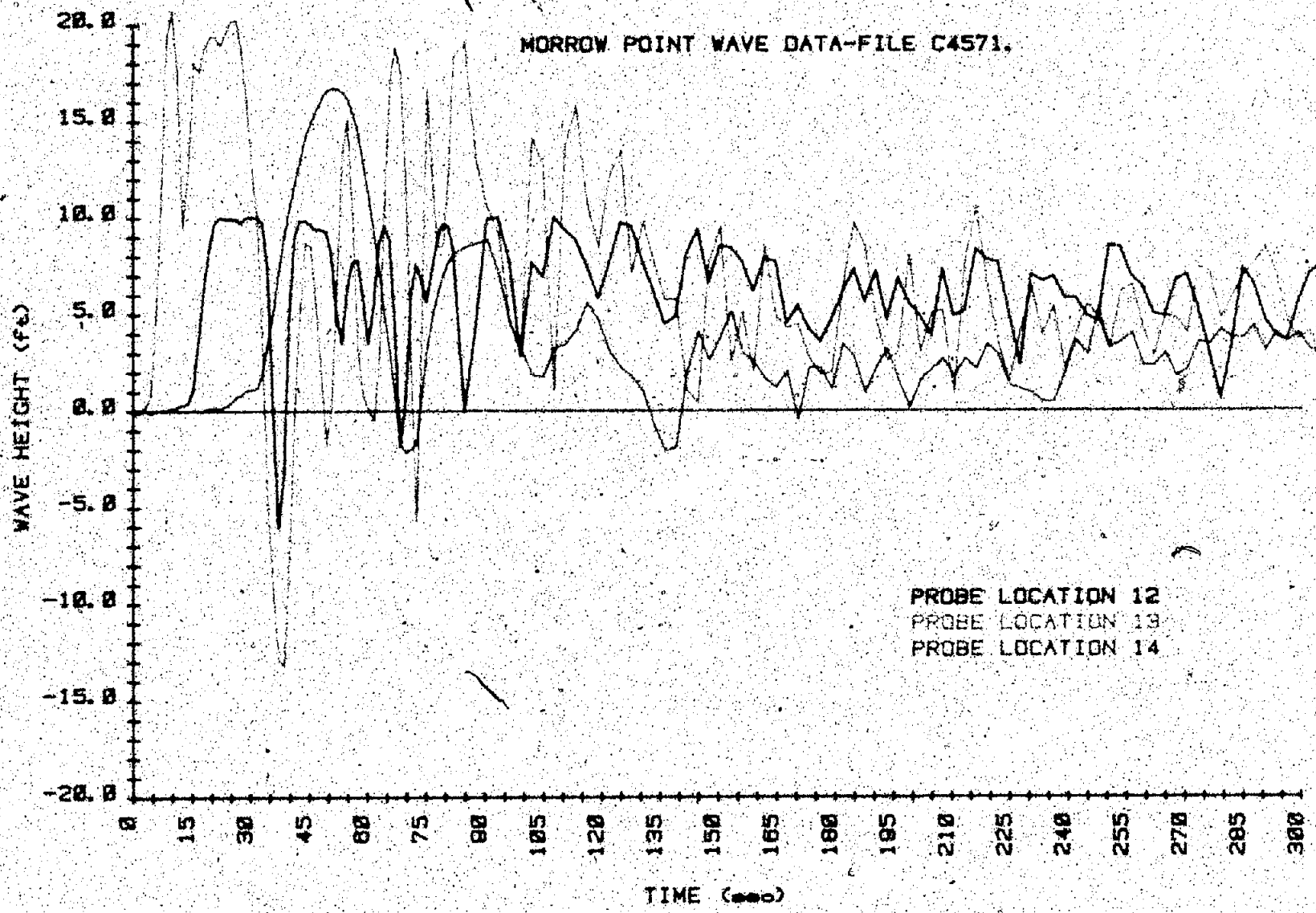

MF 151

Figure B-31. - Wave height versus time — test C4571 (4 of 5).

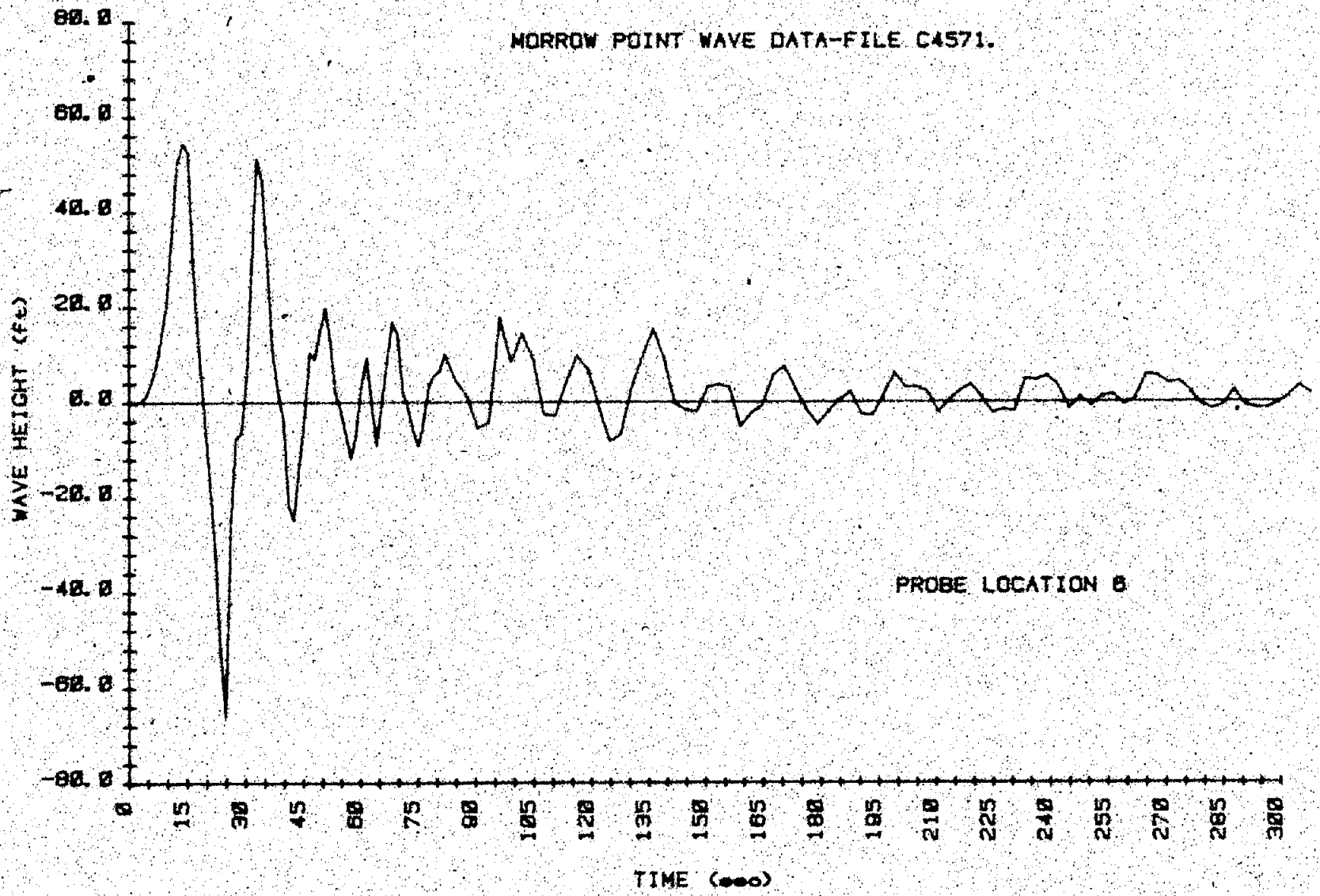

MF 152

Figure B-31. – Wave height versus time – test C4571 (5 of 5).

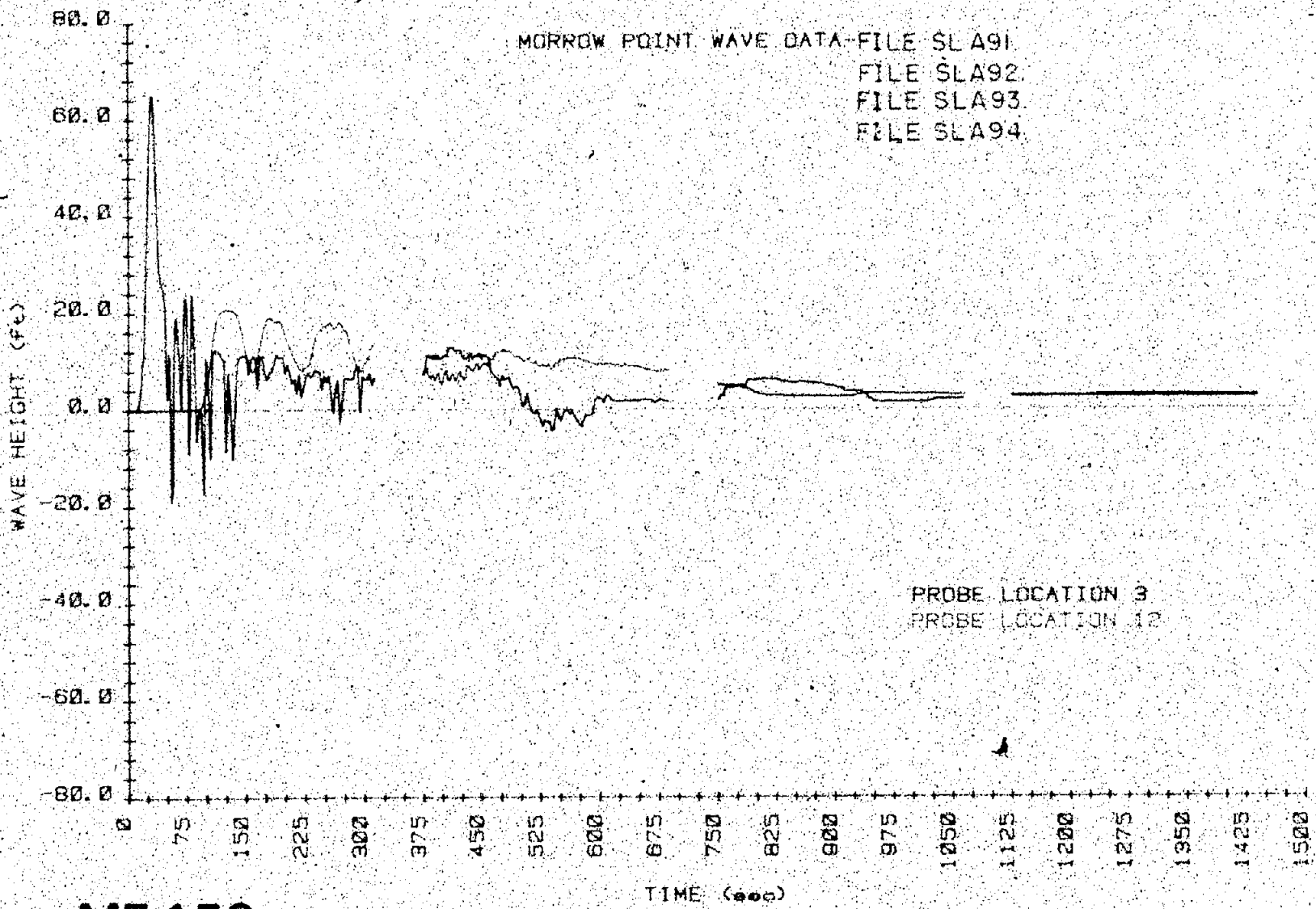

MF 153

Figure 8-32 – Wave height versus time – test SLA9 (4 Files)

END

United States Department of the Interior
Bureau of Reclamation